

**SITING
CRITERIA
FOR
DISTANCE MEASURING
EQUIPMENT**



Date: 10/19/2023

**DEPARTMENT OF TRANSPORTATION
FEDERAL AVIATION ADMINISTRATION**



**U.S. DEPARTMENT OF TRANSPORTATION
FEDERAL AVIATION ADMINISTRATION**

**ORDER
6820.14**

Effective date:
10/19/2023

SUBJ: SITING CRITERIA FOR DISTANCE MEASURING EQUIPMENT

This order provides guidance to personnel engaged in the siting of Federal Aviation Administration (FAA) Distance Measuring Equipment (DME). This order also provides guidance to FAA personnel responsible for protecting and mitigating possible adverse effects on the DME Signal-in-Space (SIS) from proposed construction around the DME facility.

This order provides guidelines that are used in conjunction with a thorough understanding of DME facility operations to arrive at the optimum facility location. The guidelines and criteria in this order are designed to be applicable to all installations, but are not required to be applied retroactively to existing installations. Application of these guidelines may be used to reduce the real estate requirements for certain existing installations. Deviations from these criteria may be permitted provided the results of a site-specific analysis indicate that operationally acceptable performance will be achieved with such deviations in place.

REBECCA Digitally signed
by REBECCA
ELLEN ELLEN GUY
GUY Date: 2023.10.19
10:14:41 -04'00'

Rebecca Guy
Vice President, Program Management Organization, AJM-0

Table of Contents

Chapter 1. General Information	1
Chapter 2. The DME System	4
Chapter 3. DME Signal Characteristics and Performance Considerations	10
Chapter 4. Antenna Considerations.....	46
Chapter 5. DME Siting Requirements.....	78
Chapter 6. Site Selection, Project Engineering and Facility Establishment.....	94
Appendix A. Acronyms.....	98
Appendix B. Reference Documents	100
Appendix C. DME Performance	103
Appendix D. Antenna Performance	192
Appendix E. Echo Location	220
Appendix F. DME Math Modeling.....	237

List of Figures

Figure 2-1. FAA DME/DME RNAV Service Architecture.....	5
Figure 2-2. DME Two-way Ranging Concept.....	7
Figure 2-3. Effects of Terrain in Producing Specular and Diffuse Reflection.....	8
Figure 2-4. DME Siting Roughness Criterion.....	9
Figure 3-1. Terminal DME SSV	12
Figure 3-2. High Altitude (H) and Low Altitude (L) DME SSVs	12
Figure 3-3. DME Low (DL) and DME High (DH) Service Volumes	13
Figure 3-4. A Hypothetical LOS Blockage Scenario.....	15
Figure 3-5. Illustration of DME Multipath Sources.....	16
Figure 3-6. DME Object Consideration Area (OCA)	18
Figure 3-7. Diffraction Gain.....	20
Figure 3-8. Knife Edge Diffraction Geometry	21
Figure 3-9. Shadowing Silhouette Used When Performing Ray Tracing.....	22
Figure 3-10. Level Run Flight Measurement Profile	24
Figure 3-11. Example Fading Data Produced by Level-run Flight Measurement Profile	24
Figure 3-12. Radiation Through an Electrically Large Rectangular Aperture.....	25
Figure 3-13. Diffraction Silhouette Used When Performing Ray Tracing	27
Figure 3-14. TOA Processing With and Without Multipath.....	29
Figure 3-15. Multipath Pulses From Same Reply Cycle Arriving Slightly Later Than Direct Pulses.....	30
Figure 3-16. Example of Pulse Deformation for Late-arrival Multipath	30
Figure 3-17. Multipath Pulse and Direct Pulse Parameters	32
Figure 3-18. Multipath Pulse Influence on Direct Pulse Time-of-Arrival Threshold.....	33
Figure 3-19. Early and Late Multipath Pulse to Direct Pulse Timing Regions	35
Figure 3-20. DME/N Error vs. Relative τ -delay, M/D ratio, In-phase Case.....	36
Figure 3-21. DME/N Error vs. Relative τ -delay, M/D ratio, Out-of-phase Case	36
Figure 3-22. Early and Late Arrival Zone Summary for -6.5 dB and -20 dB M/D Ratios	38

Figure 3-23. Examples of Resonant Antennas	44
Figure 4-1. Annotated DME Antenna Vertical Pattern	47
Figure 4-2. Annotated DME Antenna Omni-directional Horizontal Pattern	48
Figure 4-3. Annotated DME Antenna Uni-directional Horizontal Pattern	49
Figure 4-4. Annotated DME Antenna Bi-directional Horizontal Pattern	50
Figure 4-5. Illustration of Longitudinal Multipath	51
Figure 4-6. Illustration of Lateral Multipath	51
Figure 4-7. Signal-In-Space Results from Adding Direct and Reflected Signals	52
Figure 4-8. Worst-Case: Signal-In-Space Is at Minimum Amplitude	53
Figure 4-9. Best-Case: Signal-In-Space Is at Maximum Amplitude	53
Figure 4-10. More Realistic Vertical Representation of DME High Service Volume	54
Figure 4-11. dB Systems, Inc. DME Antenna Directivities	56
Figure 4-12. dB Systems, Inc. DME Antennas Minimum Directive Gain	56
Figure 4-13. dB Systems, Inc. DME Antennas Minimum Directive Gain - Detail View	57
Figure 4-14. dB Systems, Inc DME Antennas Minimum Directive Gain for 5100A, 510A, and 5100A/7° Models	57
Figure 4-15. dB Systems, Inc. DME Antennas Minimum Directive Gain for 540 and 900E Models	58
Figure 4-16. Generic Two-ray Model for Signal Reflections from the Ground	60
Figure 4-17. Pictorial Depiction of Surface Roughness Criteria	61
Figure 4-18. Example Output for the Rough Surface Analysis, Including Results for All Scenarios	62
Figure 4-19. Fading Results for Commonly Used DME Antennas, Typical Antenna Site	63
Figure 4-20. dBs 5100A Worst-case Fading for Water Only Surface Conditions	64
Figure 4-21. Example of Corrugated Surface Profiles	65
Figure 4-22. Application of Particular Surfaces to Earth Only Fading Bounds	65
Figure 4-23. Example Fading Results for Worst-Case and Best-Case Conditions	66
Figure 4-24. Level Run Flight Test Profile with Example Simulated and Measured Signal- strength Results	69
Figure 4-25. Example of Migrating Nulls with Increased Antenna Height	70
Figure 4-26. Alignment of Level Run and Fading Bound Plots	71
Figure 4-27. Illustration of Migrating Peak/Nulls with Stationary Fading Bound Envelope	72
Figure 4-28. Correlation Between Level-run and Fading Bound Plots	73
Figure 4-29. Fading Bound Equation Symmetry About Horizon	75
Figure 4-30. Vector Wheel Diagrams for Figure 4-31	75
Figure 4-31. DME/N Time Delay vs. Multipath Error for an In-phase and Out-of-phase Multipath Conditions	76
Figure 5-1. Vertical Subtending Angle Illustration	80
Figure 5-2. Horizontal Subtending Angle Illustration	80
Figure 5-3. Lateral Multipath Illustration	81
Figure 5-4. Longitudinal Multipath Illustration	84
Figure 5-5. Two-level Flat Terrain	85
Figure 5-6. Two-level Up-Slant Terrain	86
Figure 5-7. Two-level Down-Slant Terrain	87
Figure 5-8. One-level Up-Slant Terrain	88
Figure 5-9. One-level Down-Slant Terrain	89

Figure 5-10. Illustration of Obstruction of Longitudinal	92
Figure C-1. A Hypothetical LOS Blockage Scenario	106
Figure C-2. Illustration of DME Multipath Sources	107
Figure C-3. Illustration of Longitudinal Multipath	109
Figure C-4. Illustration of Lateral Multipath	110
Figure C-5. Roughness Criterion	112
Figure C-6. Pictorial Depiction of Rayleigh and Fraunhofer Criteria for Surface Roughness .	112
Figure C-7. Signal-In-Space Results from Adding Direct and Reflected Signals	113
Figure C-8. Worst-Case: Signal-In-Space at Minimum Amplitude.....	114
Figure C-9. Best-Case: Signal-In-Space at Maximum Amplitude.....	114
Figure C-10. Scenario for Calculating Radius of the First Fresnel Zone.....	116
Figure C-11. Scenario for Calculating Radius of First Fresnel Zone When Distance to Receiver is Much Larger than Distance to Structure.....	117
Figure C-12. Reflection and Refraction at Smooth Plane Surfaces	119
Figure C-13. Ray Tracing from Many Points on an Illuminated Surface	119
Figure C-14. Ray Tracing Showing the Boundaries for Incident and Reflected Rays	120
Figure C-15. Ray Tracing for a 3D Building	121
Figure C-16. Example of Echo Ellipsoids for a Given Time-delay	122
Figure C-17. Geometry for Echo Ellipse	123
Figure C-18. Plan View Showing a Building Near a Potential DME Antenna Site	124
Figure C-19. Time Delay Calculations Scenario	125
Figure C-20. Geometrical Relationship for Multipath Scalloping Equation	127
Figure C-21. Example Error Trace with Scalloping Effect Illustrated	127
Figure C-22. Bode Plot of Generic DME Interrogator Output Filter.....	128
Figure C-23. Half Amplitude Find Function Used in DME/N for TOA Determination	130
Figure C-24. DAC Function Used in DME/P for TOA Determination	131
Figure C-25. DME Object Consideration Area (OCA).....	133
Figure C-26. Diffraction Gain.....	135
Figure C-27. Knife Edge Diffraction Geometry	136
Figure C-28. Signal Blockage/Clearance Scenarios	137
Figure C-29. Flight profile and Signal Strength Analysis, Part 1	139
Figure C-30. Flight Profile and Signal Strength Analysis, Part 2.....	140
Figure C-31. Qualitative Zonal Assessment of Signal Attenuation Due to Shadowing	141
Figure C-32. Shadowing Silhouette used when Performing Ray Tracing	143
Figure C-33. Level Run Flight Measurement Profile	144
Figure C-34. Example Fading Data Produced by Level-run Flight Measurement Profile	145
Figure C-35. Example Fading Results for Worst-Case-Phase and Best-Case-Phase Conditions	146
Figure C-36. Shadowing and Reflection Multipath Signal Strength Relationships.....	147
Figure C-37. Radiation Through an Electrically Large Rectangular Aperture	148
Figure C-38. Qualitative Zonal Assessment for Signal Attenuation Due to Fading.....	150
Figure C-39. Diffraction Silhouette Used When Performing Ray Tracing.....	151
Figure C-40. TOA Processing With and Without Multipath	153
Figure C-41. Multipath Pulses From Same Reply Cycle Arriving Slightly Later than Direct Pulses.....	154
Figure C-42. Example of Pulse Deformation for Late-arrival Multipath	155

Figure C-43. Multipath Pulse and Direct Pulse Parameters.....	156
Figure C-44. Multipath Pulse Influence on Direct Pulse Time-of-arrival Threshold	157
Figure C-45. Early and Late Multipath Pulse to Direct Pulse Timing Regions.....	159
Figure C-46. Pulse Deformation Snapshots In-phase for an M/D Ratio of -6.5 dB	161
Figure C-47. Pulse Deformation Snapshots Out-of-phase for an M/D Ratio of -6.5 dB	162
Figure C-48. DME/N Error versus Relative τ -delay, M/D Ratio, In-phase Case	163
Figure C-49. DME/N Error versus Relative τ -delay, M/D Ratio, Out-of-phase Case.....	164
Figure C-50. In-phase Multipath Arrival Zones with Indications for -6.5 dB M/D Ratio.....	166
Figure C-51. In-phase Multipath Arrival Zones with Indications for -20 dB M/D Ratio.....	167
Figure C-52. Out-of-phase Multipath Arrival Zones with Indications for -6.5 dB M/D Ratio	168
Figure C-53. Out-of-phase Multipath Arrival Zones with Indications for -20 dB M/D Ratio .	169
Figure C-54. Early and Late Arrival Zone Summary for -6.5 dB and -20 dB M/D Ratios	170
Figure C-55. DME Transponder Receives and Replies to a Sequence of Aircraft Interrogations	171
Figure C-56. Downlink and Uplink Sequences.....	171
Figure C-57. Multipath TOA Relative to Direct Pulse Scenarios for First Pulse Timing	174
Figure C-58. Interpretation of Time Diagram for Computing Absolute Time-delay Values ...	176
Figure C-59. Multipath Case – 1st Pulse of Same Reply Interfering with 2nd Pulse of User Aircraft Reply.....	178
Figure C-60. Multipath Case – 2 nd Pulse of Earlier Reply Interfering with 1 st Pulse of User Aircraft Reply.....	179
Figure C-61. Multipath Case – 1 st Pulse of Earlier Reply Interfering with 1 st Pulse of User Aircraft Reply.....	179
Figure C-62. Multipath Case – 2 nd Pulse of Earlier Reply Interfering with 2 nd Pulse of User Aircraft Reply.....	180
Figure C-63. Multipath Case – 1 st Pulse of Earlier Reply Interfering with 2 nd Pulse of User Aircraft Reply.....	180
Figure C-64. Uplink Echo Ellipsoids Based on Aircraft B Geometry	182
Figure C-65. Interrogation Replies are Jittered (Asynchronously) to Prevent Multipath Interference.....	184
Figure C-66. Multipath Object Locations of Interest within Echo Ellipsoid 1	185
Figure C-67. Plan View Showing a Building Near a Potential DME Antenna Site	187
Figure C-68. Time Delay Calculations Scenario	188
Figure C-69. Determining Vertical Profile Factor	190
Figure D-1. dBs 5100A Directivity vs. Elevation Angle	197
Figure D-2. dBs Antenna Model 5100A Fading Analysis Best Case/Worst Case Phase - Earth Only Surface Conditions	198
Figure D-3. dBs 5100A/7° Directivity vs. Elevation Angle	201
Figure D-4. dBs Antenna Model 5100A/7° Fading Analysis	202
Figure D-5. dBs 510A Directivity vs. Elevation Angle	204
Figure D-6. dBs Antenna Model 510A Fading Analysis	205
Figure D-7. dBs 540 Directivity vs. Elevation Angle.....	207
Figure D-8. dBs Antenna Model 540 Fading Analysis.....	208
Figure D-9. dBs 900E Directivity vs. Elevation Angle.....	210
Figure D-10. dBs Antenna Model 900E Fading Analysis	211
Figure E-1. Multipath Overview	221

Figure E-2. Examples of Multipath Delay (Big Picture)	222
Figure E-3. Combined Pulse (In-phase).....	223
Figure E-4. Combined Pulse (Out-of-phase).....	223
Figure E-5. Ellipsoid Overview	224
Figure E-6. Vertical Slice through an Ellipsoid	225
Figure E-7. Difference in Distance to Ellipse vs Ellipsoid Intersection with Terrain	226
Figure E-8. Ellipse Variation as Function of Pulse Delay Variation	227
Figure E-9. Ellipse Variation as Function of Transmitter to Multipath is Varied	228
Figure E-10. Ellipse Variation Ensemble.....	229
Figure E-11. Ellipse Parameters.....	233
Figure E-12. Locating Possible Reflection Source	235
Figure F-1. Sample Model Scenario to Describe Plots	238
Figure F-2. Sample 2-dimensional (a) Range Error, (b) Lock Status Plot, and (c) Signal Strength	239
Figure F-3. Sample Heatmap (a) Range Error, (b) Lock Status, and (c) Signal Strength Plot .	240
Figure F-4. Wind Turbine (a) Dimensions and (b) Model Set-up	242
Figure F-5. (a) Range Error, (b) Lock Status and (c) Signal Strength for Case 1 at 1,000 feet	243
Figure F-6. (a) Range Error, (b) Lock Status, and (c) Signal Strength Results for Case 2 at 3,000 feet.....	243
Figure F-7. (a) Range Error, (b) Lock Status, and (c) Signal Strength Results for Case 3 at 5,000 feet.....	244
Figure F-8. Solar Panel Array Dimensions	244
Figure F-9. (a) Range Error, (b) Lock Status, and (c) Signal Strength Results of Solar Array Above Antenna Base.....	245
Figure F-10. Solar Panel Array Model Scenario Signal Strength Results at 1,000 feet	245
Figure F-11. Longitudinal Multipath of Solar Panel Array	246
Figure F-12. Signal Strength along Radials 15 and 60 at 1,000 feet.....	247
Figure F-13. Irrigation Equipment Dimensions	248
Figure F-14. Screen Capture of Irrigation Equipment in Model.....	248
Figure F-15. Illustration of Irrigation System Model Set-up	249
Figure F-16. (a) Range Error, (b) Lock Status, and (c) Signal Strength Results of Irrigation System at 500 feet Distance	249
Figure F-17. Dimensions of Model ATCT.....	250
Figure F-18. Illustration of ATCT Model Set-up.....	250
Figure F-19. (a) Range Error, (b) Lock Status, and (c) Signal Strength Results of 1,000 feet Distance.....	251
Figure F-20. Lock Status of (a) 6,000 and (b) 7,000 feet ATCT Distance	251
Figure F-21. Lock Status of (a) 15° and (b) 30° at 6,000 feet ATCT Distance.....	252
Figure F-22. Diagram of Model Communication Towers	253
Figure F-23. Illustration of Communication Tower Model Set-up.....	254
Figure F-24. (a) Range Error, (b) Lock Status, and (c) Signal Strength of Monopole at 1,000 feet.....	254
Figure F-25. (a) Range Error, (b) Lock Status, and (c) Signal Strength of Lattice Tower at 1,000 feet.....	255
Figure F-26. Illustration of Cylindrical Structure Model Set-up	256
Figure F-27. (a) Range Error, (b) Lock Status, and (c) Signal Strength of Fuel Tank at 2,000 feet	

..... 256
Figure F-28. Lock Status of Fuel Tank at 6,000 feet for (a) X and (b) Y-channel Transmitter 257

List of Tables

Table 3-1. Summary of DME Service Volumes 13
Table 4-1. Minimum Gain Values for dB Systems, Inc. DME Antennas 55
Table 5-1. Antenna Length and Near-field Protection Cylinder Distance 79
Table 5-2. Scattering Object Distance and Subtending Angle Criteria 82
Table D-1. DME Environmental Specification for dBs Antennas 193
Table D-2. Characteristics Common to dBs DME Antenna Models 194
Table D-3. Characteristics Common to Configurations of the dBs Antenna Model - dBs 5100A
..... 195
Table D-4. Characteristics Unique to Configurations of the dBs Antenna Model - dBs 5100A
..... 195
Table D-5. Characteristics Common to Configurations of the dBs Antenna Model - dBs
5100A/7° 199
Table D-6. Characteristics Unique to Configurations of the dBs Antenna Model - dBs 5100A/7°
..... 200
Table D-7. Characteristics Common to Configurations of the dBs Antenna Model - dBs 510A
..... 203
Table D-8. Characteristics Unique to Configurations of the dBs Antenna Model - dBs 510A 203
Table D-9. Characteristics of the dBs Antenna Model - dBs 540 206
Table D-10. Characteristics of the dBs Antenna Model - dBs 900E 209

Chapter 1. General Information

1. Purpose of This Order

This order provides guidance to personnel engaged in the siting of Federal Aviation Administration (FAA) Distance Measuring Equipment (DME). This order also provides guidance to FAA personnel responsible for protecting and mitigating possible adverse effects on the DME Signal-in-Space (SIS) from proposed construction around the DME facility.

This order provides guidelines that are used in conjunction with a thorough understanding of DME facility operations to arrive at the optimum facility location. The guidelines and criteria in this order are designed to be applicable to all installations, but are not required to be applied retroactively to existing installations. Application of these guidelines may be used to reduce the real estate requirements for certain existing installations. Deviations from these criteria may be permitted provided the results of a site-specific analysis indicate that operationally acceptable performance will be achieved with such deviations in place.

2. Audience

This order provides guidance for all personnel responsible for planning the installation or troubleshooting of existing DME facilities in the National Airspace System (NAS).

3. Where Can I Find This Order?

- a. On the Technical Library website at:

<https://nas.amc.faa.gov/phoenix/views/technicalLibrary.xhtml>

- b. On the Directives website at:

https://employees.faa.gov/tools_resources/orders_notices/

4. Cancellation

This order does not cancel an existing order.

5. Explanation of Policy Changes

There are no changes to an existing order.

6. Application

The criteria in this order apply to new DME-only establishments or relocated DME facilities. These criteria may also be used to predict the impact of changes to the local environment (e.g., construction) on the performance of existing facilities. Changes to existing facilities for the sole purpose of obtaining compliance with these criteria are not required, but may be implemented to reduce the real estate requirements associated with decommissioned Very High Frequency Omni-directional Range (VOR)/DME and Tactical Air Navigation (TACAN) sites where the DME is to remain in use (see Chapter 5 for more details). For all other instances, FAA Order 6820.10, “VOR, VOR/DME, and VORTAC Siting Criteria” will apply to those facilities.

7. Directive Verbs

The material in this order contains FAA criteria, recommended practices, and other guidance materials, which require the use of certain directive verbs such as, **MUST**, **SHOULD**, **WILL**, and **MAY**. In this order the explicit meaning of the verbs are as follows:

- a. **MUST.** The action is mandatory. For example: “The DME must provide accurate range information along all published procedures where the DME is used for position information.”
- b. **SHOULD.** The action is desirable or recommended. For example: “The vertical subtending angle from the DME antenna to any obstruction should be below 1° for all objects to minimize shadowing.”
- c. **WILL.** The action is to be taken in the future. For example: “The report will recommend the appropriate DME system and antenna type.”
- d. **MAY.** The action is permissible. For example: “Buildings beyond 5 nmi need not be evaluated unless, based on engineering judgement, it is deemed the structure may impact system performance.”

8. Procedures

- a. **Standards and Tolerances (Ground Equipment).** The standards and tolerances for the DME are contained in FAA Order JO 6730.2, “Maintenance of Distance Measuring Equipment (DME) Facilities,” and the applicable instruction books. Note that for installation purposes, the initial tolerances and limits must apply.
- b. **Airborne Signal-in-Space (SIS) Performance Requirements.** The airborne SIS requirements in this order are based on information available at the time of publication in FAA Order 8200.1, “United States Standard Flight Inspection Manual (USSFIM).”

9. DME Siting and Installation

The goal of any DME installation is to provide a DME signal which will provide information sufficient to assist aircraft in navigating to their desired location in the Area Navigation (RNAV), en route, or terminal environment. The ability to attain this objective depends to a great extent on the proper siting and performance of each DME system. If the DME is collocated with another facility, that facility siting order must also be considered when siting the DME.

10. Siting Effects on DME Operations

The ability of the DME system to provide reliable and accurate slant range information depends primarily upon the un-obstructed propagation of the SIS. The greatest detriment to the DME SIS is the presence of reflecting and signal blocking objects such as terrain, vegetation, irrigation equipment, Air Traffic Control Towers (ATCTs), communication towers, and cylindrical structures. The guidance presented in this order will enable the siting engineer to choose the optimum site for installation. Math modeling techniques may be employed to predict the probable location, magnitude, and duration of DME

disturbances caused by multipath and shadowing conditions.

11. DME Establishment Criteria

- a. **DME Establishment.** A DME may be established to support en route or terminal procedures. The FAA performed DME coverage analysis to estimate the total number of DMEs necessary to meet the DME/DME RNAV goals from the Performance Based Navigation (PBN) NAS Navigation Strategy 2016. This analysis resulted in a solution set which relies on existing high power FAA DMEs, Canadian DMEs, and Military DMEs.
- b. **Physical Requirement Considerations.** The ground based equipment of the DME system requires land and infrastructure sufficient to support the DME installation. The land required for a typical installation should be adequate to assure DME SIS is not impacted by obstructions in the vicinity of the antenna and guard against future growth or development. Infrastructure required for a DME installation includes roads, utilities and communication lines. The shelter where the DME equipment is installed must also be located close enough to the DME antenna so as not to exceed the limitations set forth by any particular DME's installation manual.
- c. **Equipment Type and Configuration Considerations.** Equipment type and antenna configurations used in DME establishments, either en route or terminal, should be chosen to fit the need for which the DME is intended to fill. Consideration should be given not only to siting DME equipment to account for current terrain, obstructions, and multipath predictions, but also for future vegetation growth and planned development around the DME facility.

12. DME Components as Obstructions

For DME installations on or near airports, the siting engineer must consider the effects of the DME components themselves as obstructions. These considerations should include guidance given in FAA Order 8260.3 "United States Standard for Terminal Instrument Procedures (TERPS)", 14 CFR Part 77, and applicable FAA Advisory Circulars (ACs) such as AC 150/5300-13 "Airport Design", and AC 70/7460-1 "Obstruction Marking and Lighting".

Chapter 2. The DME System

1. Introduction

The purpose of this chapter is to introduce the DME Siting Engineer to the basic operating principles of the DME system, describing, at a high level, Normal DME (DME/N) system operation, the DME facility and its components.

2. DME Service Requirements

DME range information is used to support en route, arrival, and departure operations, as well as approach, landing, and missed-approach operations. For these applications, DME is used in conjunction with other navigational aids (NAVAIDs) such as VOR and the Instrument Landing System (ILS). RNAV operations can also be supported through the use of multiple DME signals and appropriately equipped aircraft. This service is called DME/DME RNAV and can be used as a robust backup to Global Positioning System (GPS) navigation during GPS outages.

- a. **Procedure Support.** DMEs provide procedure support to a number of instrument approach procedures throughout the NAS. Support may include, but is not limited to, defining a fix along an ILS or defining a DME arc for a procedure. DMEs may be installed solely for procedure support or they may be used for both procedure support and en route guidance.
- b. **DME/DME RNAV Service Requirements.** The FAA is expanding the existing DME/DME RNAV service across the Contiguous United States (CONUS) to enable DME/DME RNAV equipped aircraft to continue PBN operations during Global Navigation Satellite System (GNSS) disruptions without the need for an Inertial Reference Unit (IRU). This service minimizes additional pilot and controller workload and maintains NextGen capacity and efficiency benefits in Class A airspace, as well as at the busiest Navigation Service Group (NSG)-1 and select NSG-2 airports during GNSS disruptions.

To further aid in the expansion of the DME/DME RNAV Service, the FAA is also increasing the standard service volumes of existing and future DME installations. The resulting DME/DME RNAV service architecture will provide a resilient navigation service for the NAS in CONUS. DME/DME RNAV Service will be required in 99% of the airspace above 18,000 feet Mean Sea Level (MSL) in eastern CONUS and above 24,000 feet MSL in the Western United States Mountainous Area (WUSMA) and up to Flight Level (FL) 450. The RNAV Service area also includes airspace from 1500 feet Above Ground Level (AGL) to 18,000 feet east and 24,000 feet in WUSMA around NSG-1 and select NSG-2 airports. Figure 2-1 below depicts the DME/DME RNAV Service Architecture.

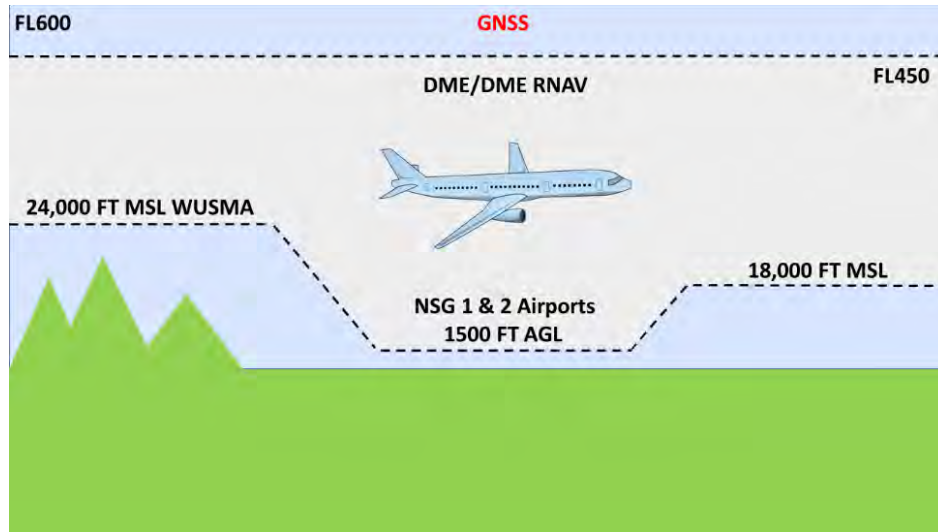


Figure 2-1. FAA DME/DME RNAV Service Architecture

3. DME System Components

- a. **Ground Equipment.** The DME ground equipment consists of four major components: a transponder, an antenna, a monitor, and a control unit.
 - i. **Transponder.** The transponder is the ground based radio transceiver that sends out broadcast replies to aircraft in the area that are interrogating on its frequency. There are several DME types currently in use by the FAA, these include: Cardion model FA-9639 and FA-9783 DME, ASII model 1118 DME, Selex models FA-30600 and FA-30601 DME, Thales models FA-18200 and 415SE DME, and Wilcox models FA-9996, and FA-10391 DME.
 - ii. **Antenna.** There are currently three types of antenna systems available for installation with the DME depending on site requirements: omni-directional, uni-directional, and bi-directional. The antenna system is composed of a collinear stack of dipoles. Arrangement of those dipoles determine the vertical radiation pattern. The main lobe of the vertical pattern generally occurs at an elevation angle between 3° to 5°. An alternate antenna that has been approved for use in the NAS on a case-by-case basis through local NAS Change Proposal (NCP) has the main lobe at 7°. Antenna Considerations provide greater detail on the antenna types referenced above.
 - iii. **Monitor.** The DME monitors the following parameters: reply delay, reply efficiency, pulse spacing, pulse count, identification, radiated power, receiver sensitivity, and transmitter frequencies. Reply delay and reply efficiency are measured by using only the transponder replies to interrogations from the signal generator section of the monitor. Reply delay is the fixed delay (usually 50 or 56 microseconds (μs)) of the DME station, the time between the reception of a valid interrogation and the transmission of a reply to that interrogation. Reply efficiency is the ratio of transponder replies to a given number of interrogations, expressed as

a percentage. The signal monitor portion of the monitor, which is used with the monitor signal generator to measure system delay and reply efficiency, also measures pulse spacing, pulse count, identification, and power output of all transponder replies. The monitor also supplies signals to the test unit for pulse viewing and measurements during testing and alignment. If one of the parameters exceeds a preset limit, a fault signal is sent to the station control unit.

- iv. **Control Unit.** The DME control unit provides manual and automatic control of the DME station. It also provides manual station turn on or turn off; and, if a dual-transponder-equipped station is used, the manual selection allows a choice of equipment, No. 1 or No. 2. For a single-equipment station, any alarm will alert personnel at the remote monitoring point and result in a station shutdown. For a dual-equipment station the same is true, except that the initial alarm results in a transfer from main to standby equipment. Alarms at the remote site, such as an air traffic control tower, are indicated by the remote status indicator or Remote Monitoring and Logging System (RMLS). Signals from the DME station are transmitted to the status indicator via a telecommunication line or to a radio transceiver. The status indicator will indicate the exact status of the DME station.

b. Airborne Equipment

- i. **Interrogator.** The aircraft interrogator decodes its own distance replies from transmissions to other aircraft by locating a time-delay period that remains essentially constant between a group of its own interrogation pulses and a series of reply pulses transmitted by the ground station. The aircraft uses an automatic process, which sets up a search pattern each time the aircraft interrogator is tuned to a new station. The process tests various delay intervals by checking the number of successive replies received within a uniform period. At some particular interval, the repetition rate of the reply matches the repetition rate of the interrogations. Reply pulse-pairs are the only ones that have the same spacing between pairs as the random interrogation pulses from the aircraft. When the two kinds of pulses are determined to be synchronous, the airborne receiver locks on to the reply pulses and automatically tracks the ground station.

4. DME Theory of Operation

- a. **Basic Principle of Operation.** An interrogator in the aircraft transmits signals to the DME ground station. A transponder at the ground station receives the signals, and after a fixed time delay has elapsed transmits replies to the aircraft. The aircraft interrogator measures the elapsed time for the exchange, which is proportional to the slant range distance between the aircraft and the ground station.
- b. **DME Radio Frequencies (RFs).** DMEs operate on frequencies between 960 Megahertz (MHz) and 1215 MHz. The interrogator in the aircraft transmits between 1025 MHz and 1150 MHz, with the DME ground station transmitting on a frequency that is 63 MHz higher or 63 MHz lower than the aircraft interrogator frequency.

- c. **DME Frequency Channels.** DME frequencies are divided into 252 channels, consisting of 126 X-channels (1X-126X), and 126 Y-channels (1Y-126Y). The main difference between the X and Y-channels is the spacing of the pulse-pairs and the reply delay of the DME ground station.
- d. **DME Pulse-Pair Spacing and Delay.** The DME transmits pulse-pairs at specific pulse-pair spacing depending on if it is an X-channel or a Y-channel. The pulse-pair spacing for an X-channel is $12\mu\text{s}$, and the spacing for a Y-channel is $36\mu\text{s}$. Ground station reply delay is also channel dependent. For X-channel this delay is $50\mu\text{s}$ and for Y-channel the delay is $56\mu\text{s}$.
- e. **DME Slant Range Measurements.** Figure 2-2 depicts the standardized two-way ranging technique used by the DME. When the aircraft pilot or flight management computer selects a ground station, the airborne interrogator sends out distance interrogation pulses on the receiving channel frequency assigned to the ground station. These airborne pulses are received by the ground station receiver, delayed a fixed amount, and distance replies are transmitted back to the aircraft on the assigned channel. Since radio energy travels at a known and constant speed, the distance between the aircraft and ground station is determined by the elapsed time between the initial transmission of the interrogation and the reception of the reply from the ground station.

There is a $50\mu\text{s}$ delay or a $56\mu\text{s}$ delay (for X or Y-channel, respectively) between reception of the aircraft signal and transmission of the reply. Timing circuits on the aircraft measure the time intervals between the interrogation and reply, subtract the 50 or $56\mu\text{s}$ delay, and convert the remaining time difference to distance. Distance is displayed on an indicator and/or digitally transmitted to other devices.

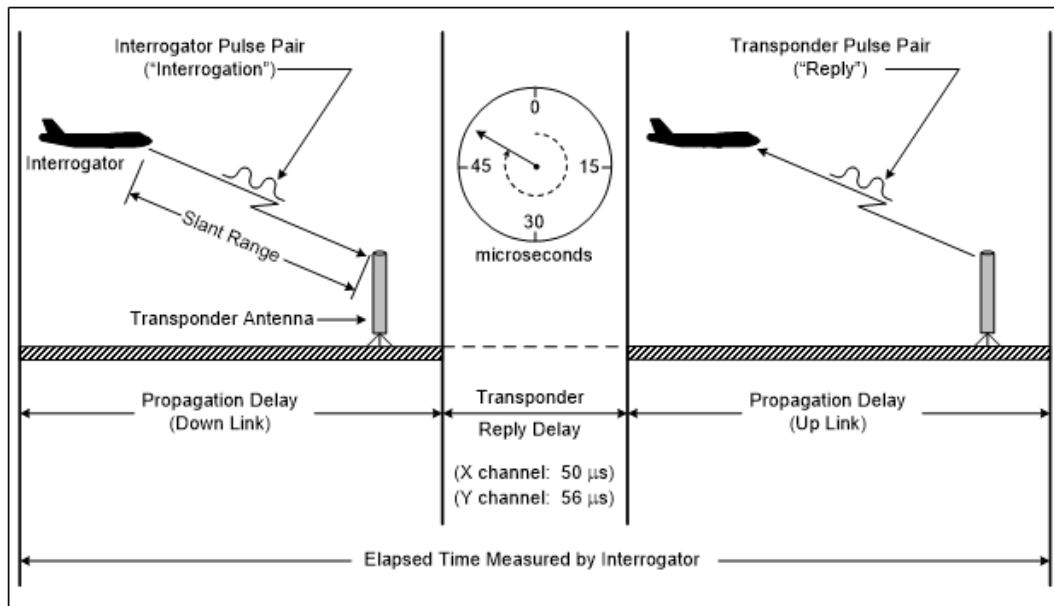


Figure 2-2. DME Two-way Ranging Concept

- f. Station Ident.** The ground station transmits an international Morse code approximately every 30 seconds. Pulse coding allows an audio signal to be generated which enables the aircraft to identify the station.
- g. Distance Replies.** The distance replies are the DME signals which provide the slant range distance from the DME ground station to the interrogating aircraft.
- h. Squitter.** Squitter is a pulse-pair transmitted by the transponder, which are not in response to interrogations. The squitter pulse-pairs are identical to standard reply pulse-pairs and occur random in time. Since they are not synchronous with an interrogator's interrogation, it is not decoded as a reply and is ignored. The number of squitter pulse-pairs transmitted is varied to maintain a minimum number of pulse-pairs transmitted by the transponder. Variations occur as the number of aircraft interrogating a facility varies. Airborne interrogators use the ensemble of transmitted pulse-pairs to detect presence of a DME facility without interrogating the ground station and to set the receiver gain.
- i. Precedence of Signals.** To prevent interference between various components of the ground station output, there is an order of precedence for each signal in the overall train of pulses. In the DME equipment, the order of priority is identification, distance replies, and squitter pulses. During the identification cycle key down period, distance reply pulses are not transmitted.
- j. Signal-In-Space (SIS) Propagation.** The objective of successful siting is to avoid the harmful effects of multipath within the required service volume of the DME. In general terms multipath is the condition where the receiving antenna gets the radio transmission via two or more paths. Radio signals reflected off the ground or a counterpoise is called longitudinal multipath, and signals reflected off objects such as buildings and trees is called lateral multipath.

As illustrated in Figure 2-3, reflection can be specular or diffuse. Specular reflection provides a stronger signal in a specific direction than does diffuse reflection. Hence, if specular reflection causes undesirable interference, the interference can be expected to be relatively strong. Diffuse reflection from a rough surface is unpredictable in its effects. If the reflecting area is sufficiently large it may cause multipath problems.

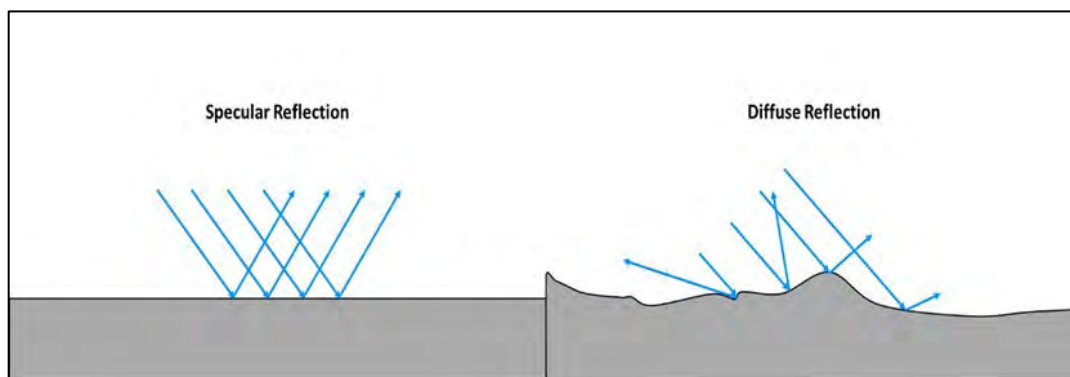


Figure 2-3. Effects of Terrain in Producing Specular and Diffuse Reflection

Judgement is required to determine whether or not a particular ground will be seen as rough or smooth by the electromagnetic energy. The Rayleigh and Fraunhofer criteria are established standards used to characterize surface roughness. Both criteria classify a surface as rough or smooth based on the phase difference between signals reflected from two different points on the surface. The Rayleigh criterion classifies a surface as rough when the value for “h” exceeds $\lambda/(8\sin\gamma)$, whereas the Fraunhofer criterion classifies a surface as rough when the value for “h” exceeds $\lambda/(32\sin\gamma)$. The Fraunhofer criterion is less conservative from a fading analysis perspective and, realistically, many sites may not present that way. Conversely, the Rayleigh criterion is more conservative and may exclude some sites that are slightly rough. As such, an intermediate criterion for DME siting – which falls in the middle of both criteria previously mentioned – was established and is shown by the red trace in Figure 2-4. Note that for small grazing angles (i.e., γ approaching zero) a very irregular ground can still act as a smooth reflective surface.

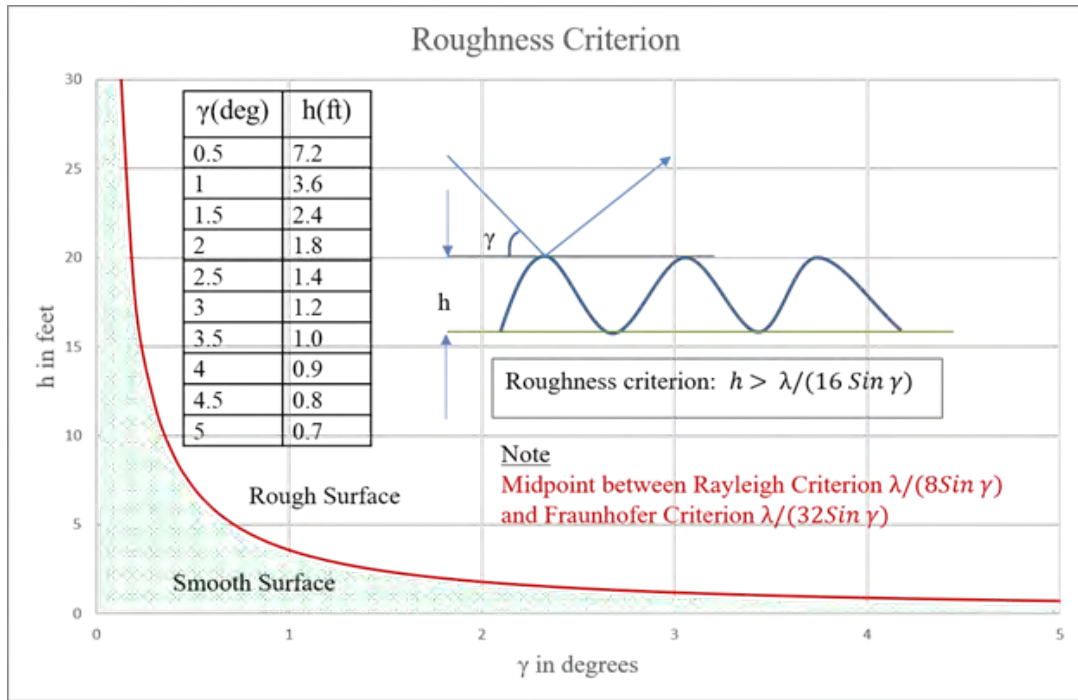


Figure 2-4. DME Siting Roughness Criterion

Chapter 3. DME Signal Characteristics and Performance Considerations

1. Introduction

The purpose of this chapter is to provide key background material on DME performance characteristics and RF concepts relevant to the analysis of such characteristics. The discussion addresses DME service provisioning, signal characteristics of interest, system performance, and performance considerations, as well as the related performance analysis techniques.

Appendix C provides a more detailed discussion of the topics mentioned in the following sections. Additionally, Appendix C provides tutorial information, and discusses topics not presented or summarized in this chapter because they pertain to DME system design concepts and related background information.

2. DME Service Provisioning Overview

This section discusses high-level DME functions and service provisioning, as well as ranging and identification functionality in terms of signal strength and quality.

a. DME Functions and Service Provisioning

- i. **DME Functions.** DME performs the following three high-level functions: Ranging, Identification, and Interfacing with the RMLS. The usability of the Ranging and Identification functions are dependent on the SIS and its characteristics. Typically, the Identification functionality is assured when the SIS provides operationally acceptable Ranging accuracy performance, i.e., signal strength and accuracy performance that meet DME system-level requirements, such as those in FAA Order FAA-E-2996, “Performance Specification for Distance Measuring Equipment (DME)”. Thus, the focus hereafter addresses concepts and parameters related to achieving such Ranging performance, as well as the means to assess the impact of a specific siting condition on such performance. RMLS functionality relies on modern, reliable telecommunication services. If such services are available, RMLS performance is not considered to be a major factor in siting a DME system.
- ii. **DME Service Provisioning.** The goal of DME Service Provisioning is to provide DME service within the prescribed service volumes. This goal implies that Ranging and Identification are the essential, navigation-enabling functionalities that are to be provided. Ranging and Identification support the pilot’s situational awareness and position location for conventional flight operations, as well as lateral guidance for DME/DME RNAV flight operations. It is important to note that DME service may be adversely impacted if the guidance in this document is not applied correctly. The impacts that could be experienced by the user include degradation of accuracy performance, service outages within portions of the service volume due to inadequate signal strength, and insufficient ground station reply rate. In such cases, the service may not fully support en route, arrival, approach, missed-approach, departure, and DME/DME RNAV flight operations within the intended service volume.

- b. DME Signal Coverage and Accuracy.** DME Ranging and Identification functionality are dependent on signal coverage and signal accuracy.

To ensure adequate DME signal coverage for the user the DME must meet the minimum signal strength requirements. This minimum signal strength is required at the DME receiver to ensure proper operation in terms of pulse-pair decoding and ranging accuracy as well as to ensure frequency protection and acceptable immunity to noise effects.

The DME signal is considered to be of sufficient accuracy if: (1) the DME pulse-pairs incident at the user receiver result in range accuracy performance that meets the minimum distance accuracy requirement and result in the interrogation continuously operating in track mode (i.e., no loss of lock); and (2) the Morse code and voice identification are correct, clear, and identifiable.

The minimum signal strength and minimum distance accuracy requirements are specified in the USSFIM to ensure sufficient signal coverage and signal accuracy within the prescribed service volumes. Flight inspection will restrict the use of the DME in areas of the service volume, or may remove a facility from service, if the facility does not meet any of the signal accuracy requirements. Failure to meet signal coverage requirements is not used as a sole determination for restricting or removing a facility from service if a solid stable DME lock is present.

DME ground station equipment is designed to provide acceptable signal coverage and accuracy throughout the DME service volumes. DME ground station transmitters are typically specified at either 1,000W or 100W. An output power of 1,000W is generally used to support the High Altitude (H), Low Altitude (L), DME Low (DL) and DME High (DH) service volumes. The reduced high altitude requirement of the DL service volume provides additional flexibility in making channel assignments for supporting DME/DME RNAV network coverage. An output power of 100W is typically used to support Terminal (T) service volumes and is generally sufficient to support Standard Instrument Approach Procedures. The DME ground stations also employ signal processing techniques such as echo suppression to improve the signal accuracy of the replies.

- c. DME Service Volumes.** DME service volumes are defined by the cylindrical volume of airspace where the DME signal is expected to be received by an aircraft from a particular DME. There are five defined service volumes for DMEs in the NAS, three defined Standard Service Volumes (SSVs), and two defined DME/DME RNAV SSVs.

The three SSVs are:

1. Terminal (T) (Figure 3-1)
2. Low Altitude (L) (Figure 3-2)
3. High Altitude (H) (Figure 3-2)

The two DME/DME RNAV SSVs are:

1. DME Low (DL) (Figure 3-3)
2. DME High (DH) (Figure 3-3)

Most SSVs are serviced by 1000W transmitters, with the exception of the T class DME SSV which is usually serviced by a 100W transmitter. A detailed description of these service volumes can be found in Table 3-1.

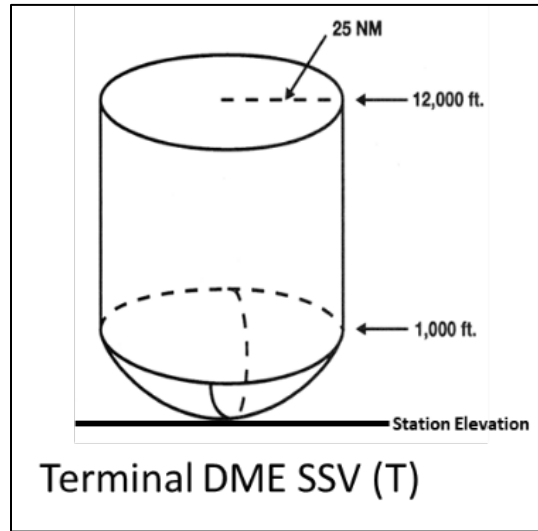


Figure 3-1. Terminal DME SSV

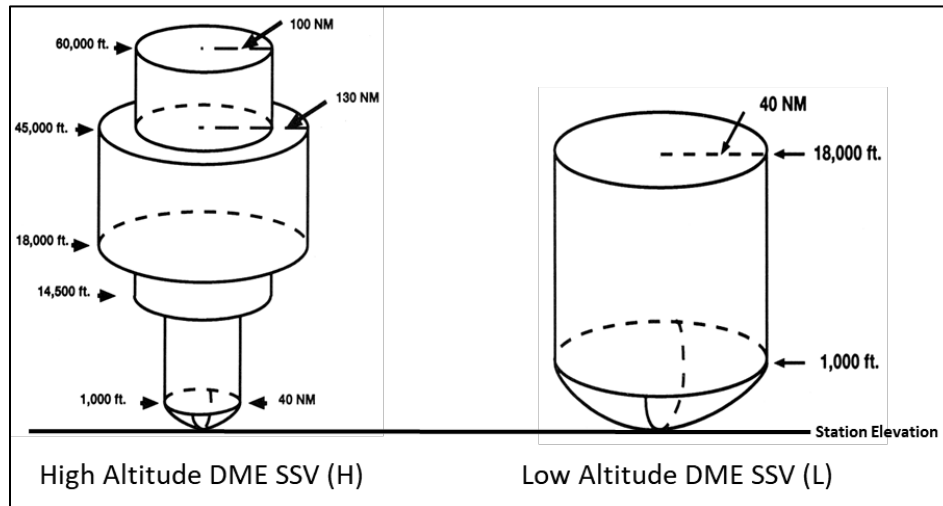


Figure 3-2. High Altitude (H) and Low Altitude (L) DME SSVs

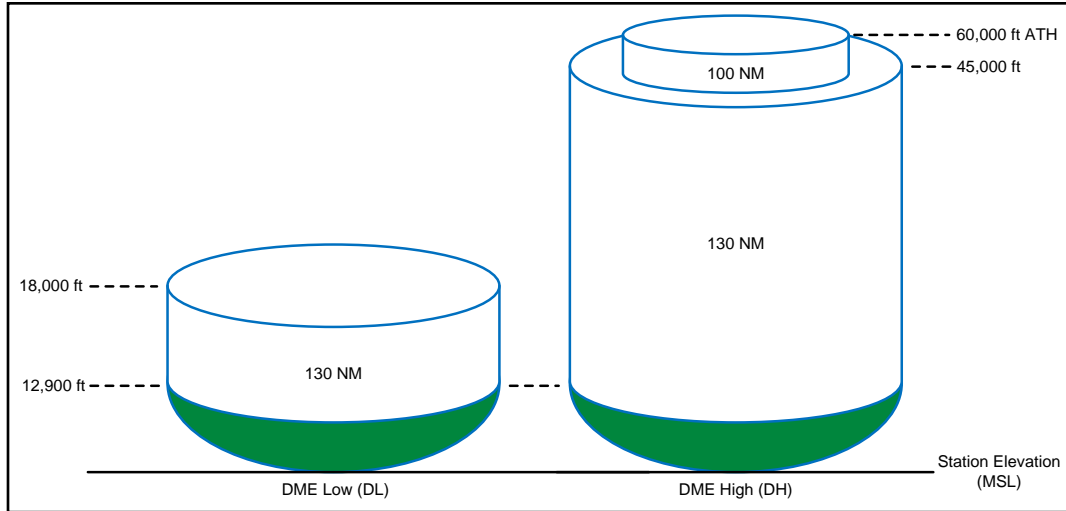


Figure 3-3. DME Low (DL) and DME High (DH) Service Volumes

Table 3-1. Summary of DME Service Volumes

Service Volume Designator	Altitude and Range Boundaries
T (Terminal)	From 1,000 feet AGL up to and including 12,000 feet AGL at radial distances out to 25 nmi.
L (Low Altitude)	From 1,000 feet AGL up to and including 18,000 feet AGL at radial distances out to 40 nmi.
H (High Altitude)	From 1,000 feet AGL up to and including 14,500 feet AGL at radial distances out to 40 nmi. From 14,500 feet AGL up to and including 60,000 feet AGL at radial distances out to 100 nmi. From 18,000 feet AGL up to and including 45,000 feet AGL at radial distances out to 130 nmi.
DL (DME Low)	From 1,000 feet AGL up to and including 18,000 feet AGL at radial distances out to 130 nmi.
DH (DME High)	From 1,000 feet AGL up to and including 45,000 feet AGL at radial distances out to 130 nmi. From 45,000 feet AGL up to and including 60,000 feet AGL at radial distances out to 100 nmi.

3. DME Signal Characteristics of Interest

This section introduces the DME signal characteristics of interest. The material includes definitions of terms such as signal strength and ranging accuracy, as well as the parameters that can affect them. Discussions of these parameters and their effects are presented in subsequent sections of this chapter.

- a. **Signal Strength Factors.** The discussion above established that signal coverage is directly tied to signal strength. Insufficient signal strength can also affect accuracy performance in the real world, primarily in terms of susceptibility to noise effects and

RF interference. The equipment design, the associated installation and configuration practices, and the environment surrounding the transmitter/receiver antenna all influence the signal strength required or achieved within the service volume.

The relevant equipment design characteristics include ground station receiver sensitivity, decoder performance, pulse shape attributes, transmitter output power, and three-dimensional antenna gain properties. Signal attenuation due to cable (type and length) and connector losses is the primary concern when it comes to the equipment installation and configuration process. These factors are addressed during the equipment design and installation procedure approval process, and thus they are not of concern to the siting engineer. Signal attenuation due to cable (type and length) and connector losses affect the transmitted power incident at the ground station antenna and only need to be considered by the siting engineer when the proposed site includes a large distance between the ground equipment and the antenna.

Lastly, signal strength can be affected by the environment surrounding the ground station antenna. Environmental or site-specific factors include Line-of-Sight (LOS) blockage issues, which occur when the direct or visible path between the antenna and a reception point is blocked by a structure, hill, or wooded area. Equipment must therefore be located such that it provides for sufficient LOS clearance over or around objects in the vicinity of the ground station antenna.

Figure 3-4 shows a hypothetical LOS blockage situation. If the direct line between the antenna and the receiver passes through the structure, as shown with the red line, then it is assumed that there is a LOS blockage. If, however, there is enough clearance over or around the structure, as shown with the green line, then it is presumed that the LOS is not blocked. In the practical sense, the effective blockage is determined by how much of the first Fresnel Zone around the LOS line falls on the structure. This concept is discussed further in Section 4 of this chapter.

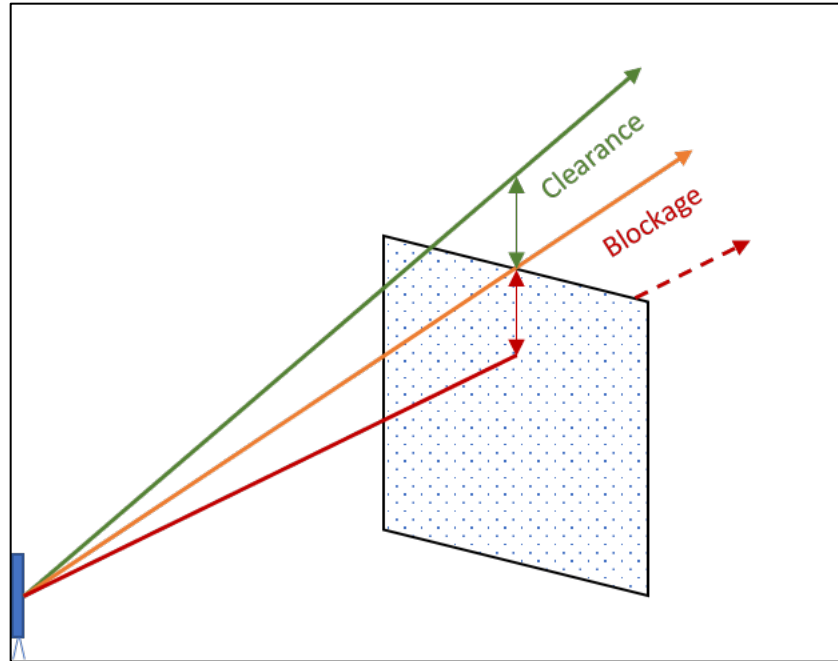


Figure 3-4. A Hypothetical LOS Blockage Scenario

Aside from signal blockage, signal scattering (reflections and diffractions) from the terrain can also result in signal nulling and fading, which can adversely affect signal strength.

- b. Ranging Accuracy Factors.** DME equipment design errors and limitations are factors that can adversely affect ranging accuracy. Specifically, equipment intrinsic errors in the signal transmission and receiver processing can induce ranging errors. However, it is assumed that the ground and airborne equipment have already been properly designed and qualified according to DME equipment requirements (per FAA-E-2996, RTCA DO-189, and TSO-C66) such that the contribution of DME equipment to ranging error is within acceptable limits.

Ranging accuracy can also be affected by environmental or site-specific factors that cause signal blockage (as discussed above), multipath, or both. As shown in Figure 3-5, the signal radiated by the DME antenna can also be reradiated (or “scattered”) by objects in the environment including buildings, trees, and mountains. Because these scattered signals traverse different signal paths to the receiver, they are commonly referred to as “multipath.” Multipath can cause DME signal pulse-shape deformations, which can translate to ranging error during DME receiver processing. Multipath can be categorized as longitudinal, lateral, or a combination of the two.

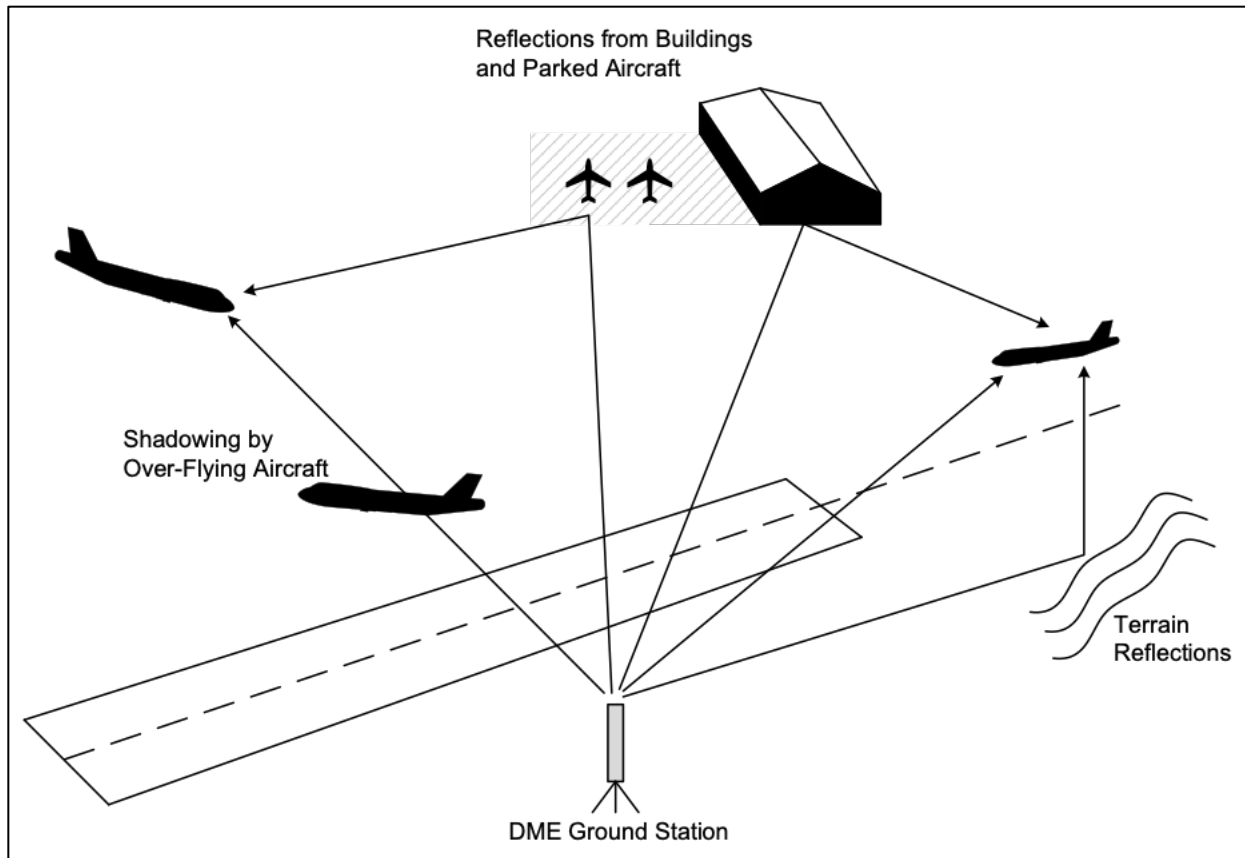


Figure 3-5. Illustration of DME Multipath Sources

Parameters that affect ranging accuracy are as follows:

1. **Multipath-to-Direct (M/D) Signal Ratio:** The ratio between the magnitude of the multipath signal and the magnitude of the direct signal.
2. **Relative Time Delay (τ):** The difference between the Time of Arrival (TOA) of the multipath signal relative to the TOA of the direct path signal.
3. **Relative Phase:** The phase of the multipath signal relative to the phase of the direct signal.
4. **Motion Averaging:** The reduction in the magnitude of both sinusoidal-like and noise-like multipath induced errors caused by the motion of an aircraft when flying through a multipath interference region.
5. **TOA Technique:** The measurement method used to determine the TOA of a detected DME pulse (i.e., pulse envelope). The interrogator uses this arrival time to determine the range from the transponder, whereas the transponder uses TOA to initiate the reply delay timing function.

4. DME System Performance

The application of the siting criteria presented herein is intended to identify an antenna site that satisfies all the siting criteria presented in this order. The first step in finding such a site is to identify a location that will enable adequate SIS performance in terms of coverage and accuracy. Only when it has been determined that a candidate site enables such performance to be achieved within the required service volume should compliance with the remaining criteria be pursued.

Enabling adequate SIS performance in terms of coverage and accuracy is achieved by finding locations where the site-specific environmental effects (aka multipath) will be sufficiently controlled. In developing this Order, analyses were performed to characterize the effect on SIS performance due to multipath caused by objects near the DME ground station antenna. These characterizations were used to generate general guidance criteria that is denoted as the Object Consideration Area (OCA), which is shown in Figure 3-6.

It should be noted that the OCA consists of the following two components: 1) a near-field protection cylinder surrounding the DME antenna that was established to protect the near-field radiation pattern of the ground station antenna; and 2) a conical sloped surface that is defined by a vertical 1° subtending angle that extends upward from the base of the DME antenna. All objects should be below this surface to control the effects of multipath and shadowing within the DME service volume. In some cases, it may not be possible to identify such a site at the designated facility location, and it becomes necessary to consider sites that result in an object or objects being located within the OCA. In this case, the effect on signal strength and ranging accuracy caused by multipath from each object must be evaluated.

Additional guidance on application of these criteria is provided below in Section 5 of this chapter, as well as Chapter 5.

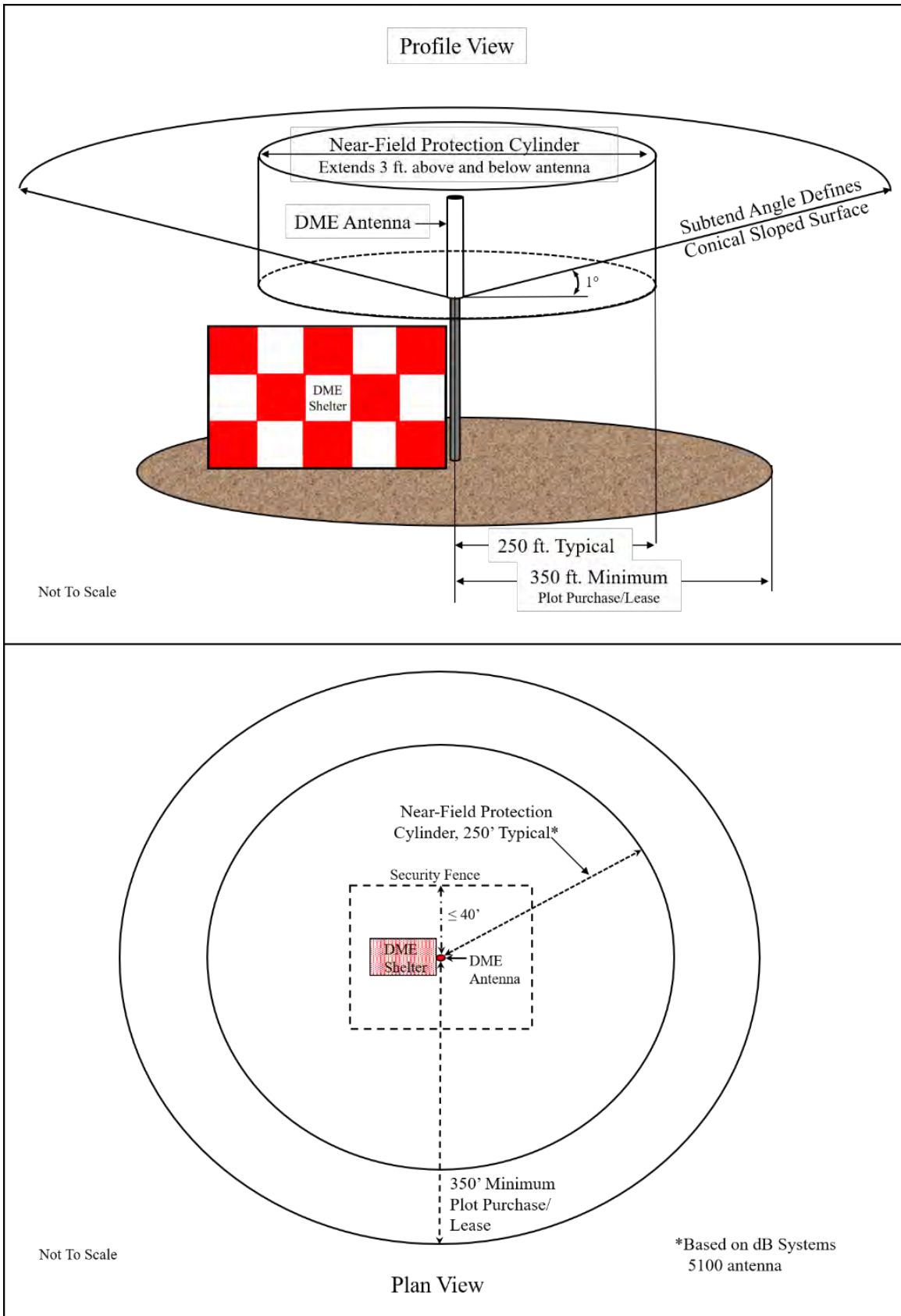


Figure 3-6. DME Object Consideration Area (OCA)

The balance of this section discusses the factors that influence DME system performance from a SIS perspective. First, signal attenuation due to either blockage of the LOS signal path by objects in the environment (aka shadowing) or fading effects caused by multipath are discussed in Section 4.a. Second, discussions in Section 4.a focus on characterizing the effects multipath can have on ranging accuracy. In each section, methods for estimating the magnitude of the impact are presented.

- a. Signal Strength.** The signal radiated by the DME ground station should meet minimum signal strength requirements to the greatest extent possible within the applicable service volume, which will normally be one of the volumes shown in Figure 3-1. Service volumes are used when assigning the transmit frequency for a facility to ensure frequency protection from co-channel and adjacent channel interference and that the DME interrogator (i.e., the airborne avionics) can receive and properly process ground station replies to interrogations.

The primary factor addressed during the site selection process is the control of multipath effects by the proper application of siting criteria. The effects of longitudinal multipath (Figure 4-5) on signal strength are primarily controlled by the DME antenna design. Information regarding DME antenna performance is provided in Chapter 4 and Appendix D. The effects of signal blockage (Figure 3-4) and lateral multipath (Figure 4-6) are controlled by selecting a suitable antenna site.

- i. Evaluating Signal Attenuation Due to Blockage/Shadowing.** Three terms must be defined before discussing signal attenuation due to blockage and shadowing:
 - 1. **LOS:** the geometrical straight-line path between a transmitter and receiver antenna.
 - 2. **Fresnel Zone:** the locus of points surrounding the LOS path where the path length difference from the transmitter to receiver antenna is an integer multiple of the half-wavelength compared to the direct LOS path.
 - 3. **LOS Region:** the three-dimensional region defined by the first Fresnel Zone surrounding the LOS between the transmitter antenna and the receiver antenna where most of the radiated power is concentrated.

In order to ensure that sufficient signal strength exists at a given receiver location, the LOS region must be free of objects. When an object or structure exists within or penetrates this region, the potential for excessive signal attenuation within the service volume should be evaluated. This section describes a qualitative method for performing such an evaluation based on the amount of LOS region obstruction caused by an object.

Analysis of the diffraction gain for an obstruction within the LOS region has shown that the strength of the signal received is a function of the obstruction size, its proximity to the LOS path, and the size of the Fresnel Zone at the obstruction

location. The amount of obstruction caused depends on both the dimensions of the object and its orientation with respect to the direct LOS path. For example, a rectangular object having a width and depth each of 10 feet can create an obstruction zone 14 feet wide when the vertical faces of such an object are oriented 45° to the LOS path.

The diagram in Figure 3-7 depicts the normalized electric field received as a function of the Fresnel-Kirchhoff Parameter (FKP) for the case of normal incidence edge diffraction (aka knife edge diffraction) of the DME signal by an infinite half plane (see Figure 3-8). Because the analysis considers a normalized electric field, the trace shown in Figure 3-7 can be interpreted as diffraction gain, where a value of less than one denotes attenuation of the received signal compared to that received for the unobstructed case. Likewise, a value greater than one signifies amplification of the signal.

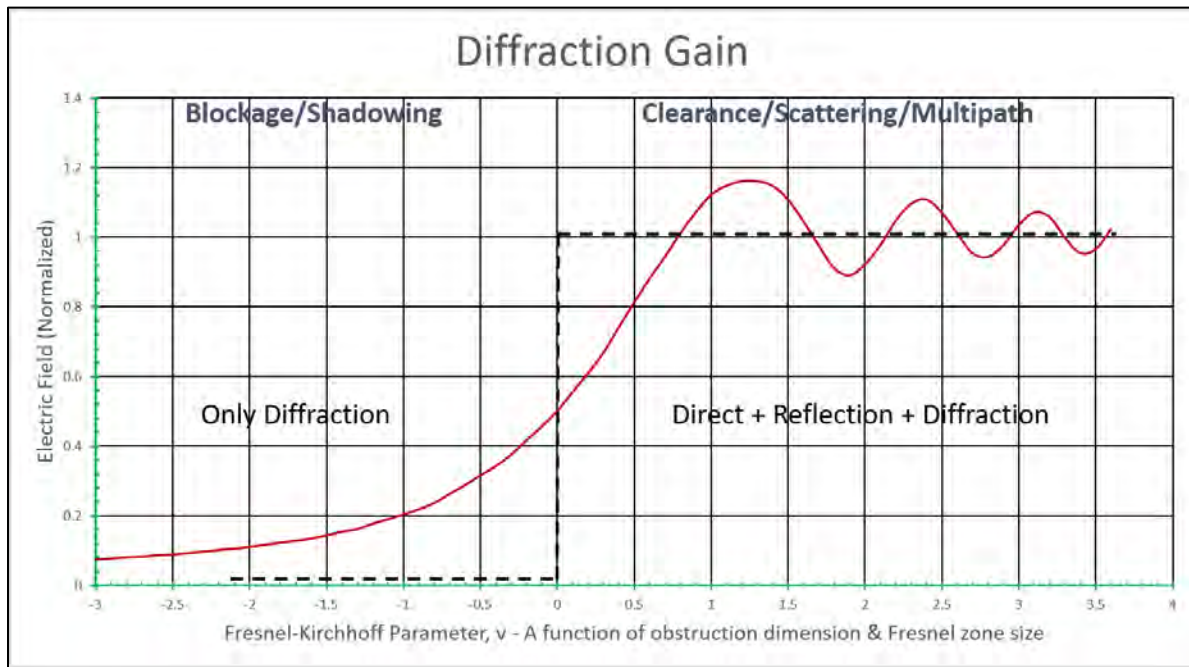


Figure 3-7. Diffraction Gain

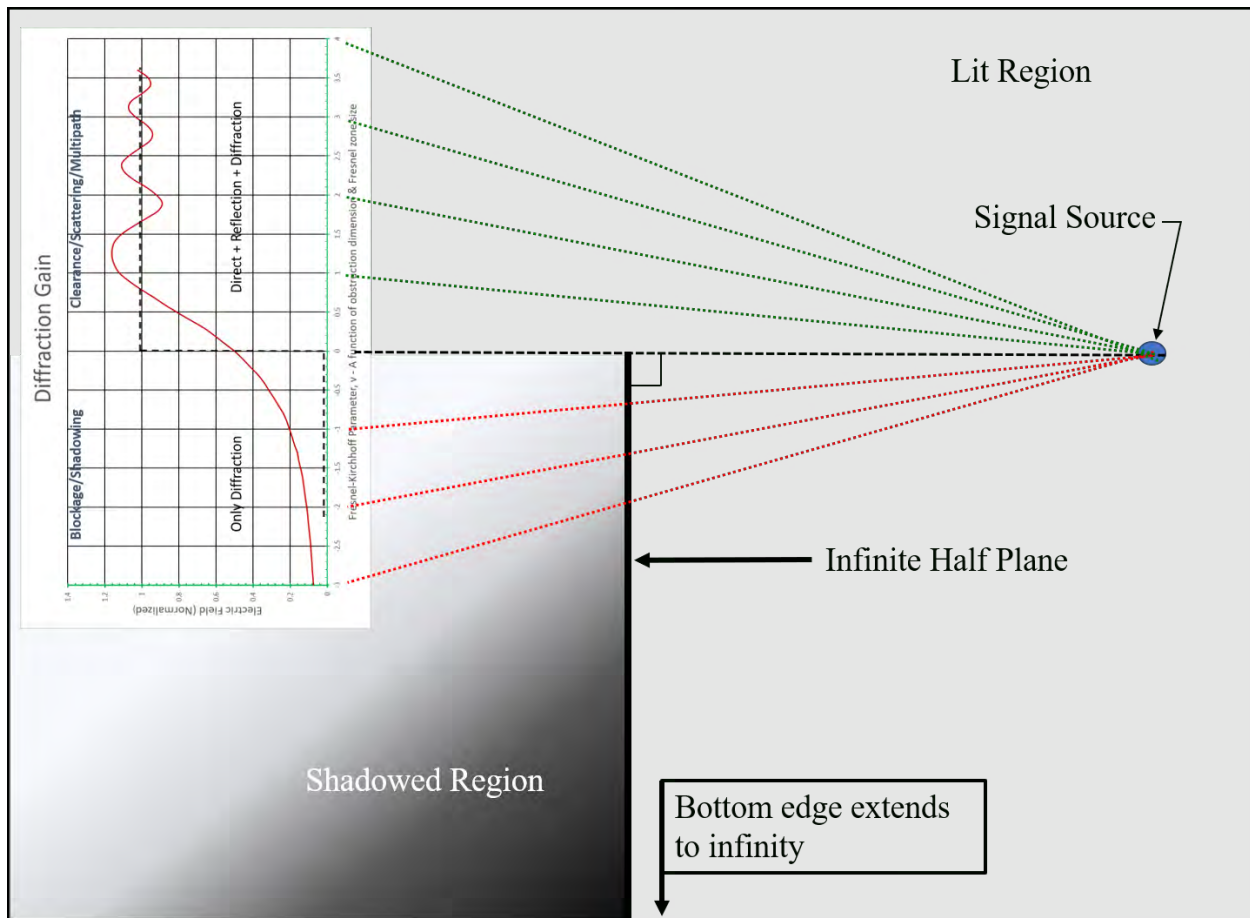


Figure 3-8. Knife Edge Diffraction Geometry

The FKP is a function of the Fresnel Zone size and the amount of clearance between the LOS path and the closest edge of the obstruction. That is, the portion of the obstruction that penetrates the Fresnel Zone around the LOS path to the reception point determines the amount of signal attenuation or amplification that results. The “Blockage/Shadowing” area shown in Figure 3-7 is the area where most of the Fresnel Zone is penetrated by the object, including blockage of the geometrical LOS between the transmitter and receiver antennas. In this case, significant obstruction of the LOS region occurs, which results in shadowing (i.e., significant signal attenuation) because only the diffracted field is received at the reception point. In the “Clearance/Scattering/Multipath” area, the amount of obstruction clearance determines the magnitude of the total field that is received at the obstruction point. Again, the amount of signal attenuation or amplification is in comparison to the unobstructed case.

Initially, signal strength behavior as the LOS region transitions from the full signal blockage case to the full signal clearance case is discussed. That is, the FKP transitions from minus one to plus one, respectively. The discussion then progresses to analyzing the signal strength behavior during a level-run flight profile that passes behind a rectangular shadowing object. Initially, the height of the profile is well below the top edge of this object, which results in the aircraft passing through the deeply shadowed region caused by

a structure. This portion of the analysis focuses on characterizing the effect on signal strength as a function of the horizontal location of the aircraft relative to the shadowed region. The next portion of the analysis characterizes the effect on signal strength as a function of the vertical location of the level run flight profile relative to the top of the rectangular shadowing object. Both characterizations are done in terms of the diffraction gain curve of Figure 3-7. Finally, the two one-dimensional analyses are combined to formulate a rudimentary approach that can be used to make qualitative assessments when performing a site survey, which in its simplest form is shown in Figure 3-9.

As illustrated in Figure 3-9, the volume of space in which signal strength may be adversely affected by a shadowing structure can quickly be identified by adding a shadowing silhouette around the structure and performing ray tracing as shown. The idea to be conveyed is that once LOS clears the shadowing object by at least one Fresnel Zone radii, the full signal clearance condition occurs and the signal strength approaches that of the unobstructed case as depicted in Figure 3-6. This approach provides a basic analysis of the shadowing caused by the structure.

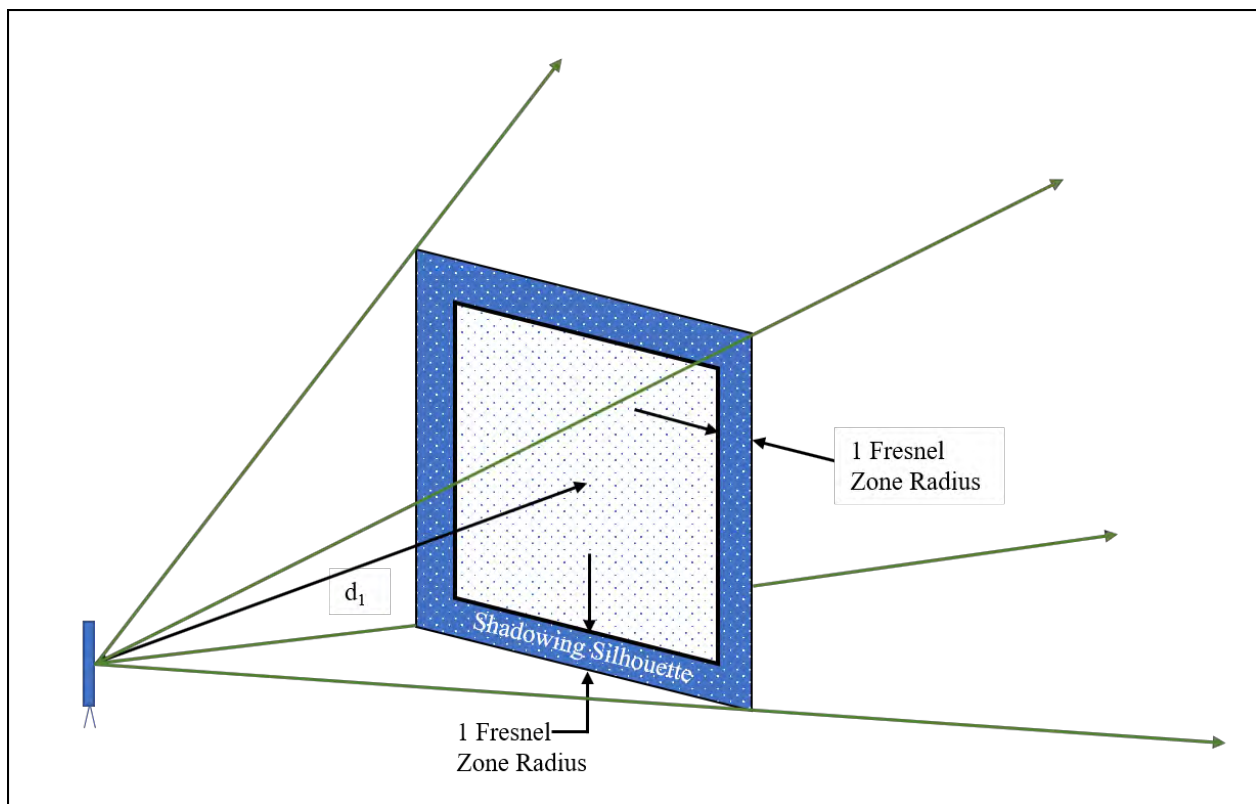


Figure 3-9. Shadowing Silhouette Used When Performing Ray Tracing

- ii. **Evaluating Signal Attenuation Due to Fading.** As previously stated, meeting the coverage requirement throughout the service requires the DME design to incorporate characteristics that provide resistance to, or sufficient control of, signal fading caused by multipath effects. Similarly, it was noted that multipath can be categorized as longitudinal, lateral, or a combination of the two.

- (a) **Longitudinal Multipath:** The scattering geometry that causes longitudinal multipath is illustrated in Figure 4-5 which depicts signal reflection from the ground as an ever-present source of longitudinal multipath. An antenna counterpoise, or center-pivot irrigation equipment located radially from the DME facility antenna are other examples of multipath objects that can cause longitudinal multipath.

A straight-level-run flight test maneuver (i.e., a level run), or simulated flight path towards or away from a ground-based transmitting antenna, can be used for collecting signal strength data that enable the assessment of signal coverage. For example, the level run profile illustrated in Figure 3-10 can be used to produce signal strength plots like that shown in Figure 3-11. The signal reflected from the ground will interact with the direct signal to cause fading (i.e., attenuation) and/or amplification. The relative phase between the direct and reflected signal (i.e., multipath) determines if attenuation or amplification occurs, and this phase is a function of the geometry between the transmitter antenna, scatterer, and receiver antenna. Because the aircraft is in motion, the relative phase is constantly changing and the signal strength will cycle through maximums and minimums as shown in Figure 3-12.

The required vertical pattern characteristics for approved DME antennas provide resistance to, or sufficient control of, signal fading caused by multipath effects for typical ground plane situations and antenna heights. Therefore, a signal fading analysis to determine the effects of ground reflection on signal strength is not required in such cases. Atypical situations may require analysis, either via manual calculations or computer modeling. A full analysis of ground reflection effects is documented in “Development of Ground Reflection Multipath Allocations for Supporting a DME Link Budget Analysis”, Ohio University, May 2020 (Reference Z).

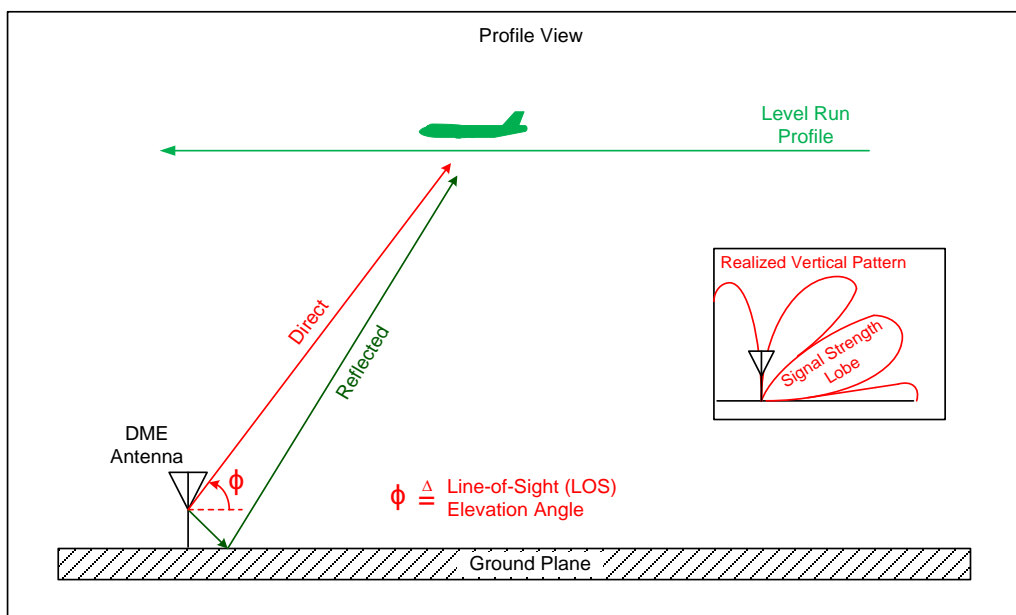


Figure 3-10. Level Run Flight Measurement Profile

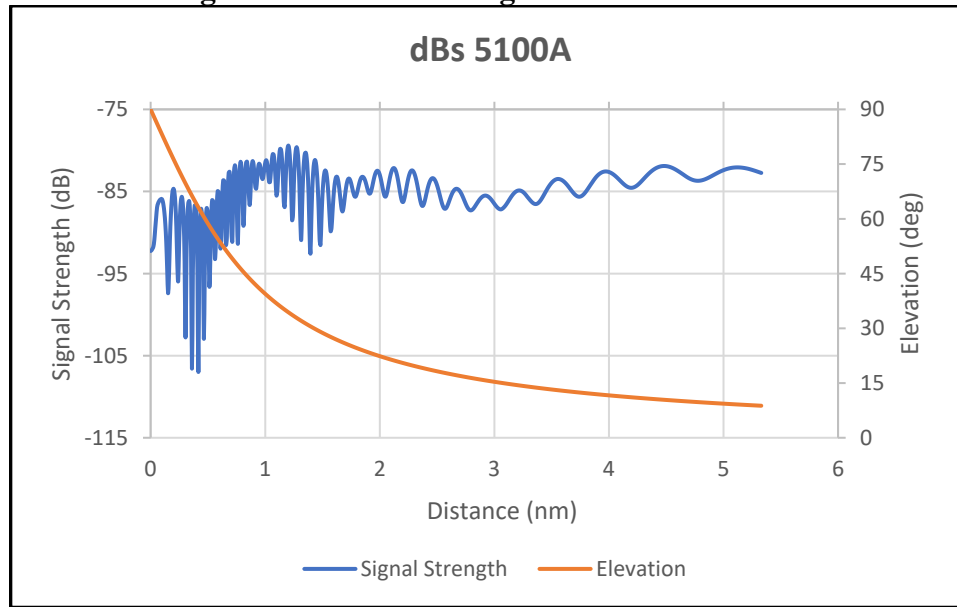


Figure 3-11. Example Fading Data Produced by Level-run Flight Measurement Profile

- (b) **Lateral Multipath:** Multipath from structures in the vicinity of the DME antenna can also cause signal fading. Again, multipath from such structures can be categorized as longitudinal, lateral, or a combination of the two, which primarily affects where the multipath will be projected into the service volume. The important distinction of this situation compared to that of the ground reflection case is that the dimensions of the structure are finite, unlike that of the ground plane (i.e., Earth surface) the antenna is mounted above. Among other properties, the size of a reflecting surface greatly influences the strength of the multipath, which in turn determines the depth of fading that may occur. The dimensions of a structure also influence the location and size of the multipath region produced. While ray tracing can be used to define the geometrical boundaries of a multipath region, additional analysis is required to evaluate the depth of signal fading (i.e., signal attenuation) that may occur within a given multipath region.

One such analysis method is developed using two different approaches as described in Appendix C. The first approach examines the relationship between signal attenuation in a shadowed region and the strength of the signal reflected into the corresponding multipath and diffraction regions. Assuming that this structure does not absorb that energy (or absorbs very little of it), conservation of energy is applied to determine (or approximate) the strength of the reflected signal within the multipath region. That is, areas of strong signal attenuation in the shadowed region have a corresponding area of strong multipath reflections in the opposite direction. Likewise, areas of minimal or no attenuation have corresponding areas of minimal or essentially zero diffracted signal energy. To identify the signal fading regions in this case, the source antenna location is used in combination with Snell's Law of Reflection and ray tracing. This approach should be sufficient to enable one to

perform qualitative analysis of fading effects.

The Physical Optics technique used for calculating radiation through an electrically large aperture can be applied for calculating the multipath and diffracted signal levels as shown in Figure 3-12. While the numerical calculations required are not trivial, the application of this technique to the case of signal reflection provides an intuitive understanding of signal reflection behavior. To apply this technique to the case of signal reflection by a rectangular object, the multipath object is replaced by its complementary aperture, and image theory is applied to determine the location of the source, which is shown as a “DME Image Antenna” in the figure. Strong multipath signals are present in the area where a direct LOS path exists from the image antenna to the reception point, and this area is denoted as the “Multipath Reflection Region” in the figure. Outside this region, the multipath signal present is due to energy diffracted by the aperture edges. The magnitude of this signal falls off as a function of Fresnel Zone radii much like that for the knife edge diffraction case. To identify the signal fading regions in this case, the image antenna location is used in combination with the complementary rectangular aperture plus ray tracing.

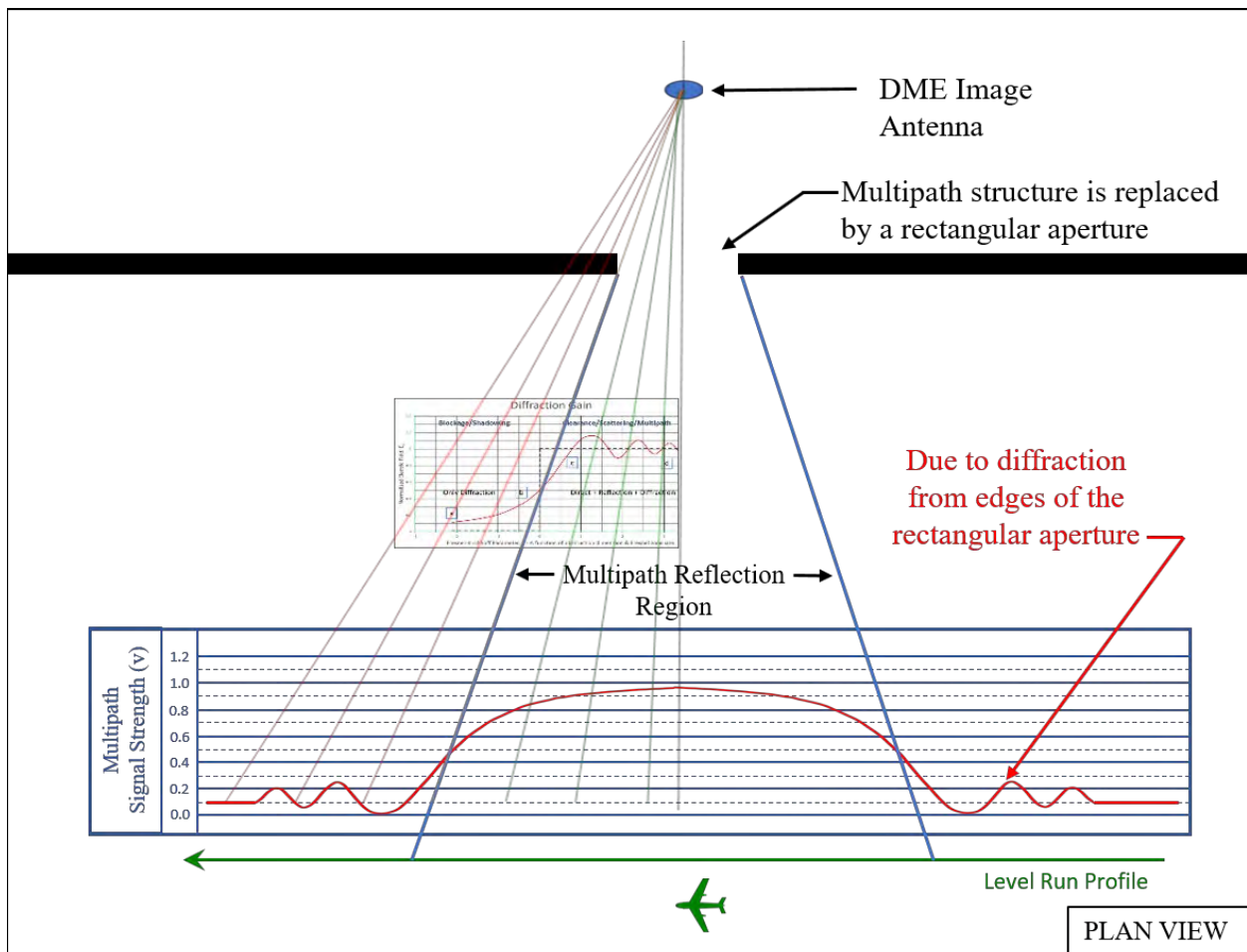


Figure 3-12. Radiation Through an Electrically Large Rectangular Aperture

As done for the case of shadowing by a rectangular object, the two one-dimensional analyses for each approach are separately combined to formulate two rudimentary approaches. These approaches can be used to make qualitative signal fading assessments when performing a site survey, which in their simplest form are shown in Figure 3-9. As illustrated in this figure, the volume of space in which signal strength may be affected by fading caused by a multipath structure can quickly be identified by adding a diffraction silhouette around the structure and performing ray tracing as shown in Figure 3-13. The idea to be conveyed is that once LOS clears the shadowing object by at least one Fresnel Zone radii, the diffracted signal strength is about 14 decibel (dB) below the direct signal and at this point fading effects will become minimal. These two approaches provide a basic analysis of the fading caused by the structure.

Also, the analysis will also identify the volume of space where ranging errors may exceed desired levels or even be out-of-tolerance, depending on the dimensions of the structure. Conversely, outside of this volume of space, the magnitude of the multipath signals diffracted from structure edges is expected to be at least 14 dB below the direct signal (i.e., M/D ratio \leq -14 dB). As discussed further in Section 4.b.iv, the magnitude of the resulting ranging errors are expected to be on the order of 100 feet (see Figure 3-20 and Figure 3-21) in most cases.

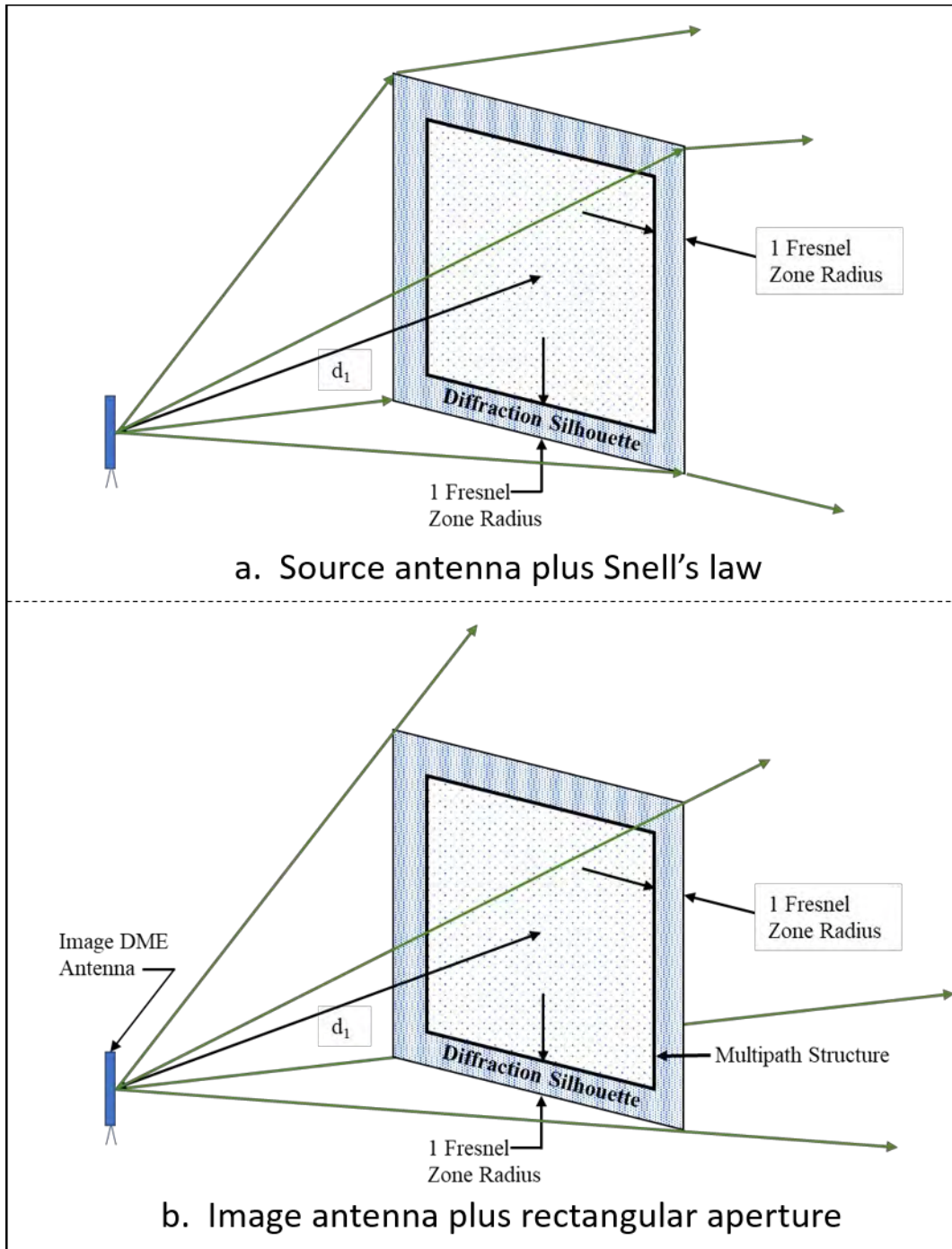


Figure 3-13. Diffraction Silhouette Used When Performing Ray Tracing

- a. **Evaluating ranging error due to multipath.** This section characterizes multipath and how it affects the SIS. The discussion includes information about how the SIS is processed to make a TOA determination, how this processing influences multipath error magnitudes, and multipath arrival zones. The section closes with an example multipath analysis.

- i. **Overview.** This section starts with a discussion of TOA signal processing and how multipath affects the TOA measurement. A foundational discussion follows regarding how multipath can deform the shape of the pulse used by the DME receiver for the TOA measurements and how this deformation results in ranging error. Plots of worst-case error magnitudes as a function of M/D ratio, relative phase, and relative time delay are presented. These plots are then analyzed to define relative time-delay bounds that describe early and late multipath arrival zones about the direct-signal pulse used for the TOA measurement (i.e., the TOA measurement pulse). Multipath arriving within these zones has the potential to generate measurable ranging errors, including errors with magnitudes large enough to impair operational performance in some cases.

- ii. **TOA Processing and Multipath.** It is important to understand how the DME SIS is processed and how multipath is analyzed. In the absence of multipath interference, the DME pulse-pairs arrive at the reception point without deformation. When a multipath-free signal is processed as illustrated in Appendix C, Figure C-23, the half amplitude find function processing that is used for the TOA determination (DME/N) outputs waveforms as shown in Figure 3-12(A). This represents the processed DME signal in the SIS domain. When multipath interference is present, the DME pulse-pairs could arrive at the reception point with or without deformation. When this signal is processed as illustrated in Figure C-23, the half amplitude find function processing that is used for the TOA determination (DME/N) outputs waveforms as shown in Figure 3-14(A). As with Figure 3-14(A), this represents the processed signal in the SIS domain. It should be noted that Figure 3-14(A) and Figure 3-14(B) appear similar and in the SIS domain the receiver cannot de-construct the composite pulse into the direct and multipath signal components. Therefore, when the impact of multipath effects on the DME signal is analyzed, it is necessary to do so in the Multipath Analysis Domain. In this domain, the direct and multipath components are combined to produce the composite signal, which is then analyzed to determine the resulting range error.

Figure 3-14(D) shows how the composite pulse is made up of the direct pulse (dotted-line) and the multipath pulse (red-line). By examining how the direct and multipath signals combine to form the resultant composite pulses in the Multipath Analysis Domain, a better understanding of how multipath can impact the DME signals is gained. Therefore, the Multipath Analysis Domain will be used in this chapter to illustrate multipath effects on the DME signal. Figure 3-14(D) further shows the half-amplitude points of the Direct and Composite Pulses (T_d Direct, T_d Composite) and therefore how the multipath can affect the TOA. The way the multipath pulse affects the direct pulse (pulse deformation) as well as its impact on the TOA is discussed next.

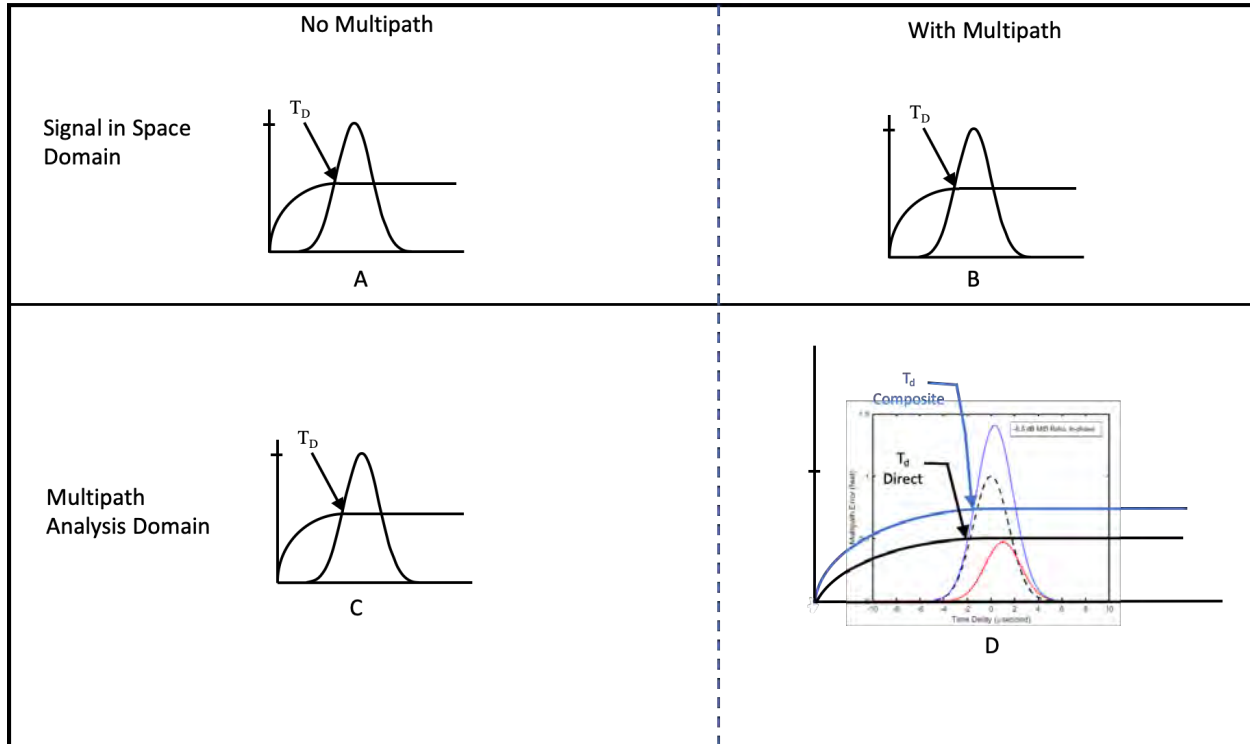


Figure 3-14. TOA Processing With and Without Multipath

- iii. **Pulse Deformation Fundamentals.** This section examines when and how a multipath pulse affects the shape of the composite pulse that is used for making the TOA determination. The concept presented is applicable whether the first pulse or second pulse of the pair is used for the range measurement. This independence is achieved because the multipath pulse parameters (i.e., amplitude, phase, and arrival time) are defined relative to the direct pulse that is used for the measurement. That is, they are defined by an M/D signal ratio, relative time delay (τ), and relative phase as previously discussed.

Multipath pulses may be a result of direct pulses that are reflected from objects as small as an outdoor equipment enclosure, or as large as a mountain range. Because they initially propagate to an intermediate location, they travel a longer propagation path from the transmitter to the receiver antenna than the corresponding direct pulses. Regardless of their amplitude or relative phase, the multipath pulses will not interfere with the direct pulses unless the multipath path pulse arrives at the receiver antenna while the direct pulse is also being received; this interference condition is depicted in Figure 3-15 below. The discussion that follows validates this condition and provides the background necessary for quantifying the range of time-delay values that constitute a “same time” arrival.

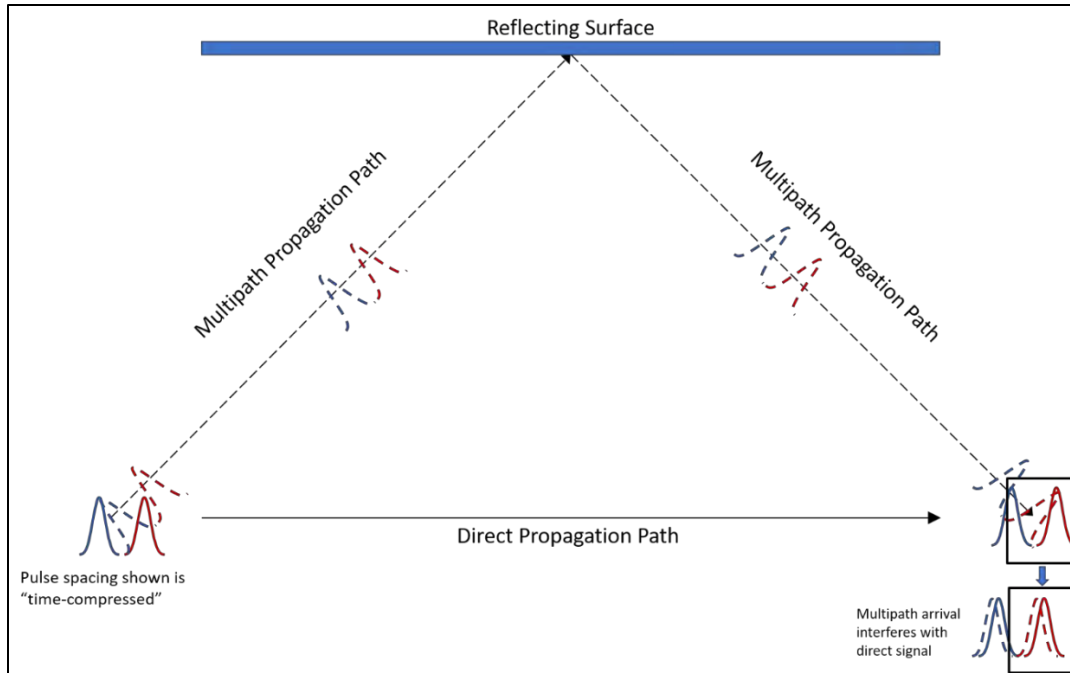


Figure 3-15. Multipath Pulses From Same Reply Cycle Arriving Slightly Later Than Direct Pulses

Figure 3-16 illustrates the manner in which the multipath scenario of Figure 3-15 results in a deformed pulse in the Multipath Analysis Domain. This scenario results from the simplest multipath case, which is when the multipath of the same interrogation or reply cycle arrives slightly later than the direct signal. The deformed pulse in this case results from the in-phase multipath combining with the direct signal to form the composite signal, which has a different TOA point than the direct signal. The way in which deformed pulses are formed is examined later in this section.

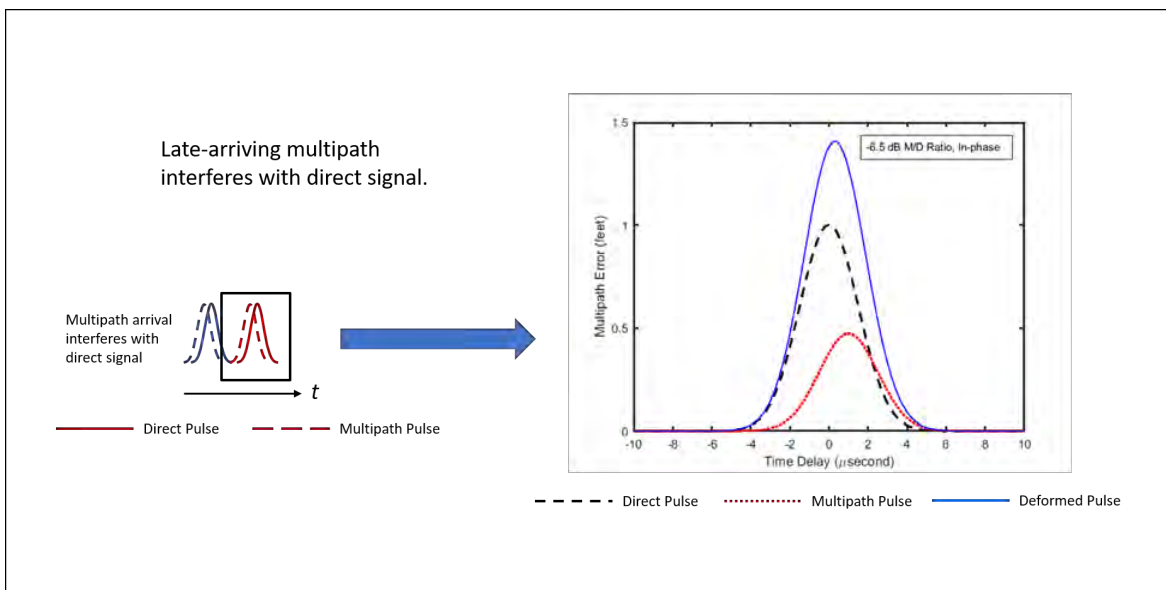


Figure 3-16. Example of Pulse Deformation for Late-arrival Multipath

As previously discussed, the half-voltage point of the leading edge of the timing pulse is used for TOA determination for DME/N. The pulse used for making the TOA determination has changed over time as previously discussed in Section 4.b.ii with early generation equipment using the second pulse of the pair while modern designs use the first pulse. In either case, the way in which the composite timing pulse is deformed can change the TOA location, thus inducing ranging error due to multipath. Next, it is necessary to examine how the multipath pulse can deform a direct pulse.

Figure 3-17 depicts a multipath pulse and a direct pulse. In this scenario the time delay between the two pulses is large enough that the multipath pulse does not deform the direct pulse. This is because the multipath pulse in the area to the right of point B does not have sufficient energy to deform the direct pulse enough to affect the location of the TOA point. This same situation is true for the area to the left of point A, which will become relevant as the discussion progresses. Because the TOA location is unchanged, this case does not induce any ranging error. In layman terms, this “no effect on ranging” condition holds true for two cases: either the multipath pulse arrives “too early”, or it arrives “too late” in time relative to the direct pulse. That is, they are two distinct pulses as far as the receiver is concerned.

While this condition may not pose a problem for range measurement, it can still cause performance problems. Specifically, the pulse decoder in the receiver may reject the unaffected direct pulse due to a pulse spacing issue when the amplitude of the multipath path pulse is close (≈ 1 dB) to that of the direct. If this condition persists long enough, it can cause a receiver unlock condition, which causes the ranging service to become unavailable until the condition ceases.

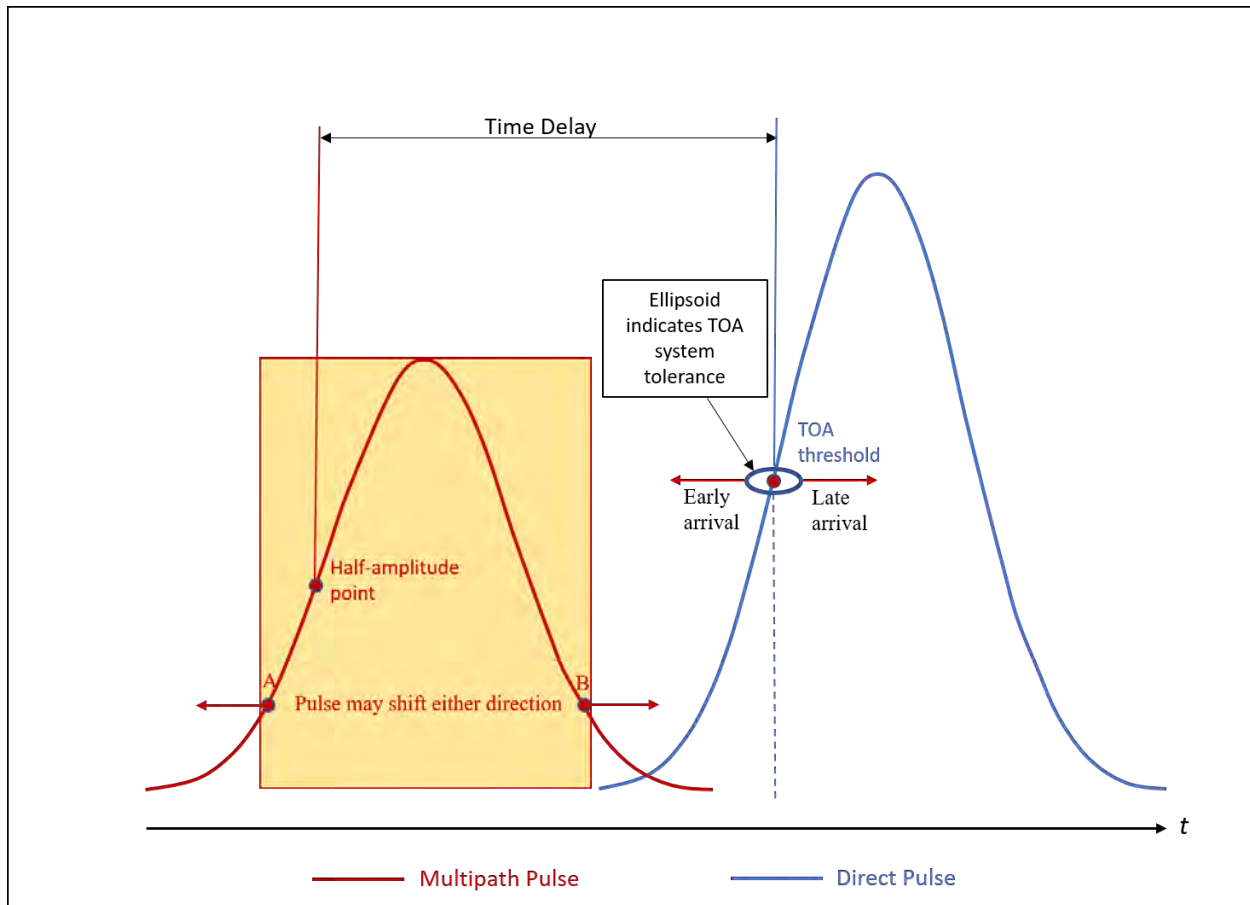


Figure 3-17. Multipath Pulse and Direct Pulse Parameters

The next step is to illustrate how the TOA location shifts when the multipath pulse overlays the direct pulse. As discussed above, the magnitude of the multipath pulse can add to (in-phase condition) or subtract from (out-of-phase condition) the magnitude of the direct pulse. In either case, the result may be a deformed composite pulse, meaning deformed in the sense that the TOA location is shifted from that of the direct pulse only location. The in-phase condition where the multipath pulse adds to the magnitude of the direct pulse is illustrated in Figure 3-16. The out-of-phase condition, where the magnitude of the multipath pulse is subtracted from the direct pulse, is addressed in the following section.

The analysis illustrating the shift in the TOA location is conducted in the Multipath Analysis Domain by moving the multipath pulse shown in Figure 3-17 from left to right while the direct pulse stays fixed. Figure 3-18 illustrates this progression by showing three cases as the multipath pulse moves from left to right. Figure 3-18(A) depicts the multipath arriving earlier than the direct pulse. In this case, the time delay is such that the two pulses combine to create a deformed composite pulse having a TOA location noticeably shifted from that of the direct pulse. When part of the multipath pulse inside the yellow box shown in Figure 3-18(A) begins to combine with the direct pulse, the magnitude of the multipath pulse adds to the magnitude of the direct pulse, resulting in a deformed pulse. Furthermore, it should

be noted that the yellow box shown in Figure 3-18(A) identifies the portion of the multipath pulse that has an amplitude large enough to generate a deformed composite pulse when it is added to the direct pulse. The exact location of points A and B on the multipath pulse depends on the M/D ratio and relative phase, which is explored further in the subsections that follow.

The red and blue vertical lines at the top of Figure 3-18(A) run through the half-amplitude (half-voltage) points of the deformed composite pulse and the direct pulse, respectively. These lines illustrate that the deformed composite pulse has a TOA that is shifted to the left compared with the direct pulse, which induces range error because the TOA has changed. It is important to note that the TOA will be out-of-tolerance if its location falls outside of the ellipsoid boundary (as shown at the top in Figure 3-18(A)).

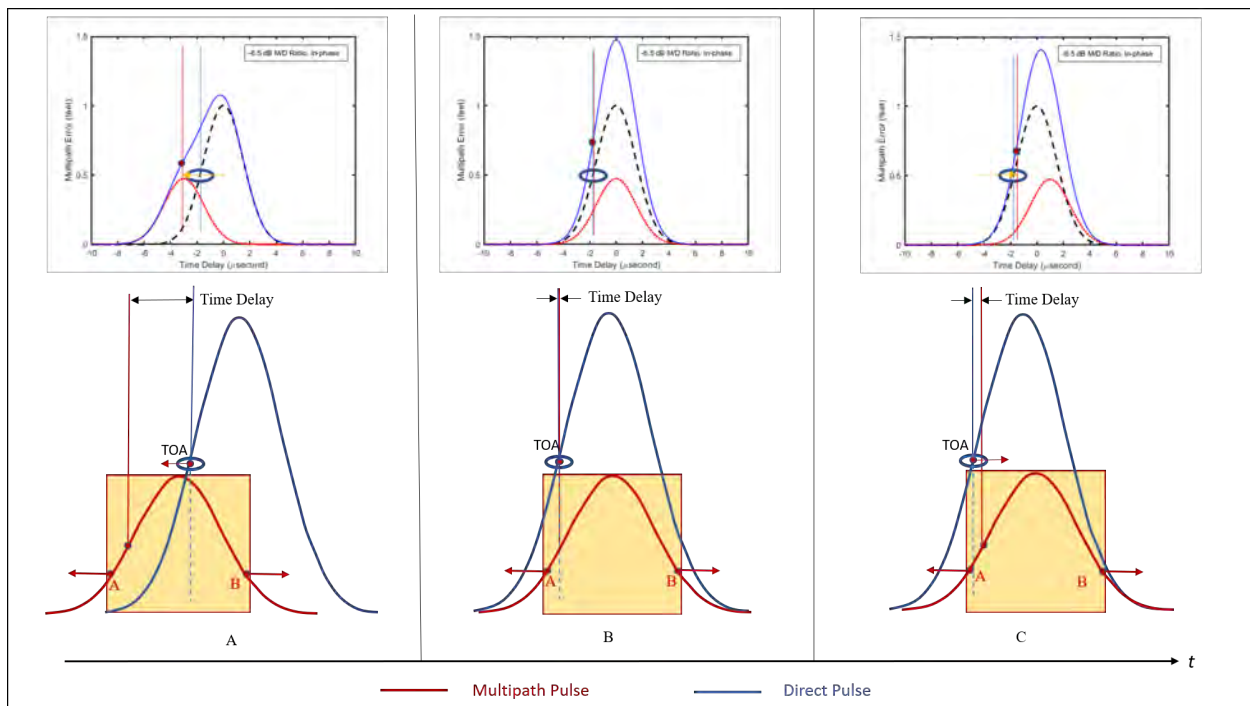


Figure 3-18. Multipath Pulse Influence on Direct Pulse Time-of-Arrival Threshold

As the multipath pulse continues to move to the right, it gets to a point where the multipath pulse completely overlays the direct pulse. This situation is shown in Figure 3-18(B). The magnitude of the multipath pulse adds to the magnitude of the direct pulse, again creating a composite pulse. As previously explained, the red and blue vertical lines shown at the top of Figure 3-18(B) run through the half-amplitude (half-voltage) points of the composite pulse and the direct pulse, respectively. These lines illustrate that, in this case, the composite pulse has a TOA that is same as the direct pulse, which results in zero range error. That is, no deformation occurred in terms of a range error being introduced, and the effect in this case is analogous to amplification of the direct pulse. For the out-of-phase case, the effect is analogous to attenuation of the direct pulse. It is important to note that when the time delay is zero, a multipath pulse does not cause a range error to occur.

As the multipath pulse continues to move to the right, it gets to a point where the multipath arrives later than the direct pulse, and the time delay is just enough for the two pulses to continue to combine. As with Figure 3-18(A), part of the multipath pulse inside the yellow box shown in Figure 3-18(A) is still combining with the direct pulse. The magnitude of the multipath pulse adds to the magnitude of the direct pulse, resulting in a deformed composite pulse. The red and blue vertical lines shown at the top of Figure 3-18(C) run through the half-amplitude (half-voltage) points of the composite/deformed pulse and the direct pulse, respectively. These lines illustrate that this deformed composite pulse has a TOA that is shifted to the right as compared with the direct pulse, which induces range error.

Based on the preceding discussion, three multipath arrival zones about the direct pulse have been developed, and these zones are classified as “early”, “late-short”, and “late-long” as illustrated in Figure 3-19. Time delay is the parameter that determines if a multipath pulse will arrive within one of these three zones. Multipath that has an “early” time delay will distort the portion of the pulse used to estimate the TOA and therefore has the potential to result in significant range error. Multipath categorized as “late-short” results in a deformed pulse, but with less range error than an “early” pulse. The “long-delay” multipath does not cause ranging errors, since it does not distort the portion of the direct-signal pulse that is processed to estimate the pulse TOA. The above characterization assumes that the magnitude of the direct pulse is larger than that of the multipath pulse.

The magnitude of the range error is a function of the M/D ratio, the TOA of the multipath relative to the direct signal (time-delay), the phase of the multipath signal relative to the direct, and the multipath scalloping frequency resulting from receiver motion in the dynamic case.

While the discussion to this point focused on describing the conditions where multipath may cause ranging error, the presence of multipath can also cause a receiver unlock condition as previously noted. The DME receiver is required to validate each pulse-pair by confirming that the pulse width and spacing fall within prescribed tolerances. Multipath having an amplitude very similar to that of the direct pulse, but arriving outside the arrival zones discussed above, can cause pulse spacing violations. Similarly, multipath arriving within these zones may cause pulse width violations, even when arriving within the “late-long” arrival zone. If any of these conditions, or a combination thereof, persists long enough, it can cause a receiver unlock condition, which causes the ranging service to become unavailable until the condition ceases.

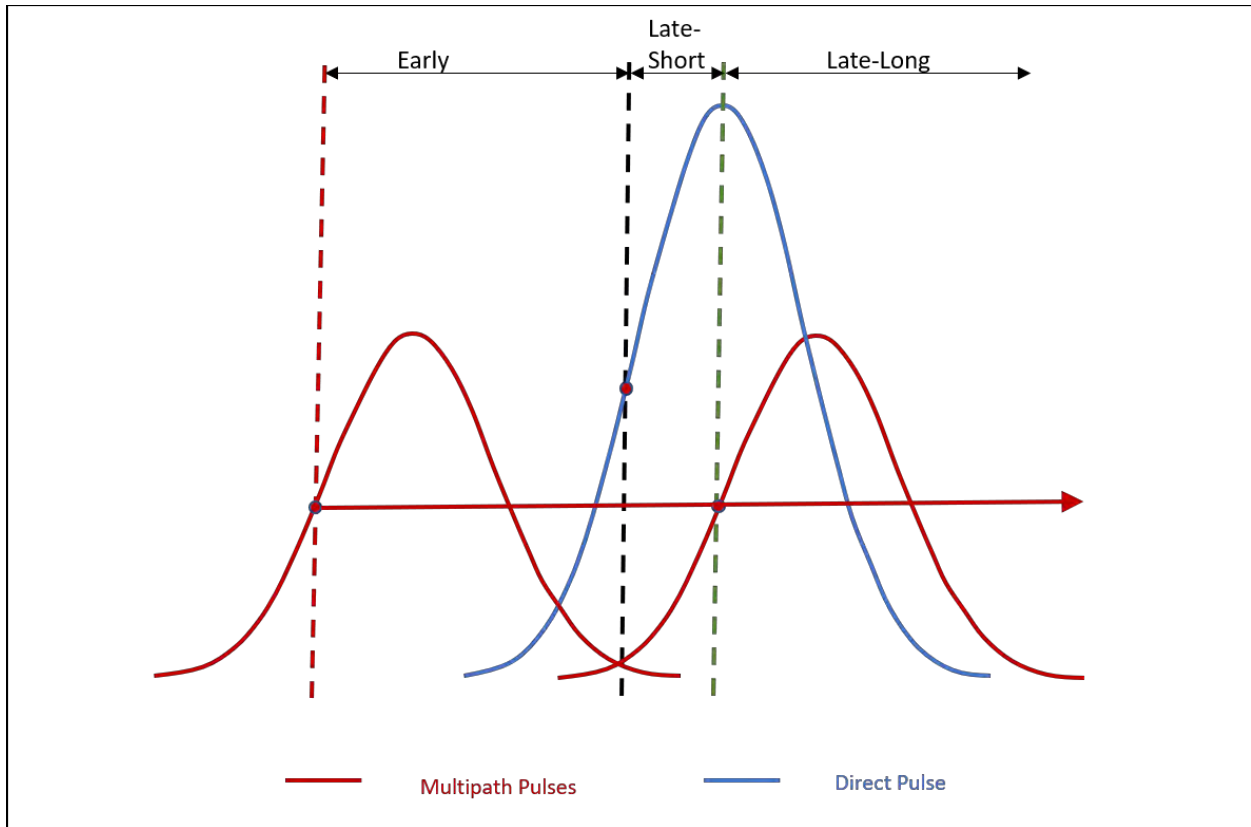


Figure 3-19. Early and Late Multipath Pulse to Direct Pulse Timing Regions

- iv. **Characterization of Multipath Error Magnitudes.** A worst-case analysis was performed to characterize ranging error magnitudes as a function of M/D ratio and time delay. The results of this analysis are presented in Figure 3-20 and Figure 3-21, which show the multipath range error (aka multipath error) resulting from deformed pulses for both in-phase and out-of-phase conditions. The M/D ratios in these figures vary from -6.5 dB to -20 dB.

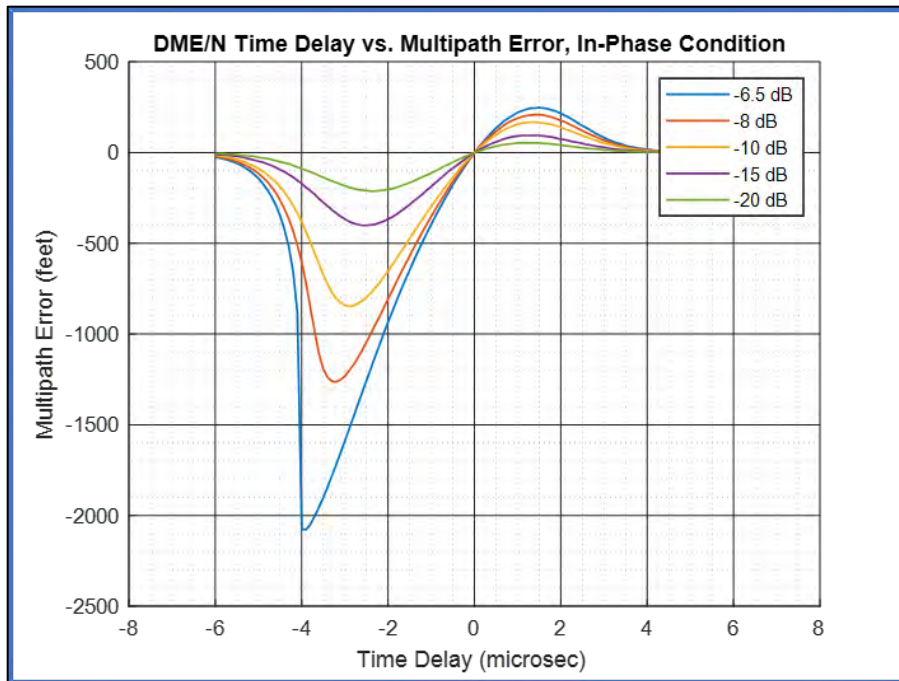


Figure 3-20. DME/N Error vs. Relative τ -delay, M/D ratio, In-phase Case

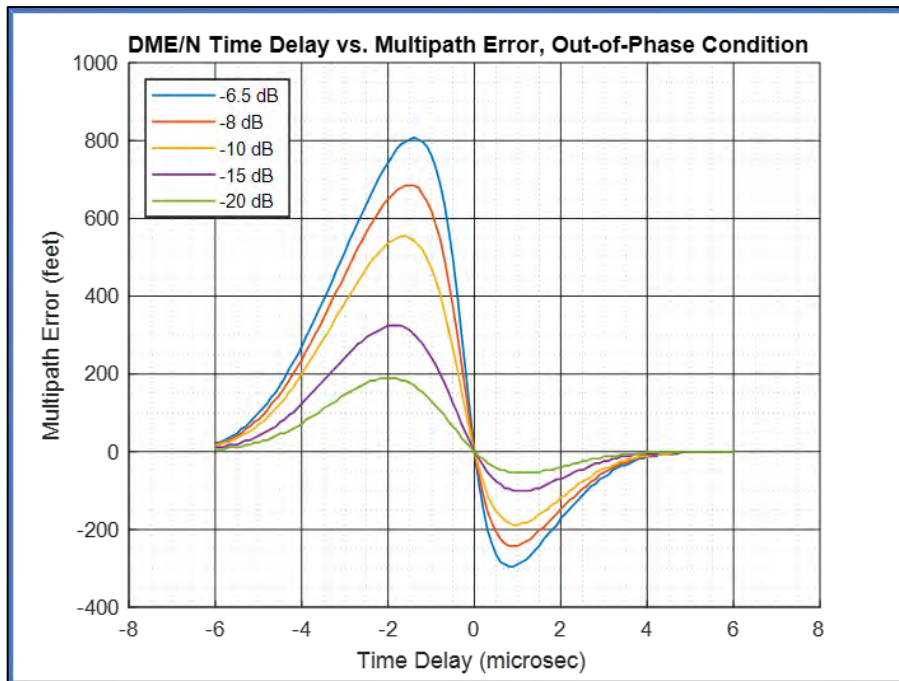


Figure 3-21. DME/N Error vs. Relative τ -delay, M/D ratio, Out-of-phase Case

It is important to note that Figure 3-20 and Figure 3-21 illustrate curves with a range of M/D ratios from -20 dB to -6.5 dB for analytical purposes. Paragraph 2.2.14.a in RTCA DO-189 states: "...the interrogator shall operate normally, including decoding and ranging accuracy in the presence of echo or multipath conditions where the reflected signal level is not greater than -10 dB with respect to the desired

signal.” Thus, when the results of a fading or error analysis yield a M/D ratio greater than -10 dB, it should be realized that this situation is likely problematic from a performance perspective. In this case, further action may be required to mitigate the impact and the action required will depend on the particulars of the situation (i.e., consider a different antenna location, change in new construction plan, et cetera).

- v. **Defining Multipath Arrival Zone.** A worst-case analysis was performed to quantify the time-delay values that define the multipath arrival zones shown qualitatively in Figure 3-17. These values are a function of M/D ratio, relative phase, and the error threshold used to define what constitutes a “measurable” range error. The M/D ratios and relative phase conditions used to generate Figure 3-20 and Figure 3-21 were also used for this analysis, and an error threshold of 50 feet was adopted.

The results are summarized in Figure 3-22. Depending on the M/D ratio, the multipath pulse can affect the thresholding point of the direct pulse when arriving as early as 5.6 μ s before the direct pulse arrival, or as late as 3.3 μ s after the direct pulse arrival. Larger M/D ratios result in wider arrival zones.

Given that the requirement to use the first pulse of the pair for TOA determination was adopted on January 1, 1989 (Reference DD), the primary concern for DME site selection purposes is the Late-Short Arrival Zone for ranging error considerations. Particularly, the case when an object is present in the DME OCA, large enough in size to generate multipath with M/D ratios greater than -20 dB, and the portion of the multipath region having time-delay values falling within the Late-Short Arrival Zone is operationally significant. It is important to be mindful of cases where the M/D ratio exceeds -10 dB because multipath arriving in the Late-Long Arrival Zone can cause receiver unlock conditions to occur as previously discussed.

The Early Arrival Zone shown in Figure 3-22 is included for completeness. Given the DME system design concept, this arrival zone is only relevant when second pulse timing is used. In this case, TOA determination is susceptible to range measurement errors due to the effects of multipath from first pulse echoes on the second pulse of the pair. This situation is not a factor considered during the site selection process given that more than 30 years have passed since the use of first pulse timing became the requirement.

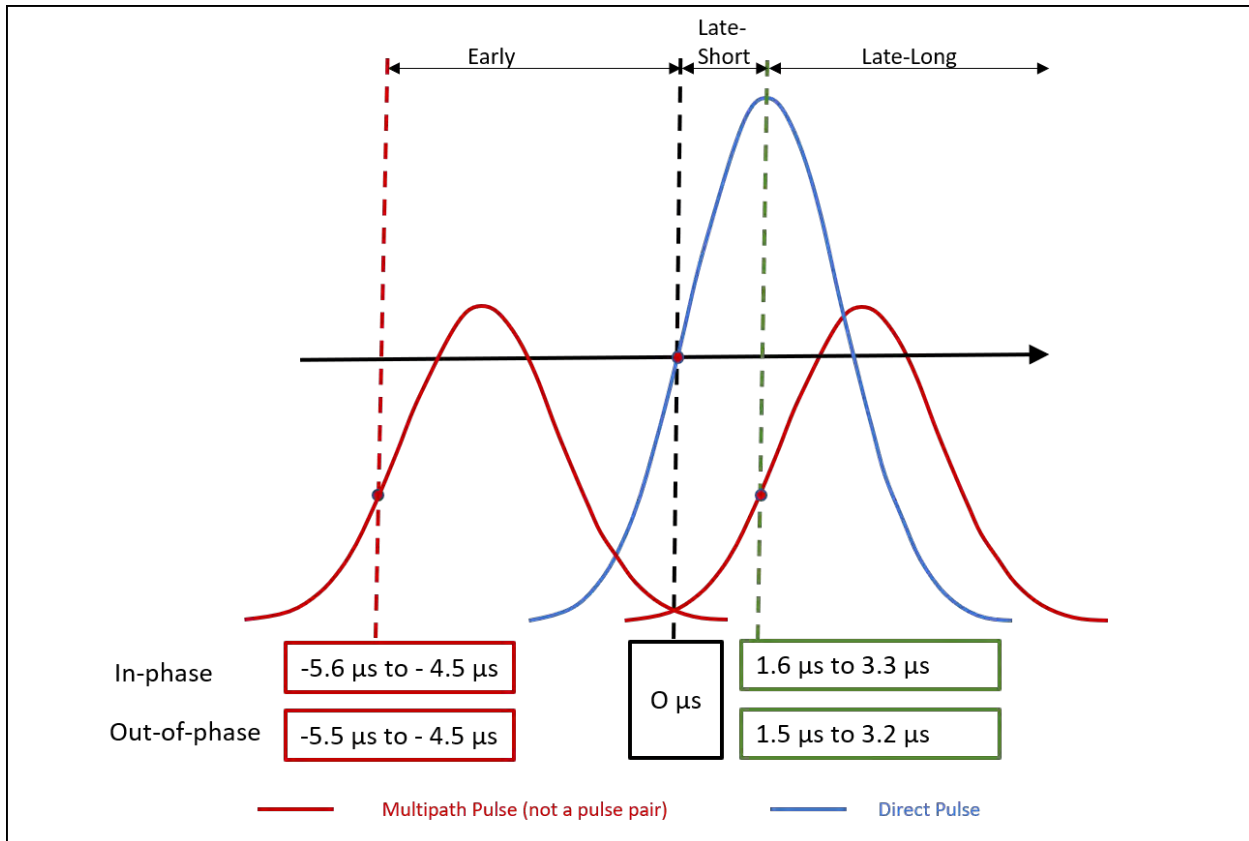


Figure 3-22. Early and Late Arrival Zone Summary for -6.5 dB and -20 dB M/D Ratios

- c. **Site Testing Using Mobile DME.** Mobile DME systems are also available. These systems can be utilized by siting engineers to provide a facility/signal to be used at a proposed site or to provide an interfering signal to test an operational installation. When used as a proposed facility/signal the mobile unit can be modified (physical position or operational parameter) to directly assess the effect of the modification on the DME SIS for a proposed site. The mobile unit can also be used as a potential interference source to assess operational site irregularities. A fully operational mobile DME can be deployed quickly and can be utilized to verify if a particular DME siting location will provide an acceptable DME SIS. Once operational, FAA flight check can be utilized to evaluate the SIS and determine if it is within the evaluation tolerances.

5. DME Performance Considerations

This section discusses DME performance considerations related to the OCA, antenna types, antenna performance, signal blockage and shadowing, multipath, and resonant structures.

- a. **Object Consideration Area (OCA).** The DME OCA (see Figure 3-6) is the area centered about the DME antenna where, ideally, all objects and structures are removed. A cylindrical volume surrounding the DME antenna has been established to protect the near-field radiation pattern of the DME antenna since objects within this area can alter the antenna's radiation pattern. The electromagnetic properties of the radiated signal are more complex in the near-field compared to those in the far-field, and consequently, the analysis of signal scattering by objects in the near-field is a complex undertaking.

Therefore, the near-field should be free of all objects, except for the DME equipment shelter, antenna, and security fence.

Also, a subtending angle of 1.0° extending upward from the base of the DME antenna is used to define a conical, sloped surface. All objects should be below this surface to control the effects of multipath and shadowing within the DME service volume. If the removal of all objects is not practical, then any objects located within the OCA should have their possible impact evaluated to determine the objects' effect on the DME SIS. Additional information regarding the OCA and its application is provided in Section 3 of Chapter 5.

- b. Antenna Types.** This section gives an overview of antennas that are available for use in the NAS. A review of antenna terminology as well as additional performance information on the antennas listed below can be found in Chapter 4 and Appendix D.
- i. **Standard Antenna(s).** The standard antenna type deployed within the NAS is the omni-directional antenna. Examples of this type of antenna are the dBs Model 5100A and the dBs Model 510A. The omni-directional horizontal pattern and achieved gain (≥ 8 dBi) of these antenna models, as well as other FAA-approved antenna models, makes them capable of providing adequate signal coverage throughout the DME service volumes shown in Figure 3-1. Therefore, these models are well suited for supporting terminal and en route DME flight operations. The vertical pattern of these antenna models typically have a beamwidth of greater than 5.0° and a nominal beam tilt (area of maximum radiated energy) between 2.0° and 5.0° above the horizon.. These characteristics, combined with other vertical pattern performance requirements, provide resistance to signal fading caused by ground reflections.
 - ii. **Special Purpose Antenna(s).** Special purpose antennas are available for deployment within the NAS when unique siting conditions exist. Uni-directional and bi-directional antennas each utilize unique horizontal patterns. The bi-directional antenna pattern has two primary lobes of energy in the horizontal plane, whereas the uni-directional has just one primary lobe. These antennas can be used for terminal and en route DME applications and can be used to provide maximum DME signal coverage in special/unique situations. These antennas are similar to the omni-directional antenna mentioned above in the sense that the vertical pattern of this antenna has a nominal beam tilt (area of maximum radiated energy) between 2.0° and 5.0° above the horizon.

Antennas with a higher vertical beam tilt are also available as a solution when unique siting conditions exist. This type of antenna is typically utilized in instances where additional radiation tilt is needed to minimize ground reflections (multipath). An example of this antenna is the dBs 5100A/7 $^\circ$.

High performance antennas that provide increased gain and vertical pattern shaping are available for siting conditions that require improved fading control. An example

of this antenna is the ultra-high gain dBs 540.

c. Antenna Performance

- i. **Antenna Height.** Both the free-space vertical pattern characteristics and the height of the antenna above the ground affect the realized vertical pattern of an installed antenna. The height determines the number of nulls or minima that are introduced into the pattern. The region between two nulls is commonly referred to as a (signal strength) lobe. The number of lobes introduced into the vertical pattern is proportional to antenna height, so with increased height, more lobes are generated. Additional information on how antenna height affects performance can be found in Chapter 4 and Chapter 5.
- ii. **Fading.** As previously discussed, fading results when multipath signals arrive at the receiver antenna out-of-phase with the DME direct signal. This situation ultimately reduces the signal strength and therefore signal coverage may be adversely impacted. The parameters that affect fading are: surface conditions, such as water or soil; surface roughness height; and the phase relationship of the multipath signal to the direct signal (i.e., the relative phase).

Signal reflection from the ground below the DME antenna is an ever-present source of longitudinal multipath. Therefore, meeting the coverage requirement throughout the service requires the DME antenna design to incorporate characteristics that provide resistance to, or sufficient control of, signal fading caused by such multipath effects. Performance considerations relevant to providing resistance to, or sufficient control of, signal fading caused by multipath effects include: sufficient vertical pattern slope in the vicinity of the horizon; relatively low-level below horizon sidelobes; and relatively high-level above the horizon sidelobes (i.e., shoulders). The required vertical pattern characteristics for FAA-approved DME antennas provide sufficient control of signal fading for typical antenna heights and ground plane situations.

Fading effects may be more pronounced for situations where the DME antenna is mounted over a smooth ground plane, such as when a large sector of water surrounds the antenna. Conversely, fading effects will be diminished when installing the antenna over a rough ground plane, such as furrowed earth or a corrugated surface. The presence of dense vegetation on the ground plane may cause the signal reflected from the ground to be more diffuse in nature, and thus fading effects will be less prominent than fading for the typical ground plane situation. It should be realized that the presence of such vegetation may be a seasonal or temporary situation.

The presence of trees may result in a situation where the signal reflected from the ground is blocked by the tree line while the direct signal from the antenna is unobstructed because the treetops are just below the subtending angle. In this case, fading due to ground reflections may be mitigated, or substantively reduced, in the

portion of the service volume where shadowing of the reflected signal occurs. The magnitude of the reduction can depend on the types of trees, the size of the wooded area, and the density of the trees within this area; the reduction may also be a seasonal or temporary situation.

The presence of a tilted, sloped, or a slowly undulating ground plane typically affects the location of the maxima and minima of the fading pattern compared to the level ground case. A ground plane is considered slowly undulating when the length of the swells and troughs are many Fresnel Zones wide.

Additional information on fading and how fading affects SIS performance can be found in Chapter 4.

- d. Signal Blockage and Shadowing.** Signal blockage (aka shadowing) occurs when the LOS region between the DME ground station antenna and the reception point is blocked by a stationary or moving object. A stationary object can be a permanent object or a moving object that has temporarily stopped.

Examples of permanent objects include equipment enclosures and shelters; antenna or antenna arrays; towers; buildings and hangars; above ground storage tanks; trees and vegetation; and hilly or mountainous terrain. These objects must be clear of the OCA, meaning outside of the near-field cylindrical volume and below the conical surface defined by the subtending angle (see Figure 3-6). Objects located within this area should have their impact evaluated through data analysis, or math modeling, or both, to determine the shadowing effect each object has on the DME SIS.

Examples of moving objects include vehicles and aircraft; mobile irrigation systems; construction, agricultural, snow removal, and landscape equipment; and construction cranes. Moving objects should keep clear of the near-field cylinder when in motion and clear of the OCA when parked or stationary. Otherwise, their impact must be evaluated through data analysis, or math modeling, or both, to determine the shadowing effect each object has on the DME SIS.

When an evaluation is required, it should determine and consider the amount of signal attenuation expected to occur within the shadowed region. The portion of the shadowed region where the amount of attenuation poses a threat to achieving the minimum signal strength requirement should be identified and noted. A conservative approach is to assume that this threat exists whenever a full signal blockage condition exists, see Appendix C, Figure C-28.

The duration of time that the receiver is likely to be exposed to this condition should be evaluated as well. While the volume of space shadowed by an object must be determined and considered, the shape of the volume influences the duration of time that the DME receiver is likely to be subjected to reduced signal strength. This exposure time determines if the effects of passing through a shadowing region will be observable in the receiver output or cause an unlock condition. For example, consider a shadowed

region to be a tunnel in the sky. When the tunnel is long and narrow, it is less likely that any particular flight path will align with the tunnel for a given amount of time (i.e., receiver coast period) compared to the case when the tunnel is long and wide.

In the end, the nature of the impact is determined by considering the amount of signal attenuation expected to occur; the location of the shadowed region within the service volume; the duration of time that the receiver may be exposed to an inadequate signal level condition; the impact to conventional procedures to be supported by the facility; and the effect of coverage gaps on the DME/DME RNAV network performance. In some cases, the outcome of such an evaluation may indicate that the identification of a more suitable antenna location should be pursued because the impact to flight operations is undesirable.

Note: The DME RNAV Service Map (DRSM) can be applied to assess the effect of coverage gaps on DME/DME RNAV network performance. See Site Selection, Project Engineering and Facility Establishment for additional information on the DRSM.

Additional information regarding the effect of signal shadowing on system performance can be found in Chapter 5 and Appendix F.

- e. **Multipath.** As previously discussed, the signal radiated by the DME antenna can also be reradiated (or “scattered”) by objects in the environment. The reradiated signals traverse different signal paths to the receiver, thus they are commonly referred to as “multipath.” Multipath can cause DME signal pulse-shape deformations, which can translate to ranging error during DME receiver processing. Also, multipath can cause signal fading and receiver unlock conditions. As previously discussed, multipath can be categorized as longitudinal, lateral, or a combination of the two.

Both stationary and moving objects within the vicinity of the DME ground station antenna can generate multipath. The examples of stationary and moving objects given in Section D above can also be sources of multipath. Permanent objects must be clear of the OCA. Moving objects should keep clear of the near-field cylindrical volume when in motion and clear of the OCA when parked or stationary. Otherwise, their impact must be evaluated through data analysis, or math modeling, or both, to determine the multipath effect each object has on the DME SIS.

When an evaluation is required, it should determine and consider the range of M/D ratios expected to occur within the multipath and diffraction regions shown in Appendix C, Figure C-26.

The M/D ratio will vary within these regions and the ratio at any particular reception point determines the possibility of operationally significant signal fading, receiver unlock conditions, and operationally significant ranging accuracy degradation. For the purpose of this discussion, a fading condition is considered operationally significant when the usable distance for the ground station is reduced by 10 percent or more.

Similarly, an accuracy degradation of 200 feet or more is considered operationally significant.

The portion of the multipath and diffraction regions where the amount of signal fading poses a threat to achieving the minimum signal strength requirement should be identified and noted. A conservative approach is to assume that this threat exists whenever ray tracing indicates that the projection of the first Fresnel Zone lies entirely within the diffraction silhouette shown in Figure 3-13. In this case, the M/D ratio would be expected to exceed -9 dB, which is sufficient for causing operationally significant signal fading. The -9 dB value assumes that the minimum signal strength requirement can be met within the service volume with that ground station operating at the -3 dB power alarm limit. The duration of time that the receiver is likely to be exposed to this condition should be evaluated as well.

The portion of the multipath and diffraction regions where the M/D ratio poses a threat of a receiver unlock condition occurring should be identified and noted. A receiver unlock condition is possible whenever the M/D ratio equals or exceeds -10 dB. A conservative approach is to assume that this threat exists whenever ray tracing indicates that the projection of the first Fresnel Zone lies entirely within the diffraction silhouette shown in Figure 3-13. The duration of time that the receiver is likely to be exposed to this condition should be evaluated as well.

The portion of the multipath and diffraction regions where the M/D ratio poses a threat of a range accuracy degradation condition occurring should be identified and noted. Such a threat is considered possible when the M/D ratio equals or exceeds -10 dB (see Appendix C, Figure C-50 and Figure C-51). It is reasonable to assume that this threat exists whenever ray tracing indicates that the projection of the first Fresnel Zone lies entirely within the diffraction silhouette shown in Figure 3-13. When such a threat exists, the Late-Short Arrival Zone boundary shown in Figure 3-19 should be determined using the appropriate time-delay values from Figure 3-20. A time-delay value of 3.3 μ s can be used as the default value for this part of the analysis. The sector from the multipath object to the Late-Short Arrival Zone boundary identifies the portion of the multipath and diffraction regions where ranging accuracy may be impacted. The duration of time that the receiver is likely to be exposed to this condition should be evaluated as well.

In the end, the nature of the impact is determined by considering the amount of airspace where operationally significant signal fading, receiver unlock conditions, and operationally significant ranging accuracy degradation conditions may occur; the location of the airspace within the service volume; the duration of time that the receiver is likely to be exposed to any of these conditions; the impact to conventional procedures to be supported by the facility; and the effect of coverage gaps and accuracy degradation on the DME/DME RNAV network performance. In some cases, the outcome of such an evaluation may indicate that the identification of a more suitable antenna location should be pursued because the impact to flight operations is undesirable.

Additional information regarding the effect of multipath on system performance can be found in Chapter 5 and Appendix C.

- f. Resonant Structures.** A resonant structure will radiate electromagnetic energy very efficiently when stimulated at its resonant frequency. The stimulus could result from a directly applied voltage or induced voltage caused by an incident electromagnetic field. An antenna is an example of a resonant structure that radiates electromagnetic energy when a sinusoidal voltage is applied at its input, and examples of resonant antennas are shown in Figure 3-23. In this case, it is intended that these structures broadcast a desired signal. As illustrated in this figure, there is a distinct relationship between the physical size of the antenna structure and its resonant frequency (or very narrow band of frequencies).

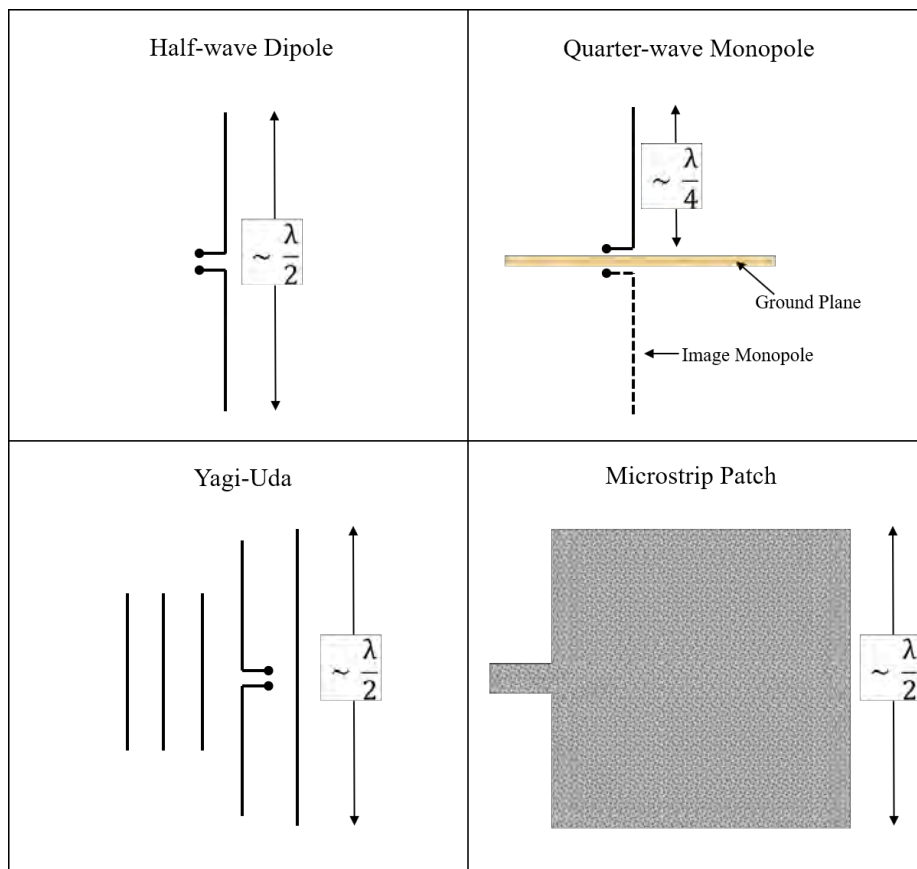


Figure 3-23. Examples of Resonant Antennas

However, when exposed to an external electromagnetic field, these same types of structures can reradiate that field, which may be unintended. That is, the reradiated field becomes a source of multipath that can adversely impact the DME SIS. In this case, resonant structures can be metal strips (e.g., wire), isolated metallic patches, slotted surfaces, or cavities.

During a site survey, it is challenging to identify such structures because their physical size is on the order of inches at DME frequencies. A single resonant

structure is rarely a threat in terms of signal shadowing or multipath because of its finite physical size at DME frequencies unless it is in very close proximity to the DME antenna.

In some cases, the effects of resonant structures may not be identified until flight tests are performed, or user complaints are received. When the application of conventional location techniques identifies an area that does not contain an obvious (i.e., large) multipath object, it should be realized that a resonant structure may be the cause.

Chapter 4. Antenna Considerations

1. Introduction

The purpose of this chapter is to provide key background material on DME antenna performance characteristics for antenna models currently used in the United States NAS. This material will assist the siting engineer in choosing the appropriate antenna configuration and location to maintain the integrity and quality of the DME service.

As previously discussed in Chapter 3, Ground Based NAVAIDs are classified according to their intended use and each classification has a designated service volume. The FAA has engineered the correct signal strength and frequency protection within the service volumes; therefore the DMEs, like all NAVAIDs, are available for use only within their service volume. For information on service volumes for co-located facilities please refer to the specific facility type siting order.

The discussion that follows focuses on those performance characteristics that are relevant to the installed system performance, specifically the vertical and horizontal antenna pattern characteristics. Tutorial information is provided regarding the vertical and horizontal pattern characteristics of common DME antennas and RF concepts relevant to analyzing antenna performance. Because the ground above which the antenna is mounted provides an ever-present source of signal reflection (i.e., multipath), detailed discussion is presented regarding the effect of resulting multipath on both signal strength and accuracy. The effect of antenna height and vertical pattern performance on signal fading (i.e., attenuation) characteristics is discussed, including the interpretation of fading analysis data as it relates to achieved coverage performance measured during flight inspection.

For performance characteristics of commonly-used antenna types refer to Appendix D.

2. DME Antenna Performance Characteristics

This section provides tutorial information on DME antenna performance characteristics relevant to the installed system performance. The pattern characteristics discussed include gain, slopes, beamwidth(s), tilt, and sidelobe levels. Parameter values for the vertical and horizontal pattern characteristics of common DME antennas are given.

a. DME Antenna – The Vertical Plane. A typical radiation pattern of the DME antenna in the vertical plane is shown in Figure 4-1. The diagram is annotated and shows the important characteristics of the vertical pattern. Some of the characteristics shown are:

1. The peak gain (tilt): This normally lies between 2° and 5° above the horizon.
2. Width of primary lobe (beamwidth): The width of the primary lobe is greater than 5°.
3. Gain at horizon: The gain at horizon is greater than 6 dB below the peak gain.
4. Slope at horizon: The radiation pattern slope at the horizon influences the fading performance at very low elevation angles. A steeper slope will give an improved multipath to direct ratio.
5. Gain at $-50 \leq \theta \leq -6$: At least 8 dB lower than the maximum level at the shoulder.

6. Sidelobes below horizon: The sidelobes below horizon, between 6° below and 50° below must be at least 8 dB lower than peak of the major lobe above the horizon.
7. Shoulders: Sidelobes above the horizon.
8. Gain at $6 \leq \theta \leq 15$: Greater than 20 dB below the peak.
9. Gain at $15 \leq \theta \leq 45$: Greater than 30 dB below the peak.

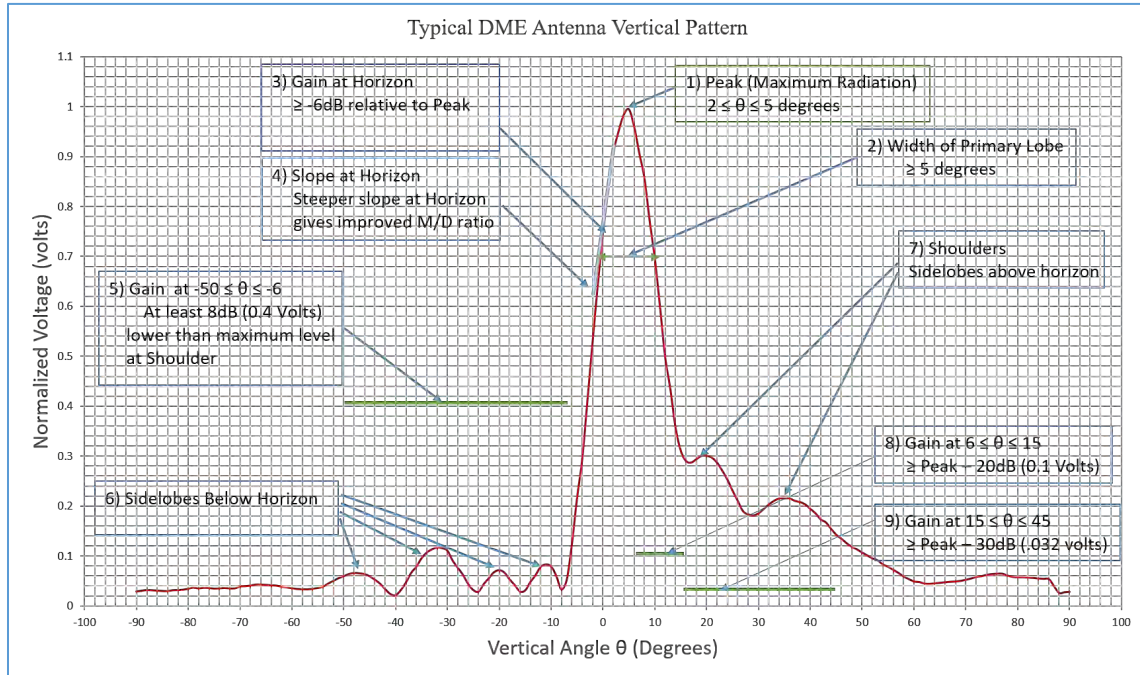


Figure 4-1. Annotated DME Antenna Vertical Pattern

- b. DME Antenna – The Horizontal Plane.** The horizontal radiation pattern of the DME antenna depends on the particular model. The antennas are available in omni-directional, uni-directional, and bi-directional models.

Figure 4-2 below is a typical horizontal pattern for an omni-directional DME antenna. All around the antenna in the horizontal plane, the gain of the antenna remains the same. However, due to slight imperfections in the physical antenna and system feed, some ripples will be experienced where the gain may vary slightly, not to exceed ± 1 dB circularity, in the pattern.

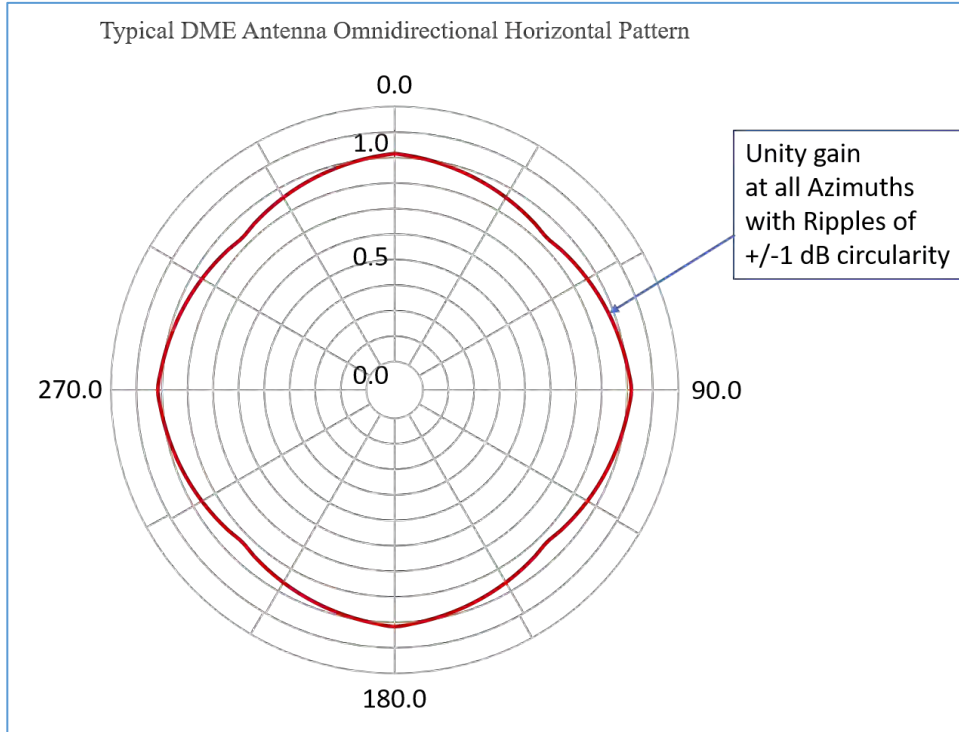


Figure 4-2. Annotated DME Antenna Omni-directional Horizontal Pattern

The horizontal pattern for a uni-directional antenna is shown in Figure 4-3. The diagram is annotated and shows the important characteristics of the horizontal pattern for a uni-directional antenna. Some of the characteristics shown are:

1. The peak gain: This is the gain of the major lobe which is normally in the favored or forward direction. The peak gain (A) is more than that of the omni-directional antenna.
2. Gain on the back lobe: The gain (B) on the back lobe is significantly reduced from the gain in the major lobe on the forward direction.
3. Front-to-Back Ratio = A/B: The ratio of the major lobe gain to the back-lobe gain. A/B Ratio ≥ 10 dB.
4. Half Power Beam Width (HPBW): The HPBW is the width of the major lobe. HPBW $\geq 70^\circ$.

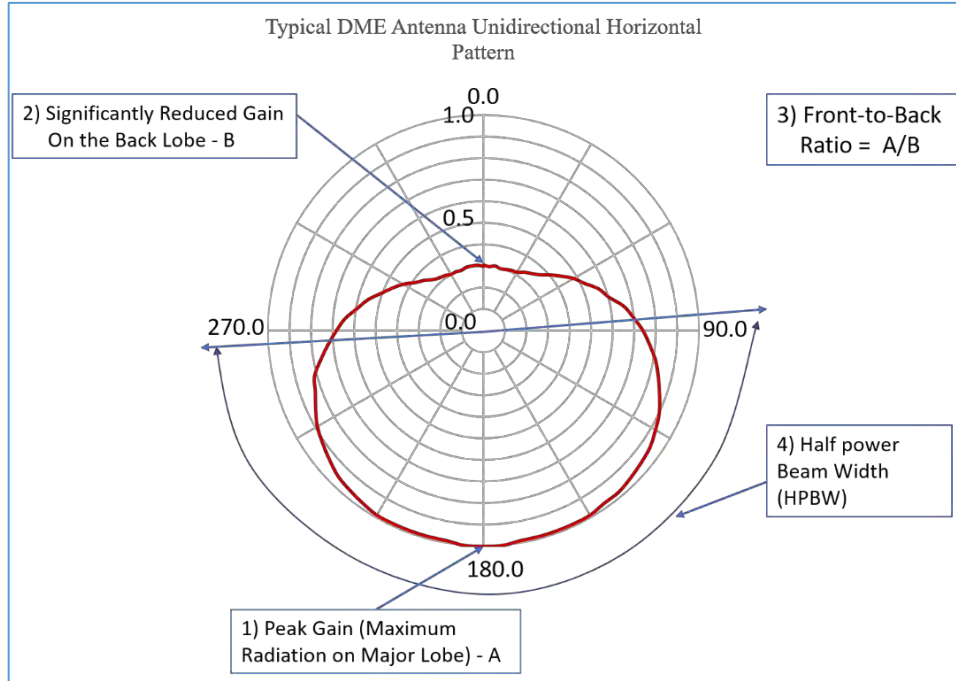


Figure 4-3. Annotated DME Antenna Uni-directional Horizontal Pattern

The horizontal pattern for a bi-directional antenna is shown in Figure 4-4. The diagram is annotated and shows the important characteristics of the horizontal pattern for a bi-directional antenna. Some of the characteristics shown are:

1. Major lobes: There are two major lobes 180° apart. The peak gains of the two lobes are approximately the same. The peak gain is less than the uni-directional antenna gain. The Ratio of the Major lobe gain to gain on the side must be greater than 10 dB.
2. Half Power Beam Width (HPBW): The HPBW of the two major lobes are approximately the same. The HPBW $\geq 20^\circ$.
3. Decreased Gains: There are two areas of significantly decreased gains on either side of the major lobes' directions.

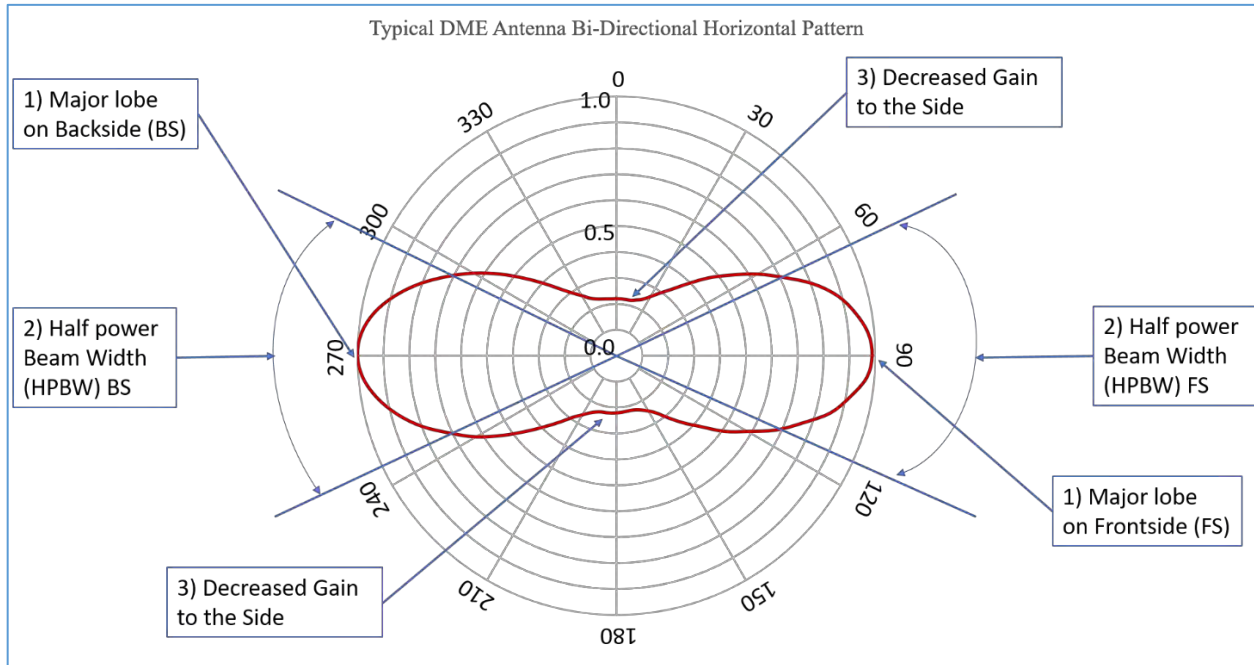


Figure 4-4. Annotated DME Antenna Bi-directional Horizontal Pattern

3. Radio Frequency (RF) Concepts Review

Appendix C provides tutorial information regarding the parameters and RF concepts used to estimate the effects of multipath on the DME SIS. The section provides a brief review of the parameters and concepts applicable to characterizing antenna performance, and a familiarity with the information in Appendix C is assumed. Parameters and concepts applicable to antenna performance are discussed in the paragraphs below.

- a. Multipath.** As discussed in Chapter 3, objects near the DME antenna can block or cause multipath that adversely impact DME performance. It was also noted that multipath can be categorized as longitudinal, lateral, or a combination of the two.

Longitudinal multipath occurs when the DME antenna is placed over a large flat surface commonly referred to as a ground plane. In the absence of other objects, the DME signal arrives at the aircraft via two paths (see Figure 4-5): the LOS path (direct path), and the ground reflected path (i.e., the multipath). Examples of objects that could be the source of longitudinal multipath are flat earth, antenna counterpoise, and center-pivot irrigation equipment located radially from the DME facility antenna. For flat, level ground, the direct and multipath signals will be in the same vertical plane and this special case is called longitudinal multipath.

Lateral multipath occurs when the DME antenna is located in the vicinity of a reflective object as shown in Figure 4-6. Like longitudinal multipath, the DME signal arrives at the aircraft via the direct and reflected paths, however, these paths are in the same horizontal plane. Examples of objects that could be the source of lateral multipath are buildings, hangars, air traffic control towers, monopoles, wind turbines, cell towers, and irrigation equipment.

Most multipath signals will be a combination of longitudinal and lateral multipath; that is, neither strictly the longitudinal nor lateral case.

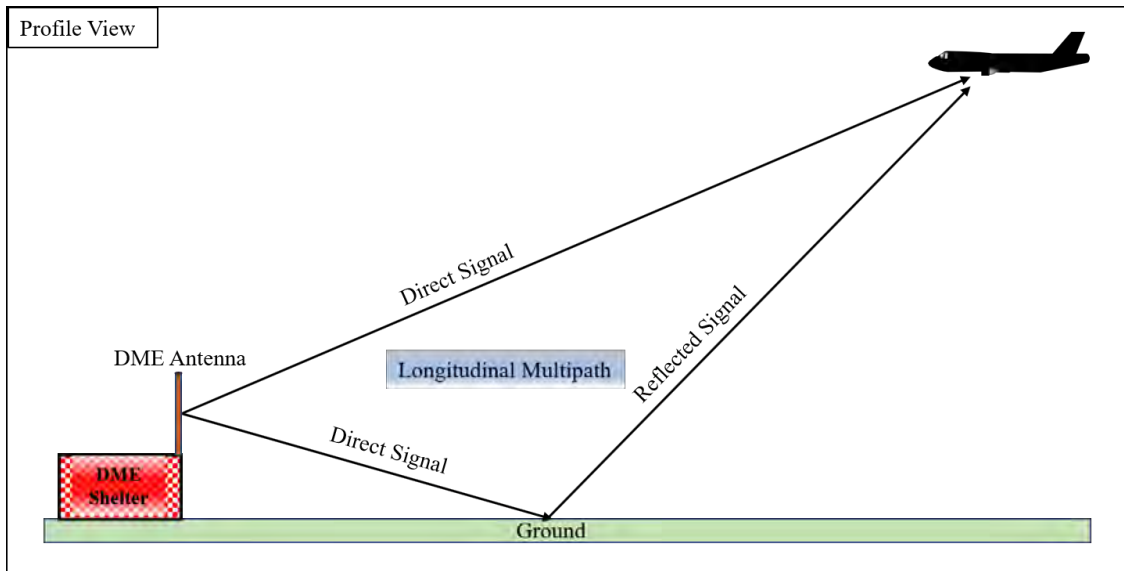


Figure 4-5. Illustration of Longitudinal Multipath

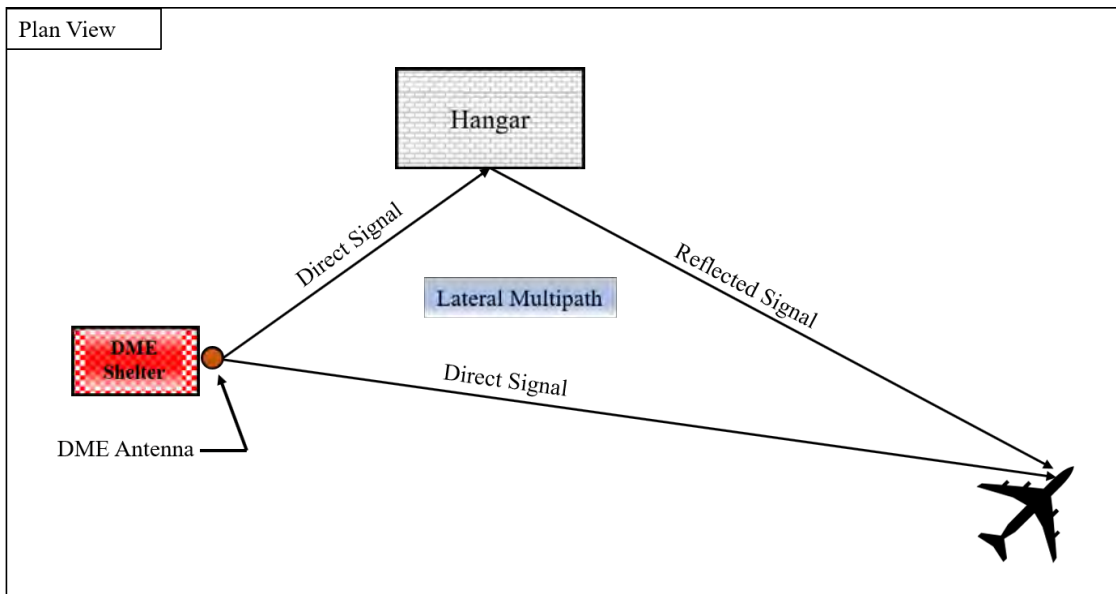


Figure 4-6. Illustration of Lateral Multipath

- b. Multipath-to-Direct (M/D).** The M/D signal strength ratio is defined as the ratio between the magnitude of the multipath signal and the magnitude of the direct signal. The multipath signal could be caused by the reflection of the DME signal by a single source, such as the ground. Alternatively, it may be the vector sum of all the multipath signals caused by re-radiation of the DME signal by the ground, as well as objects and terrain in the vicinity of the DME antenna. This ratio is commonly stated as a logarithmic ratio (e.g., -10 dB).

- c. **Relative Phase and the Vector Wheel.** Electromagnetic waves can be represented mathematically as vectors having a magnitude and phase. How two waves combine in space, or analytically, depends on their magnitudes and the phase of one wave relative to the other. The phase of one wave relative to the other is the parameter referred to as the relative phase (ϕ_r). Similarly, how two DME signals combine depends on their magnitudes and their relative phase.

Because the ground above which the antenna is mounted provides an ever-present source of signal reflection (i.e., multipath), understanding how this multipath alters the SIS provides insight into how system performance may be affected by such ground reflections. The vector wheel (see Figure 4-7) can be used to illustrate the vector sum of the direct and ground reflection signals that together produce the SIS. This reflection can add to, or subtract from, the direct signal. The extent to which it adds or subtracts to the direct depends on the relative phase relationship as shown by parameter " ϕ_r " in Figure 4-7, and the SIS vector is found by vectorially adding the reflected ray to the direct ray as shown. The parameter " ϕ_r " can have any value between 0° and 360° , which means the SIS arrowhead can "touch" any location on the dashed circle shown in Figure 4-7.

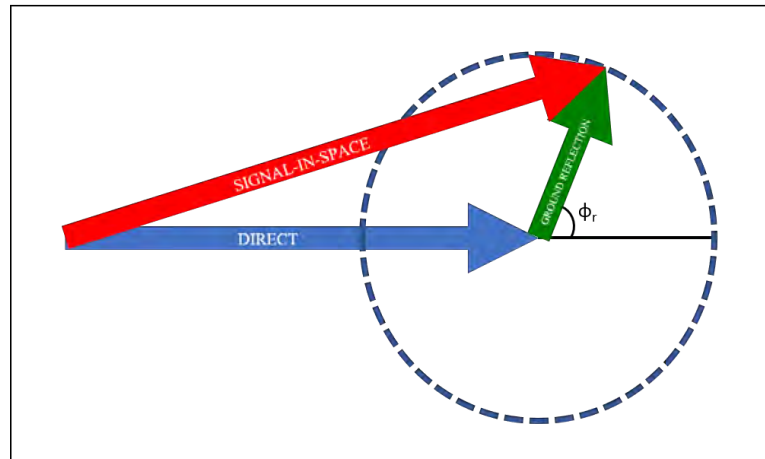


Figure 4-7. Signal-In-Space Results from Adding Direct and Reflected Signals

One is usually interested in bounding the effect that multipath can have on system performance. The nature of the parameter being evaluated typically determines whether an upper bound, lower bound, or both are of interest. The vector wheel can be used to illustrate these bounds. A reflection that is 180° out-of-phase will be subtracted completely from the direct signal. This condition results in the worst-case decrease in the magnitude of the SIS, as shown in Figure 4-8. When the ground reflection phase is 0° relative to the direct signal, the reflection is completely in-phase, and the ground reflection adds completely to the direct signal. This best-case scenario is depicted in Figure 4-9.

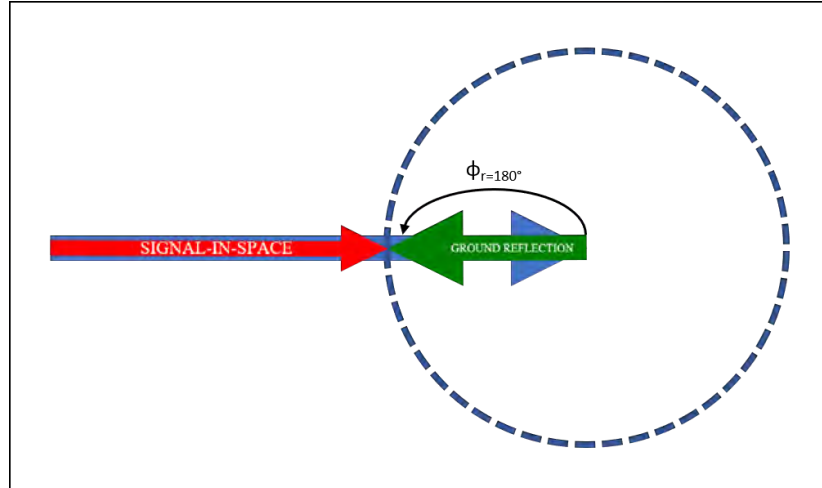


Figure 4-8. Worst-Case: Signal-In-Space Is at Minimum Amplitude

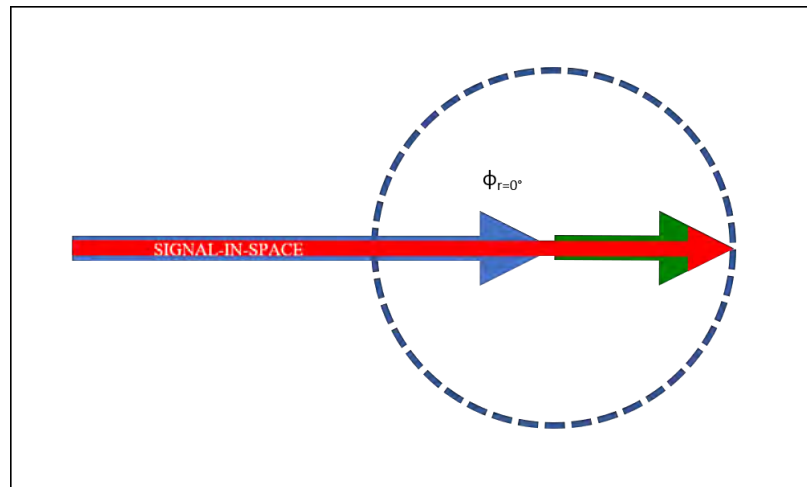


Figure 4-9. Best-Case: Signal-In-Space Is at Maximum Amplitude

4. Antenna Performance

The top-level operational requirements are signal availability and signal quality, which relate to coverage and accuracy, respectively. Signal availability is directly tied to signal strength because a minimum signal level is required to assure proper interrogator operation in terms of pulse-pair decoding and ranging accuracy. Achieving the required signal level is dependent on: transmitter output power; cable loss due to attenuation and mismatch; antenna directive gain; and, resistance to signal attenuation (i.e., fading) caused by multipath. Resistance to multipath effects also aids accuracy performance and such resistance is achieved by the combination of signal format, antenna design, and proper antenna siting. The subsections that follow discuss antenna performance as it relates to coverage and accuracy.

- a. **Coverage.** The design of DME antennas is driven by the requirement to provide coverage throughout the DME service volume as discussed in Chapter 3, Section 2.c. As previously stated, the operational performance requirement is providing the minimum signal strength required to assure proper interrogator operation. Meeting the

operational requirement at the distant service volume boundaries determines the directive gain characteristics of the antenna. These characteristics are discussed in section 4.a.i.

Meeting this requirement throughout the service volume requires the antenna design to incorporate characteristics that provide resistance to, or sufficient control of, signal fading caused by multipath effects. These characteristics are discussed in section 4.a.ii.

- i. **Directive Gain.** In Figure 4-1, example vertical pattern data are provided in the form of normalized voltage plotted against elevation angle. This format gives general insight into the coverage performance when one considers a drawing of the service volumes with a more representative vertical aspect ratio compared with those shown in Figure 3-1. For example, the image shown in Figure 4-10 provides a more realistic vertical representation of the DME High Service Volume assuming a flat earth model; this drawing illustrates that the beam of maximum radiation should be between 0.9° and 5.6° . When the heights shown in Figure 4-10 are interpreted as barometric altitudes, the range of elevation angles shifts downwards due to earth curvature and the range is approximately 0.0° to 4.4° .

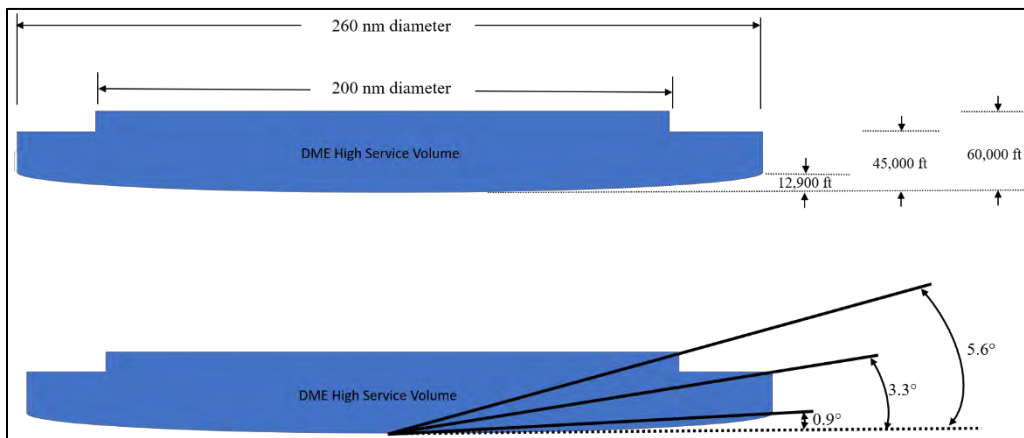


Figure 4-10. More Realistic Vertical Representation of DME High Service Volume

An understanding of the fading and coverage performance of one antenna compared to another can be gained by comparing plots of normalized voltage versus elevation angle (see Figure 4-11). However, this does not provide the most representative comparison because the antenna models have different peak gain values. Therefore, a better understanding may be gained when one considers plots of directive gain versus elevation angle.

Normalized linear directivity plots for the dB Systems, Inc. antennas are shown in Figure 4-11. Table 4-1 shows the minimum gain for each antenna as obtained from the manufacturer's web site.

Table 4-1. Minimum Gain Values for dB Systems, Inc. DME Antennas

dB Systems, Inc. Antenna Model	Minimum Gain (dB)
5100A	9
5100A/7°	9
510A	8
540	12
900E*	9

*TACAN Antenna operating in DME mode.

The directivity for each antenna has been converted to dBi using the following formula:

$$\text{Gain } (\theta) = 20 * \log[\text{directivity voltage } (\theta)] + \text{minimum antenna gain}$$

Several useful examples of minimum directive gain plots are shown in Figure 4-12 through Figure 4-15. Figure 4-12 shows the minimum logarithmic directive gain for each of the antennas. Figure 4-13 is a detail view of Figure 4-12 with a smaller y-axis scaling that provides better resolution of main beam characteristics. The data traces shown in Figure 4-13 are further divided into two groups for ease of viewing. Figure 4-14 displays traces for the most commonly-used antennas, which are the dBs 5100A, dBs 5100A/7°, and dBs 510A. Figure 4-15 shows the traces for the high-performance dBs 540 and the dBs 900E.

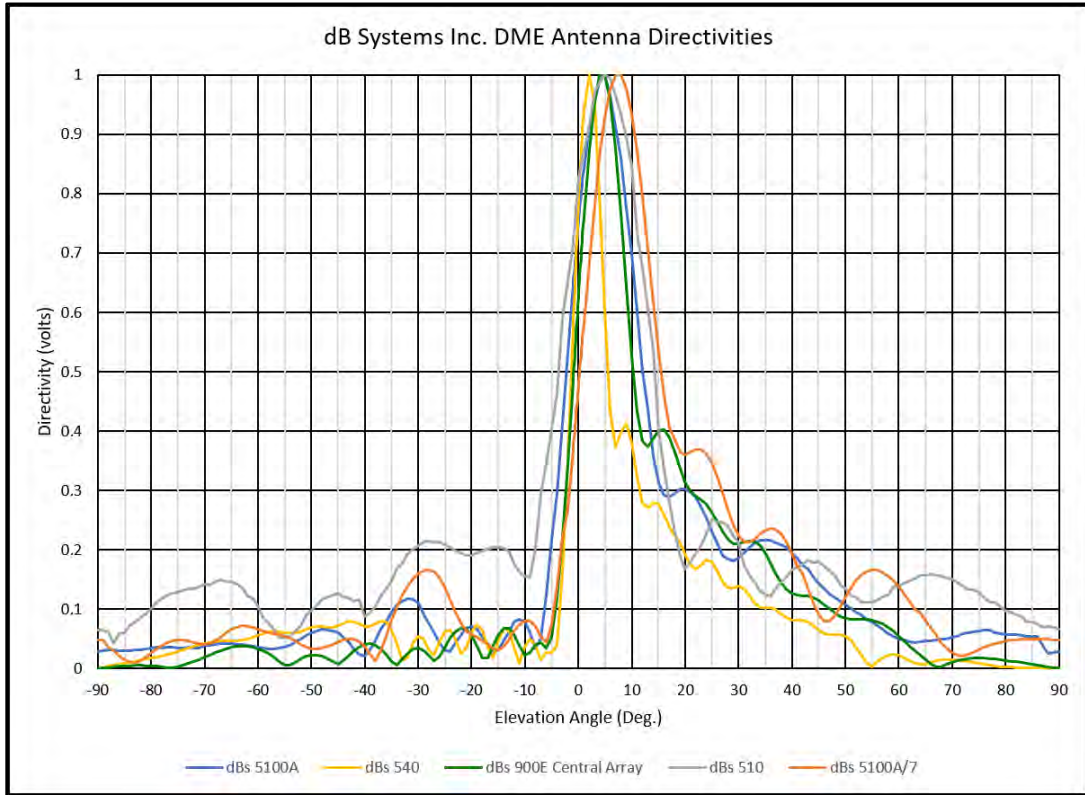


Figure 4-11. dB Systems, Inc. DME Antenna Directivities

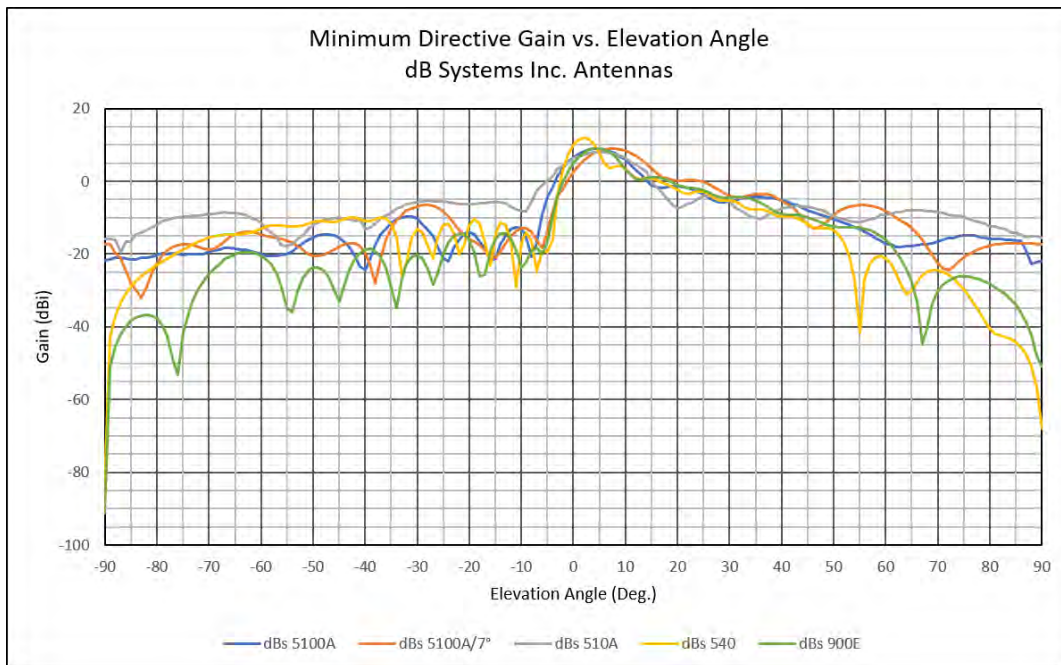


Figure 4-12. dB Systems, Inc. DME Antennas Minimum Directive Gain

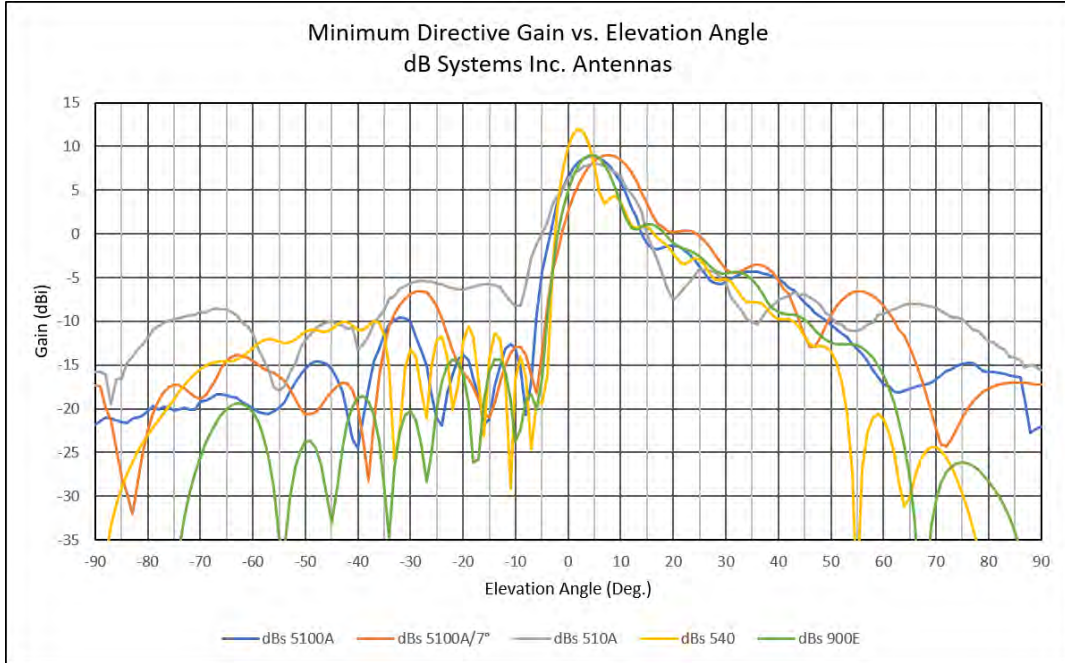


Figure 4-13. dB Systems, Inc. DME Antennas Minimum Directive Gain - Detail View

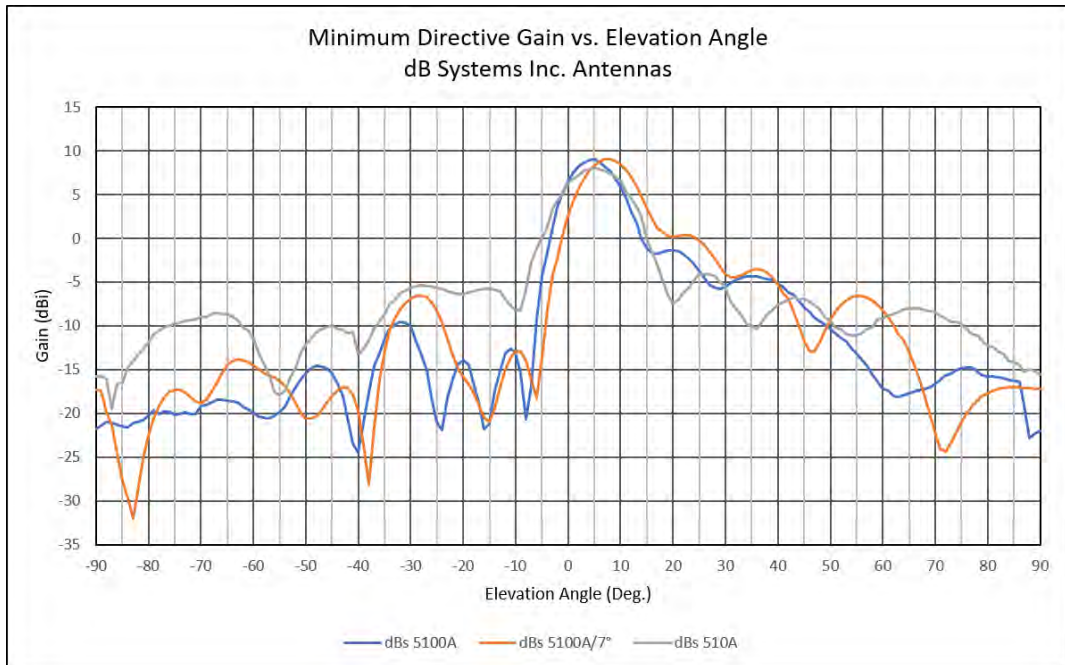


Figure 4-14. dB Systems, Inc DME Antennas Minimum Directive Gain for 5100A, 510A, and 5100A/7° Models



Figure 4-15. dB Systems, Inc. DME Antennas Minimum Directive Gain for 540 and 900E Models

The circular nature of the service volumes shown in Figure 3-1 indicate that the DME antenna should have an omni-directional horizontal pattern. Most modern antenna designs achieve near-perfect performance in this plane with the variation being on the order of ± 1 dB.

Based on the discussion above, the antenna performance characteristics relevant to meeting signal coverage requirements at the distant service volume boundaries include the antenna gain, a directive vertical pattern with the main lobe center around 3° , and an omni-directional horizontal pattern. Additional information regarding antenna pattern requirements can be found in Section 3.3 of Order FAA-E-2996, “Performance Specification for Distance Measuring Equipment (DME).”

- ii. **Signal Fading.** As previously stated, meeting the coverage requirement throughout the service volume requires the antenna design to incorporate characteristics that provide resistance to, or sufficient control of, signal fading caused by multipath effects. Similarly, it was noted that multipath can be categorized as lateral, longitudinal, or a combination of the two.

a) **Lateral Multipath**

Regarding lateral multipath, the circular nature of the DME service volumes (see Figure 3-1) requires the DME antenna to have an omni-directional horizontal pattern. Consequently, objects in the vicinity of the DME antenna will be illuminated and lateral multipath will be generated. Thus, meeting the omni-directional pattern requirement directly competes with the desire to control the effects of lateral multipath on signal coverage. Therefore, proper site selection is the means typically used to eliminate lateral multipath or control the severity of its

effects within operationally significant air space. This same approach is taken for multipath having either a predominantly lateral or significant lateral component.

b) Longitudinal Multipath

As previously stated, the ground above which the DME antenna is mounted provides an ever-present source of longitudinal multipath. It is important to understand how this multipath alters the SIS and the effect these alterations have on system performance. The vector wheel concept (see Figure 4-7) was used previously to illustrate qualitatively how ground reflection can add to, or, subtract from, the direct signal. Both the worst-case (180°) and best-case (0°) relative phase conditions were introduced. The discussion in this section will build upon this qualitative understanding by summarizing the results of a comprehensive study that was performed to characterize the signal attenuation (i.e., worst-case) or amplification (i.e., best-case) that can occur due to reflection of the DME radiated signal by the ground.

As part of the study, a two-ray model of signal propagation was formulated and applied to evaluate the effect on the SIS due to signals reflected by both idealized and real-world ground plane materials (see Figure 4-16). The signal received by an aircraft consists of both direct and ground-reflected rays. The typical DME antenna free space vertical patterns are shown in Figure 4-11 and shows that the pattern is directive. This means that the magnitude of the direct and reflected rays can be different depending on their departure angle from the DME antenna. Thus, vertical pattern differences were taken into consideration when performing the study.

The effects of ground plane materials and surface roughness on the strength of the reflected ray were also considered. When the ground plane is smooth, the magnitude of the ground-reflected ray is multiplied by the Fresnel Reflection Coefficient. If the ground plane is not smooth, the magnitude of the ground-reflected wave is multiplied by both the Fresnel Reflection Coefficient and a rough surface reduction factor. For each elevation angle, the magnitude of the positive-angle direct signal is either reduced or amplified by the magnitude of the negative-angle reflected signal, depending on the relative phase of the reflected signal.

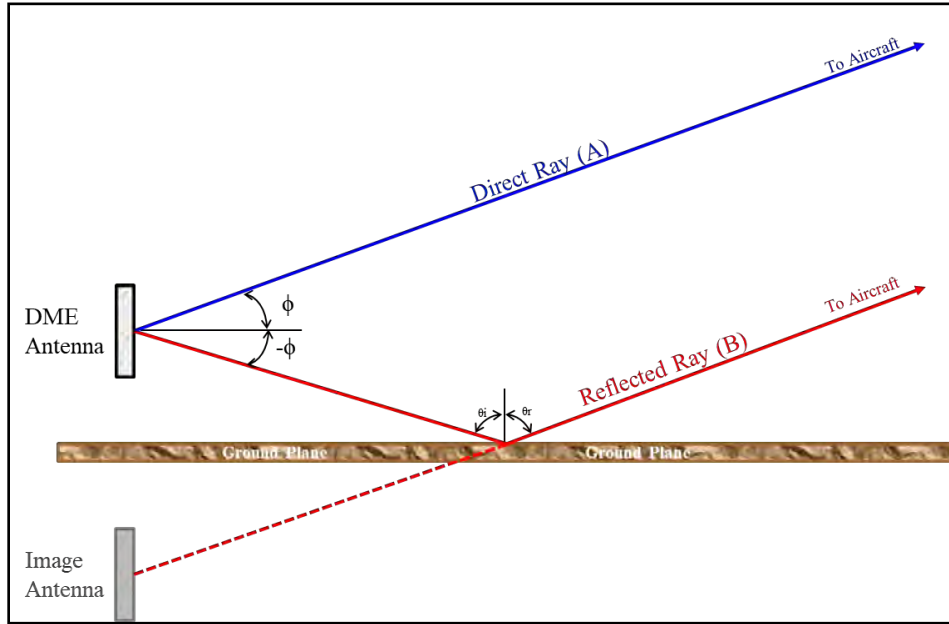


Figure 4-16. Generic Two-ray Model for Signal Reflections from the Ground

1) Overview of Fading Due to Ground Reflection

When considering longitudinal multipath, the worst-case fading occurs where the ground plane material is a Perfect Electric Conductor (PEC), which is a theoretical condition that does not exist in the real world. Worst-case fading occurs for PEC materials because the magnitude of the Fresnel Reflection Coefficient is one for all elevation angles. To provide conservative, yet more representative results, the dielectric properties of real-world materials were used to calculate worst-case fading values for three groups of earth surface conditions: Water and Earth, Water Only, and Earth Only.

Since each group includes two or more surface conditions, further analysis was performed. For each group it was determined which condition yields the Fresnel Reflection Coefficient with the largest magnitude for a given elevation angle. This magnitude was then established as the reflectivity bound for that elevation angle for the group being considered. This process was performed for each elevation angle to obtain a reflectivity bound versus elevation angle curve for each surface condition group.

For each of the three earth surface conditions, fading charts were generated based on ground surface roughness. In Figure 4-17 below, the regions representing smooth, non-smooth and rough surface conditions – based on the standard deviation (h) of the heights of the ground – are shown in different color codes. The green area represents the smooth region of the Fraunhofer region. The blue area represents the rough region of the Rayleigh criterion. An intermediate criterion, which falls in the middle of the Fraunhofer and Rayleigh regions, was established as shown in red in Figure 4-17. Based on this intermediate criterion, a surface is “smooth” when the Root Mean Square (RMS) value of the surface height is less than $\lambda/16$. Surfaces

where the value for “h” ranges from $\lambda/16$ to $\lambda/8$ are considered as “non-smooth”, and surfaces are considered “rough” when the value for “h” exceeds $\lambda/8$.

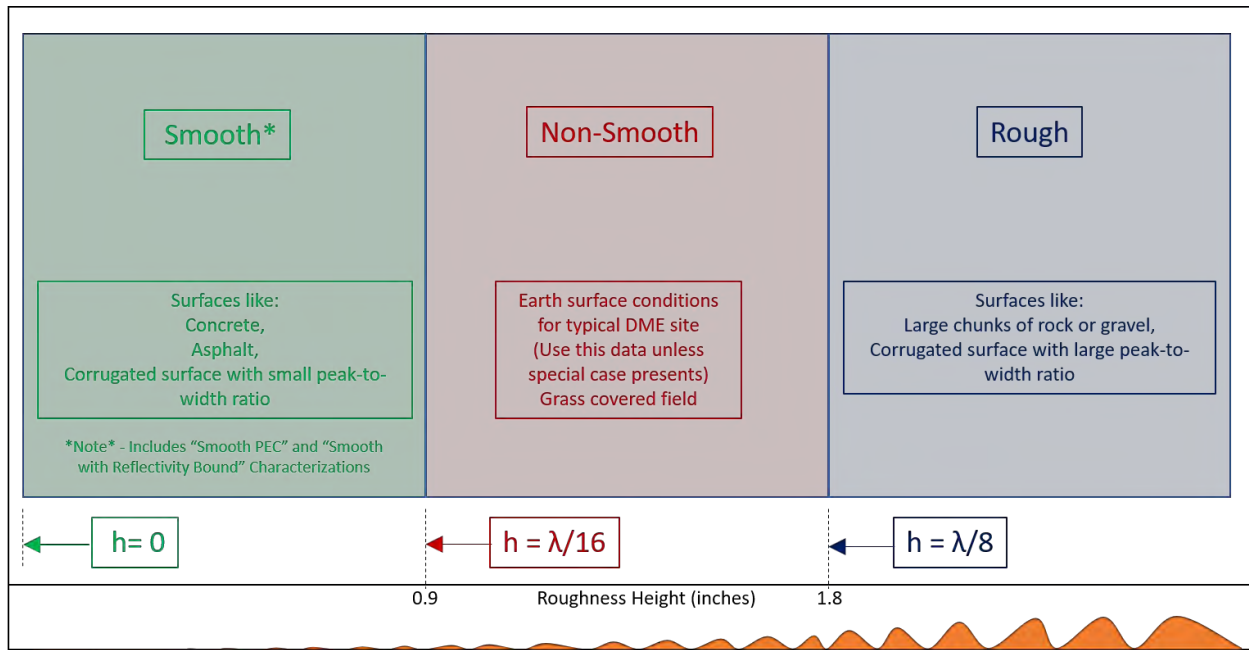


Figure 4-17. Pictorial Depiction of Surface Roughness Criteria

An example of fading output for Earth Only surface conditions is shown in Figure 4-18, including the results obtained for the previously-mentioned roughness scenarios. The “Worst Case” designation refers to the 180-degree relative phase of the reflected signal to the direct signal. Note that a “Rough” surface has the smallest fading margin.

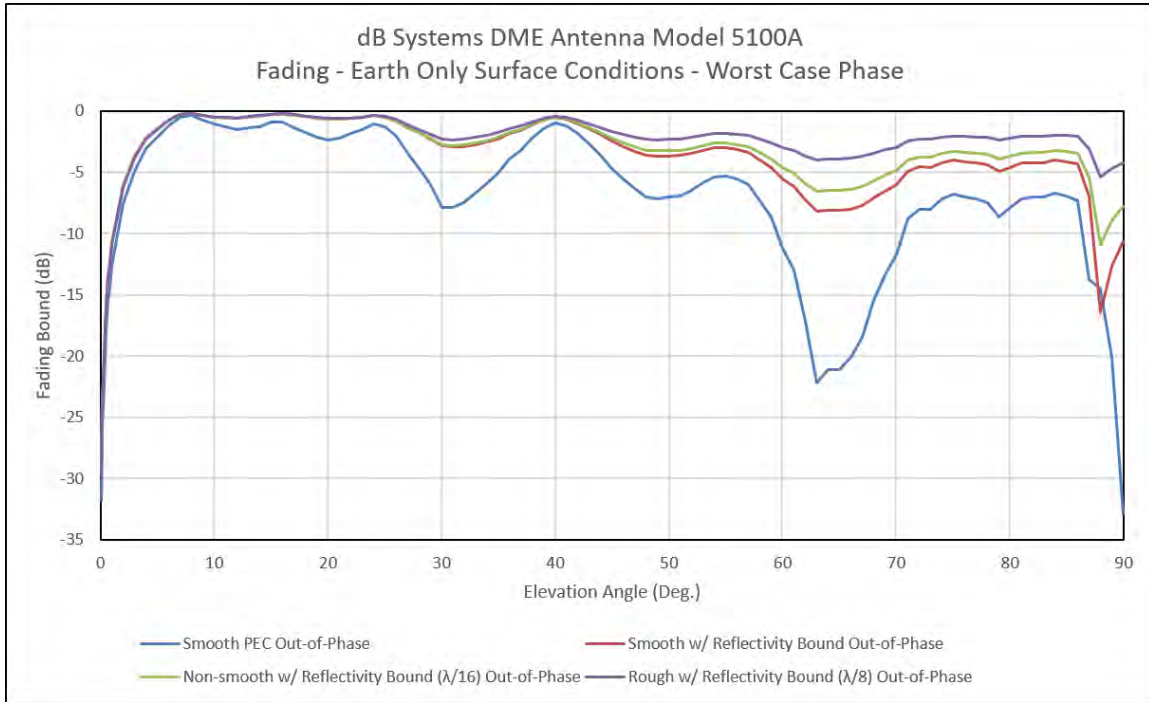


Figure 4-18. Example Output for the Rough Surface Analysis, Including Results for All Scenarios

The next step was to determine which of the three surface condition groups (Earth Only, Water Only, Water and Earth) best correlates with the surface conditions typical of most DME antenna sites. While there are and will be cases where a significant portion or sector of the ground plane is water, these will be outlier cases. Such cases are best handled by site-specific analysis, which among other things, may take into consideration the fading data presented herein (see Figure 4-20) that is relevant to each specific case. The majority of sites are likely to present as Earth Only cases (see Figure 4-22), which leaves the four surface roughness traces on the Earth Only plot for further contemplation.

At DME signal wavelengths, the $\lambda/16$ standard deviation for the roughness height corresponds to about 0.6 inches, or maximum height variations in the range of 0.9 inches. Thus, most installation sites encountered in the NAS will likely be classified as either the non-smooth or rough surface case. This is not to say that one will not encounter sites classified as the smooth case, just that these cases may be more effectively handled through site-specific analysis.

While the $\lambda/8$ standard deviation for the roughness height corresponds to about 1.2 inches, or maximum height variations in the range of 1.8 inches, it is advised to assume a greater margin of fading. Therefore, most sites will present as cases where the $\lambda/16$ case (Earth Only) curve can be applied. Figure 4-19 shows this data for the three DME antenna models commonly used in the NAS.

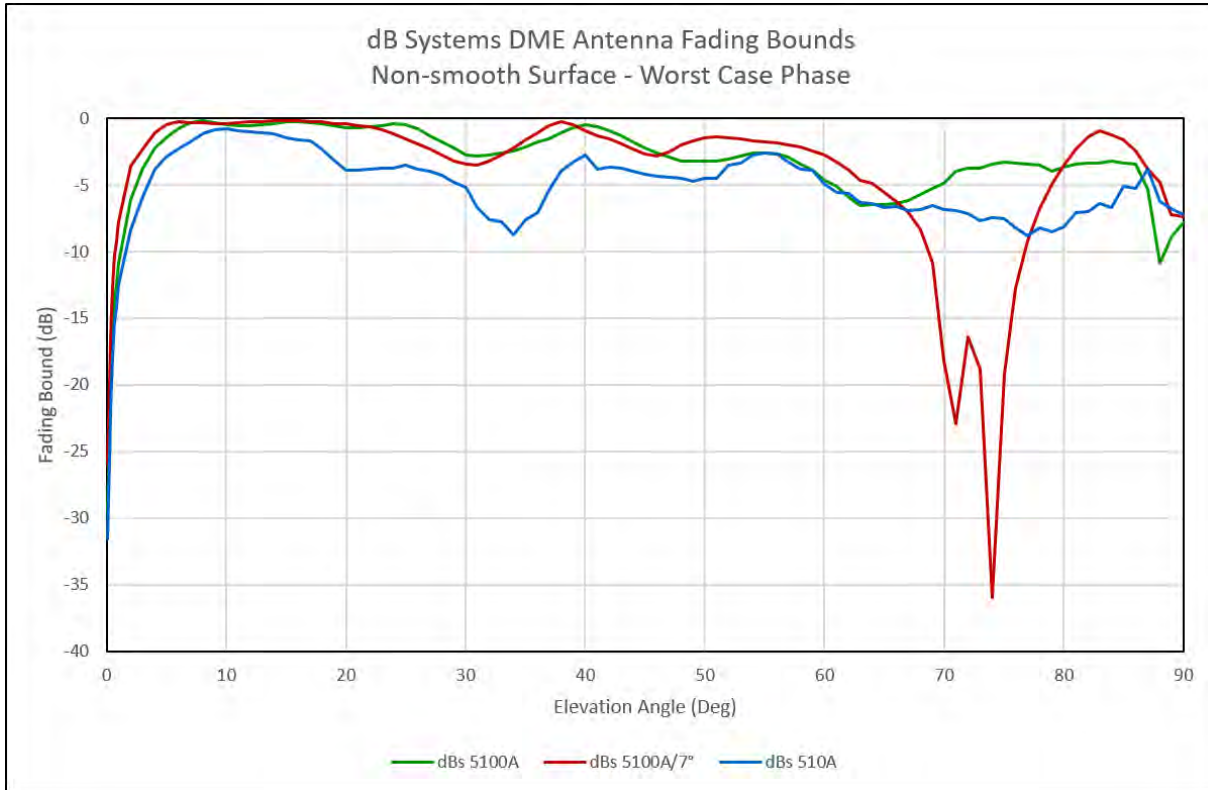


Figure 4-19. Fading Results for Commonly Used DME Antennas, Typical Antenna Site

2) Application of Fading Analysis Results

This section provides example applications of the fading analysis results. These examples discuss the selection of both a representative surface condition group and roughness height criterion.

A DME installation that is next to an ocean coastline or large inland body of water will be subject to a reflection surface with rough water or waves, as well as smooth water under calm conditions. Because of the smooth water conditions, the worst-case fading is characterized by the “Smooth PEC” Water Only trace as shown in Figure 4-20. Note that the fading results apply only to the sector where the ground plane is water, such as a level run along radials in that area.

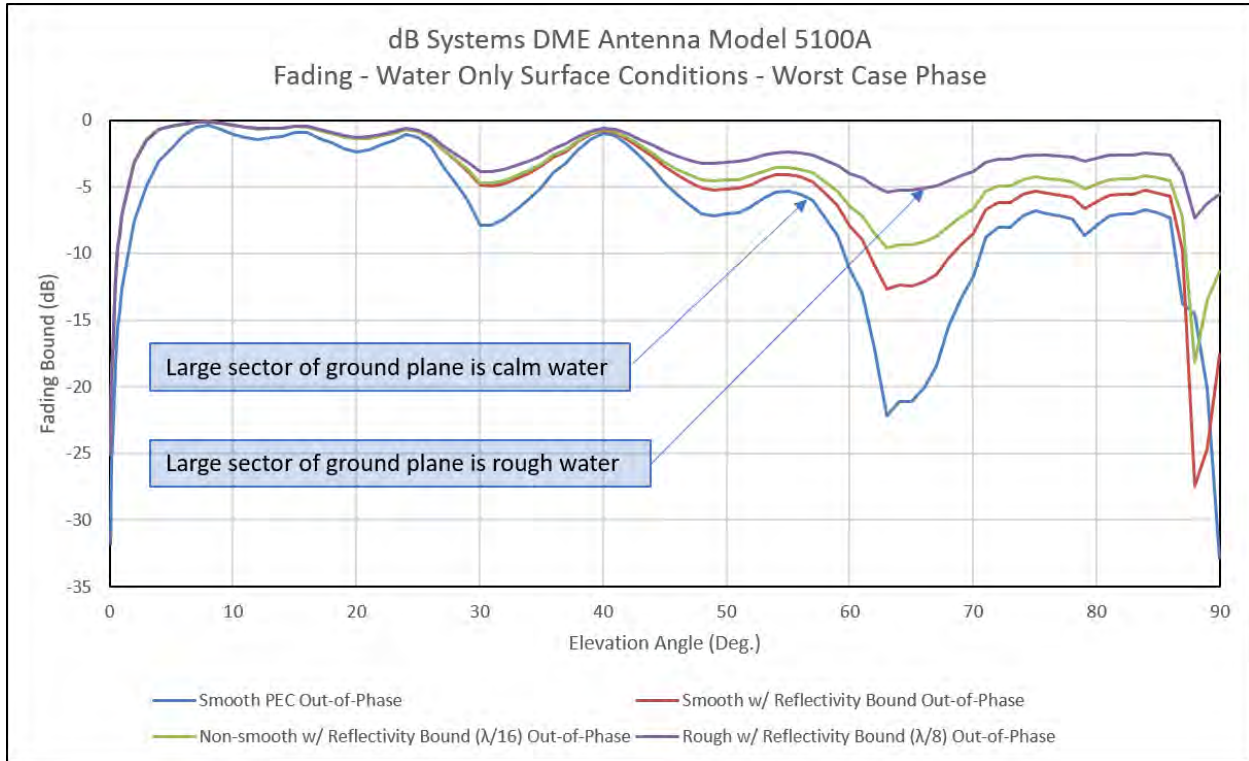


Figure 4-20. dBs 5100A Worst-case Fading for Water Only Surface Conditions

If a large sector of the ground plane is smooth concrete or asphalt, fading results will be between the “Smooth w/ Reflectivity Bound” and “Non-Smooth w/ Reflectivity Bound” results. The amount of variation in the concrete (e.g., age, troweled/brush finishing) or asphalt (e.g., age, coarse aggregate, fine aggregate, rolled) surfaces will determine which curve is more appropriate. Due to the many variables with concrete and asphalt surfaces, the most conservative characterization would be that these surfaces present as the “Smooth w/ Reflectivity Bound” case.

A metal roof top or large counterpoise may present differently depending on the height variations of the surface. An example of this is a corrugated surface. When the length of the trough is an appreciable portion of the wavelength and the peak is a much smaller fraction of the wavelength as shown in Figure 4-21(a), the surface should present as the PEC case. Depending on its dimensions, a corrugated surface may also present as shown in Figure 4-21(b). This case will exhibit characteristics of a rough surface, the $\lambda/8$ case of Figure 4-22, when the corrugation is ≈ 1.5 inches or higher.

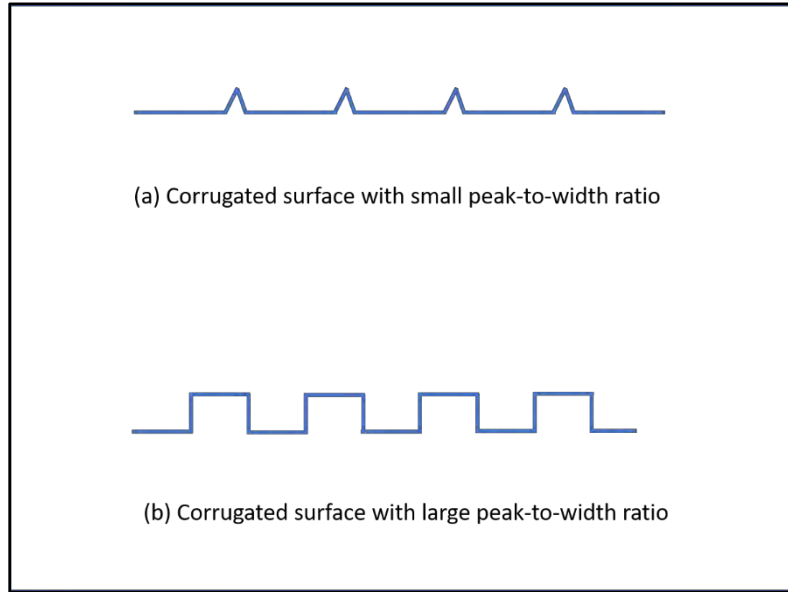


Figure 4-21. Example of Corrugated Surface Profiles

Surfaces that exhibit larger roughness profiles, such as areas filled with large chunks of rock or gravel, suggest that the use of the “Rough ($\lambda/8$)” might be the most appropriate. The application of these cases is shown pictorially in Figure 4-22.

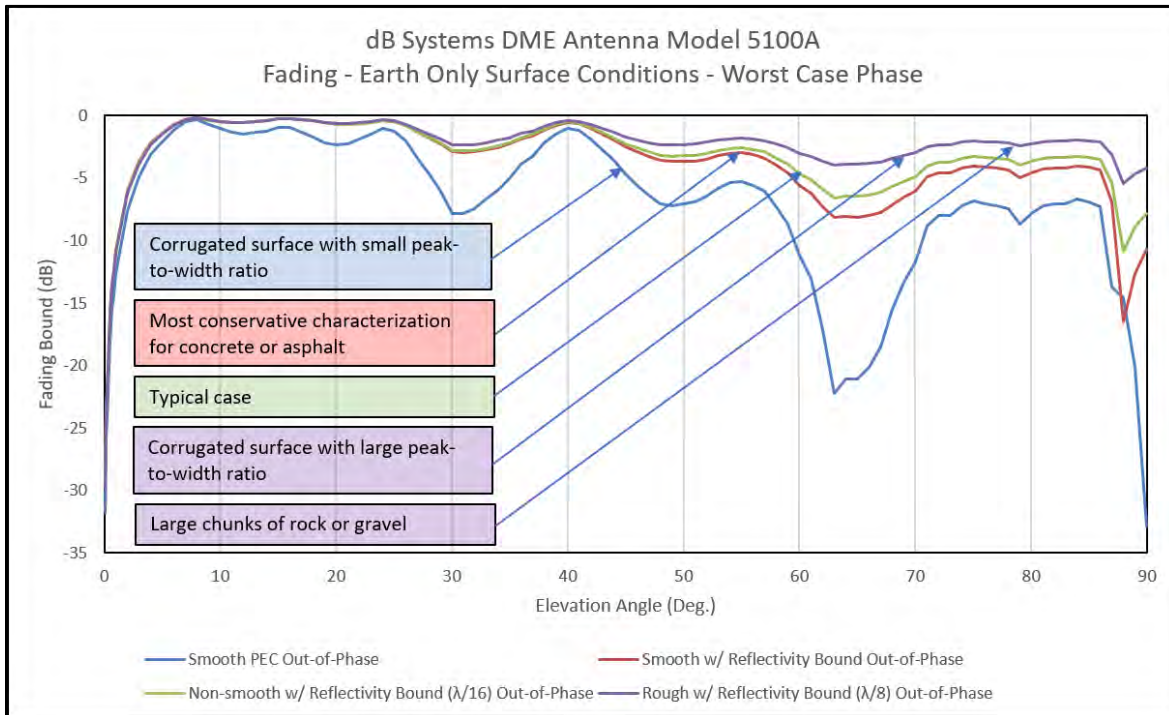


Figure 4-22. Application of Particular Surfaces to Earth Only Fading Bounds

In the discussion above, signal fading analysis was done on surfaces with varying roughness using the worst-case scenario relative phase condition. That is, the case when ground reflection (longitudinal) multipath is out-of-phase ($\phi_r = 180^\circ$) relative to the direct signal. Next, knowledge of the in-phase and out-of-phase multipath relative to the direct signal and vector wheel concept will be combined. Figure 4-23 shows fading analysis results for both the worst-case and best-case relative phase conditions. As the vector wheel inset shows, the ground reflection is 180 electrical degrees out-of-phase with the direct signal for the worst-case condition. This condition results in the fading data having negative values, which indicates there is a reduction in signal strength compared to free-space conditions. Similarly, for the best-case phase condition, the vector wheel inset shows that the ground reflection is completely in-phase with the direct, which “amplifies” the SIS.

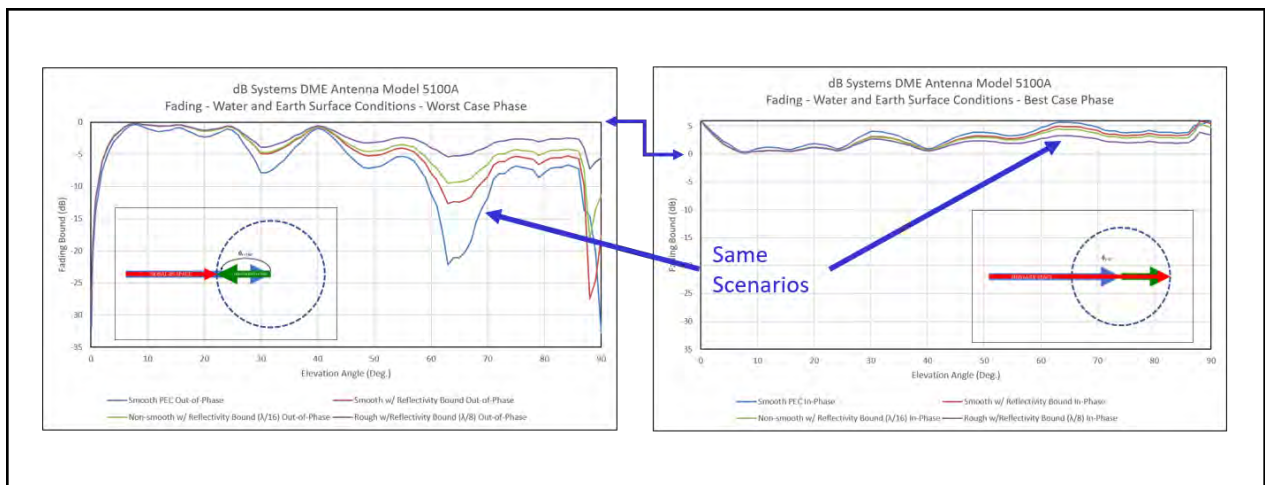


Figure 4-23. Example Fading Results for Worst-Case and Best-Case Conditions

3) Interpretation of the Fading Analysis Results

Fading data is available for the following five dB Systems DME antenna models:

1. dBs 5100A;
2. dBs 5100A/7°;
3. dBs 510A;
4. dBs 540; and
5. dBs 900E.

For each antenna, data plots are available that characterize both the worst-case fading (out-of-phase condition) and the best-case amplification (in-phase condition) caused by ground reflection multipath for select surface conditions. The availability of this data aids the characterization of signal coverage performance, and can be used to support DME siting efforts.

Such characterizations aid siting criteria development, antenna site selection, and antenna installation decisions. Proper interpretation of the fading data presented in

the preceding sections is key to understanding how it relates to signal coverage performance. This topic is addressed next, followed by discussion regarding application of the results to support siting criteria efforts.

A straight-level-run flight test maneuver (i.e., a level run), or simulated flight path towards or away from a ground-based transmitting antenna, can be used for collecting signal strength data that enable the assessment of signal coverage. For example, the level run profile illustrated in Figure 4-24(a) can be used to produce signal strength plots like those shown in panels (b), (c), and (d) of this figure.

The general trend of the signal strength plot follows what is known as the free space loss curve, which accounts for the spreading of a finite amount of transmitter power over an increasingly larger spherical surface as the signal energy propagates away from the transmitter antenna. A bias between calculated and measured signal strength data may be introduced depending on how rigorously one accounts for transmitter output power, cable losses, and antenna gain. Scattering of the radiated signal by objects in the environment can also affect the signal strength measured at any given point in space. As previously mentioned, the signal reflected from the ground will interact with the direct signal to cause fading (i.e., attenuation) or amplification.

The amount of fading or amplification depends on those factors previously discussed, with the predominant factor being how much signal energy is radiated towards the ground. In the case of a dipole antenna, significant energy is radiated towards the ground, and as the results of Figure 4-24(b) show, significant (i.e., 10s of dB) fading occurs. Conversely, the vertical pattern of most DME antennas limits the amount of energy radiated towards the ground, which greatly reduces signal fading effects as the results of Figure 4-24(c) and Figure 4-24(d) illustrate. It should be noted that while signal fades may be 10s of dB deep, the maximum amplification will be limited to 6 dB in the case of ground reflection (or the case of a signal multipath source).

In addition to the free-space vertical pattern characteristics of an antenna, the height of the antenna above ground also affects the realized vertical pattern of an installed antenna. The height determines the number of nulls or minima that are introduced into the pattern. The region between two nulls is commonly referred to as a (signal strength) lobe, which is illustrated by the inset to Figure 4-24(a). The number of lobes introduced into the vertical pattern is proportional to antenna height, with increased height generating more lobes as demonstrated in Figure 4-25. The “slicing” through these lobes on a level run generates oscillations in the signal strength data as previously shown in Figure 4-24.

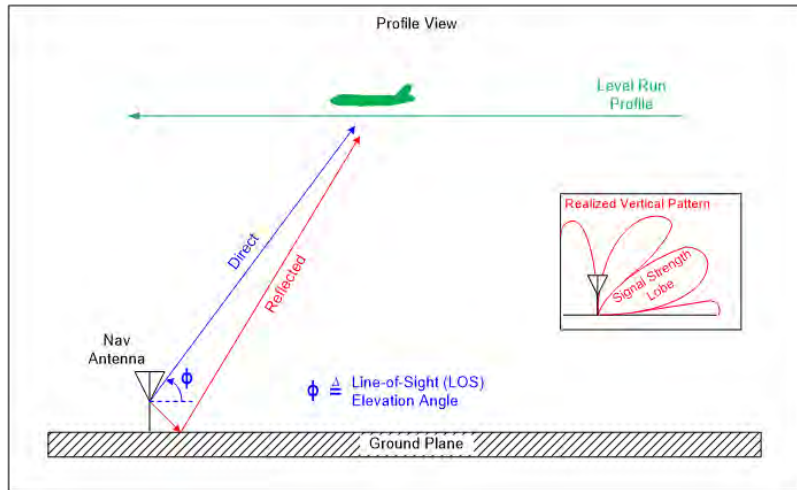
The discussion will now focus on describing the relationship between a fading bound plot and the coverage performance measured during a level-run maneuver. While not representative of the typical case for an installed DME transponder antenna, the results for the smooth PEC case will be used for the purposes of this

discussion because the fading effects can be easily distinguished from other effects (e.g., free space loss). As Figure 4-26(a) illustrates, the horizontal plot axis is distance whereas the axis for the fading bound plots is in elevation angle, see Figure 4-26(c). It should also be noted that the direction for decreasing elevation angle is reversed in these two plots. This situation is addressed by flipping the entire fading bound plot horizontally as shown in Figure 4-26(d). The entire chart (including the descriptive text) is shown as a reverse image to distinguish it from the standard fading plot format to avoid confusion regarding the X-axis of this on particular chart (decreasing elevation angle) with the standard plots (increasing elevation angle). Figure 4-26(b) shows elevation angle versus distance for nine level run heights, and the resulting family-of-curves show an exponential-like mapping. That is, most of the fading bound plot corresponds to the last 10 miles or less of the level run, depending on aircraft height, see Figure 4-26(d).

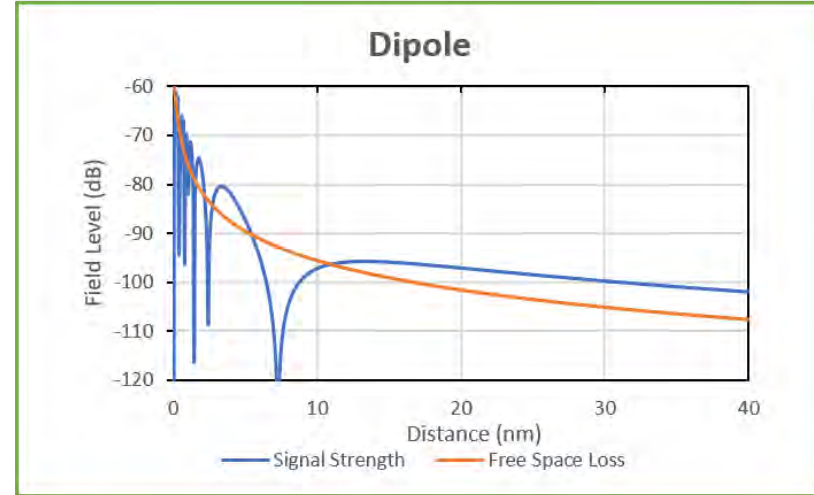
It has been stated previously that antenna height affects the realized vertical pattern, yet the fading results provided herein are not a function of antenna height. The peaks and nulls in the instantaneous signal strength plot will migrate horizontally (i.e., either left or right) as the antenna height is increased or decreased. This occurs because changing the antenna height introduces a shift in the relative phase between the direct and reflected rays for a given reception point. That is, it affects the angular starting point of the reflected ray on the vector wheel. The same situation holds true for the case where the height of the level run (i.e., receiver antenna height) is increased or decreased. Also, changes in ground plane conditions (e.g., from dry soil to wet soil) can cause migration of the peaks and nulls; the amplitude of the reflected signal may change as well.

However, the same maximum and minimum values will be observed through each complete rotation of the vector wheel. The amplitude of the reflected ray is largely a function of elevation angle because both the vertical pattern of the antenna and magnitude of the reflection coefficient are a function of elevation angle. The outcome of the relationships discussed in this paragraph and the preceding paragraph is that the signal strength peaks and nulls migrate horizontally with a change in antenna and/or level run heights, while the fading bound envelope is stationary in space. Figure 4-27 illustrates these relationships.

Ultimately, the relationship between a fading bound plot and the coverage performance measured during a level run maneuver is that the bound describes the envelope produced by the oscillations in the signal strength data. This envelope will be superimposed on other “trends”, most notably free-space loss and the vertical gain characteristics of the DME transponder (and interrogator) antenna as illustrated in Figure 4-28.



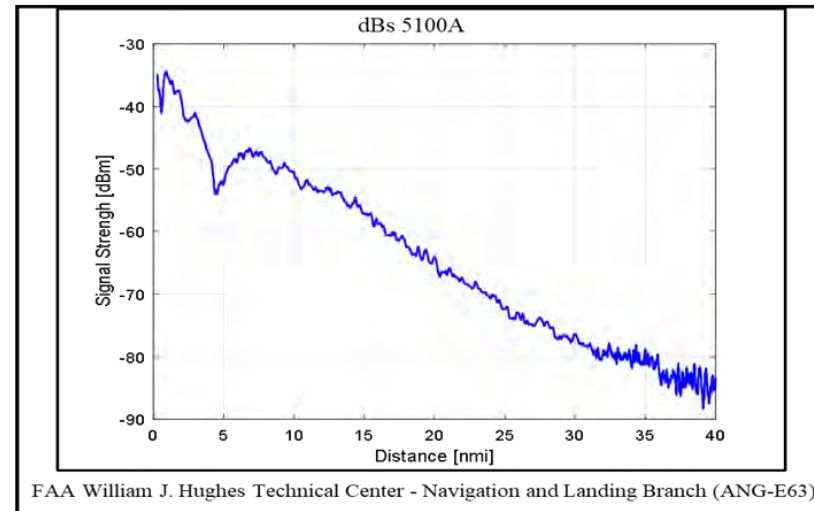
(a) Level run profile



(b) Simulated, 14' antenna height



(c) Simulated, 14' antenna height



(d) Measure, 14' antenna height

Figure 4-24. Level Run Flight Test Profile with Example Simulated and Measured Signal-strength Results

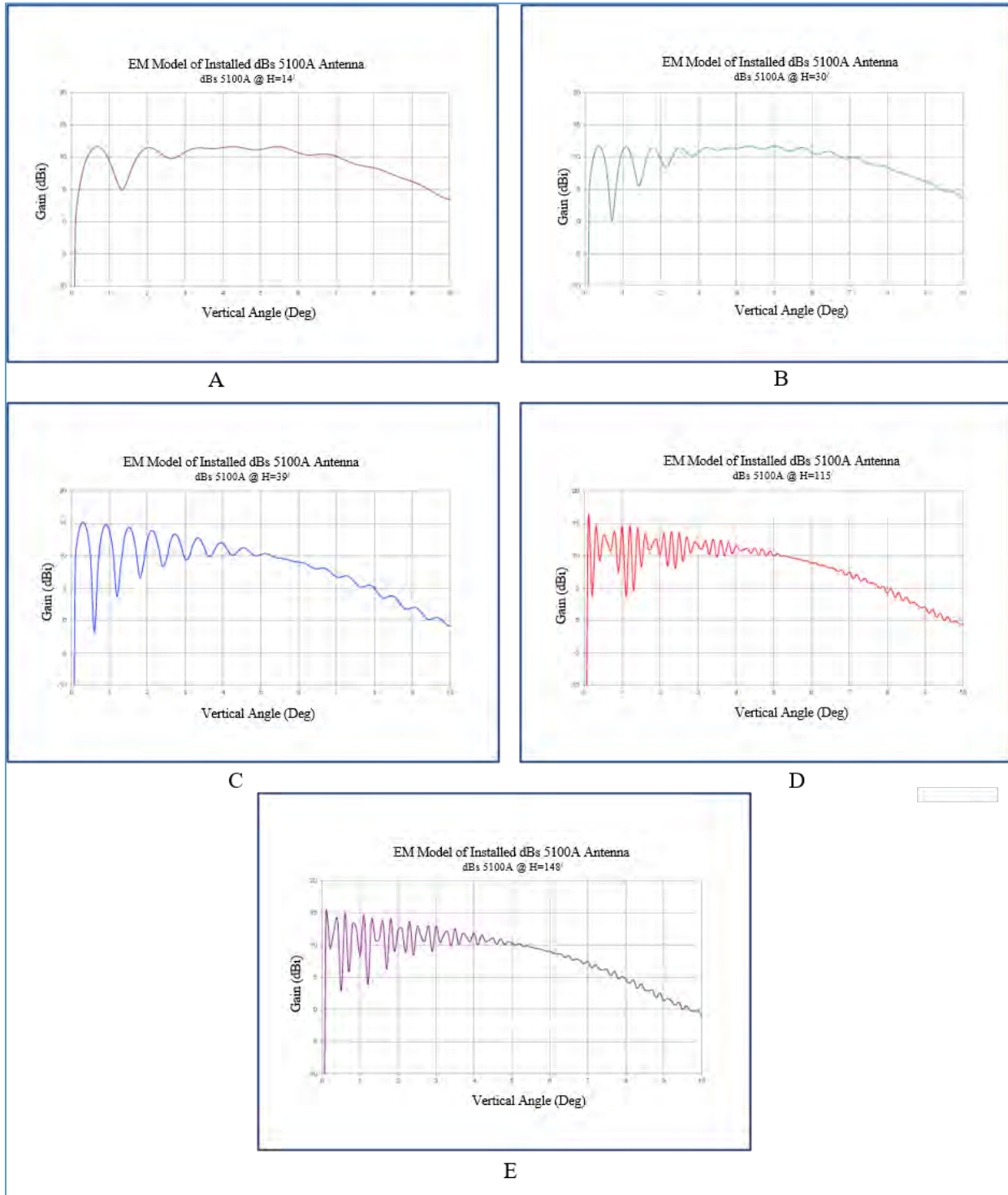


Figure 4-25. Example of Migrating Nulls with Increased Antenna Height

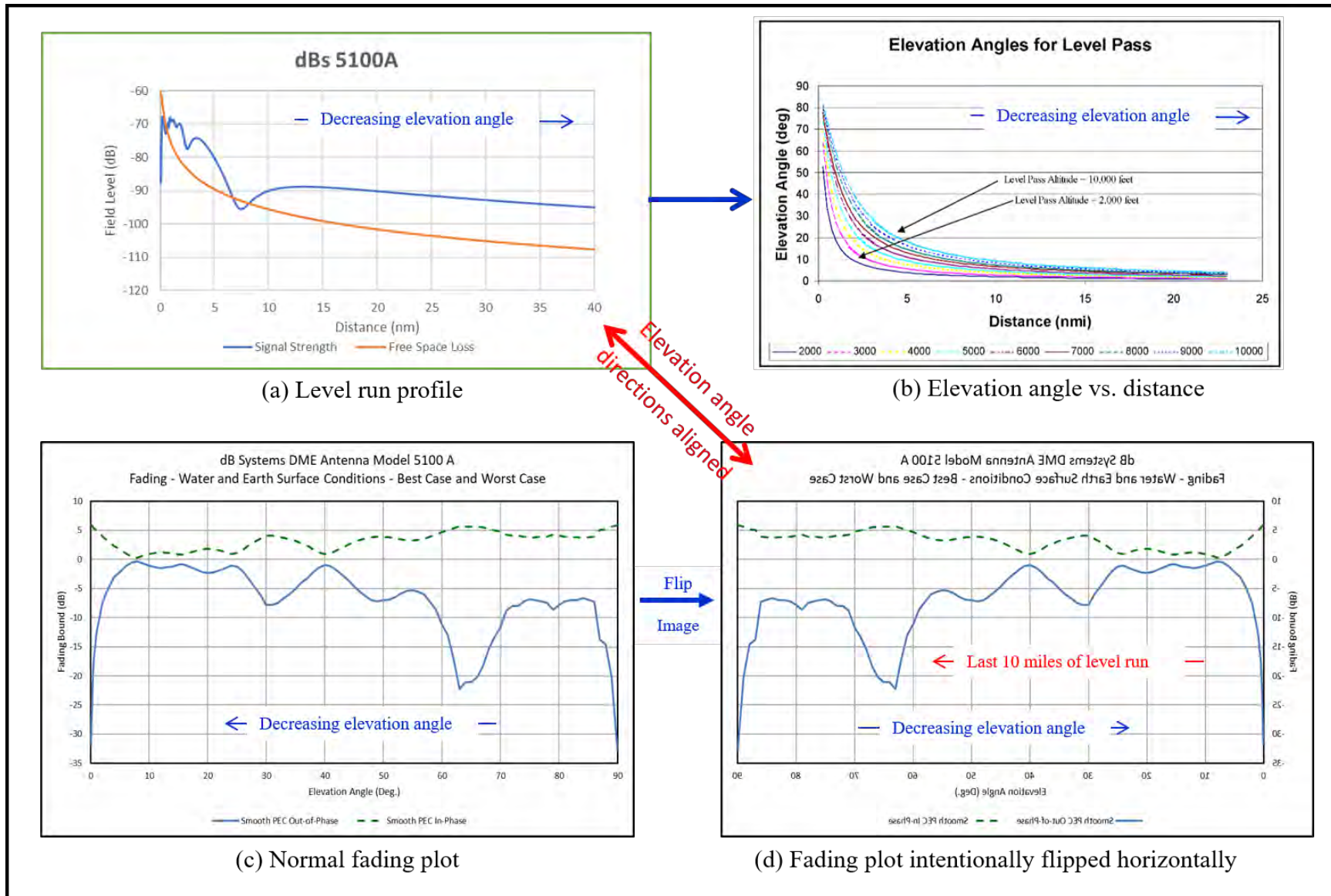
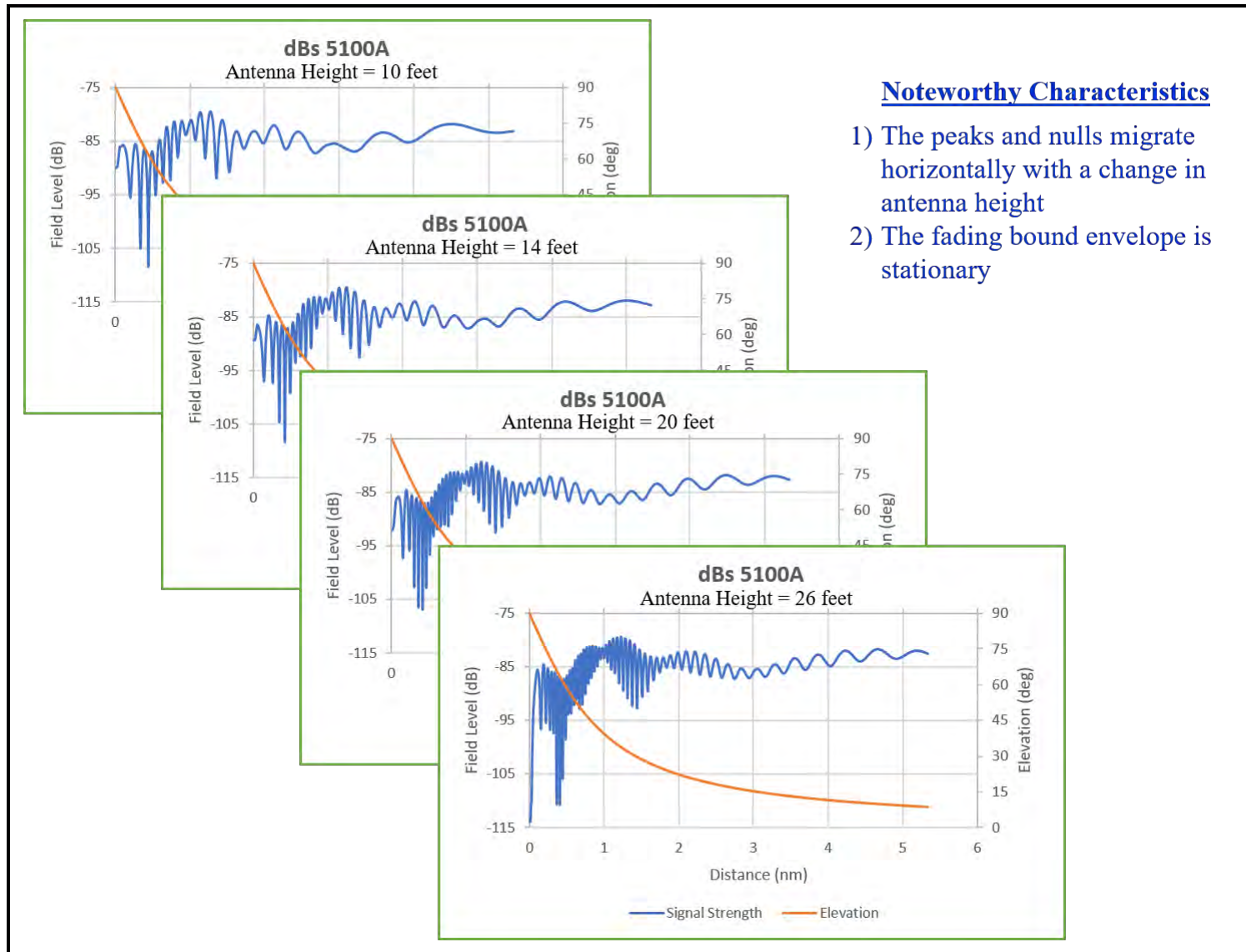


Figure 4-26. Alignment of Level Run and Fading Bound Plots



Noteworthy Characteristics

- 1) The peaks and nulls migrate horizontally with a change in antenna height
- 2) The fading bound envelope is stationary

Figure 4-27. Illustration of Migrating Peak/Nulls with Stationary Fading Bound Envelope

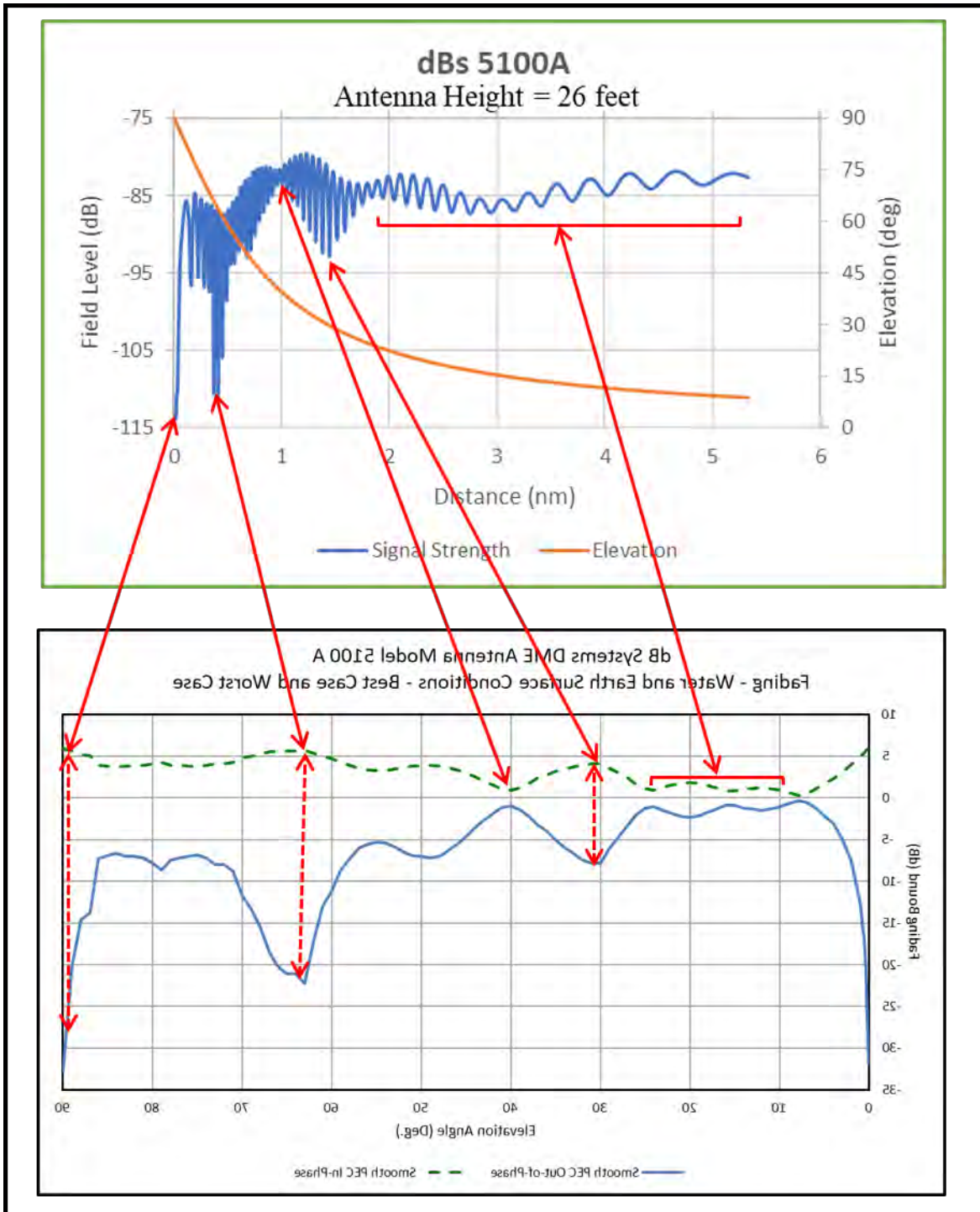


Figure 4-28. Correlation Between Level-run and Fading Bound Plots

Based on the discussion above and information presented in Reference Z, the antenna performance characteristics relevant to providing resistance to, or sufficient control of, signal fading caused by multipath effects include sufficient vertical pattern slope in the vicinity of the horizon; relatively low-level below

horizon sidelobes; and relatively high-level above the horizon sidelobes (i.e., shoulders). The relatively-low versus relatively-high condition is met when the ratio between the shoulder lobes and the sidelobes is about 2:1 (6 dB). As previously stated, additional information regarding antenna pattern requirements can be found in section 3.3 of Order FAA-E-2996.

The phrase “relatively low-level” and “relatively high-level” are used in reference to the desired sidelobe performance because the equation used to calculate the fading bound has symmetry about the horizon as shown in Figure 4-29. In this case, the equation shown considers just the vertical pattern contribution for the worst-case relative phase condition ($\phi_r=180^\circ$). At 10° , the above horizon level is nearly an order of magnitude greater than the below horizon level. The circle in the vector wheel diagram has a “small” relative radius indicating that the ground reflection multipath has “relatively” little influence compared to the direct signal (Figure 4-30(a)). At 30° , the above and below horizon levels are more comparable. The circle in the vector wheel diagram has a “large” relative radius indicating that the ground reflection multipath has “similar” influence compared to the direct signal (Figure 4-30(b)).

It is important to note that a DME antenna with exceptionally low below-horizon sidelobes will greatly minimize longitudinal multipath. The slope of the radiation pattern relative to the horizon has an influence on the fading performance at low elevation angles. A steeper slope will give an improved M/D signal strength ratio, thus better fading performance, however, this characteristic must be balanced with the requirement to provide sufficient gain at the horizon to ensure coverage at the lower service volume extremes.

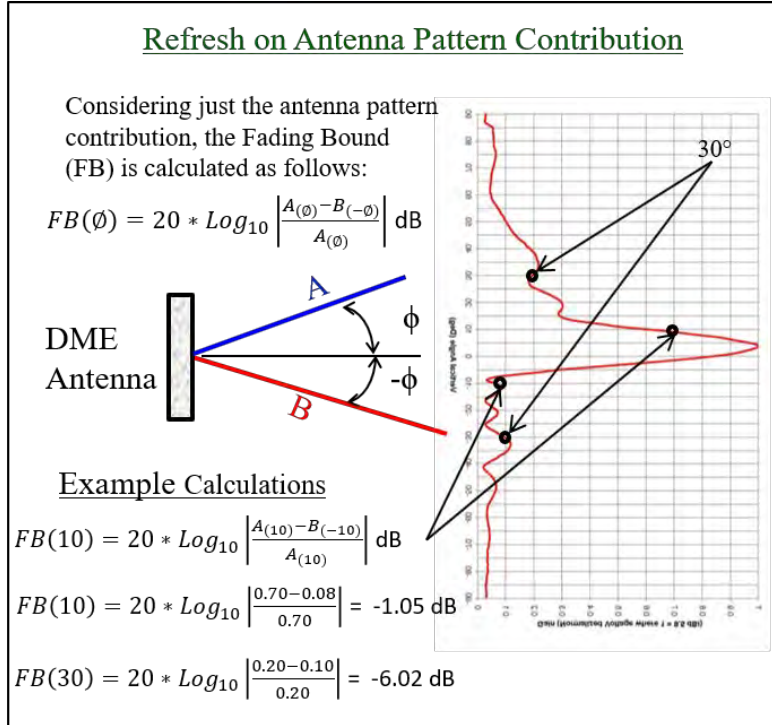


Figure 4-29. Fading Bound Equation Symmetry About Horizon

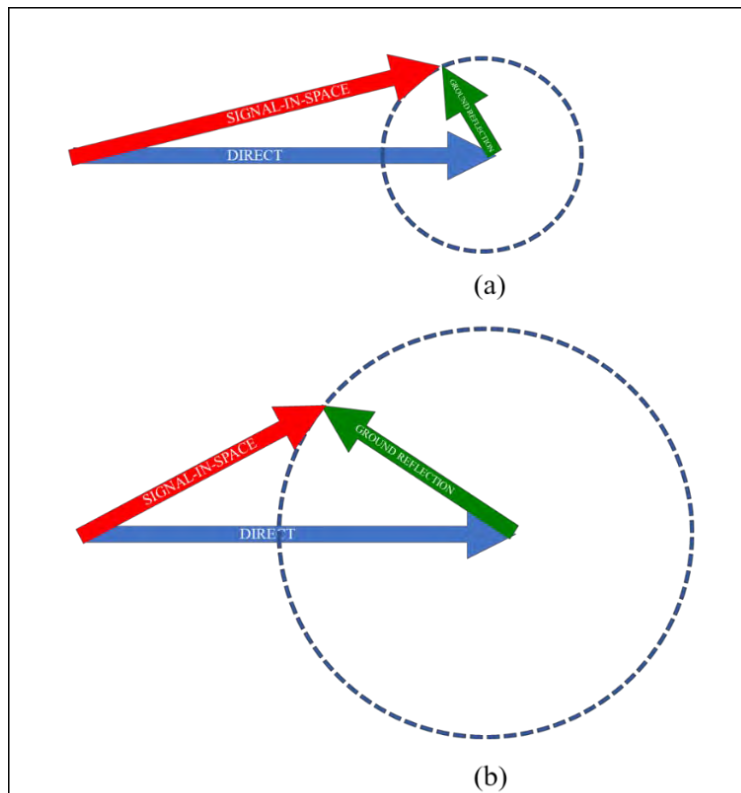


Figure 4-30. Vector Wheel Diagrams for Figure 4-31

- b. Signal Quality.** The typical DME antenna is designed for providing omni-directional coverage. Because this is the standard requirement, lateral multipath is typically handled by proper siting to ensure errors do not exceed tolerances. There may be some rare cases where large range errors in limited sectors of the service volume may be unavoidable or could be mitigated by directive horizontal patterns.

The DME antenna is mounted above the ground which means that longitudinal multipath (ground reflection) will always be a concern. DME signal fading due to this multipath is an issue, however it can be controlled by vertical pattern shaping within the design of the DME antenna. This vertical pattern shaping limits the amount of signal energy towards the ground. The effect of longitudinal multipath on accuracy is limited because the path length difference (time delay) will be limited. For example, an antenna mounted at a height of 20 feet will have an indirect signal path length that is 40 feet longer than the direct signal path (20 feet above ground) for the antenna, plus 20 feet below horizon for the image antenna). A 40-foot path difference corresponds to about 40 nanoseconds in timing error. The maximum multipath error is enclosed within the red dots at the axis origins of Figure 4-31(a) and (c). Figure 4-31(b) shows that a 40 nanosecond timing error corresponds to a DME multipath error of less than 15 feet for the in-phase condition. Figure 4-31(d) shows less than 40 feet of multipath error for the out-of-phase condition.

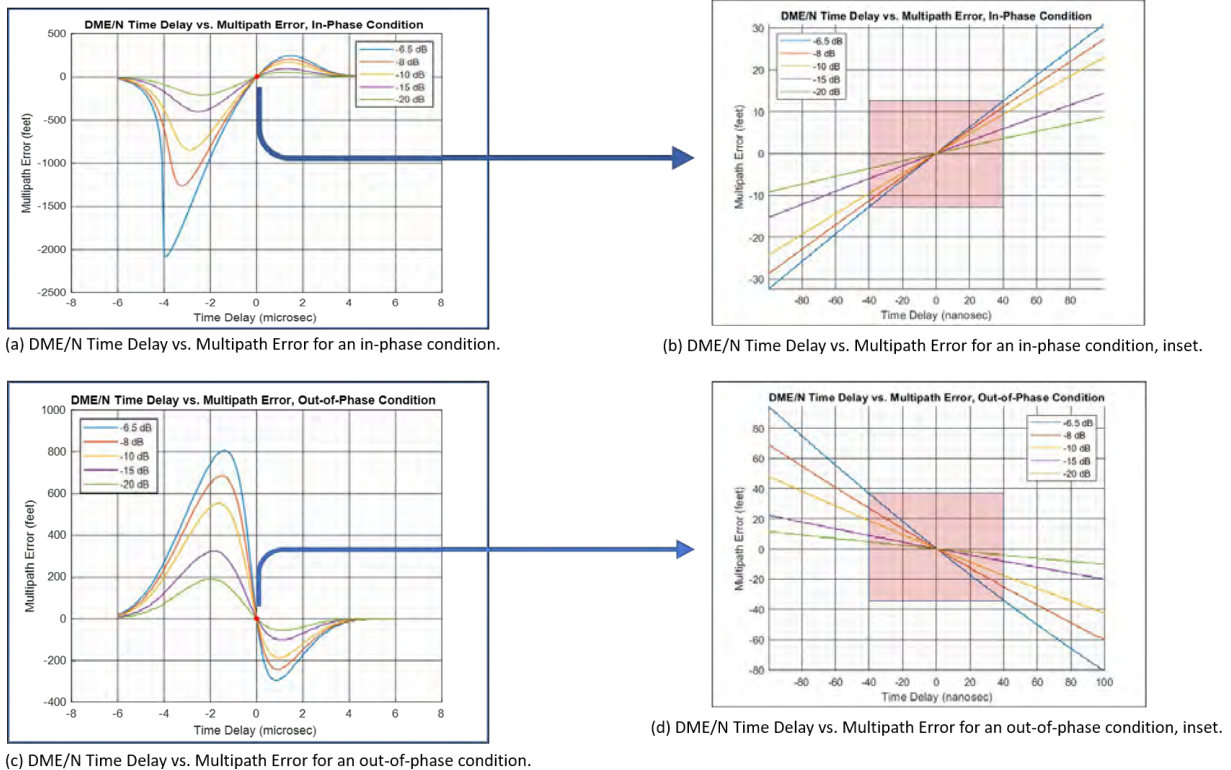


Figure 4-31. DME/N Time Delay vs. Multipath Error for an In-phase and Out-of-phase Multipath Conditions

- c. Directional Horizontal Pattern Applications.** As previously stated in Section 4.a.ii the circular nature of the DME service volumes (see Figure 3-1) requires the DME antenna to have an omni-directional horizontal pattern, which will illuminate objects in the vicinity of the DME antenna potentially producing lateral multipath. Therefore, proper site selection is the means typically used to eliminate lateral multipath or control the severity of its effects within operationally significant air space.

However, there may be rare cases where the use of a DME antenna having a directional horizontal pattern provides a means for overcoming a troublesome multipath, coverage, or spectrum engineering situation. The use of such an antenna will result in some portion(s) of the DME service volume lacking sufficient signal coverage, which may have an operational impact. For this approach to be viable, the operational benefit gained must outweigh the impact caused by the resulting coverage gap. Reference Y examined the use of bi-directional antennas to support ILS operations in frequency congested regions. Another example would be the use of a uni-directional DME antenna to support ILS operations in a “box canyon” mountainous region.

- d. Multipath Modeling.** DME multipath modeling software is available. When the software is properly utilized, it can predict the effect that various siting conditions have on DME facility performance. This modeling software is useful in predicting DME signal disturbance, whether for a new DME site that poses challenging siting conditions (mountainous terrain), an existing DME site when new construction near a DME facility has been proposed, or to compare the performance achieved by the use of different antenna models. Additional information regarding multipath models can be found in Chapter 5 and Appendix F.

Chapter 5. DME Siting Requirements

1. Introduction

The purpose of this chapter is to provide specific requirements when siting a DME facility. It also provides information on obstruction types, errors caused, and possible mitigation to the affected DME SIS. Mitigation of certain siting conditions, including antenna height and types are discussed in this chapter to help overcome adverse siting conditions.

2. Plot Purchase/Lease

It is recommended that a minimum 350 feet radius, or 700 foot by 700 foot (approximately 11 acres), plot around the DME antenna be purchased or leased by the FAA. A radius of 350 feet should provide an adequate buffer to protect the near-field for most DME installations, however, certain locations may require a larger plot to assure adequate DME performance. Reasons for the increased area required may be a result of many conditions including, but not limited to, inability to limit future encroachment, or type of DME equipment (antenna) used. To justify a smaller land purchase/lease area for the installation of a DME facility, a thorough analysis should be performed to ensure the DME SIS will be adequately protected. Refer to Chapter 6 for activities related to site acquisition.

- a. **Application to Existing DME-Only Facilities.** In order to apply this Siting Criteria to existing DME-only sites (for example, where a VOR has been decommissioned) for the purpose of reducing the required clear zone around a facility, an analysis should first be conducted. The analysis should consider the antenna type and height, as well as other site specific details necessary to determine the appropriate OCA and the plot size required to protect the DME SIS. Both the OCA cylinder (for the particular DME antenna type and site frequency) and the 1° vertical subtending angle from the base of the antenna should be protected. A survey may be necessary to evaluate the surrounding terrain and structures. Consideration should also be given to potential tree growth and future development when determining the final plot size. It should also be noted that not all antenna types currently used to provide DME service have been evaluated in the development of this Order.

3. Object Consideration Area (OCA)

- a. **Definition.** As defined in Chapter 3, Section 4, the DME OCA (see Figure 3-6) is comprised of two components, the near-field protection cylinder and the area above a 1° vertical subtending angle from the base of the antenna. The near-field protection cylinder is the area centered about the DME antenna where, ideally, all objects and structures are removed. The near-field protection cylinder is a cylindrical volume surrounding the DME antenna, and has been established to protect the near-field radiation pattern of the DME antenna since objects within this area can alter the antenna's radiation pattern. The electromagnetic properties of the radiated signal are more complex in the near-field compared to those in the far field, and consequently, the analysis of signal scattering by objects in the near-field is a complex undertaking. Therefore, the near-field should be free of all objects, except for the DME equipment

shelter, antenna, and security fence.

The OCA is also comprised of a vertical subtending angle of 1° extending upward from the base of the DME antenna, which is used to define a conical, sloped surface. All objects should be below this surface to control the effects of multipath and shadowing within the DME service volume. If the removal of all objects is not practical, then any objects located within the OCA should have their possible impact evaluated to determine the objects' effect on the DME SIS.

Table 5-1 shows the relation between the length of the DME antenna and frequency versus the size of the DME near-field protection cylinder, and is the justification for the 250 feet radius of the near-field protection cylinder. As you can see from the table if an antenna longer than 10 feet is used a corresponding increase in the near-field protection cylinder must also occur, and subsequently a larger plot may need to be purchased or leased by the FAA.

Table 5-1. Antenna Length and Near-field Protection Cylinder Distance

Antenna Length	Near-field Distance (960 MHz)	Near-field Distance (1215 MHz)
3'	17.7 feet (5.4 meters)	22.3 feet (6.8 meters)
4'	31.2 feet (9.5 meters)	39.4 feet (12.0 meters)
6'	70.2 feet (21.4 meters)	89 feet (27.1 meters)
6.5' (dB Systems 5100A)	82.3 feet (25.1 meters)	104.3 feet (31.8 meters)
8'	125 feet (38.1 meters)	158.1 feet (48.2 meters)
10'	195.2 feet (59.5 meters)	247 feet (75.3 meters)
11.5' (dB systems 540)	258.2 feet (78.7 meters)	326.8 feet (99.6 meters)
12'	281.2 feet (85.7 meters)	355.6 feet (108.4 meters)

- b. Security Fence.** The security fence should be no higher than the base of, and must be located no farther than 40 feet from, the DME antenna.
- c. Transient Obstructions.** Transient obstructions (vehicles and maintenance equipment) can be tolerated during maintenance operations in this area, as long as they are not taller than the base of the DME antenna. Transient objects that are higher than the base of the antenna should be evaluated to determine if, based on engineering judgement, the penetration may impact system performance. This evaluation should occur before the transient objects are allowed to operate in the OCA.

4. Subtending Angles

a. Vertical Subtending Angle

- i. Definition.** The vertical subtending angle is the angle between a line extending horizontally from the base of the DME antenna and a line extending from the base of the DME antenna and the top of the obstruction. Figure 5-1 illustrates this angle.

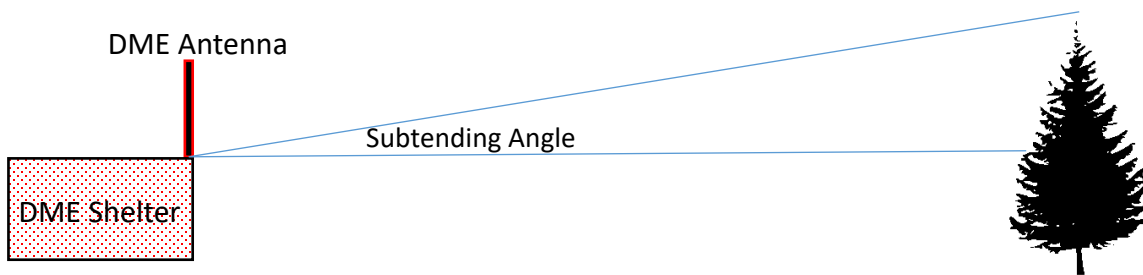


Figure 5-1. Vertical Subtending Angle Illustration

- ii. **Angle.** The vertical subtending angle from the DME antenna to any obstruction should be below 1° for all objects to minimize shadowing. Objects may be permitted to penetrate this if, based on engineering judgement and evaluation, it is determined the penetration will not impact system performance.

b. Horizontal Subtending Angle

- i. **Definition.** The horizontal subtending angle is the angle in the azimuth plane which is occupied by an object. Figure 5-2 illustrates this angle.

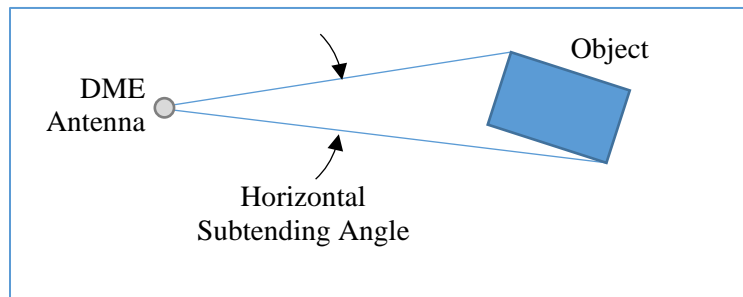


Figure 5-2. Horizontal Subtending Angle Illustration

- ii. **Angle.** The horizontal subtending angle from the DME antenna to any obstruction should be less than 1° for all objects to minimize lateral multipath and shadowing. Objects may be permitted to exceed this angle if, based on engineering judgement and evaluation, it is determined the penetration will not impact system performance.

5. Vegetation

- a. **Definition.** Vegetation is divided into two categories; trees and other. Trees, for the purposes of this document, are any naturally growing plant that has a minimum full grown height 20 feet or higher. Other vegetation is any naturally growing plant with a maximum full grown height less than 20 feet.
- b. **Trees.** Trees present a unique scattering object to the DME SIS. Multipath from a row of trees is unlikely. Trees act as attenuators to the DME signal, reducing the signal

strength to areas beyond the trees. Raising the antenna so the vertical subtending angle is less than 1° should mitigate most of the shadowing impact in the DME service volume introduced by trees. This mitigation and its consequences are discussed further in Section 10 of this chapter.

- c. **Other.** Other types of vegetation (e.g., grass, shrubs and crops) should be below the base of the DME antenna within the OCA and below a 1° vertical subtending angle beyond the OCA to minimize signal degradation. Crop irrigation equipment is discussed in Section 6.a.iii.d of this chapter.

6. Multipath

Multipath could be categorized as lateral, longitudinal, or a combination of the two. Most multipath signals will be a combination of longitudinal and lateral multipath; that is, neither strictly the longitudinal nor lateral case. Lateral and longitudinal multipath are described in the following paragraphs.

a. Lateral Multipath

- i. **Definition.** Lateral multipath occurs when the DME antenna is located in the vicinity of a reflective object as shown in Figure 5-3. Like longitudinal multipath, the DME signal arrives at the aircraft via direct and reflected paths; however, in this case, these paths are in the same horizontal plane. Examples of objects that could be the source of lateral multipath are buildings, hangars, air traffic control towers, monopoles, wind turbines, cell towers, and irrigation equipment.

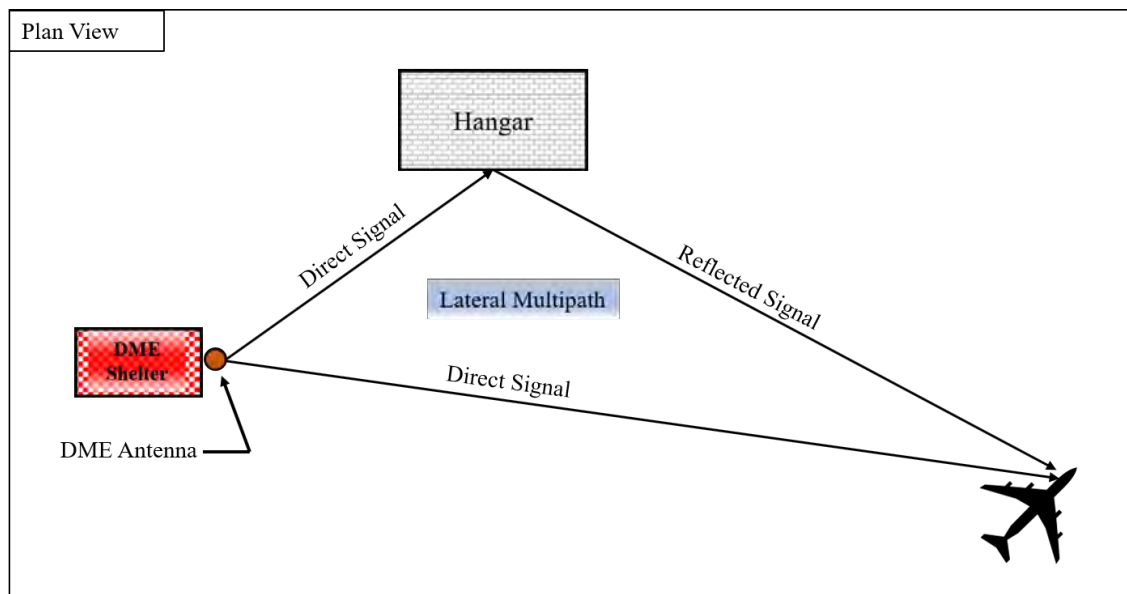


Figure 5-3. Lateral Multipath Illustration

- ii. **Issues.** Lateral multipath delays the arrival times of DME pulses potentially causing range errors or unlocks.
- iii. **Scattering Object Distance and Subtending Angle Criteria.** Table 5-2 summarizes the information in the following paragraphs. The potential impact on DME performance should be evaluated for all objects that do not meet the distance and subtending angle criteria tabulated in Table 5-2.

Table 5-2. Scattering Object Distance and Subtending Angle Criteria

Scattering Object Distance and Subtending Angle Criteria		
Object	Distance	Vertical Subtending Angle
Buildings	> 350'	< 1.0° btwn 0-5 nmi*
Wind Turbine - Single	> 2,000'	< 2.0°
Wind Turbine - Multiple	> 10,000'	< 1.0°
Solar Farms	> 350'	Below antenna base height
Irrigation Equipment	> 350'	Below antenna base height
ATCTs	> 7,000' (X-channel) > 4,000' (Y-channel)	< 1.0° (X-channel) < 2.0° (Y-channel)
Comm Towers	> 2,000'	< 2.0°
Cylindrical Structures	> 10,000' (X-channel) > 5,000' (Y-channel)	< 0.5° (X-channel) < 1.0° (Y-channel)
Other Objects	> 350'	< 1.0°

*The criteria applies for vertical and horizontal subtending angle.

- a) **Buildings.** If a building is located between 350 feet and 5 nmi from the DME facility and does not exceed the 1° vertical or 1° horizontal subtending angles, evaluation may not be necessary. However, if the siting engineer is unsure of the potential impact of a building on the DME SIS an evaluation should be performed to ensure adequate protection of the DME SIS. Buildings beyond 5 nmi need not be evaluated unless, based on engineering judgement, it is deemed the structure may impact system performance.
- b) **Wind Turbines.** The shaft and nacelle of the wind turbines are the main components that cause lateral multipath for DMEs. A single wind turbine near a DME is allowed if it is greater than 2,000 feet from the DME and under 2° vertical subtending angle. As the number of wind turbines increases the SIS performance of the DME decreases. Multiple wind turbines must be farther than 10,000 feet from the DME and below 1° vertical subtending angle. Multiple wind turbines constitute a group of more than one wind turbine which are separated by 2,000 feet or less. The analysis used to derive these criteria is found in Section 3.a of Appendix F.
- c) **Solar Farms.** Systems installed beyond 350 feet from, and wholly below the base of the DME antenna and outside the OCA should not create any significant lateral multipath issues to the radiating DME signal. Solar farms not installed wholly below the base of the antenna should be evaluated for DME system impact. If any solar panel structures are located above the base height of the antenna, then these

structures must be evaluated either through engineering analysis, math modeling, or both. The analysis used to derive these criteria is found in Section 3.b of Appendix F.

- d) **Irrigation Equipment (Center Pivot).** Systems installed wholly below the base of the DME antenna and outside the OCA should not create any significant lateral multipath issues to the radiating DME signal. Irrigation systems within 350 feet of the DME and not installed wholly below the base of the antenna and systems should be evaluated for DME system impact. This evaluation should be conducted through engineering analysis, math modeling, or both. The analysis used to derive these criteria is found in Section 3.c of Appendix F.
- e) **Air Traffic Control Towers (ATCTs).** ATCTs are likely to be encountered at prospective DME sites particularly for on-airport DMEs. The impact of ATCTs on DMEs is highly dependent on the channel type of the DME. Y-channels are more immune to ATCTs impact due to the larger pulse-spacing. For X-channel transmitters, ATCTs must be under a 1° elevation angle measured from the base of the DME antenna and farther than 7,000 feet from the DME. For Y-channel transmitters, ATCTs must be under 2° elevation angle measured from the base of the DME antenna and farther than 4,000 feet from the DME. The analysis used to derive these criteria is found in Section 3.d of Appendix F.
- f) **Communication Towers.** Communication antenna towers may be encountered at DME sites, particularly if they are off-airport. Monopole or lattice antenna towers must be no closer than 2,000 feet from the DME. Beyond that, monopole or lattice antenna towers must be under 2° elevation angle measured from the base of the DME antenna. The analysis used to derive these criteria is found in Section 3.e of Appendix F.
- g) **Cylindrical Structures.** Lateral multipath resulting from large cylindrical structures (diameters larger than 20 feet) is particularly problematic since it scatters the signal over a wider angular sector compared to flat surfaces, which causes errors in a larger part of the service volume. For X-channel transmitters, large cylindrical structures must be under a 0.5° elevation angle measured from the base of the DME antenna and farther than 10,000 feet from the DME. For Y-channel transmitters, large cylindrical structures must be under 1° elevation angle measured from the base of the DME antenna and further than 5,000 feet from the DME. The analysis used to derive these criteria is found in Section 3.f of Appendix F.
- h) **Other Objects.** If objects not mentioned above are greater than 350 feet from the DME antenna and do not penetrate the 1° vertical and horizontal subtending angles, they need not be evaluated.

b. Longitudinal Multipath

- i. **Definition.** Longitudinal multipath occurs when the direct and reflected signals are in the same vertical plane, which typically arises when the DME antenna is placed over a large flat surface commonly referred to as a ground plane. This scenario is illustrated in Figure 5-4, with the direct (i.e., LOS path) and reflected signal paths noted. Examples of objects that could be the source of longitudinal multipath are flat earth, an antenna counterpoise, solar farms, or center-pivot irrigation equipment located radially from the DME facility antenna.

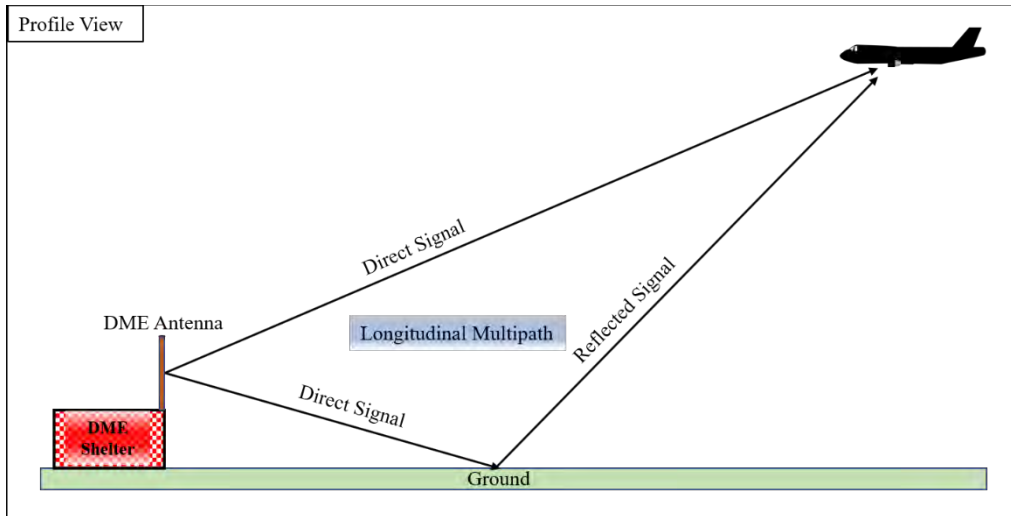


Figure 5-4. Longitudinal Multipath Illustration

- ii. **Issues.** Depending on the phase, the multiple paths can arrive either in-phase or out-of-phase at the aircraft, which determines if the effect is constructive interference leading to increased signal strength (lobes), or destructive interference leading to decreased signal strength (nulls), respectively.
- iii. **Causes.** Raising the antenna may have the adverse effect of increasing longitudinal multipath. Care should be taken to consider this effect prior to raising the antenna height to overcome certain siting conditions.
- iv. **Terrain Irregularities.** The impact of longitudinal multipath is highly dependent on the topology of the surrounding terrain. This section highlights the impact of five common terrain topology features that may be encountered at DME sites. The impact was determined by modeling each terrain topology and comparing the signal strength taken along the profile to that of a perfectly flat terrain. The reflection properties of the terrain were of average land with a relative permittivity value of 11, and a conductivity of 0.03 Siemens per meter (S/m).

- (a) **Two-level Flat.** Figure 5-5 illustrates two flat portions of terrain at two different elevations. In this topology the DME is located on the higher plane. The signal strength pattern of the two-level flat topology shows that an additional major null is introduced, compared to the flat plane topology, as a result of the second flat plane at the lower elevation.

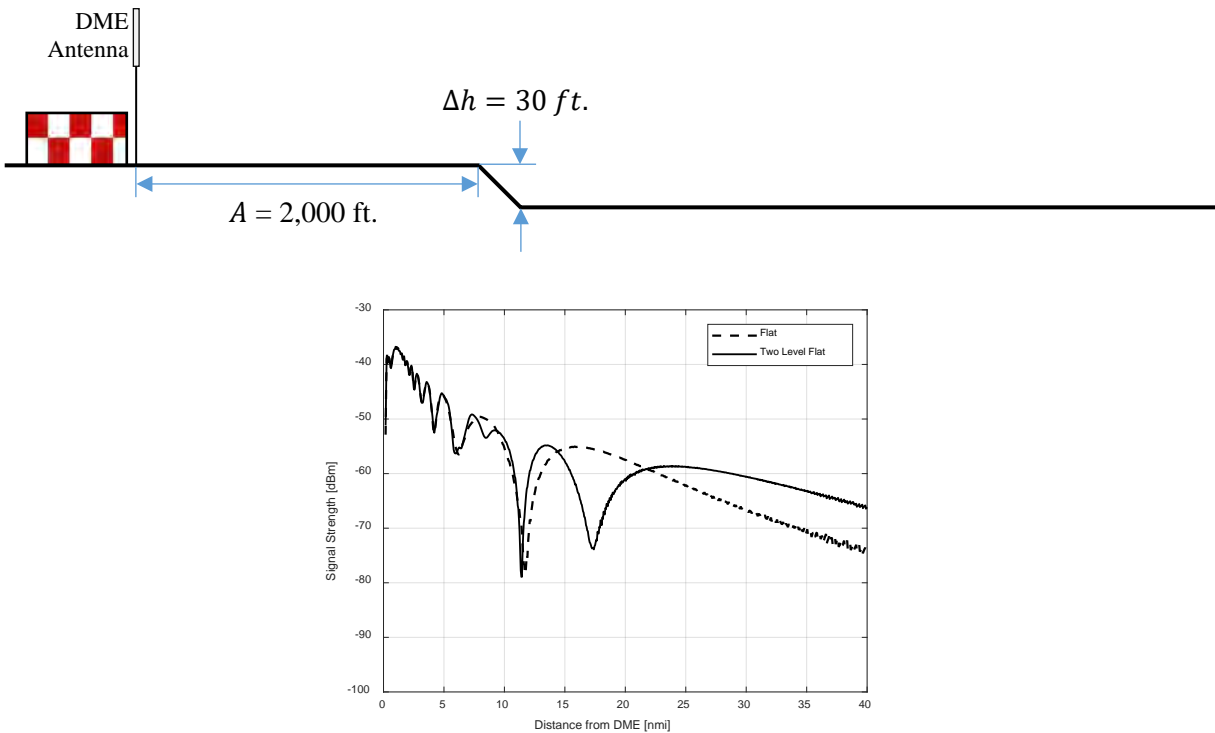


Figure 5-5. Two-level Flat Terrain

(b) **Two-level Up-Slant.** In Figure 5-6 the top level is flat and the bottom level slants up with elevation increasing as distance from DME increases. The signal strength pattern of the two-level up-slant topology shows additional nulls compared to the flat plane topology. For this topology, the nulls are deeper, more numerous, and narrower over the flat plane topology.

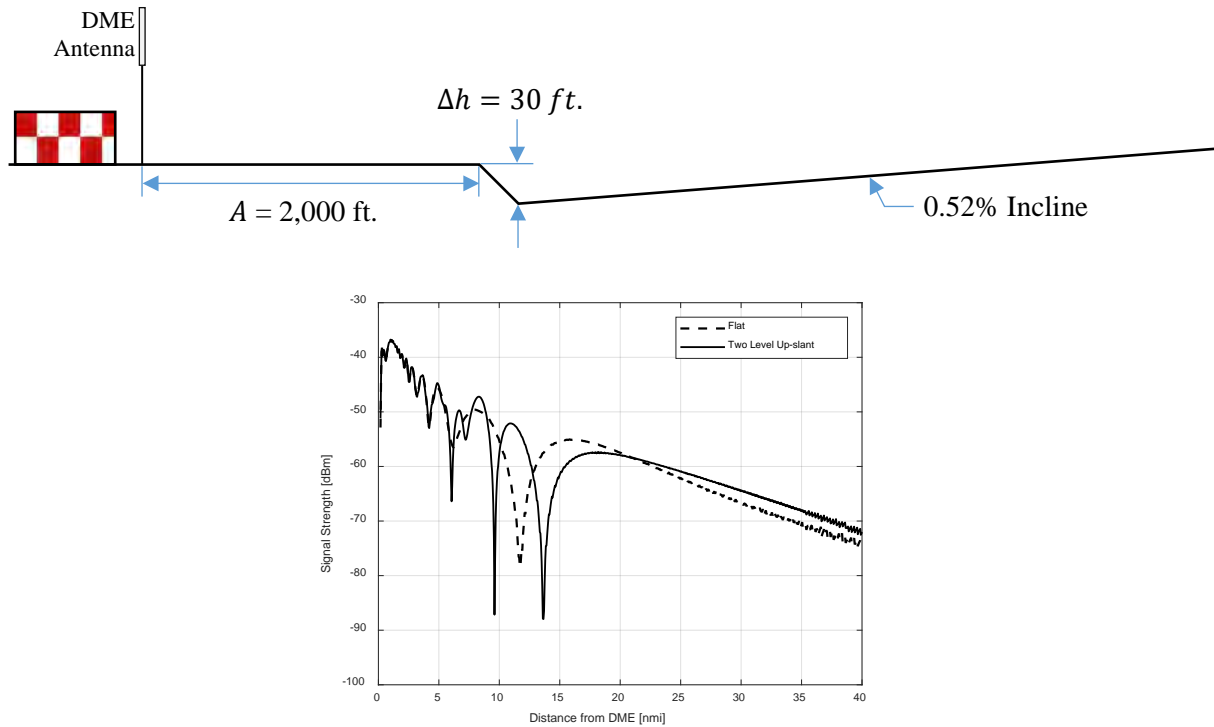


Figure 5-6. Two-level Up-Slant Terrain

- (c) **Two-level Down-Slant.** Figure 5-7 is similar to the previous topology with the exception of the bottom level, which slants down instead of up. The signal strength pattern of the two-level down-slant topology shows fewer and shallower nulls compared to the flat plane topology. Additionally, the signal strength shows improvement at the limits of coverage.

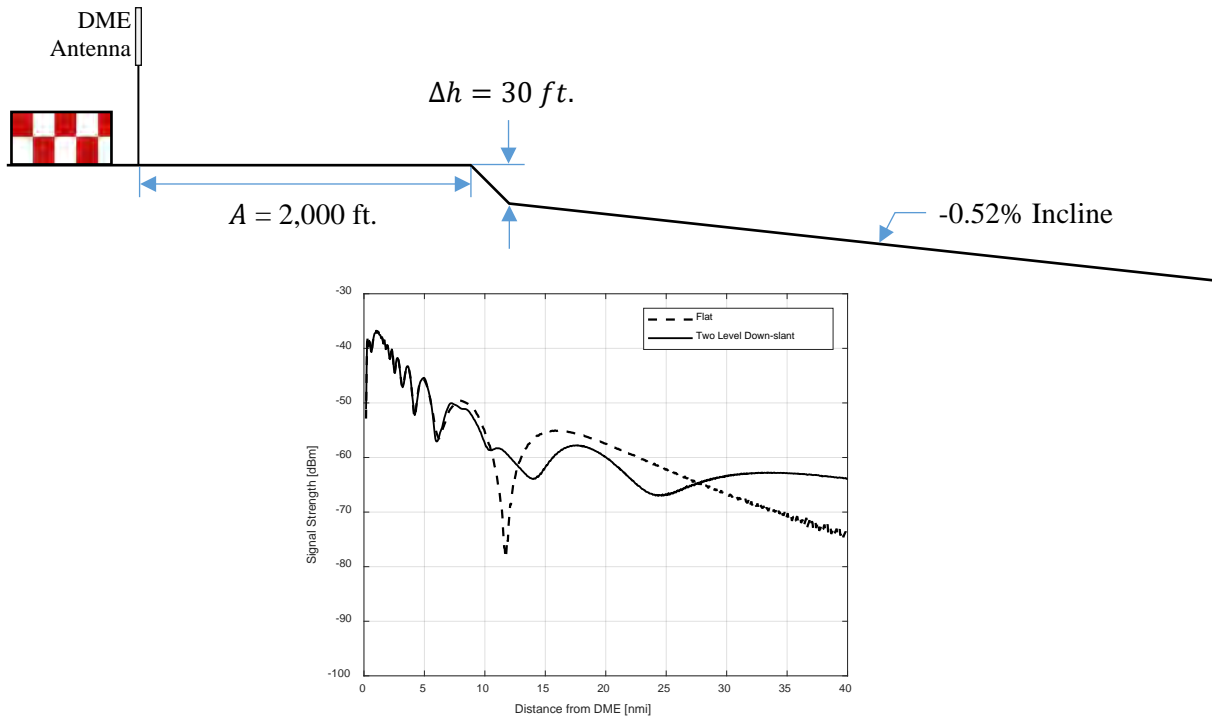


Figure 5-7. Two-level Down-Slant Terrain

(d) **One-level Up-Slant.** In Figure 5-8 a single level of terrain is flat until a certain distance then slants upwards. The signal strength pattern of the one-level up-slant topology shows the same number of nulls compared to the flat plane topology. The main null is shifted towards the DME and the signal strength past the null towards the limits of coverage is decreased.

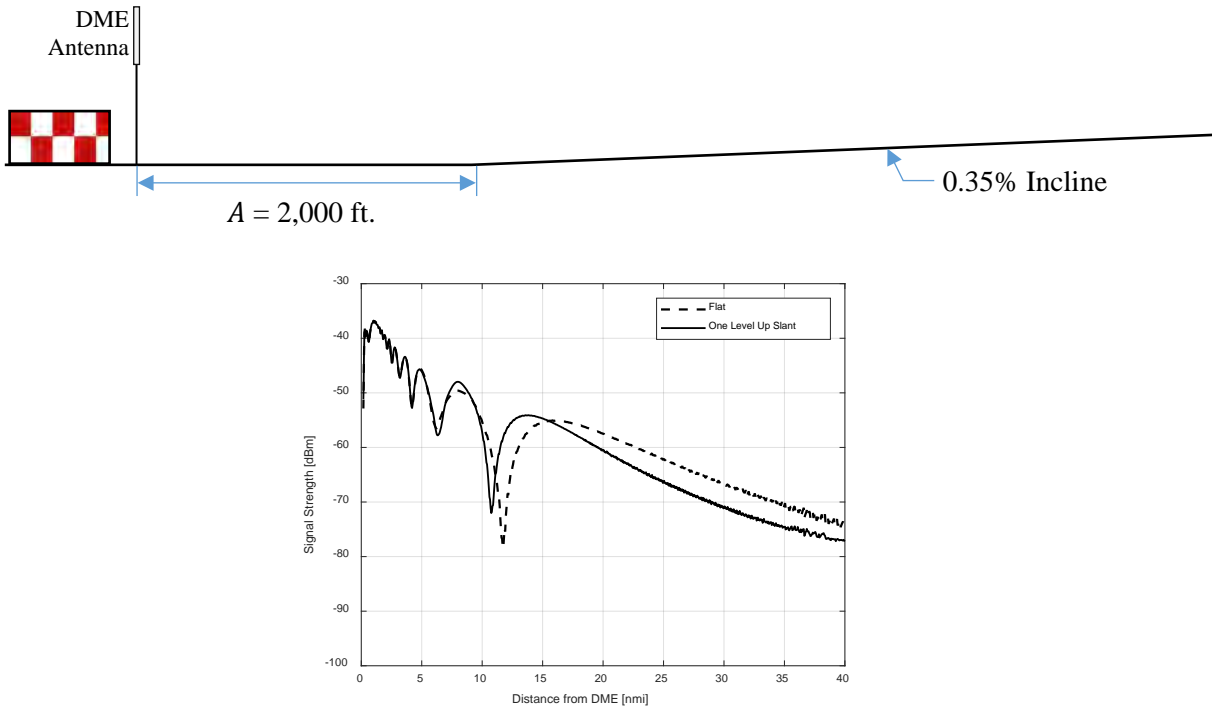


Figure 5-8. One-level Up-Slant Terrain

- (e) **One-level Down-Slant.** Figure 5-9 is similar to the previous topology except the slant direction is downward instead of upward. The signal strength pattern of the one-level down-slant topology shows the same number of nulls compared to the flat plane topology. The main null is shallower than the flat topology, and the signal strength past the null towards the limits of coverage is increased.

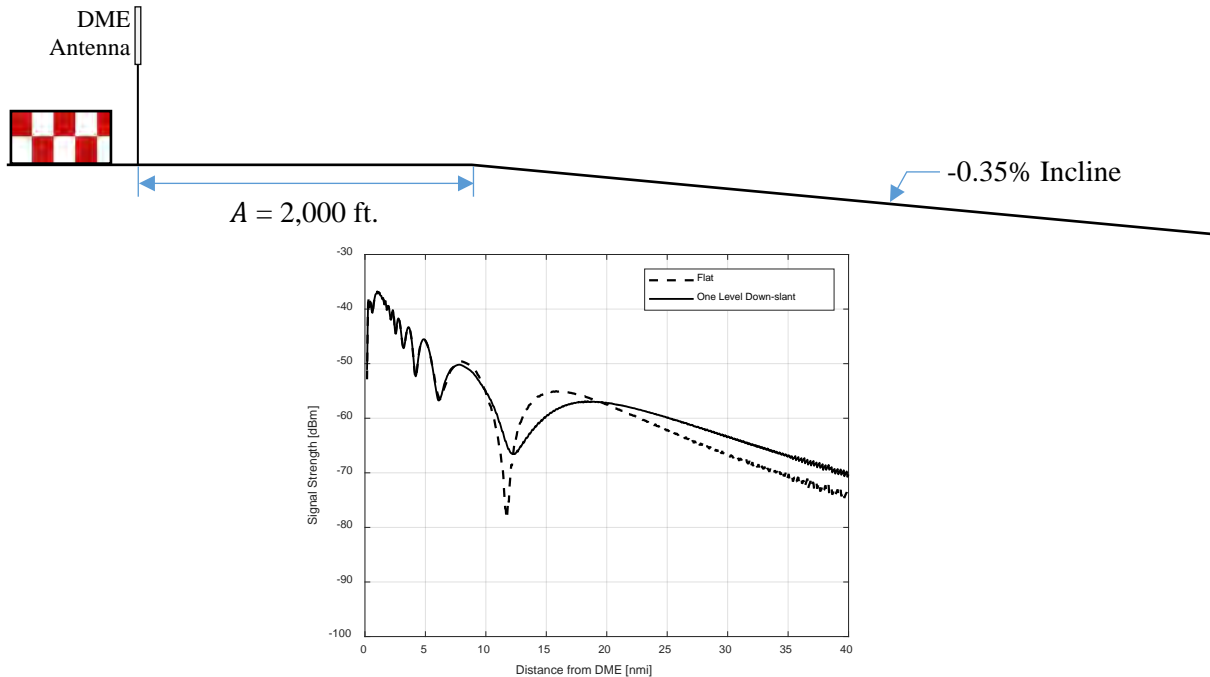


Figure 5-9. One-level Down-Slant Terrain

- (f) **Discussion.** The analysis of the modeling revealed that as the number of horizontal surfaces increases so does the number of vertical pattern lobes. Additionally, the magnitude or depth of the lobes was primarily dependent on whether the terrain sloped up or down from the facility. Up-sloping terrain showed increased null depths and down-sloping terrain showed decrease null depths. Other factors that influence the depth of the nulls are the roughness of the horizontal surfaces as well as the reflection properties. These scenarios are analogous to sites having two different antenna heights with the effective height for any one multipath geometry being dependent on which plane contains the specular reflection point.

- v. **Terrain Selection.** The topology that shows best performance in terms of longitudinal multipath is any variation of terrain sloping downwards as you get further away from the DME. In presence of irregular terrain, the DME should be installed at the highest point in the area of interest.
- vi. **Solar Farms.** The impact of solar farms is predominantly observed in terms of longitudinal multipath. Solar farm installations that are at ground level and below the antenna height show a slight benefit to DME performance in that they curb the negative effects of longitudinal multipath. The analysis used to derive these criteria is found in Section 2.b of Appendix F.

7. Shadowing/Blockage

- a. **Definition.** Shadowing is the blockage of the LOS from the ground station to the receiving aircraft by objects such as large buildings, trees, or terrain features.
- b. **Issues.** The effect of shadowing is generally reduced signal strength. This is particularly important at the limits of coverage where any additional signal strength drop will likely translate to loss of lock. The most common causes of shadowing for DME ground stations are trees, large objects, and terrain. While reduced signal strength is the primary result of shadowing, it can also amplify the effects of multipath in areas where the direct signal is attenuated by the shadowing feature and the multipath signal has a clear LOS to the aircraft. A detailed discussion on shadowing/blockage can be found in Chapter 3 and Appendix C.

8. Orientation/Plumb

- a. **Orientation.** Orientation is only significant to DME antenna installations where a uni-directional or bi-directional antenna will be installed. The main beams of these antennas should be centered on the region of coverage the DME is to service. These antennas can be adjusted so potential scatterers are not illuminated by the DME SIS to minimize multipath.
- b. **Plumb.** It is critical that all DME antennas be installed plumb (without a tilt). Since the DME antenna is already broadcasting at an angle (3° to 7°), any additional tilt (positive or negative) may reduce the service volume of the DME or illuminate scatterers that would have otherwise not been illuminated, creating multipath where none would be if the antenna was installed plumb.

9. Determining Origin of Potential Multipath Errors in Flight Inspection Data

There are techniques which can identify the origin of multipath errors. One technique uses the measured delay of the multipath signal relative to the direct signal and aircraft position of observation. This technique requires specialized, but available, flight inspection equipment that can measure the pulses of the DME signal during flights. Using this information, an ellipse can be plotted using a mapping program that will identify possible locations for multipath reflections. The path is then reviewed for reflecting surfaces. This

is not an exact process, but helps focus the search effort. This method is discussed in detail in Appendix E.

10. Mitigation of DME Siting Issues

While protection of the entire service volume of a DME is important, it must be realized that this will not always be possible and some impacts to DME performance will have to be accepted. It is vital that the siting engineer understand which portions of the DME service volume are operationally significant. This section describes some steps the siting engineer may take in order to mitigate certain siting issues.

- a. **Definition.** Mitigation is the process of trying to reduce the severity of impact of site conditions to the DME SIS by deviating from standard DME antenna installation practices.
- b. **DME Use and Mitigation.** While a perfect site with no obstructions is ideal, it is also unlikely for this condition to exist, and the siting engineer must realize that a large part of mitigation centers on the specific use of the DME. When deciding where to install a DME, and before any mitigation efforts are undertaken, the siting engineer must evaluate the intended use of the DME being installed. Knowledge of the operationally significant portions of the DME service volume will assist the engineer in determining whether a site is adequate to provide the desired DME performance.
 - i. **Terminal DME (Low Power).** If a low power DME is to be installed at a particular site, the main concern for the siting engineer is that the DME provides proper range information along all published procedures that use the DME for navigation information. While proper DME guidance is desirable within the whole terminal area service volume, this may be unachievable in the current environment. In such cases the siting engineer, should make sure all operationally significant procedures will be supported by the DME, and the engineer should utilize all tools available to them to determine the best location to install the DME to maximize performance, at a given site. The DME must provide accurate range information along all published procedures where the DME is used for position information.
 - ii. **En Route DME (High Power).** For high power DME installations the siting engineer's main concerns are terminal, en route, and DME/DME RNAV DME signal coverage. In this case the engineer must evaluate all procedures the DME is being installed to support and also RNAV coverage gaps the DME is being installed to fill. In both instances, the DME should first be evaluated for the areas intended to be serviced by the DME (terminal procedures and RNAV coverage).
- c. **Antenna Type.** Different DME antennas are available to help the siting engineer mitigate certain adverse siting conditions. These include uni- and bi-directional antennas as well as 7° antenna types. Details about these antennas and their uses are found in Chapter 4 and Appendix D of this document.

- d. Antenna Height.** The height of the DME antenna is one of the most powerful mitigation tools the siting engineer can use to overcome siting challenges. Compared to other navigation systems, DME antennas are compact and versatile allowing for installation at a wide range of heights. Raising the antenna generally reduces the impact of lateral multipath. Consequently, raising the antenna may introduce lobing in the vertical pattern of the antenna. The siting engineer should be aware of this trade-off and use it to achieve maximum coverage at a given site.
- i. Lateral Multipath Mitigation.** Increasing the antenna height has multiple benefits for lateral multipath. First, the amount of radiation that strikes an object that would cause lateral multipath decreases as the antenna height increases. This has the benefit of reducing the M/D ratio thereby reducing the impact of the multipath. Also, the vertical component of the reflection angle decreases as the antenna height increase, which reduces the area where multipath is observed. Additional information on lateral multipath can be found in Chapter 3 and Chapter 4, as well as Appendix C and Appendix D.
- ii. Longitudinal Multipath Mitigation.** The main parameters that influence the nulls are the height and radiation pattern of the antenna, and the surrounding ground properties. In order to keep longitudinal multipath to a minimum, engineers should avoid heights between 30-50 feet, particularly at sites that have large area of flat terrain around the facility. Sites surrounded by irregular terrain are less susceptible to fading since the reflections from the terrain are more dispersed. Another longitudinal multipath mitigation technique is trapping the null-producing ray. Figure 5-10 shows an illustration of a two-ray model that contains trees, which prevent the ground-reflected ray from combining with the direct ray to produce the null. Additional information on longitudinal multipath is discussed in Chapter 4.

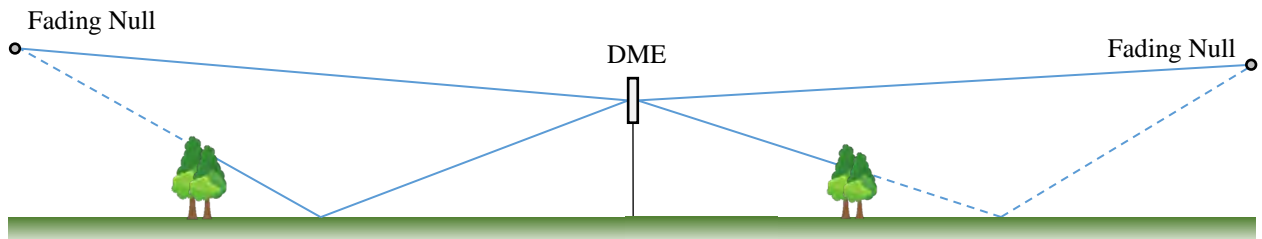


Figure 5-10. Illustration of Obstruction of Longitudinal

- e. Consequences of Mitigation.** Some mitigation efforts may lead to undesirable effects. These include, but are not necessarily limited to:
- i. Nulls.** As the antenna is raised to reduce the subtending angle to certain obstructions, nulls may be created in areas of no obstructions, resulting in degradation of service.

- ii. **Loss of Service Volume.** If alternative antennas are used (i.e., 7° antenna) loss of service volume at lower elevations may occur. Uni-directional and bi-directional antennas limit the coverage of the DME SIS. This will result in severely limited service volumes because much of the service area will not receive the DME SIS. These antennas should only be used in unique situations for en route DME installations. They may be used for terminal DME installations to overcome local adverse siting conditions especially where the main concern is the local terminal area and approach procedures.

Chapter 6. Site Selection, Project Engineering and Facility Establishment

1. Procedure for Site Selection

- a. **General.** The selection of a suitable site for a DME facility is primarily a function of performance and cost. No candidate site should be selected that does not satisfy the minimum performance requirement at a cost commensurate with the benefit to be received. Primarily, this order provides the siting engineer with techniques for estimating site performance and the effect on performance of various corrective measures. This chapter presents a methodology for selecting a DME site that meets the performance requirements of the system and the cost limitations of the program. Although detailed performance or cost estimates are beyond the scope of this order, a good first approximation is required for site selection and acquisition.
- b. **Initial Locality.** The DME type, whether terminal or en route, initially determines the general location of the DME facility. The location of a terminal facility is constrained by the actual location of the airport and the RNAV terminal procedures the DME will support. The location of en route facilities is determined largely by RNAV coverage gaps, but also by the location of the airways the DME serves and the RNAV procedures the DME may support.

2. Preliminary Survey

- a. **Map Survey.** Once the general location has been determined, candidate sites may be identified from Digital Elevation Models (DEMs) obtained from the U.S. Geological Survey of the Department of the Interior or other online topographic mapping tools. These map studies will identify, as accurately as possible, the coordinates of the candidate sites and the locations of triangulation points or other control points. These points will permit establishment of an accurate baseline and verification of coordinates in the field.
- b. **Office Survey.** The initial office survey should develop a candidate site and several alternative sites, if possible. This will save the cost and time of additional field trips if the primary candidate is determined to be unsuitable or unavailable. If the installation is to be within an existing facility, all available engineering drawings describing the site should also be assembled. Other information that does not require a site visit may also be compiled at this time. This includes some or all of the following:
 1. Ownership characteristics of the land, particularly name and address of owner(s); easements, rights-of-way or other use limitations; and zoning or use restrictions imposed by the local political jurisdictions.
 2. The possibility of using Government-owned land and existing facilities should be investigated at this time.
 3. Location of the proposed facility with respect to any nearby town or airport, roads, utility lines, and boundary lines in the vicinity.

4. Local utilities' plans for new or upgraded lines near the proposed sites and local planning districts' long-range plans that might impact these sites.
5. Site elevation should be considered, and care should be taken not to select a site that is significantly lower than the surrounding terrain.

c. Real Property Planning and Acquisition. The real property acquisition office should be advised of tentative sites so that they may initiate preliminary negotiations with property owners for use of the land.

3. Preliminary Report

a. Contents. After the information obtained in the preliminary survey has been carefully analyzed, the project engineer will prepare a report summarizing the results of the survey. The report will recommend the appropriate DME system and antenna type. It should also provide the potential locations necessary to achieve satisfactory operation. In addition, the report should include a prediction (including confidence level) of the expected performance of the facilities based on the presence of reflection sources and terrain conditions in the vicinity, and describe other problem areas or operational limitations which may affect the DME establishment. The report should recommend site testing when it is difficult to predict accurately the quality of a facility's performance. The preliminary report will also include the analysis and recommendations regarding site acquisition by the Real Property Acquisition office.

b. Concurrence. The preliminary report will be coordinated with all concerned organizations (e.g., Flight Procedures, Airports, and Technical Operations). Any non-concurrence, objections, or reservations will be resolved. For example, if the report indicates that it would not be possible to attain unrestricted DME performance, it may be necessary to compromise between the cost of selecting another site and the extent to which degraded performance may be accepted. Any changes to the preliminary report and its recommendations should be incorporated into the report.

4. Final Engineering Activities

Once concurrence of the preliminary report has been obtained, the final project engineering activities may commence. These include:

1. Determining the exact location of the DME facility.
2. Coordinating with the Real Estate Contracting Officer (RECO) to ensure access and rights for permanent or long term (or short term for site testing) have been established.
3. Scheduling the installation of any power cables, control and monitoring lines to the site.
4. Coordinating special engineering to overcome peculiar siting conditions. This includes arranging for removal or repositioning of potential interference sources.
5. Preparing instructions for the field installation engineer. This includes the DME antenna type, and special instructions and/or tests to overcome degrading site conditions.

5. Site Testing

It is not necessary or practical to conduct site tests at all locations. Modern modeling software can predict the effect of various siting conditions on facility performance. There will be locations where site testing may be practical and advisable, for example, a highly congested area where interference sources make it impossible to predict facility performance with high confidence. If site testing is required, it should be deferred until at least preliminary site improvement and obstruction removals have been completed.

- a. **Portable DME.** When practical, a portable DME may be utilized to evaluate a potential DME site. If necessary, this should be done during the final engineering activities, after initial Math Modeling indicates the site may require further evaluation.
- b. **Computerized Math Models.** Computerized math models are available and usable by personnel with a wide variety of experience levels; however, engineering knowledge of, and judgment about, the appropriate assumptions and limitations of the various models are required when applying such models to specific multipath environments.
 - i. **New Facility Math Modeling.** For new siting, and particularly for challenging siting conditions, siting engineers with little modeling and validating field experience should be cautious about performing their own modeling. It is recommended that these engineers seek modeling assistance from the FAA William J. Hughes Technical Center (WJHTC), outside engineering sources, or other more experienced FAA engineers for peer review of modeling results before making siting recommendations.
 - ii. **Existing Facility Math Modeling.** Where a DME has been installed and found satisfactory, computers and simulation techniques can be employed to predict the probable extent of DME disturbance, which may arise as a result of proposed new construction. Wherever possible, the results of such computer-aided simulation should be validated by direct comparison with actual flight measurements of the results of new construction. Again, it is recommended that the engineer with little modeling and validating field experience should seek modeling assistance from the WJHTC, outside engineering sources, or other more experienced FAA engineers.
 - iii. **Accuracy of Model Inputs.** When performing a DME modeling study, the accuracy of the inputs for scatterer definition are extremely important due to the DME wavelength. The short wavelengths of the DME signal means smaller objects impact the DME SIS as compared to longer wavelength NAVAIDs (e.g., VOR and ILS), therefore errors in scatterer definition will have significant impact to the model results and may, in fact, cause the siting engineer to make errors in judgement.
- c. **DME Computer Modeling Tools.** Several DME modeling tools exist to help the FAA engineer determine site effects on the DME SIS. These models should be used to help predict DME SIS performance at the selected site. These modeling tools include, but are not limited to the following:

- i. **FAA Navigation and Landing Branch High Fidelity DME model.** The FAA Navigation and Landing Branch developed a high fidelity DME model to help create the siting criteria contained in this document. The model can accurately predict DME SIS performance in the presence of scattering objects. Appendix F contains additional information on FAA DME Math Modeling capabilities. Detailed information about the FAA DME model and the efforts involved in validating the model can be found in Reference V.
- ii. **FAA Intranet Radio Coverage Analysis System (iRCAS).** The iRCAS is an application originally designed by the FAA Computer Aided Engineering Graphics (CAEG) group and is managed by the FAA Spectrum Engineering Group. The iRCAS application uses the limits of coverage profiles, as well as the formulaic definitions of the Radio LOS, Free Space Loss, and the IF-77 and ITM Electromagnetic Wave Propagation Model for most of the analysis modules integrated into the application. More information about iRCAS may be obtained from the FAA Spectrum Management Office.
- iii. **Ohio University Navaid Performance Prediction Model (OUNPPM).** OUNPPM has DME modeling capabilities that, as of the writing of this document, have not been validated for use by FAA personnel.
- iv. **DME RNAV Service Map (DRSM).** The DRSM is a web-based application developed by the FAA Navigation and Landing Branch available to FAA personnel to assess DME/DME RNAV service throughout the NAS. Users will be able to view near real-time DME/DME RNAV service through a browser within the FAA mission support network. The primary application is to provide a read-out of the percentages of redundant DME coverage, single DME coverage, and no DME coverage along with a list of critical DMEs for a given snapshot of service across the NAS. The tool allows one to account for, and determine impact of, planned and unplanned DME maintenance or outages. The application uses criteria set forth in AC 90-100A to determine RNAV coverage at all locations in the CONUS.

Appendix A. Acronyms

Acronym	Description
AC	Advisory Circular
ACY	Atlantic City Airport
AGL	Above Ground Level
ATC	Air Traffic Control
ATCT	Airport Traffic Control Tower
CAEG	Computer Aided Engineering Graphics
CFR	Code of Federal Regulations
CONUS	Contiguous United States
COTS	Commercial-of-the-Shelf
dB	Decibel
dBm	Decibel Milliwatts
dBs	dB Systems, Inc.
DAC	Delay-Attenuate-Compare
DEM	Digital Elevation Model
DH	DME High Altitude
DL	DME Low Altitude
DME	Distance Measuring Equipment
DME/N	DME Normal
DME/P	DME Precision
FAA	Federal Aviation Administration
FI	Flight Inspection
FKP	Fresnel-Kirchhoff Parameter
FL	Flight Level
GNSS	Global Navigation Satellite System
GPS	Global Positioning System
GS	Glide Slope
HFSS	High Frequency Structure Simulator
HPBW	Half Power Beam Width
HPDME	High Power DME
Hz	Hertz
I/O	Input/Output
ILS	Instrument Landing System
IRCAS	Intranet Radio Coverage Analysis System
IRU	Inertial Reference Unit
KML	Keyhole Markup Language
LOC	Localizer
LOS	Line-of-Sight
LPDME	Low Power DME
M/D	Multipath-to-Direct
MSL	Mean Sea Level
MHz	Megahertz
MOPS	Minimum Operational Performance Standards

Acronym	Description
NAS	National Airspace System
NAVAID	Navigational Aid
NCP	NAS Change Proposal
NMI	Nautical Mile
NSG	Navigation Service Group
OCA	Object Consideration Area
OU	Ohio University
OUNPPM	Ohio University Navaid Performance Prediction Model
PBN	Performance Based Navigation
PEC	Perfect Electric Conductor
RECO	Real Estate Contracting Officer
RF	Radio Frequency
RMLS	Remote Monitoring and Logging System
RMS	Root Mean Square
RNAV	Area Navigation
μS	Microsecond
SARPS	Standards and Recommended Practices
SBR	Shooting and Bouncing Rays
SIS	Signal-in-Space
S/M	Siemens per Meter
SSV	Standard Service Volume
TACAN	Tactical Air Navigation
TERPS	US Standard for Terminal Instrument Procedures (FAA Order 8260.3)
TOA	Time of Arrival
VHF	Very High Frequency
VOR	VHF Omni-directional Range
VORTAC	Very High Frequency Omni-directional Range Collocated Tactical Air
VSWR	Voltage Standing Wave Ratio
W	Watts
WJHTC	William J. Hughes Technical Center
WUSMA	Western United States Mountainous Area

Appendix B. Reference Documents

- A. FAA Order E-2754, Purchase Description, “DME Ground Station Antenna,” June 20, 1985.
- B. FAA Order 6820.10, “VOR, VOR/DME, and VORTAC Siting Criteria,” April 17, 1986.
- C. FAA Order E-2828a, “Antenna System, TACAN,” January 10, 1990.
- D. FAA Order STD-022d, “Microwave Landing Systems (MLS) Interoperability and Performance Requirements,” October 15, 1991.
- E. FAA Order 6830.5, “Criteria for Siting Microwave Landing Systems (MLS),” July 22, 1993.
- F. FAA Order 6480.7, “Airport Traffic Control Tower and Terminal Radar Approach Facility Design Guidelines,” April 11, 2004.
- G. FAA Order G-2100H, FAA Specification, “Electronic Equipment, General Requirements,” May 9, 2005.
- H. FAA Order E-2996, “Performance Specification for Distance Measuring Equipment (DME),” April 1, 2008.
- I. FAA Order JO 6730.2, “Maintenance of Distance Measuring Equipment (DME) Facilities,” November 13, 2009.
- J. FAA Order 6884.1, “Siting Criteria for Ground Based Augmentation System (GBAS),” December 15, 2010.
- K. FAA Order 6750.16E, “Siting Criteria for Instrument Landing Systems,” April 10, 2014.
- L. FAA Order 8200.1D, “US Standard Flight Inspection Manual (USSFIM),” November 6, 2016.
- M. FAA Order 8260.3 “United States Standard for Terminal Instrument Procedures (TERPS),” February 16, 2018.
- N. FAA, “Final Program Requirements Document (fPRD) for the NextGen Distance Measuring Equipment (DME) Program,” Version 1.1, May 13, 2020.
- O. FAA, Advisory Circular AC 150/5300-13, “Airport Design,” February 26, 2014.
- P. FAA, Advisory Circular AC 90-100, “U.S. Terminal and En Route Area Navigation (RNAV) Operations,” Change 2, April 14, 2015.
- Q. FAA, Advisory Circular AC 70/7460-1M, “Obstruction Marking and Lighting,” November 16, 2020.

- R. RTCA DO-189, “Minimum Operational Performance Standards (MOPS) for Airborne Distance Measuring Equipment (DME) Operation within the Radio Frequency Range of 960-1215 Megahertz,” September 20, 1985.
- S. TCO-C66, “Distance Measuring Equipment (DME) Operating within the Radio Frequency Range of 960-1215 Megahertz,” January 18, 1991.
- T. MIL, STD-810F, Department of Defense Test Method Standard: “Environmental Engineering Considerations and Laboratory Tests,” January 1, 2000.
- U. MIL, STD-810G, Department of Defense Test Method Standard: “Environmental Engineering Considerations and Laboratory Tests,” October 31, 2008.
- V. NAV-C3-REP-067, “Distance Measuring Equipment (DME) Siting Criteria Math Model Validation Report,” May 11, 2020.
- W. Greco, Salvatore V., “TACAN Principles and Siting Criteria,” September 1968.
- X. Kelly, Robert J., and Cusick, Danny R., “Distance Measuring Equipment and Its Role in Aviation, Advances in Electronics and Electron Physics,” Volume 68, Copyright 1968, Academic Press, Inc.
- Y. Thomas, Robert J., and DiBenedetto, Michael F., “Operational Viability of a Directive Distance Measuring Equipment (DME) Antenna in a National Airspace System (NAS) Approach and Landing Environment,” OU/AEC EER 97-02, Avionics Engineering Center, Ohio University, Athens, OH, April 1997.
- Z. DiBenedetto, Michael F.; Odunaiya, Simbo; and Thomas, Mary, “Development of Ground Reflection Multipath Allocations for Supporting a DME Link Budget Analysis,” Ohio University, May 2020.
- AA. Lo, Sherman; Chen, Yu Hsuan; Enge, Per; Peterson, Benjamin; Erikson, Robert; and Lilley, Robert, “Distance Measuring Equipment Accuracy Performance Today and for Future Alternative Position Navigation and Timing (APNT),” September 2013.
- BB. Bigham, Todd, and Snelling, Brad, “Investigation of Terminal Area Distance Measuring Equipment Signal Interference - A Case Study,” 2010.
- CC. Balanis, Constantine A., “Advanced Engineering Electromagnetics,” 2nd edition, Copyright 2012, John Wiley and Sons, Inc., ISBN 978-0-470-58948-9.
- DD. International Civil Aviation Organization, “Annex 10, Volume I – Aeronautical Telecommunications Volume I – Radio Navigation Aids,” ICAO AN 10-1, 2018.
- EE. Berz, G., and Bredemeyer, J., “Qualifying DME for RNAV Use,” Proceedings of the 15th International Flight Inspection Symposium, Oklahoma City, 2008.

FF. Berz, G.; Saini, L; Vitan, V; and Spanner, M., “Alternative PNT: What comes after DME?”
Proceedings of the 20th International Flight Inspection Symposium, Monterey, 2018.

GG. Stutzman, Warren L.; Thiele, Gary A., “Antenna Theory and Design,” Third Edition,
John Wiley and Sons, Inc., ISBN 978-0-470-57664-9.

Appendix C. DME Performance

1. Overview

The purpose of this appendix is to provide key background material on DME performance characteristics. The discussion focuses on describing those characteristics that affect signal coverage and signal accuracy, as well as the related performance analysis techniques.

The appendix begins with a high-level discussion of DME ground equipment functionality and service provisioning. The terms signal coverage and signal accuracy are introduced as the top-level operational requirements and qualitatively defined.

The next section introduces the top-level DME performance characteristics of interest, which are signal strength and ranging accuracy. The relationship between signal coverage and signal strength is explained, as is the relationship between the quality of the DME signal and ranging accuracy. Factors affecting performance are presented and defined, including site-specific factors that can be controlled by proper application of the siting criteria presented in this document. The effect of signal scattering (aka multipath) by objects in the vicinity of the DME ground station on signal strength and ranging accuracy is discussed qualitatively to set the stage for subsequent detailed discussions.

Tutorial information is provided regarding useful Radio Frequency (RF) and signal processing concepts. The RF concepts that are directly applicable to characterizing the effects that multipath has on signal strength and ranging accuracy are reviewed. General techniques that are utilized by the DME receiver for processing the DME Signal-in-Space (SIS) are also introduced.

Then, a detailed discussion regarding the factors that influence DME system performance from a SIS perspective is provided. Initially, signal attenuation due to either blockage of the line-of-sight (LOS) signal path by objects in the environment (aka shadowing), or fading effects caused by multipath, are discussed. Then, the discussion focuses on characterizing the effects multipath can have on ranging accuracy. In each instance, methods for estimating the magnitude of the impact are presented.

This appendix concludes with a brief discussion regarding when mathematical modeling or site testing with a mobile DME ground station may be required.

2. DME Service Provisioning Overview

This section discusses high-level DME functions and service provisioning, as well as ranging and identification functionality in terms of signal strength and quality.

a. DME Functions and Service Provisioning

- i. **DME Functions.** DME performs the following three high-level functions: Ranging, Identification, and Interfacing with the Remote Maintenance and Logging System (RMLS). The usability of the Ranging and Identification functions are dependent on the SIS and its characteristics. Typically, the Identification

functionality is assured when the SIS provides operationally acceptable Ranging accuracy performance, i.e., signal strength and accuracy performance that meet DME system-level requirements, such as those in FAA-E-2996. Thus, the focus hereafter addresses concepts and parameters related to achieving such Ranging performance, as well as the means to assess the impact of a specific siting condition on such performance.

RMLS functionality relies on modern, reliable telecommunication services. If such services are available, RMLS performance is not considered to be a major factor in siting a DME system.

- ii. **DME Service Provisioning.** The goal of DME Service Provisioning is to provide DME service within the prescribed service volumes. This goal implies that Ranging and Identification are the essential, navigation-enabling functionalities that are to be provided. Ranging and Identification support the pilot's situational awareness and position location for conventional flight operations, as well as lateral guidance for DME/DME Area Navigation (RNAV) flight operations.

It is important to note that DME service may be adversely impacted if the guidance in this document is not applied correctly. The impacts that could be experienced by the user include degradation of accuracy performance, service outages within portions of the service volume due to inadequate signal strength, and insufficient ground station reply rate. In such cases, the service may not fully support en route, arrival, approach, missed-approach, departure, and DME/DME RNAV flight operations within the intended service volume.

- b. **DME Signal Coverage and Accuracy.** DME Ranging and Identification functionality are dependent on signal coverage and signal accuracy.

To ensure adequate DME signal coverage for the user the DME must meet the minimum signal strength requirements. This minimum signal strength is required at the DME receiver to ensure proper operation in terms of pulse-pair decoding and ranging accuracy as well as to ensure frequency protection and acceptable immunity to noise effects.

The DME signal is considered to be of sufficient accuracy if: (1) the DME pulse-pairs incident at the user receiver result in range accuracy performance that meets the minimum distance accuracy requirement and result in the interrogation continuously operating in track mode (i.e., no loss of lock); and (2) the Morse code and voice identification are correct, clear, and identifiable.

The minimum signal strength and minimum distance accuracy requirements are specified in the USSFIM to ensure sufficient signal coverage and signal accuracy within the prescribed service volumes. Flight inspection will restrict the use of the DME in areas of the service volume, or may remove a facility from service, if the facility does not meet any of the signal accuracy requirements. Failure to meet signal coverage requirements is not used as a sole determination for restricting or removing a facility from service if a solid stable DME lock is present.

DME ground station equipment is designed to provide acceptable signal coverage and accuracy throughout the DME service volumes. DME ground station transmitters are typically specified at either 1,000W or 100W. An output power of 1,000W is generally used to support the High Altitude (H), Low Altitude (L), DME Low (DL) and DME High (DH) service volumes. The reduced high altitude requirement of the DL Service Volume provides additional flexibility in making channel assignments for supporting DME/DME RNAV network coverage. An output power of 100W is typically used to support Terminal (T) service volumes and is generally sufficient to support Standard Instrument Approach Procedures. The DME ground stations also employ signal processing techniques such as echo suppression to improve the signal accuracy of the replies.

- c. DME Service Volumes.** DME service volumes are defined by the cylindrical volume of airspace where the DME signal is expected to be received by an aircraft from a particular DME. There are five defined service volumes for DMEs in the NAS; three defined Standard Service Volumes (SSVs), and two defined DME/DME RNAV SSVs.

Most SSVs are serviced by 1000W transmitters, with the exception of the T class DME SSV which is usually serviced by a 100W transmitter. A detailed description of these service volumes can be found in Chapter 3, Figure 3-1 through Figure 3-3, and Table 3-1.

The three SSVs are:

1. Terminal (T) (Figure 3-1)
2. Low Altitude (L) (Figure 3-2)
3. High Altitude (H) (Figure 3-2)

The two DME/DME RNAV SSVs are:

1. DME Low (DL) (Figure 3-3)
2. DME High (DH) (Figure 3-3)

3. DME Signal Characteristics of Interest

This section introduces the DME signal characteristics of interest. The material includes definitions of terms such as signal strength and ranging accuracy, as well as the parameters that can affect them. Detailed discussions of these parameters and their effects are presented in subsequent sections of this appendix.

- a. Signal Strength Factors.** The discussion above established that signal coverage is directly tied to signal strength. Signal strength can also affect accuracy performance in the real world, primarily in terms of susceptibility to noise effects and RF interference. The equipment design, the associated installation and configuration practices, and the environment surrounding the transmitter/receiver antenna all influence the signal strength required or achieved within the service volume.

In this case, the relevant equipment design characteristics include receiver sensitivity, decoder performance, pulse shape attributes, transmitter output power, and three-dimensional antenna gain properties. Signal attenuation due to cable (type and length) and connector losses is the primary concern when it comes to the equipment installation and configuration process. These factors are addressed during the equipment design and installation procedure approval process, and thus they are not of concern to the siting engineer.

Signal strength can be affected by the environment surrounding the ground station antenna. Environmental or site-specific factors include LOS blockage issues, which occur when the direct or visible path between the ground station antenna and a reception point is blocked by a structure, hill, or wooded area. Equipment must therefore be located such that it provides for sufficient LOS clearance over or around objects in the vicinity.

Figure C-1 shows a hypothetical LOS blockage situation. If the direct line between the antenna and the receiver passes through the structure, as shown with the red line, it is assumed that there is a LOS blockage. If, however, there is enough clearance over or around the structure, as shown with the green line, it is presumed that the LOS is not blocked. In the practical sense, the effective blockage is determined by how much of the first Fresnel Zone around the LOS line falls on the structure. This concept is discussed further in Section 4.

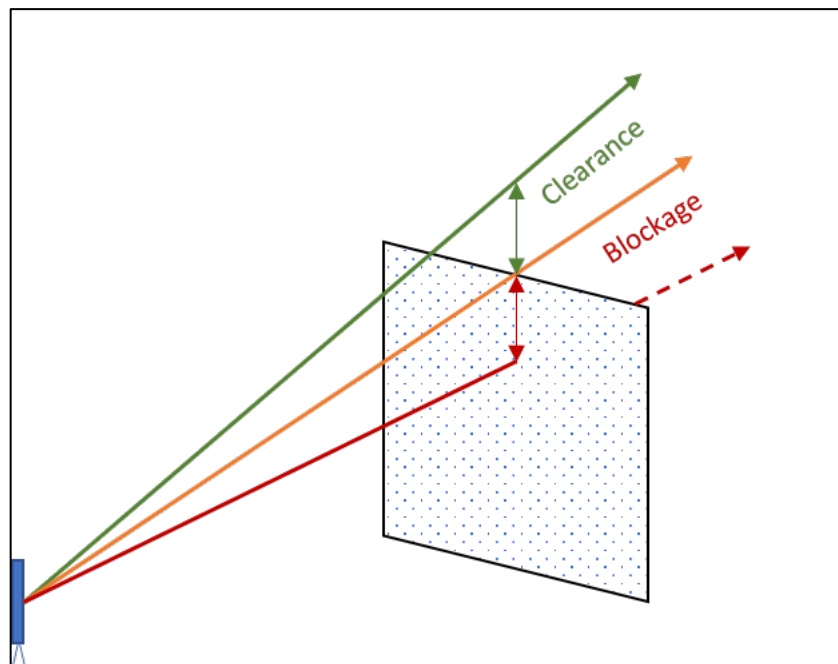


Figure C-1. A Hypothetical LOS Blockage Scenario

Aside from signal blockage, signal scattering (reflections and diffractions) from the terrain can also result in signal nulling and fading, which can adversely affect signal

strength.

- b. Ranging Accuracy Factors.** DME equipment design errors and limitations are factors that can adversely affect ranging accuracy. Specifically, equipment intrinsic errors in the signal transmission and receiver processing can induce ranging errors. However, it is assumed that the ground and airborne equipment has already been properly designed according to DME equipment requirements (per FAA-E-2996, RTCA DO-189, and TSO-C66) and that such designs limit ranging error to acceptable design levels.

Ranging accuracy can also be affected by environmental or site-specific factors that cause signal blockage (as discussed above), multipath, or both. As shown in Figure C-2, the signal radiated by the DME antenna can also be reradiated (or “scattered”) by objects in the environment including buildings, trees, and mountains. Because these scattered signals traverse different signal paths to the receiver, they are commonly referred to as “multipath.” Multipath can cause DME signal pulse-shape deformations, which can translate to ranging error during DME receiver processing. Multipath can be categorized as longitudinal, lateral, or a combination of the two.

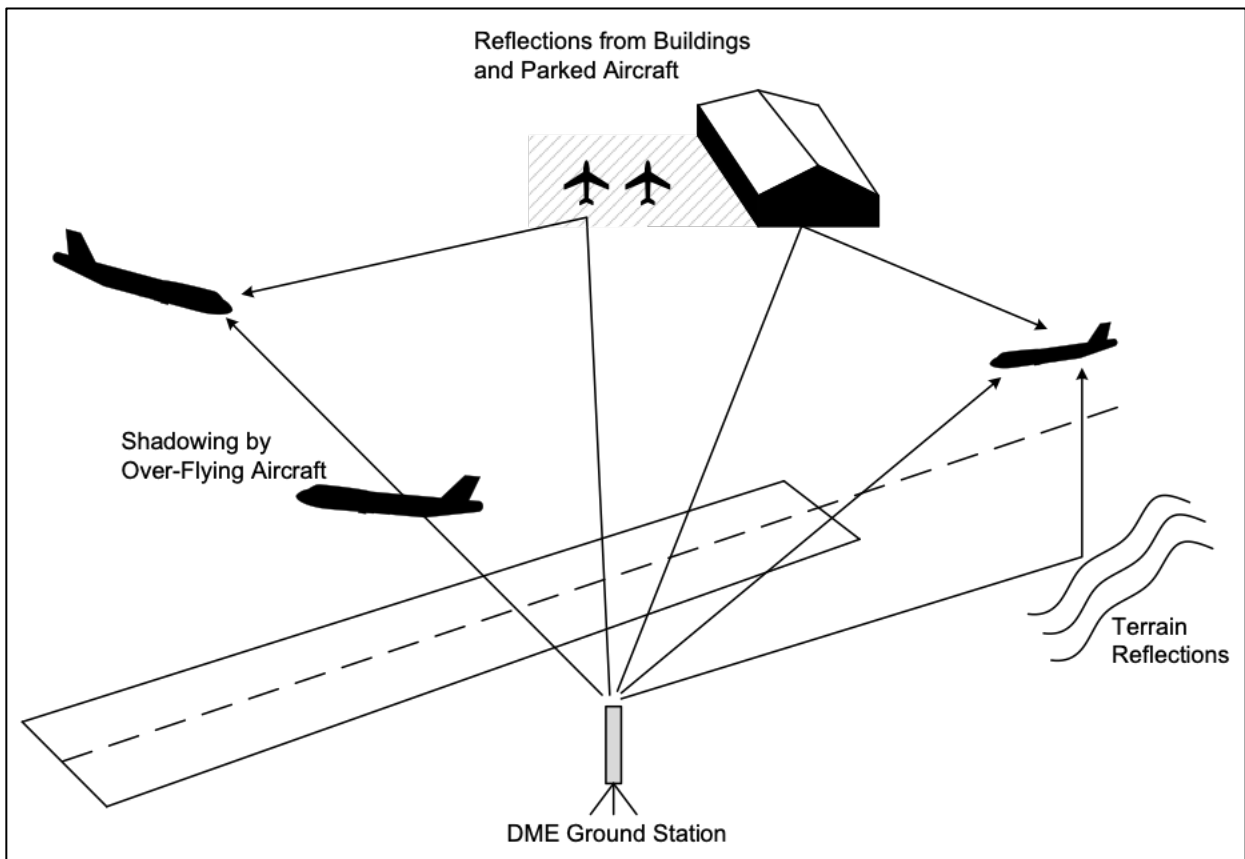


Figure C-2. Illustration of DME Multipath Sources

Parameters that affect ranging accuracy are as follows:

1. **Multipath-to-Direct (M/D) Signal Ratio:** The ratio between the magnitude of the multipath signal and the magnitude of the direct signal.
2. **Relative Time Delay (τ):** The difference between the Time of Arrival (TOA) of the multipath signal relative to the TOA of the direct path signal.
3. **Relative Phase:** The phase of the multipath signal relative to the phase of the direct signal.
4. **Motion Averaging:** The reduction in the magnitude of both sinusoidal-like and noise-like multipath induced errors caused by the motion of an aircraft when flying through a multipath interference region.
5. **TOA Technique:** The measurement method used to determine the TOA of a detected DME pulse (i.e., pulse envelope). The interrogator uses this arrival time to determine the range from the transponder, whereas the transponder uses TOA to initiate the reply delay timing function.

4. Radio Frequency (RF) and Signal Processing Concepts Review

This section introduces useful RF terms and concepts that are used to describe signal blockage/shadowing and signal multipath, as well as the impact they can have on DME signal strength and accuracy. Signal processing concepts that are utilized during receiver processing of the DME SIS are also discussed.

- a. **Useful RF Concepts.** The section provides a brief review of useful RF concepts that are directly applicable to characterizing the effects of multipath on signal strength and ranging accuracy. The following concepts are addressed below:

- i. **Multipath**
- ii. **M/D Signal Ratio**
- iii. **Relative Phase and the Vector Wheel**
- iv. **Fresnel Zone**
- v. **Ray Tracing**
- vi. **Echo Ellipsoid**

- i. **Multipath.** It was noted previously that multipath could be categorized as longitudinal, lateral, or a combination of the two. Longitudinal and lateral multipath are described in the following paragraphs.

Longitudinal multipath occurs when the direct and reflected signals are in the same vertical plane, which typically arises when the DME antenna is placed over a large flat surface commonly referred to as a ground plane. This scenario is illustrated in

Figure C-3, with the direct (i.e., LOS path) and reflected signal paths noted. Examples of objects that could be the source of longitudinal multipath are flat earth, an antenna counterpoise, or center-pivot irrigation equipment located radially from the DME facility antenna.

Lateral multipath occurs when the DME antenna is located in the vicinity of a reflective object as shown in Figure C-4. Like longitudinal multipath, the DME signal arrives at the aircraft via direct and reflected paths; however, in this case, these paths are in the same horizontal plane. Examples of objects that could be the source of lateral multipath are buildings, hangars, air traffic control towers (ATCTs), monopoles, wind turbines, cell towers, and irrigation equipment.

Most multipath signals will be a combination of longitudinal and lateral multipath; that is, neither strictly the longitudinal nor the lateral case.

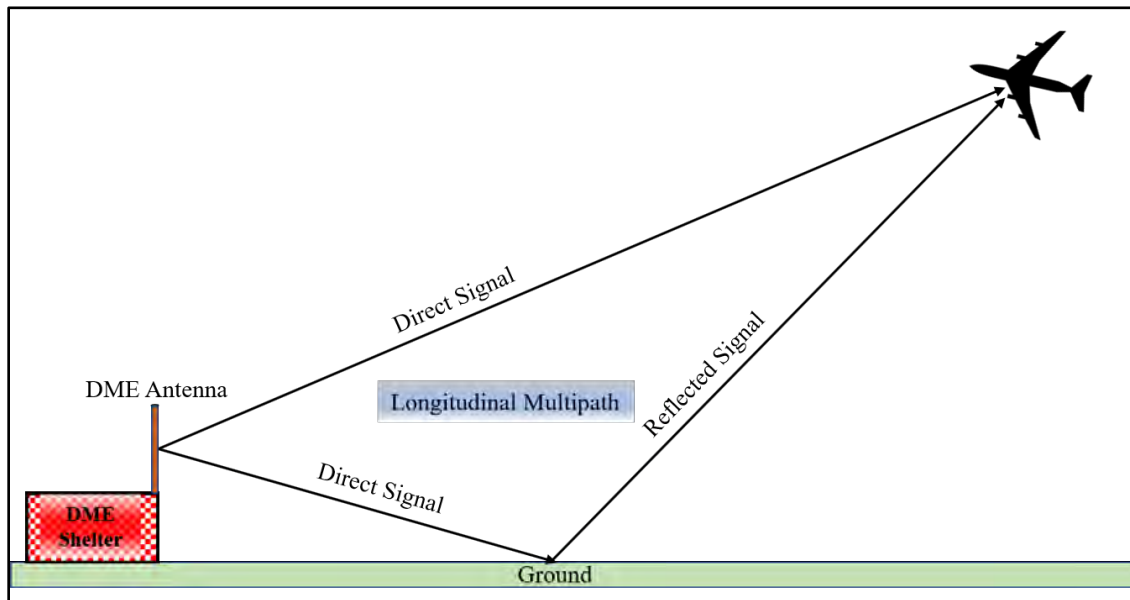


Figure C-3. Illustration of Longitudinal Multipath

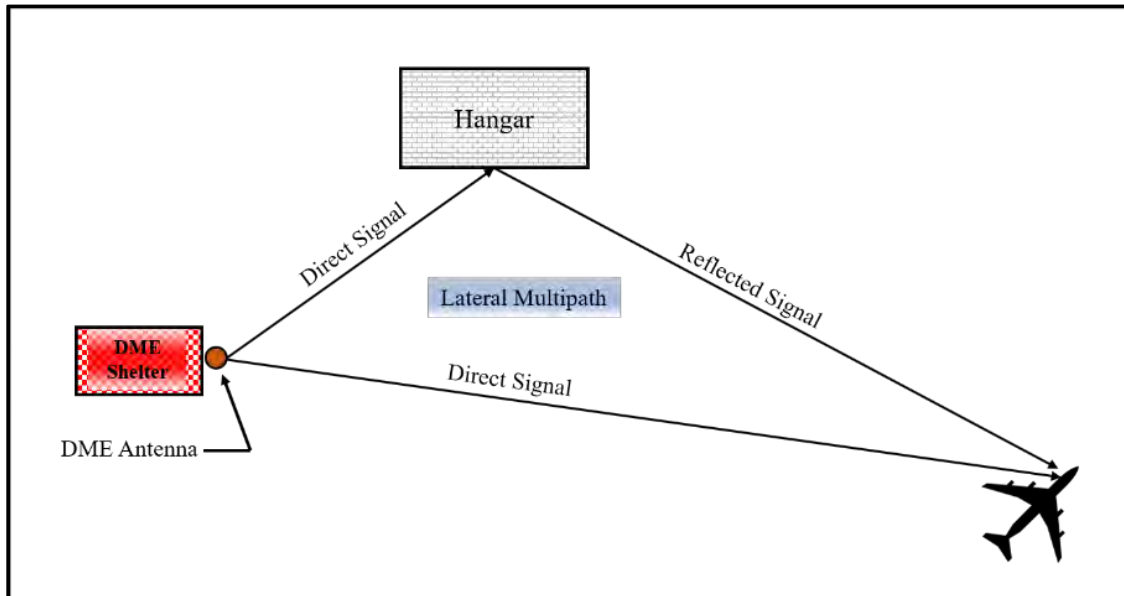


Figure C-4. Illustration of Lateral Multipath

- ii. **M/D Signal Ratio.** As noted previously, the M/D signal strength ratio is defined as the ratio of the magnitude of the multipath signal to the magnitude of the direct signal. The multipath signal could be caused by the reflection of the DME signal by a single source, such as the ground. Alternatively, it may be the vector sum of all the multipath signals from various sources, such as the ground, objects, and terrain in the vicinity of the DME antenna. Thus, computing the multipath signal strength is a more complex endeavor compared to that required for the direct signal. This ratio is commonly stated as a logarithmic ratio (e.g., -10 dB).

The topic of multipath signal strength, and the factors that affect its value, is discussed in the DME signal fading analysis conducted by Ohio University (OU). While this analysis focuses on characterizing the effect on signal strength caused by reflection of the DME radiated signal by the ground, the techniques used are applicable to multipath signal strength computation in general. A summary as it relates to the effect of surface roughness on the M/D ratio is provided below.

Multipath signal strength is affected by the incidence (or grazing) angle of the direct signal, as well as the material, size, and surface roughness of the multipath source. The material determines how efficiently the object scatters energy and is commonly denoted by the magnitude of the reflection coefficient, which can have a value of 1 or less, and results in sinusoidal type error effects. The reflection coefficient magnitude is dependent on the incidence angle as well. Size affects the amount of energy that can be scattered by the object and is typically evaluated in comparison to the first Fresnel Zone, which is discussed below.

The surface roughness of the multipath source also determines how efficiently the object scatters energy, resulting in both sinusoidal and noise type error effects. The Rayleigh and Fraunhofer criteria are established standards used to characterize

surface roughness. Both criteria classify a surface as rough or smooth based on the phase difference between signals reflected from two different points on the surface. The criteria can also utilize the surface height for this classification, as the phase difference can be expressed as a function of the height. (The Rayleigh and Fraunhofer criteria classify a surface as rough when the value for “h” exceeds $\lambda/(8\sin(\gamma))$ and $\lambda/(32\sin(\gamma))$, respectively. Further details are provided in Reference Z.) Accordingly, Figure C-5 illustrates the Rayleigh and Fraunhofer characterizations of surface roughness using the standard deviation of the heights (h) of the ground as a function of grazing/elevation angle (γ). It is important to note that the information in Figure C-5 originated in the VOR Siting manual and was modified to be applicable to DME.

The analysis in Reference Z established three surface roughness zones – smooth, non-smooth, and rough – as depicted in Figure C-6. Each of these zones is shown in the figure using different color shading, and the zones are based on the standard deviation of the heights (h) of the ground. The blue area represents the rough region of the Rayleigh criterion, while the green area represents the smooth region of the Fraunhofer criterion. The Fraunhofer criterion is less conservative from a fading analysis perspective and, realistically, many sites may not present that way. Conversely, the Rayleigh criterion is more conservative and may exclude some sites that are slightly rough.

As such, an intermediate “non-smooth” criterion – which falls in the middle of both criteria previously mentioned – was established as shown in the red region of Figure C-6. Based on this intermediate criterion, the fading analysis considers a surface to be “smooth” when the standard deviation of the surface height (i.e., h) is less than $\lambda/16$. Surfaces where “h” ranges from $\lambda/16$ to $\lambda/8$ are considered as “non-smooth”, and surfaces are considered “rough” when the value for “h” exceeds $\lambda/8$.

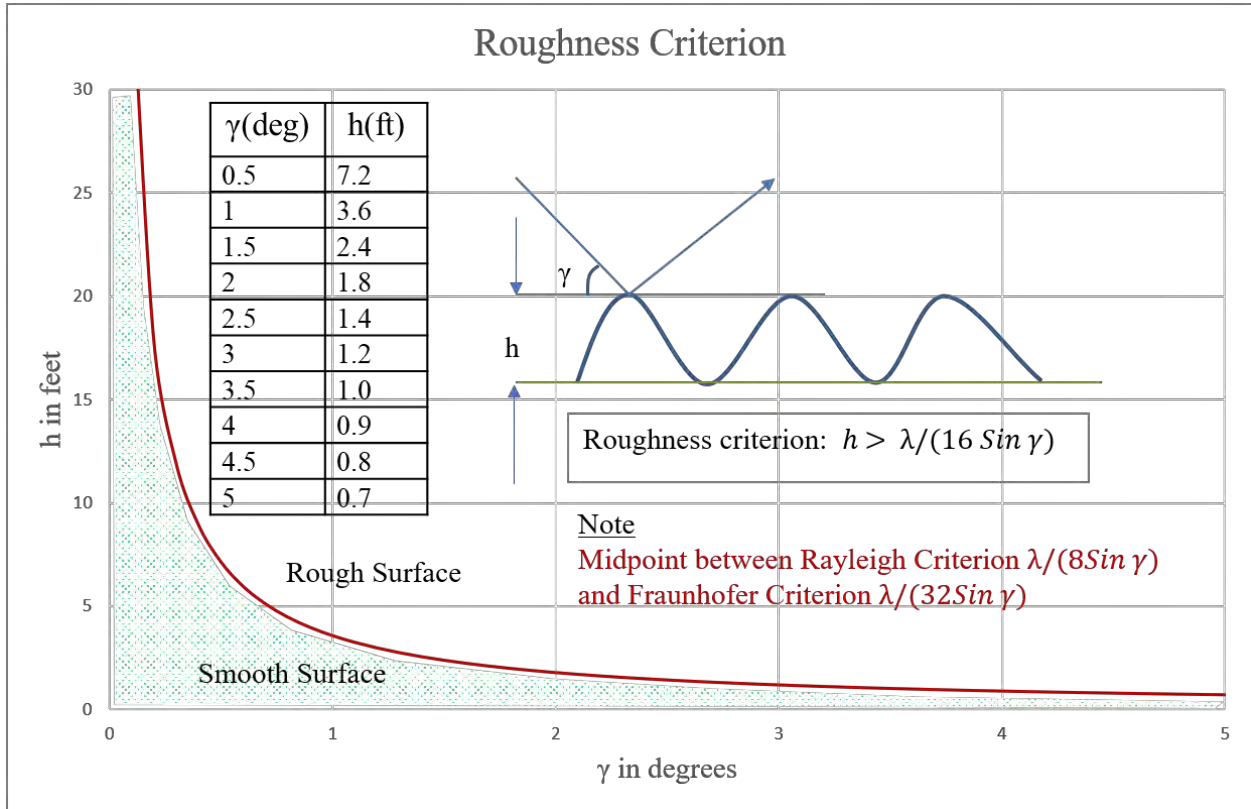


Figure C-5. Roughness Criterion

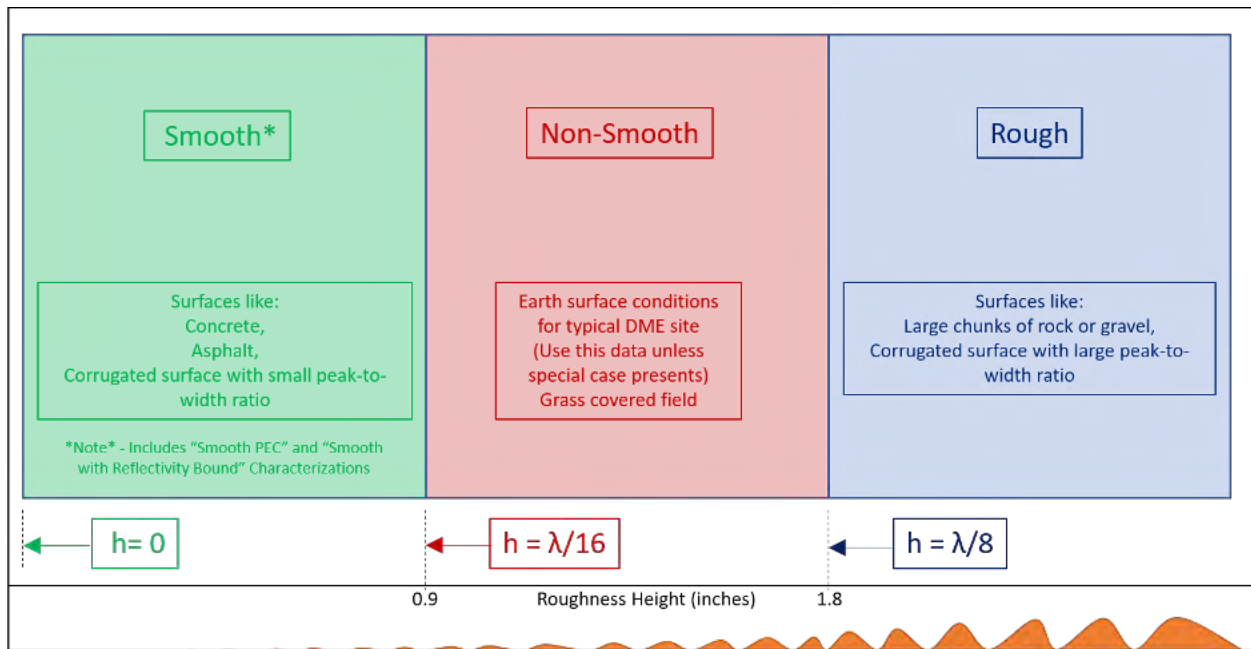


Figure C-6. Pictorial Depiction of Rayleigh and Fraunhofer Criteria for Surface Roughness

- iii. **Relative Phase and the Vector Wheel.** Electromagnetic waves can be represented mathematically as vectors having a magnitude and phase. How two waves combine in space, or analytically, depends on their magnitudes and the phase of one wave relative to the other, i.e., their relative phase (ϕ_r). Similarly, how two DME signals combine in space depends on their magnitudes and their relative phase.

Because the ground below which the antenna is mounted provides an ever-present source of signal reflection (i.e., multipath), understanding how this multipath alters the SIS provides insight into how system performance may be affected. Accordingly, the vector wheel shown in Figure C-7 can be used to illustrate the vector sum of the direct and ground reflection signals that together produce the SIS.

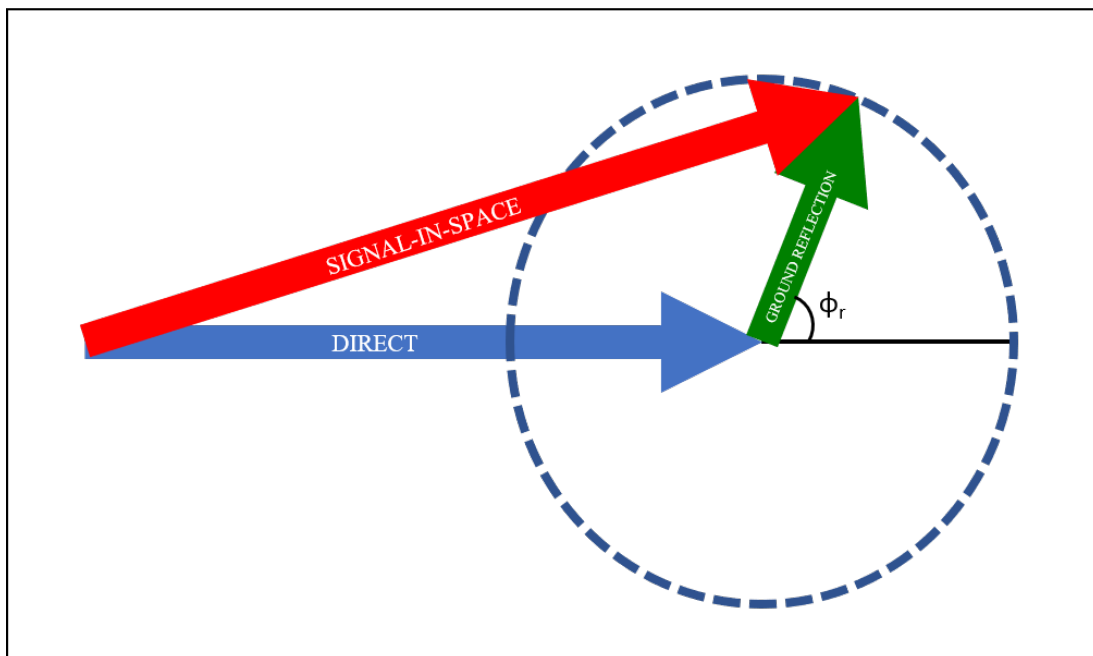


Figure C-7. Signal-In-Space Results from Adding Direct and Reflected Signals

The SIS vector is found by vectorially adding the reflected ray to the direct ray as shown in Figure C-7. It is noted that the reflected signal can add to, or subtract from, the direct signal. The extent of this addition or subtraction depends on the relative phase relationship of the two signals as shown by parameter “ ϕ_r ” in the figure. The parameter “ ϕ_r ” can have any value between 0° and 360° , which means the SIS arrowhead can “touch” any location on the dashed circle shown in the figure.

One is usually interested in bounding the effect multipath can have on system performance. The nature of the parameter being evaluated typically determines whether an upper bound, lower bound, or both are of interest. The vector wheel can be used to illustrate these bounds. A reflection that is 180° out-of-phase will be subtracted completely from the direct signal, a condition that results in the worst-case decrease in the magnitude of the SIS as shown in Figure C-8. When the ground reflection phase is 0° relative to the direct signal, the reflection is completely in-

phase, and the ground reflection adds entirely to the direct signal. This best-case scenario is depicted in Figure C-9.

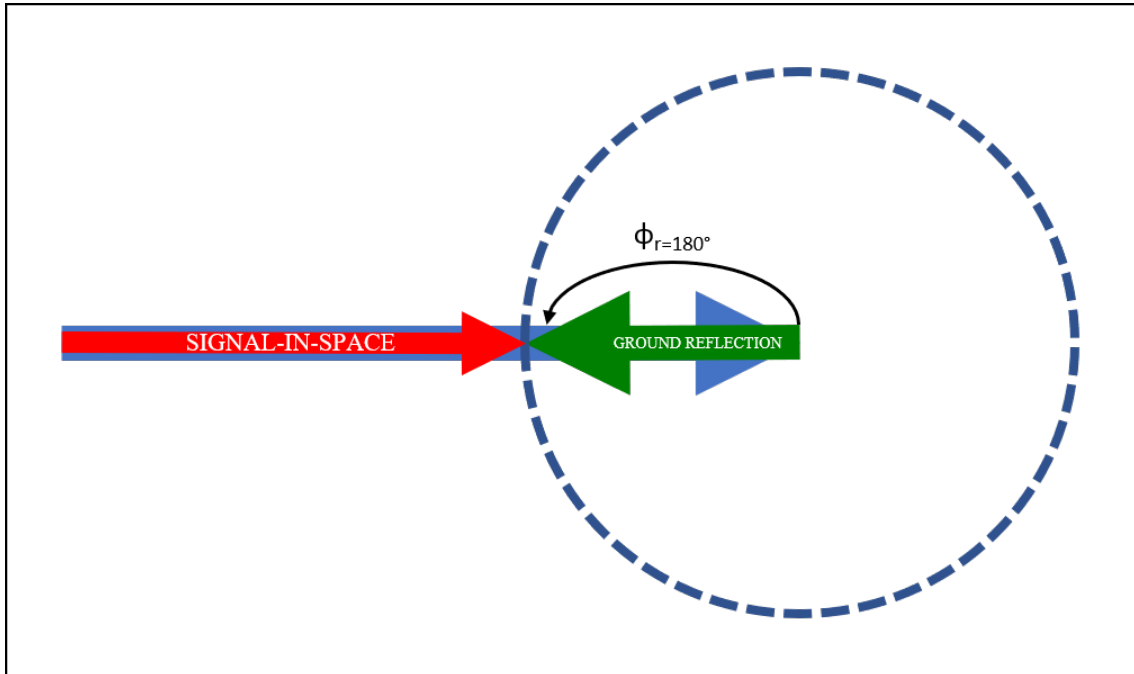


Figure C-8. Worst-Case: Signal-In-Space at Minimum Amplitude

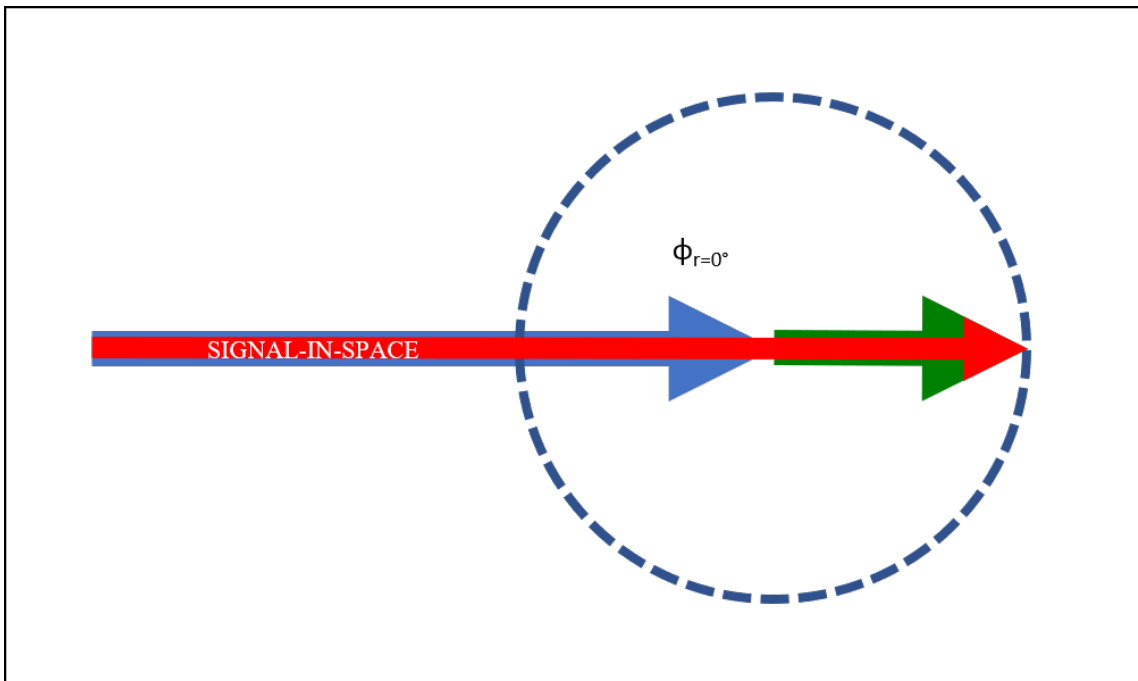


Figure C-9. Best-Case: Signal-In-Space at Maximum Amplitude

- iv. **Fresnel Zone.** In order to intuitively determine the impact of a structure on the distance information provided by DME, it is important to understand the concept of Fresnel Zone. As noted previously, signals emanating from the source antenna

can arrive at the receiver antenna or observation point by different paths. The different paths result from signal scattering by obstacles and terrain located in the vicinity of the transmitter or receiver antennas. At the receiver antenna, direct transmission from the source antenna will be present along with reflected signals from objects and from the ground. These waves arrive at the receiver antenna with different magnitudes and phases. Constructive or destructive interference will occur between the signals depending on these magnitudes and phases.

The reflected and direct signals arriving at the receiver will interfere constructively when their travel paths differ by less than a half wavelength. A large surface can have parts of the surface reflecting constructively while there are other parts reflecting destructively, again depending on the path length between the point on the surface and the point of reception. On a typical large surface there will be alternating areas of constructive and destructive interference. These areas of constructive and destructive interference, known as Fresnel Zones, are the areas that surround the optical LOS between a transmitter and a receiver antenna. The areas are concentric cylindrical elliptical shapes that encompass the electromagnetic waves after they leave the antenna.

The size of the Fresnel Zones depends on the distance between the transmitter and the receiver antennas and their heights. There are many zones, but most of the signal strength is concentrated within the first Fresnel Zone, which is the innermost area. Beyond the first Fresnel Zone, signal interference will be alternately destructive and constructive. Generally, the term “Fresnel Zone” refers to the first Fresnel Zone since most of the energy transmitted is concentrated within this zone.

The most common use of Fresnel Zone information for DME is to check for obstructions that penetrate the zone. If obstructions (such as terrain, vegetation, buildings, and towers) penetrate the Fresnel Zone, the transmitted signal can be seriously impacted. Given transmitting antenna and receiving antenna locations, the dimension of the Fresnel Zone can be calculated by simple geometry for any two-dimensional plane containing these antennas. An example scenario is presented in Figure C-10. The calculations at different points between the two antennas for the first Fresnel Zone boundary – i.e., the two-dimensional locus of points where the path difference is $\lambda/2$ – will trace an elliptical shape as shown in the diagram. This same elliptical trace would exist on any other two-dimensional plane containing the antennas. Thus, when three-dimensional space is considered, the first Fresnel Zone boundary forms the surface of an ellipsoid, with the majority of the signal energy reaching the receiver antenna “flowing” through the area contained within this ellipsoid.

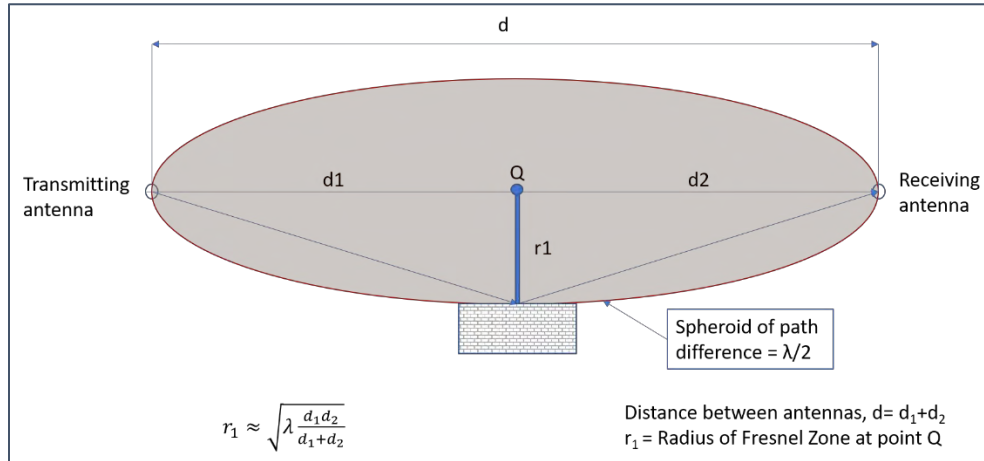


Figure C-10. Scenario for Calculating Radius of the First Fresnel Zone

In this scenario, the radius of the Fresnel Zone at point Q is computed as follows:

$$\text{Path difference, } \Delta d = \lambda/2 = \sqrt{d_1^2 + r_1^2} + \sqrt{d_2^2 + r_1^2} - d \quad \text{Equation 1}$$

$$\lambda/2 = d_1 \left(1 + \frac{r_1^2}{d_1^2}\right)^{1/2} + d_2 \left(1 + \frac{r_1^2}{d_2^2}\right)^{1/2} - d \quad \text{Equation 2}$$

$$\lambda/2 \approx \frac{r_1^2}{2} \left(\frac{1}{d_1} + \frac{1}{d_2}\right) \quad \text{Equation 3}$$

$$\xrightarrow{\text{yields}} r_1 \approx \sqrt{\lambda \frac{d_1 d_2}{d_1 + d_2}} \quad \text{Equation 4}$$

Where:

d = distance between transmitting and receiving antennas, therefore,

d = d₁ + d₂

r₁ = Radius of Fresnel Zone at point Q.

When the distance between the transmitting antenna and the structure (d₁) is much smaller than the distance from the structure to the receiving antenna (d₂) as shown in Figure C-11, the radius of the Fresnel Zone can be approximated as follows:

The distance, $d = d_1 + d_2 \approx d_2$ Equation 5

$\xrightarrow{\text{yields}} r_1 = \sqrt{\lambda d_1}$ Equation 6

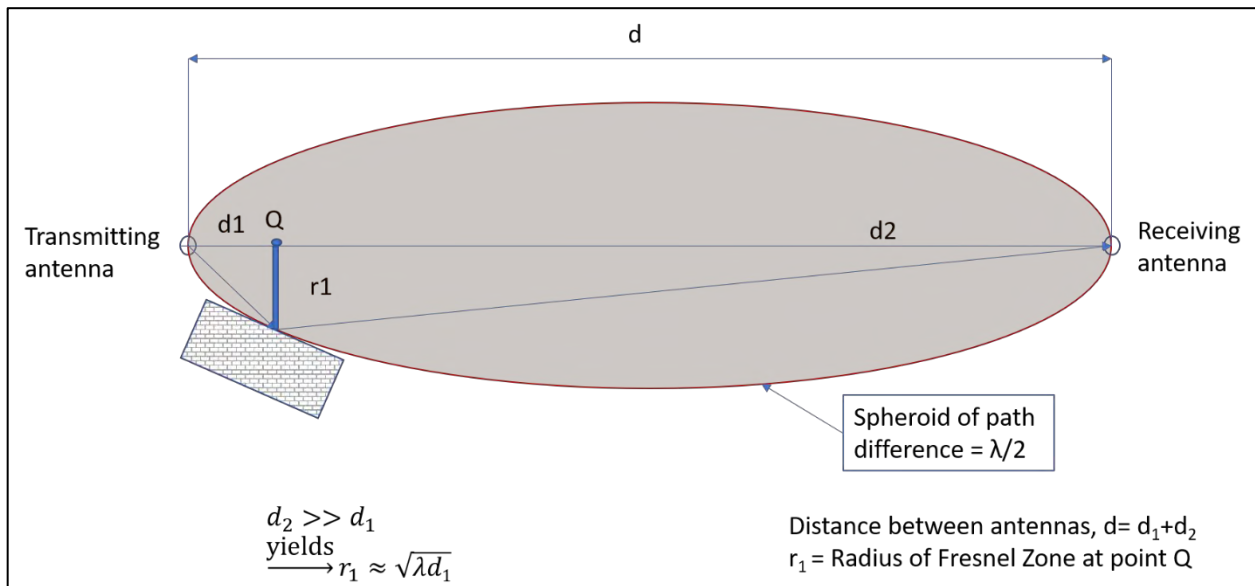


Figure C-11. Scenario for Calculating Radius of First Fresnel Zone When Distance to Receiver is Much Larger than Distance to Structure

When there are obstacles within the first Fresnel Zone, signals reflected or diffracted from these structures will add constructively at the receiver. The amount that is added on to the total signal received still depends on the size and the precise location of the structure. In addition to reflected or diffracted signals, structures in this region can also cause blockage or shadowing of signals from the receiver. Some deductions regarding the amount of signal blockage can be made based on the size of the structure.

- v. **Ray Tracing.** Ray tracing is a method of generating optical paths in a system based on the laws of geometric optics. The concept of ray tracing treats a ray as a mathematical abstraction that has a point of origin and direction only; electromagnetic properties such as energy, polarization, and the wave nature of propagation are not considered. In ray tracing, the rays travel in a straight path within a homogenous system while the direction is altered when a different medium is encountered. The ray tracing of electromagnetic waves only results in an approximation, which is usually adequate for most applications. The concept of ray tracing helps provide general ideas about areas that are illuminated by a wave, areas

that may be shadowed from the wave, and regions where multipath may be present.

Two basic laws that are important for ray tracing are the laws of reflection and Snell's laws of refraction, as indicated in Figure C-12. The laws of reflection pertain to the situation when the direction of the ray is altered at the intersection of two media such that the ray direction is cast back into the original medium. The laws of refraction address the scenario in which the direction at the media intersection is altered, but within the new medium. The path of an electromagnetic ray can be generated by successively applying the laws of reflection and refraction on an electromagnetic medium. In doing so, the electromagnetic ray can be propagated from its source to a target and thereby generate an approximate property of the propagated ray.

The laws of reflection, which are as depicted in Figure C-12(a), are as follows:

1. The incident ray, the reflected ray, and the normal to the reflection surface at the point of ray incidence all lie in the same plane;
2. The angle the incident ray makes with the normal at the point of incidence equals the angle the reflected ray makes with the same normal, (i.e., $\theta_i = \theta_r$), and;
3. The incident ray and the reflected ray are on the opposite sides of the normal.

The laws of refraction, as shown in Figure C-12(b), are as follows:

1. The incident ray, the refracted ray, and the normal to the refracting surface at the point of ray incidence all lie in the same plane; and,
2. $n_1 \sin(\theta_1) = n_2 \sin(\theta_2)$ where n_1 and n_2 are the refractive indices of media 1 and 2 respectively.

Both the laws of reflection and the laws of refraction also hold for non-planar surfaces, provided that the normal to the interface at any given point is understood to be the normal to the local tangent plane of the interface at that point.

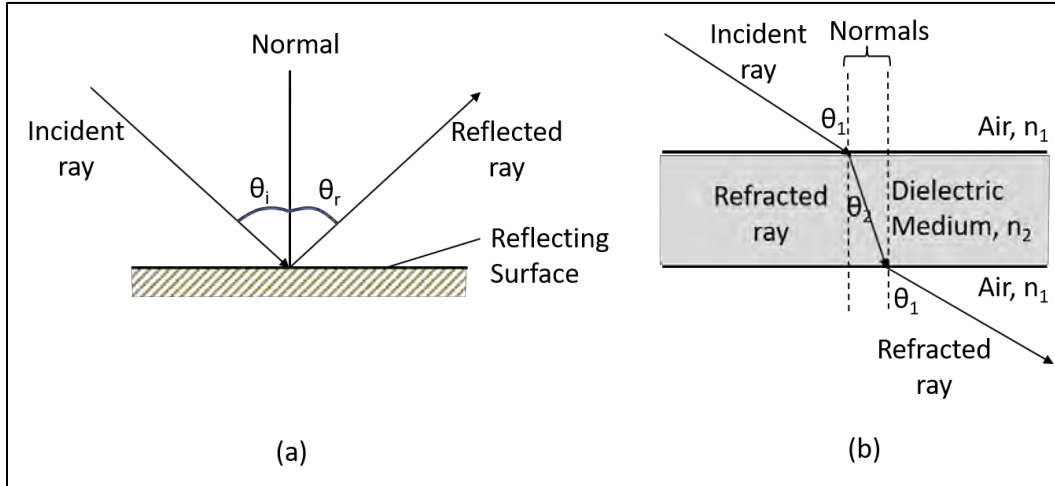


Figure C-12. Reflection and Refraction at Smooth Plane Surfaces

In ray tracing, all parts of an illuminated surface are assumed to be reflecting. Thus, for the purposes of this document, the laws of reflection are adequate to describe the ray tracing that is discussed. In this case, the reflected rays for a surface can be represented as shown in Figure C-13.

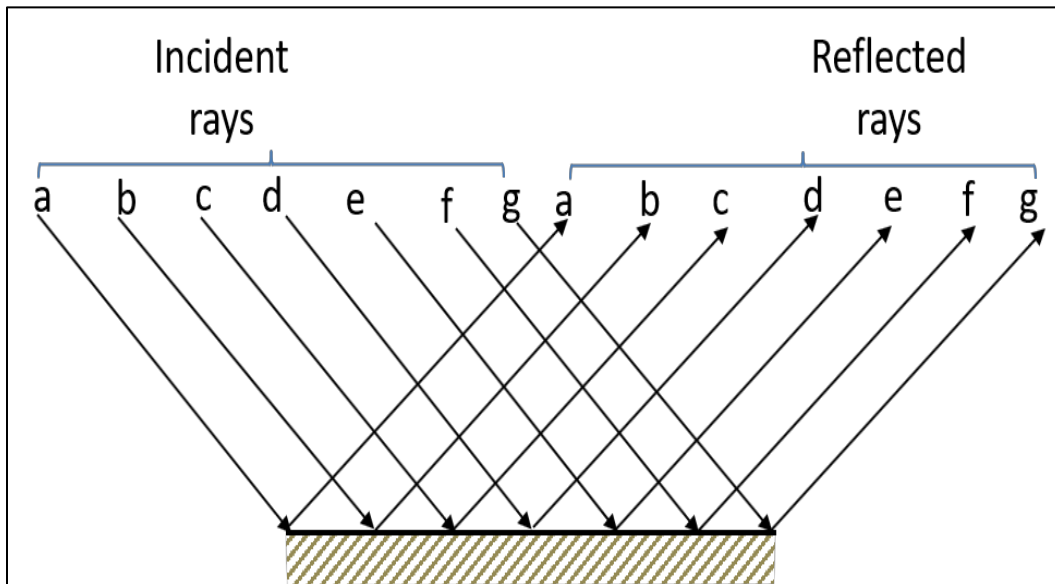


Figure C-13. Ray Tracing from Many Points on an Illuminated Surface

The diagram of Figure C-13 above can be extended such that the rays from every infinitesimal point of the illuminated surface are considered. In such a case, the reflected rays can simply be represented by a bound that encompasses the reflected rays from the extremities of the surface. For a known source point, the incident and reflected rays can thus be represented as shown in Figure C-14. The shaded region in this figure is commonly referred to as the multipath region, and though not illustrated in this figure, when the receiver or observation point lies within this region a ray directly from the source to that point would exist as well.

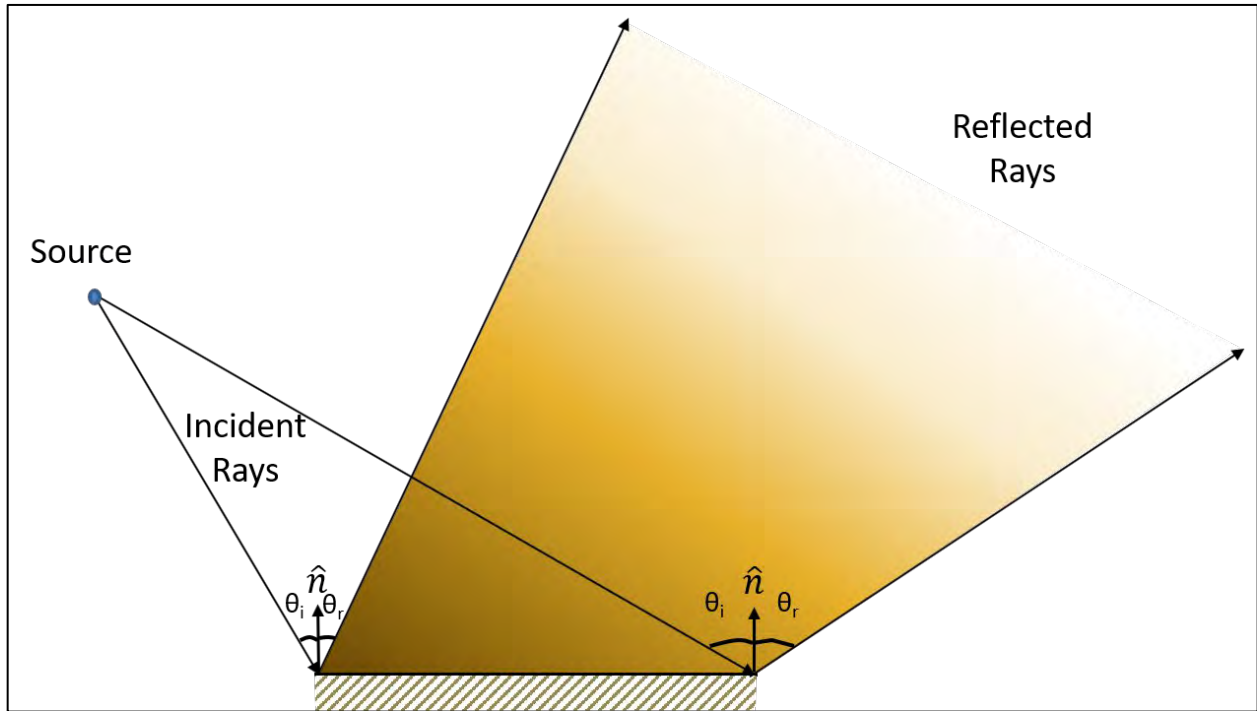


Figure C-14. Ray Tracing Showing the Boundaries for Incident and Reflected Rays

This ray tracing technique can be applied to a three-dimensional building to ascertain the direction of the reflected rays from the building as indicated in Figure C-15. It can also help to delineate the area where reception of signals is shadowed or blocked. All of these approaches help in providing a general idea of where the ray can be received, i.e., the region where multipath will be present. The analysis can then focus on this region, the values for the multipath parameters can be computed at select receiver points, and an assessment can be made regarding the potential impact to signal strength and ranging accuracy.

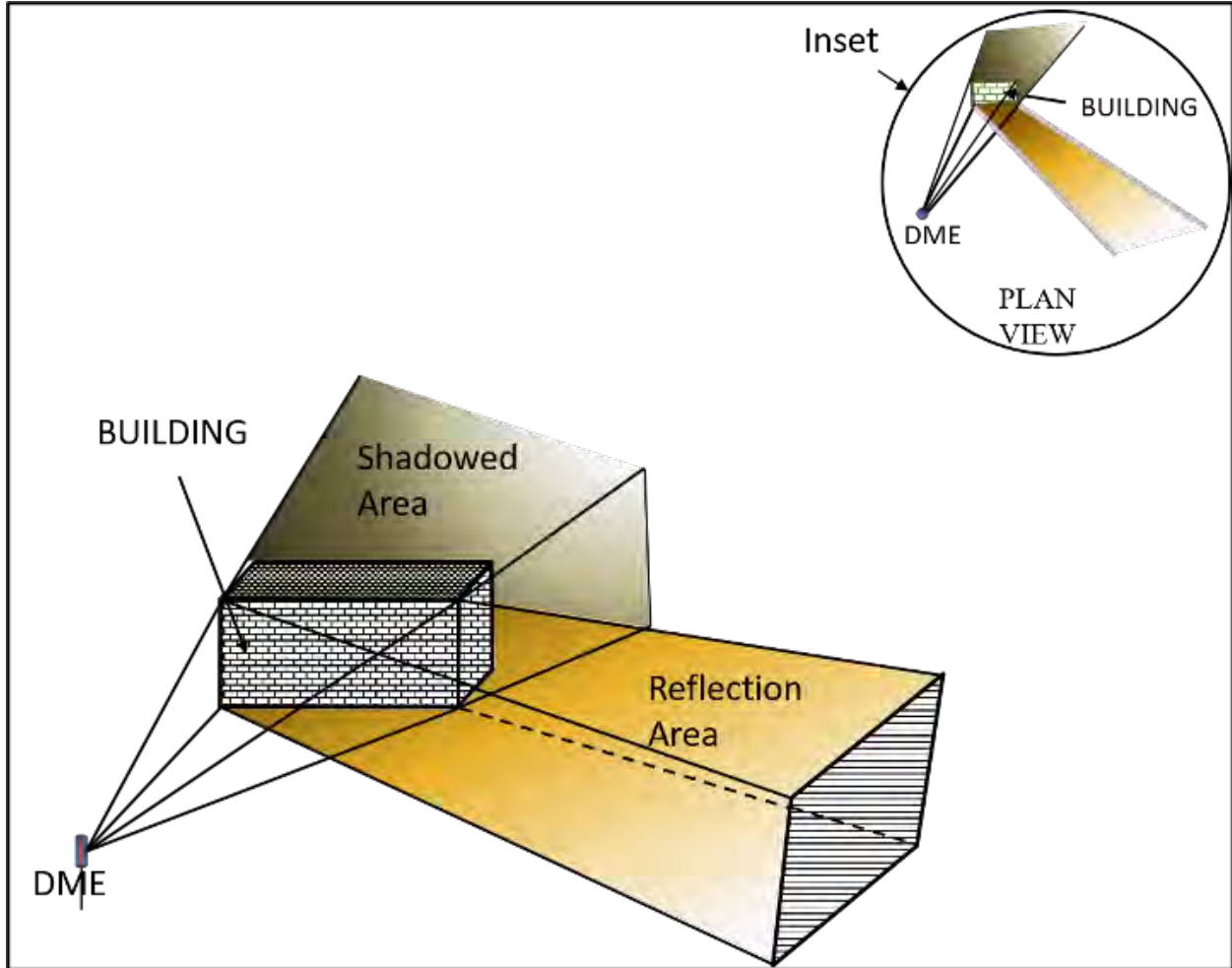


Figure C-15. Ray Tracing for a 3D Building

- vi. **Echo Ellipsoid.** Echo ellipsoids for a given time-delay value can be used to evaluate the potential for ranging error from a particular source. The echo ellipsoid for a given receiver path is used to determine the worst case scatterer locations. The echo ellipsoid migrates as the receiver moves, just like the Fresnel Zone. As previously discussed, the Fresnel Zone ellipsoid represents the locus of points where the relative path length difference is $\lambda/2$ at the source frequency. For the echo ellipsoid, the relative path length difference corresponds to a particular time-delay value, which is translated into a distance given the velocity of propagation. Simply stated, the particular time-delay value used is the latest (i.e., longest) delay value that can still cause an unacceptable ranging error to result. A detailed discussion of this topic is provided below, and in Appendix E.

Figure C-16 illustrates how an echo ellipsoid can be used to determine the potential for a structure to cause significant multipath error for DME. The profile and plan view show three buildings that can be evaluated for multipath errors. The first building penetrates the profile view ellipsoid while also sitting within the plan view ellipsoid; this indicates a possible problem. Building number two is below the

profile view ellipsoid while sitting within the plan view, which should pose no problem for meeting the multipath error tolerance. Lastly, building number three falls outside both the profile and plan view ellipsoids and again poses no multipath error tolerance problems.

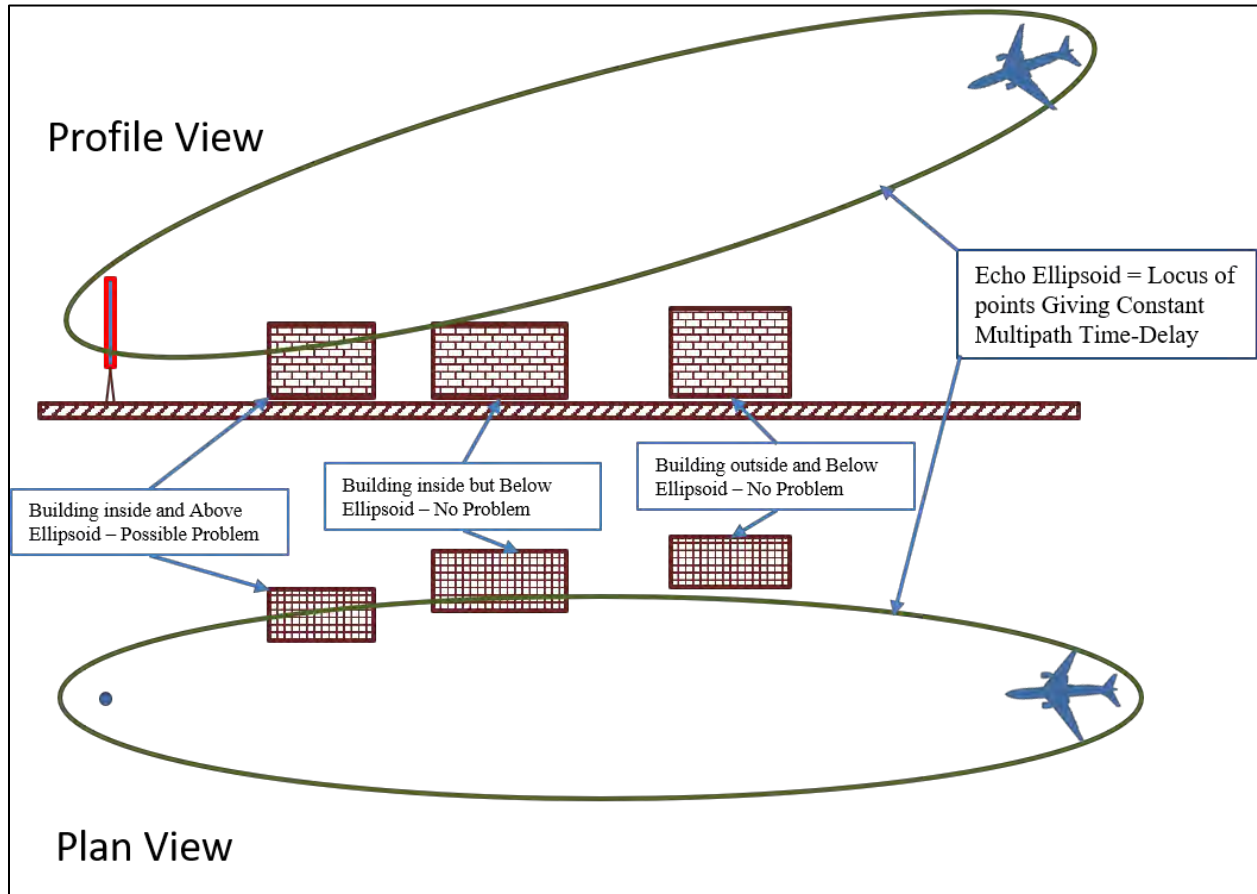


Figure C-16. Example of Echo Ellipsoids for a Given Time-delay

The delay between the measured TOA of the direct and multipath signals is used to calculate the DME distance error. If the multipath portion of the DME error tolerance allocations is known, then this allocation can be used to calculate the maximum time-delay value that can still produce such an error for an estimated M/D ratio. The locus of all points that gives this time-delay value traces an ellipsoidal shape, like the one shown above, about the source and the observation point.

The diagram in Figure C-17 shows a scenario for computing the echo ellipsoid. It is assumed here that the source is located at point S, while the observation is at point O. The signal reflections from a point C will be received by an observer at point O with a delay time (t) given by:

$$ct = r + R - d \quad \text{Equation 7}$$

where r and R are, respectively, the distances of C from the source and the observer; $d = OS$, the distance of the observer to the source; and c is the speed of light.

The locus of all points with equal delay time is an ellipsoid with the source and the observer at the focal points of the ellipse.

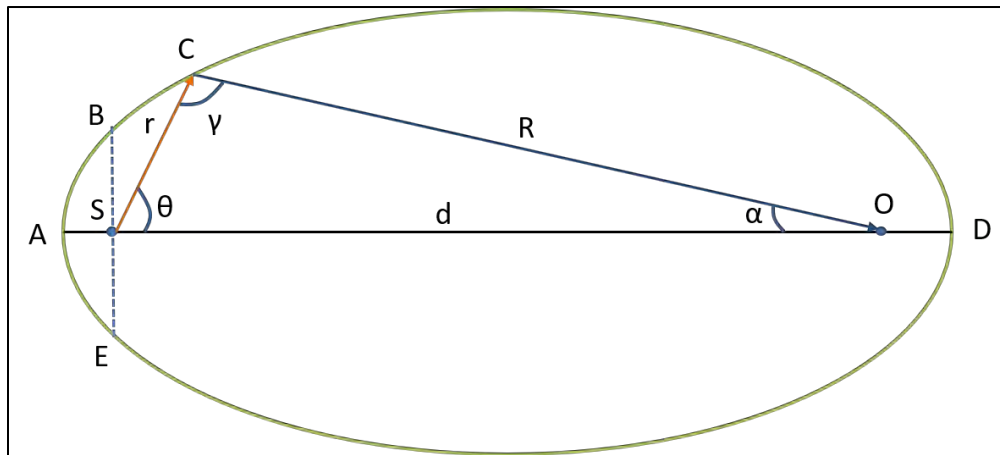


Figure C-17. Geometry for Echo Ellipse

Using the law of cosines:

$$r^2 = R^2 + d^2 - 2Rdcos(\alpha) \quad \text{Equation 8}$$

or

$$R^2 = r^2 + d^2 - 2rdcos(\theta) \quad \text{Equation 9}$$

The distance, r or R , can be expressed in terms of the delay time (t) and source distance (d) as:

$$r = \frac{d(d + ct)(1 - \cos(\alpha)) + (ct)^2/2}{d(1 - \cos(\alpha)) + ct} \quad \text{Equation 10}$$

$$R = \frac{d(d + ct)(1 - \cos(\theta)) + (ct)^2/2}{d(1 - \cos(\theta)) + ct} \quad \text{Equation 11}$$

Where:

α = the angular distance of the multipath source from the observation point, and;

θ = the angular distance of the multipath source from the signal source.

In practice, the siting engineer will survey a potential transponder antenna location and large structures may be noted/observed nearby. For example, if a large building is located close to a potential antenna site as shown in Figure C-18, multipath from the building will result in different time delays at receiver locations Rx₁, Rx₂, and Rx₃ (which are located at distances d₁, d₂, and d₃ from the antenna site, respectively). These time delays can be computed for each location to ascertain if they fall within the span of values known to cause large range errors. Typically, the upper end of the range is taken as the upper time-delay bound.

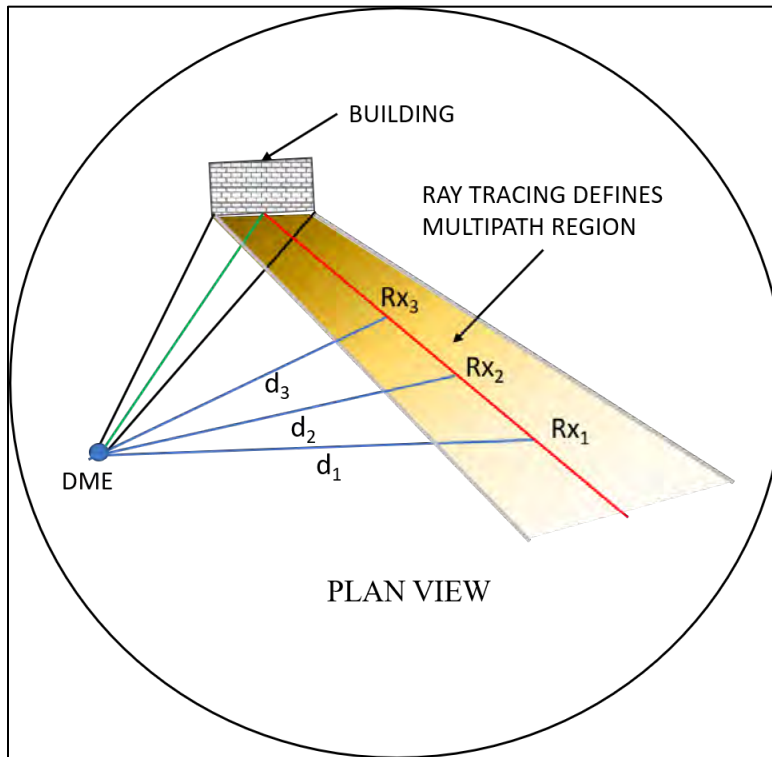


Figure C-18. Plan View Showing a Building Near a Potential DME Antenna Site

Consider a scenario where the building above is located at a distance of 5,000 feet from the DME and at an angle of 45° from a line between the DME and receiver point 2 (Rx₂), as shown in Figure C-19. Assuming the distance between the DME and Rx₂ is 10 nmi (60,760 feet), the time delay for the multipath signal arriving at

Rx₂ can be computed using Equation 9 and then Equation 7 as shown below:

$$R = \sqrt{r^2 + d^2 - 2rd\cos(\theta)} = \sqrt{5000^2 + 60760^2 - 2(5000)(60760)\cos(45^\circ)} = 57,334 \text{ ft}$$

$$\text{Time delay, } t = \frac{r + R - d}{c} = \frac{5000 + 57334 - 60760}{9.84 \times 10^8} \approx 1.6\mu\text{s}$$

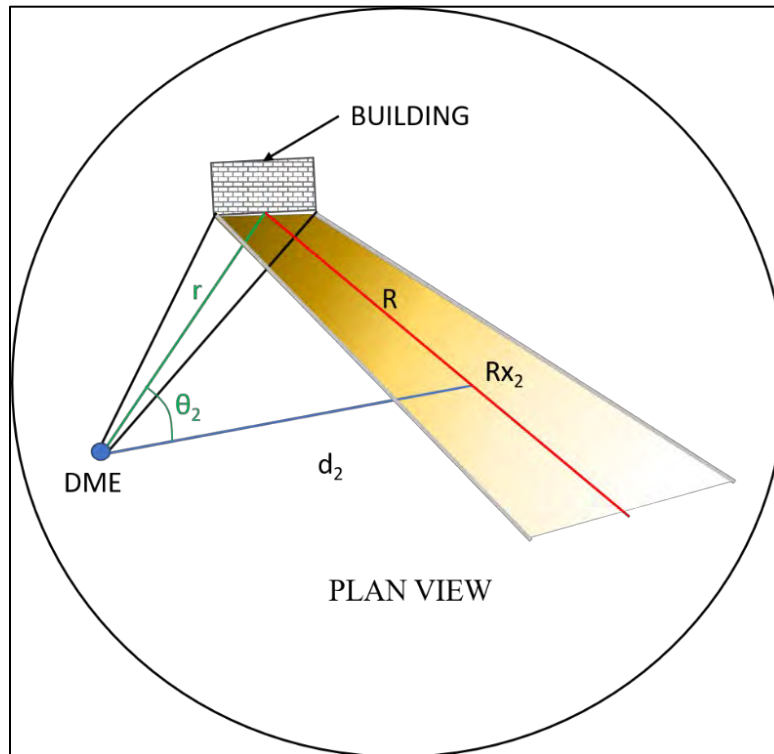


Figure C-19. Time Delay Calculations Scenario

In a similar manner to the calculations above, the time delay for Rx₁ at 12 nmi and Rx₃ at 8 nmi can also be computed to give 1.65 μs and 1.56 μs, respectively.

For a given time delay upper bound of 1.6 μs, these computations show that the Rx₂ is right on the boundary, while Rx₁ is outside the boundary and Rx₃ is within the boundary. This means that at receiver location Rx₃ the multipath from the building has the potential to adversely impact the performance of the DME system. Conversely, while at the location Rx₁ the impact on the performance will not be significant.

The method for determining the numerical value(s) for the time delay upper bound is discussed below.

b. Signal Processing Concepts. This section provides a review of signal processing concepts that are used to process the DME SIS. Concepts applicable to DME signal processing include:

- i. **Motion Averaging**
- ii. **Time-Of-Arrival (TOA) Determination**

- i. **Motion Averaging.** As previously discussed, ranging errors may result when the direct and multipath signals arrive at the receiver antenna close in time to one another. The magnitude of the error is a function of the relative phase between the direct and multipath signals, as well as the other parameters previously discussed.

The relative phase is a function of the geometry between the transmitter antenna, the scatterer, and the receiver antenna. When this geometry is fixed, the relative phase has a fixed value as well. When the geometry is dynamic, such as the case when the receiver antenna is mounted on an aircraft, the relative phase will vary with time. The rate of change in the RF carrier phase of the direct signal is a function of the velocity of propagation and the projection of the aircraft velocity onto line A in Figure C-20. Similarly, the rate of change in the RF carrier phase of the multipath signal is a function of the velocity of propagation and the projection of the aircraft velocity onto line B. In this case, the rate of change for the relative phase between the direct and multipath signals can be expressed as a “scalloping frequency,” and the scalloping frequency at any instant in time can be calculated as follows:

$$F_s = d\phi/dt = (V/\lambda)(\cos \alpha - \cos \beta) \quad \text{Equation 12}$$

As the aircraft shown in Figure C-20 continues its flight through the multipath region, the values for α and β change continuously. This change causes the scalloping frequency to change continuously as well, producing an error trace like the one shown in Figure C-21. The aircraft will fly directly towards or away from the DME transponder antenna during some flight inspection maneuvers (e.g., level runs), thus α in Equation 12 will be zero and this equation can be reduced to the following:

$$F_s = d\phi/dt = (V/\lambda)(1 - \cos \beta) \quad \text{Equation 13}$$

In this case, the scalloping portion of the flight recording can be used to compute the instantaneous scalloping frequency. Once the frequency is known, one can then compute the value for β , which provides two lines of position for the scatterer causing the multipath error, given that $\cos \beta$ equals $\cos -\beta$. Depending on the length of the scalloping signal, the process described can be repeated and two more lines of position can be determined. The intersection of two lines gives a potential, approximate location for the scatterer. Additional lines of position, or the consideration of the resulting values for other multipath parameters for each

potential location, can be used to facilitate the process of multipath source identification.

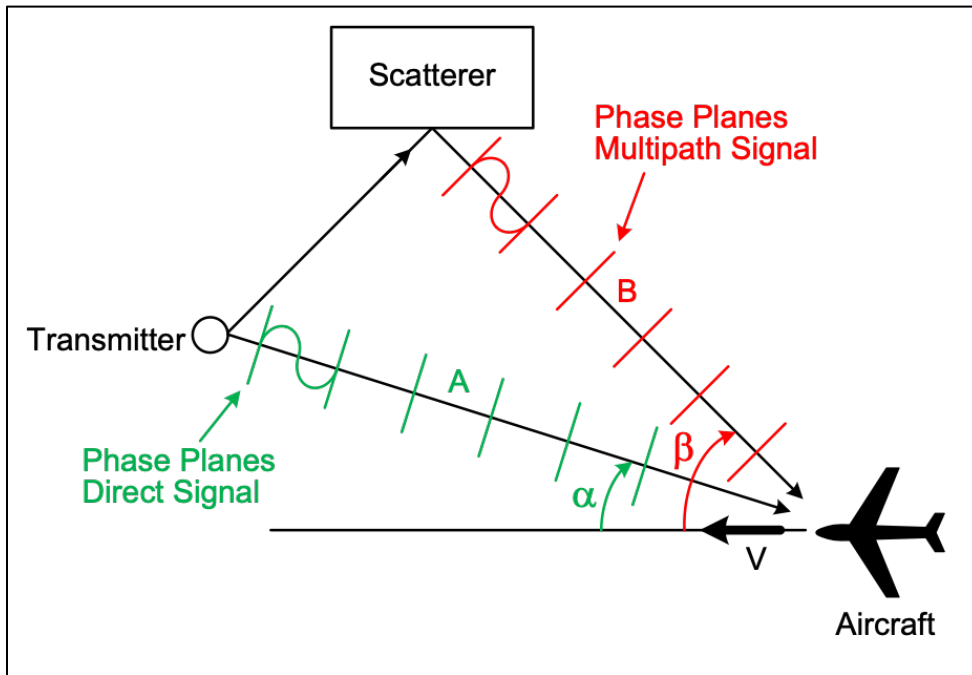


Figure C-20. Geometrical Relationship for Multipath Scalping Equation

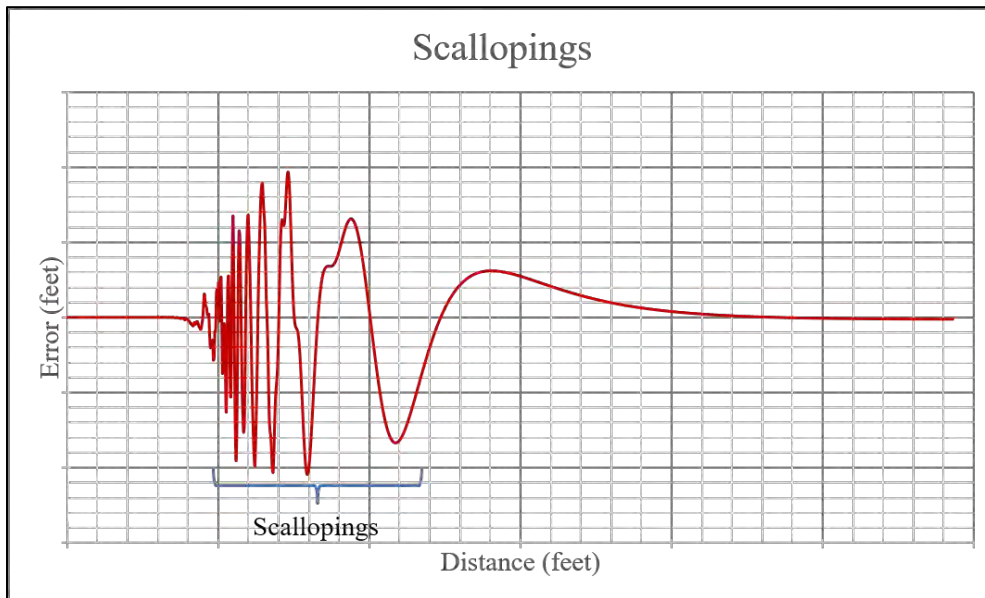


Figure C-21. Example Error Trace with Scalping Effect Illustrated

As Figure C-21 illustrates, the ranging error magnitude can oscillate rapidly with the instantaneous frequency dependent on the scattering geometry and aircraft flight profile at that instant in time. The magnitudes of such oscillation can be reduced by filtering and/or averaging the range measurements.

The mass of an aircraft provides inertial damping that limits the rate of change in the velocity of the aircraft, which in turn physically limits the rate at which an aircraft’s distance to a DME ground station can fluctuate. The knowledge of this physical constraint permits the use of a low-pass data output filter in the interrogator to reduce the effects of sinusoidal and noise-like error effects on range measurements. While the interrogator manufacturer has flexibility in the use and design of this filter, it is commonly assumed to be a single-pole (i.e., 6 dB/octave), low-pass filter with a corner frequency of 10 radians/second (i.e., 1.6 Hertz (Hz)) for the purpose of conducting a general error analysis (Reference X). The Bode plot for this filter is shown in Figure C-22. This filter can be applied to simulation results, or its characteristics used (a) to determine the amount of reduction to apply to the scalloping portion of an error trace or (b) when performing manual calculations of multipath error bounds.

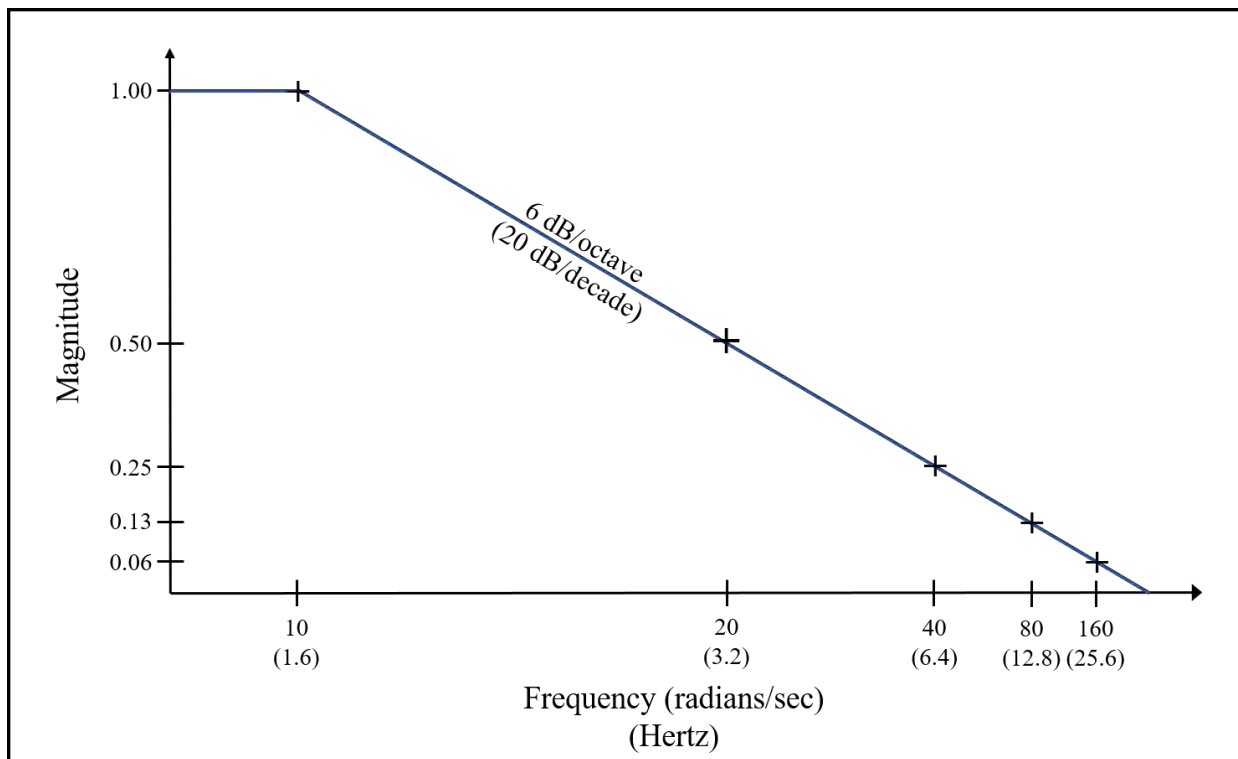


Figure C-22. Bode Plot of Generic DME Interrogator Output Filter

Generally, the interrogation rate is higher than the rate needed for accurate range measurements during normal aircraft flight dynamics. In this case, the averaging of “excessive” range measurements can be performed to reduce the effects of sinusoidal and noise-like error effects on range measurements. Beyond the application of the low-pass filter discussed above, the application of further data averaging requires knowledge of the interrogator design. The application of design-specific signal processing techniques tends to make the analysis results design specific as well. Thus, this type of analysis is not applicable to supporting the site selection process.

- ii. **Time-Of-Arrival (TOA) Determination.** The DME pulse-pair must be detected, and its TOA accurately determined, to support the ranging function. As previously mentioned, the interrogator uses this arrival time to determine range, whereas the transponder uses it to begin the reply delay timing. Envelope detection is used in DME, thus the RF carrier phase information is of no importance to range determination (Reference X).

The measurement method used must satisfy the ranging accuracy requirement under conditions typically encountered during normal flight operations. Consideration of, or tradeoffs amongst, the following items is necessary to achieve satisfactory performance in day-to-day operation:

1. Accuracy requirement;
2. Spectrum requirements;
3. Signal amplitude and pulse shape variations;
4. Multipath resistance;
5. Aircraft dynamics versus signal filtering/smoothing;
6. Measurement threshold to noise ratio;
7. Spurious noise or anomalous measurement effects; and
8. Measurement circuit or analog-to-digital converter variations and/or limitations.

A common TOA measurement technique uses a circuit or software function to compare a delayed version of the detected pulse to an attenuated version of the same pulse. The first crossover point between these two signals – that is, when the delayed signal exceeds the attenuated version – is used to determine the pulse TOA. Of course, the measurement time introduced by the technique must be taken into consideration when performing the TOA determination. While there is some flexibility in the design of the circuit or software function used, the delay and compare parameters selected must ensure that the crossover point occurs on the rising edge of the delayed pulse.

Determining where this crossover point is to occur involves making a tradeoff between good multipath performance (i.e., accuracy performance) and susceptibility to noise induced measurement anomalies (i.e., useable distance performance). The competing tradeoffs led to the development of narrow-bandwidth DME (i.e., DME/N) and precision DME (i.e., DME/P) (Reference X). DME/N is the primary system used in aviation today and is commonly referred to simply as DME.

The half amplitude find function used in DME/N for TOA determination is shown in Figure C-23. The detected pulse is delayed in one channel, while its peak is found and attenuated (6 dB) in the second channel. The channel outputs are compared, and the crossover point (T_D) is used to declare the pulse TOA. The delay must be long enough to ensure that the pulse peak is measured and attenuated, and that the corresponding output reaches the comparator slightly before the half amplitude

point of the delayed pulse.

Based on the pulse characteristic requirements contained in FAA-E-2996, the pulse peak should occur within 3,800 ns minus the time for the delayed pulse to reach its half-amplitude point (i.e., 1,900 ns), which suggests a delay of at least 2,000 ns should be used. The selection of these parameter values favors noise performance (i.e., greater range coverage), making DME/N better suited for supporting en route flight operations with multipath performance that is typically adequate for support of terminal operations.

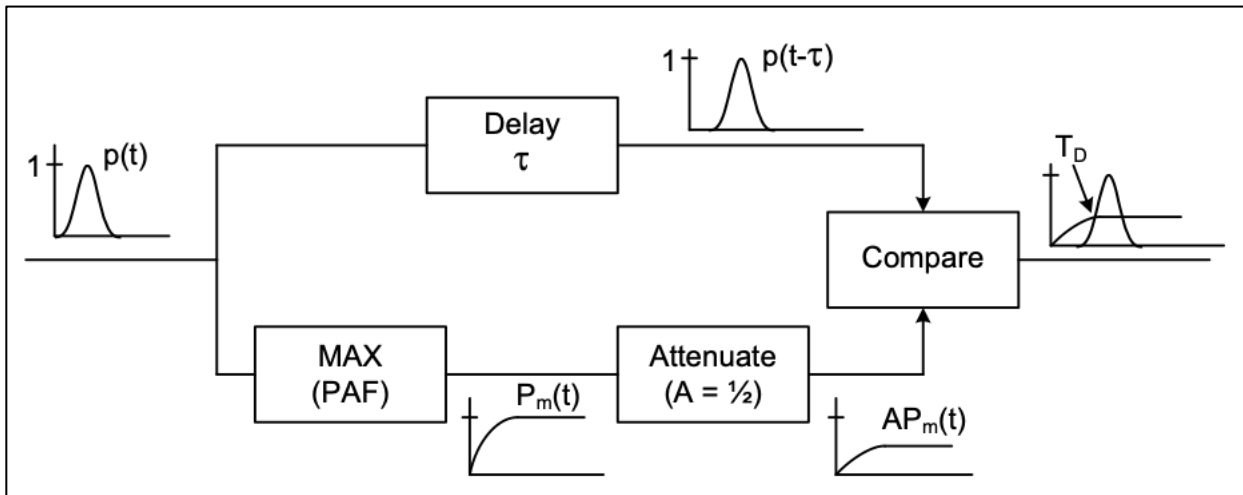


Figure C-23. Half Amplitude Find Function Used in DME/N for TOA Determination

Although DME/P equipment will not be deployed in the NAS, the Delay-Attenuate-Compare (DAC) function used for TOA determination in the DME/P Final Approach Mode region is shown in Figure C-24 for completeness. The delay and attenuation parameters are typically selected such that the crossover point occurs in the vicinity of 200 ns. The use of such parameter values, combined with the use of a pulse shape having a linear leading-edge segment (e.g., \cos/\cos^2), provides ranging accuracy ($\approx \pm 100$ feet) superior to that achieved by DME/N (RTCA DO-189). The technique greatly reduces the effects that multipath and pulse rise-time variation (which are permitted by the requirements) have on ranging accuracy. However, this accuracy performance comes at the expense of a reduced coverage volume, limiting DME/P support of flight operations to the approach region.

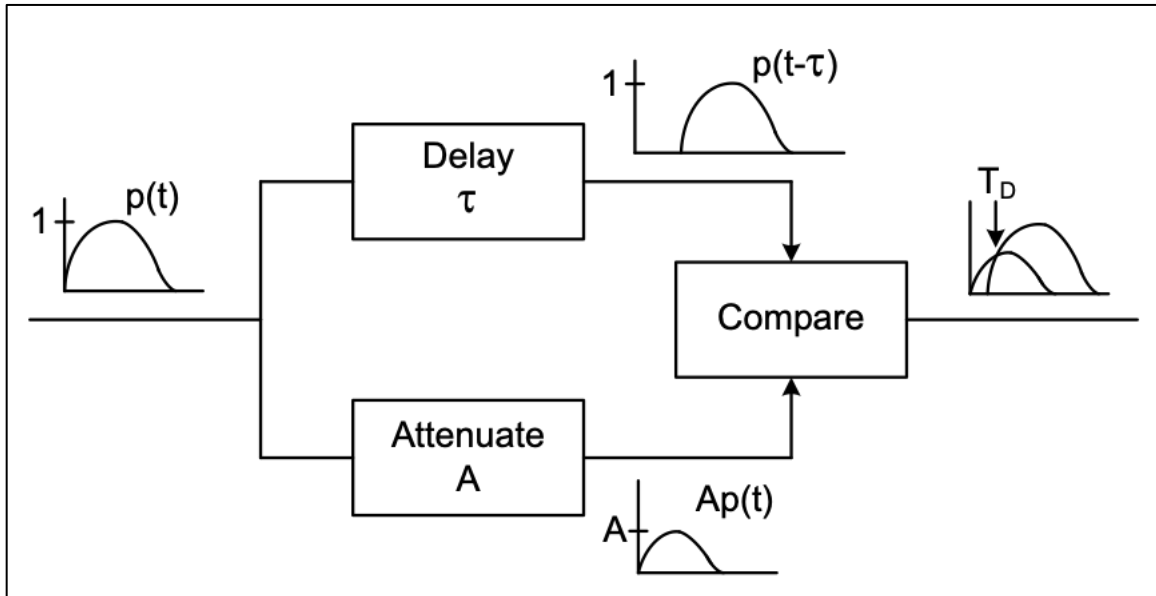


Figure C-24. DAC Function Used in DME/P for TOA Determination

The pulse used for making the TOA determination has changed over time (References R, DD, EE and FF). The use of the second pulse of the pulse-pair for TOA determination was the method used in early DME equipment. The “second pulse method” was used due to the limitations of the RC (analog) delay circuits used in early equipment designs. It should be noted that this method was susceptible to range measurement errors due to the effects of multipath from first pulse echoes on the second pulse of the pair (see Section 5.b.iii of this Appendix for additional discussion).

Advances in integrated circuitry during the late 1980s enabled the use of first-pulse timing methods. However, since many countries were unfamiliar with these methods, some DME equipment designed at that time were configurable to allow the selection of first-pulse or second- pulse timing. The use of first-pulse timing provided ranging accuracy performance improvements sufficient to enable DME/DME RNAV (now a certification requirement in some cases). Both DME/N and DME/P Standards and Recommended Practices (SARPs) require that range measurements be made using the first pulse of a valid pulse-pair (References R and DD).

5. DME System Performance

This section provides a detailed discussion regarding the factors that influence DME system performance from a SIS perspective. First, signal attenuation due to either blockage of the LOS signal path by objects in the environment (aka shadowing) or fading effects caused by multipath are discussed in Section 5.a. Then, discussions in Section 5.b focus on characterizing the effects multipath can have on ranging accuracy. In each section, methods for estimating the magnitude of the impact are presented.

a. Signal Strength. The signal radiated by the DME ground station must meet minimum

signal strength requirements everywhere within the applicable service volume, which will normally be one of the volumes shown in Figure 3-2. Compliance with this requirement ensures frequency protection from co-channel and adjacent channel interference and that the DME interrogator (i.e., the airborne avionics) can receive and properly process ground station replies to interrogations.

Factors that affect signal strength include transmitter output power; cable and connector losses; antenna pattern gain characteristics in both the horizontal and vertical planes; propagation loss incurred as the signal travels through the atmosphere; and the effect of multipath caused by objects in the vicinity of the DME ground station antenna. Most of these factors have been addressed by prior analyses (e.g., link budget) and/or operational experience, and as such, do not need to be addressed as part of the antenna site selection process.

The primary factor addressed during the site selection process is the control of multipath effects by the proper application of siting criteria. The effects of longitudinal multipath (Figure C-3) on signal strength are primarily controlled by the DME antenna design, and information regarding DME antenna performance is provided in Chapter 4 and Appendix D. The effects of signal blockage (Figure C-1) and lateral multipath (Figure C-4) are controlled by selecting a suitable antenna site, ideally a site that satisfies all the siting criteria presented in the body of this order. This is a site for which the Object Consideration Area (OCA) shown in Figure C-25 is free of objects. In some cases, it may not be possible to identify such a site at the designated facility location, and it becomes necessary to consider sites that result in an object(s) being located within the OCA. In this case, the effect on signal strength caused by multipath from this object(s) must be evaluated.

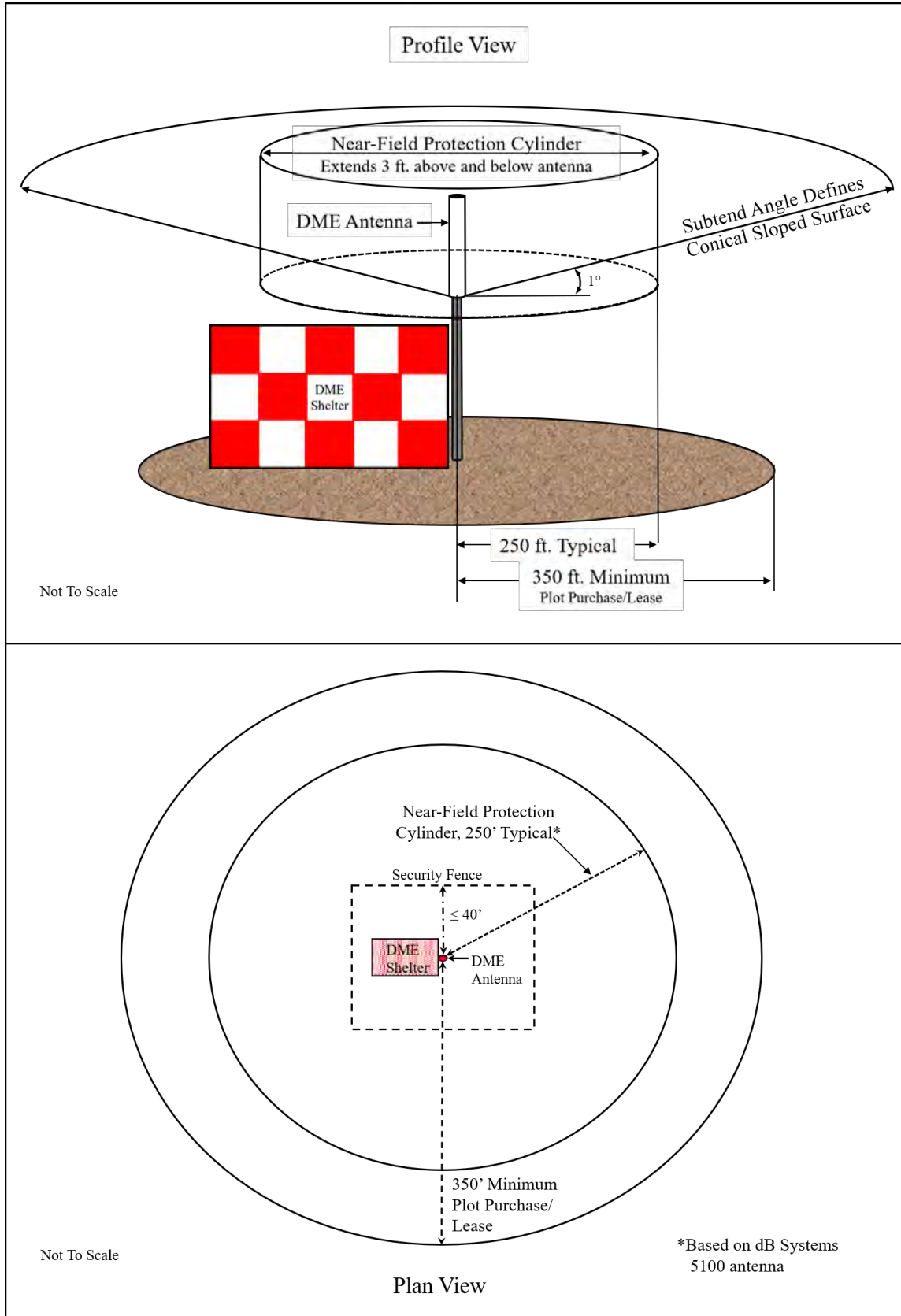


Figure C-25. DME Object Consideration Area (OCA)

- i. **Evaluating signal attenuation due to blockage/shadowing.** In order to ensure that sufficient signal strength exists at a given receiver location, the three-dimensional region (aka LOS region) defined by the first Fresnel Zone surrounding the direct LOS path between the transmitter and receiver antennas must be free of objects. In other words, a clear LOS region is to be maintained as shown in Figure C-10 and Figure C-11. When an object or structure exists within or penetrates this region, the potential for excessive signal attenuation to result within the service volume should be evaluated. This section describes a qualitative method for performing such an evaluation based on the amount of LOS region obstruction caused by an object.

Analysis of the diffraction gain for an obstruction within the LOS region has shown that the strength of the signal received is a function of the obstruction size, its proximity to the LOS path, and the size of the Fresnel Zone at the obstruction location. The amount of obstruction that is caused depends on both the dimensions of the object and its orientation with respect to the direct LOS path. For example, a rectangular object having a width and depth each of 10 feet can create an obstruction zone 14 feet wide when the vertical faces of such an object are oriented 45° to the LOS path.

The diagram in Figure C-26 depicts the normalized electric field received as a function of the FKP for the case of normal incidence edge diffraction (aka knife edge diffraction) of the DME signal by an infinite half plane (see Figure C-27). Because the analysis considers a normalized electric field, the trace shown in Figure C-26 can be interpreted as diffraction gain, where a value of less than one denotes attenuation of the received signal compared to that received for the unobstructed case. Likewise, a value greater than one signifies amplification of the signal.

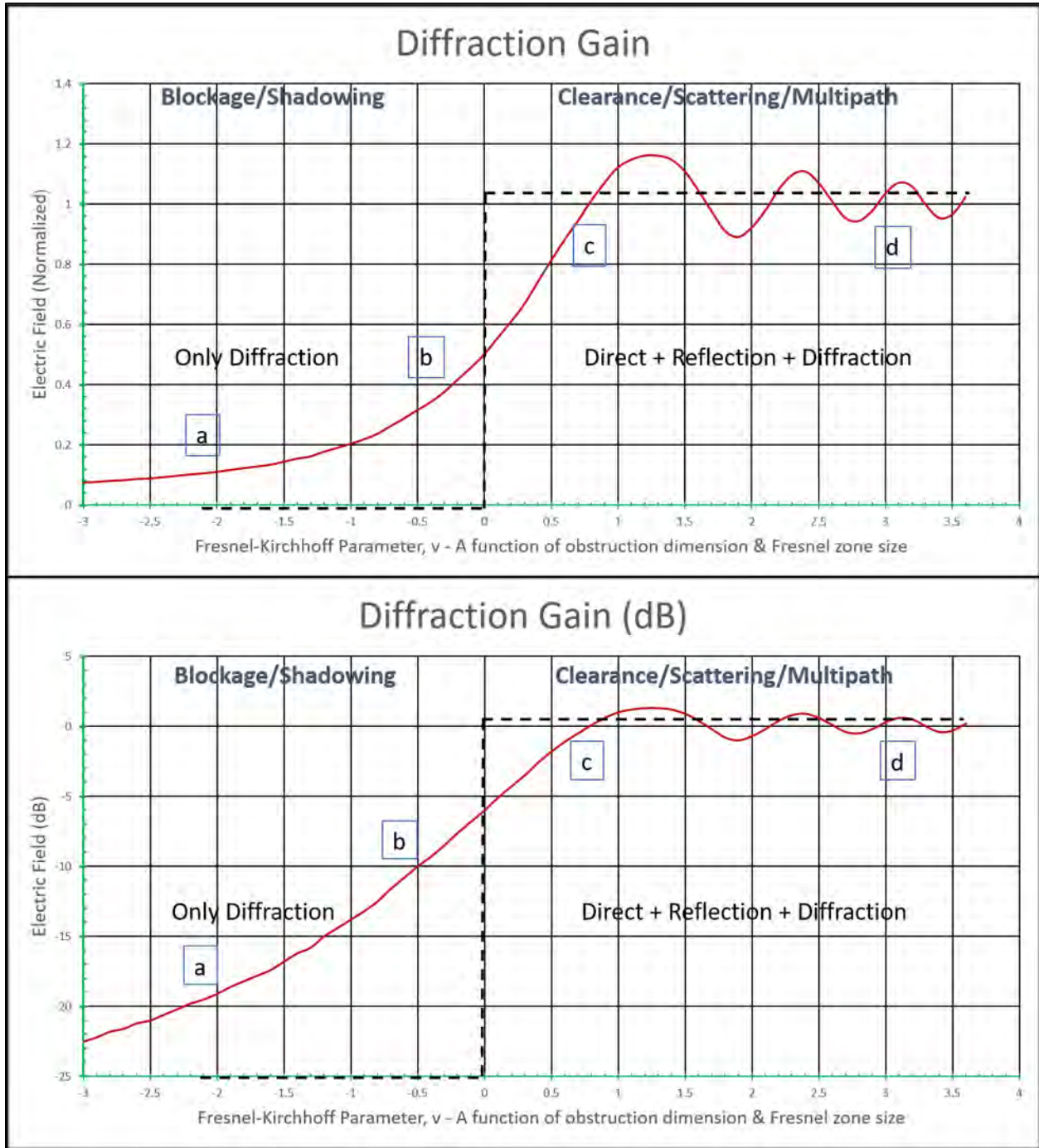


Figure C-26. Diffraction Gain

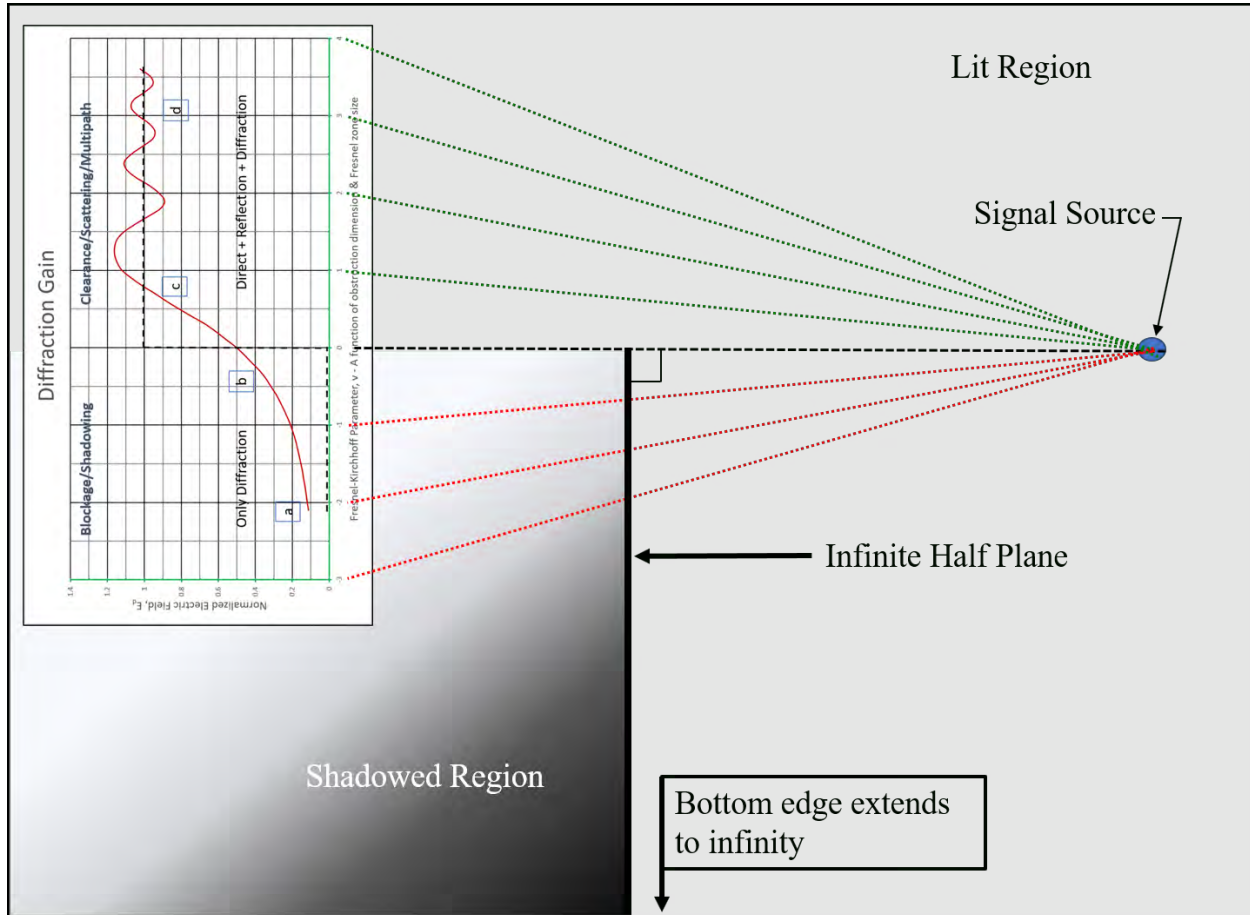


Figure C-27. Knife Edge Diffraction Geometry

The FKP is a function of the Fresnel Zone size and the amount of clearance between the LOS path and the closest edge of the obstruction. That is, the portion of the obstruction that penetrates the Fresnel Zone around the LOS path to the reception point determines the amount of signal attenuation or amplification that results. The “Blockage/Shadowing” area shown in Figure C-26 is the area where most of the Fresnel Zone is penetrated by the object, including blockage of the geometrical LOS between the transmitter and the receiver antennas. In this case, significant obstruction of the LOS region occurs, which results in shadowing (i.e., significant signal attenuation) because only the diffracted field is received at the reception point. In the “Clearance/Scattering/Multipath” area, the amount of obstruction clearance determines the magnitude of the total field that is received at the obstruction point. Again, the amount of signal attenuation or amplification is in comparison to the unobstructed case.

The phenomenon explained above is illustrated further by the four scenarios shown in Figure C-28. It should be noted that the term “blockage” is used for scenarios where the geometrical LOS is blocked by the object, and conversely, the term “clearance” is used for scenarios where it is unobstructed. Scenario (a) depicts full signal blockage because the whole of the first Fresnel Zone is on the structure and

the entire LOS region is obstructed. In this case, only the field diffracted by the edges of the object is received at the reception point, and this field is very weak because the structure edges are some distance away from the first Fresnel Zone boundary and the reception point is directly behind the structure. That is, the geometrical LOS pierce point is far removed from the structure edges as well. In scenario (b), the LOS region is only partially blocked and the pierce point is still on the structure. These conditions indicate that more of the radiated signal will still reach the reception point via diffraction and that this point is still within the shadowed region. If, for example, a half of the Fresnel Zone is blocked, this can lead to about 6 dB drop in signal strength. Scenario (c) illustrates a partial signal clearance condition, and in contrast to scenario (b), the pierce point is off the structure and clearance for the majority of the LOS region is achieved. In scenario (d), the LOS region fully clears the obstructing structure with the signal strength being similar or equal to that of the object free case. In scenarios (c) and (d), the pierce point is off the structure indicating that the reception point is in what is referred to as the “lit region”.

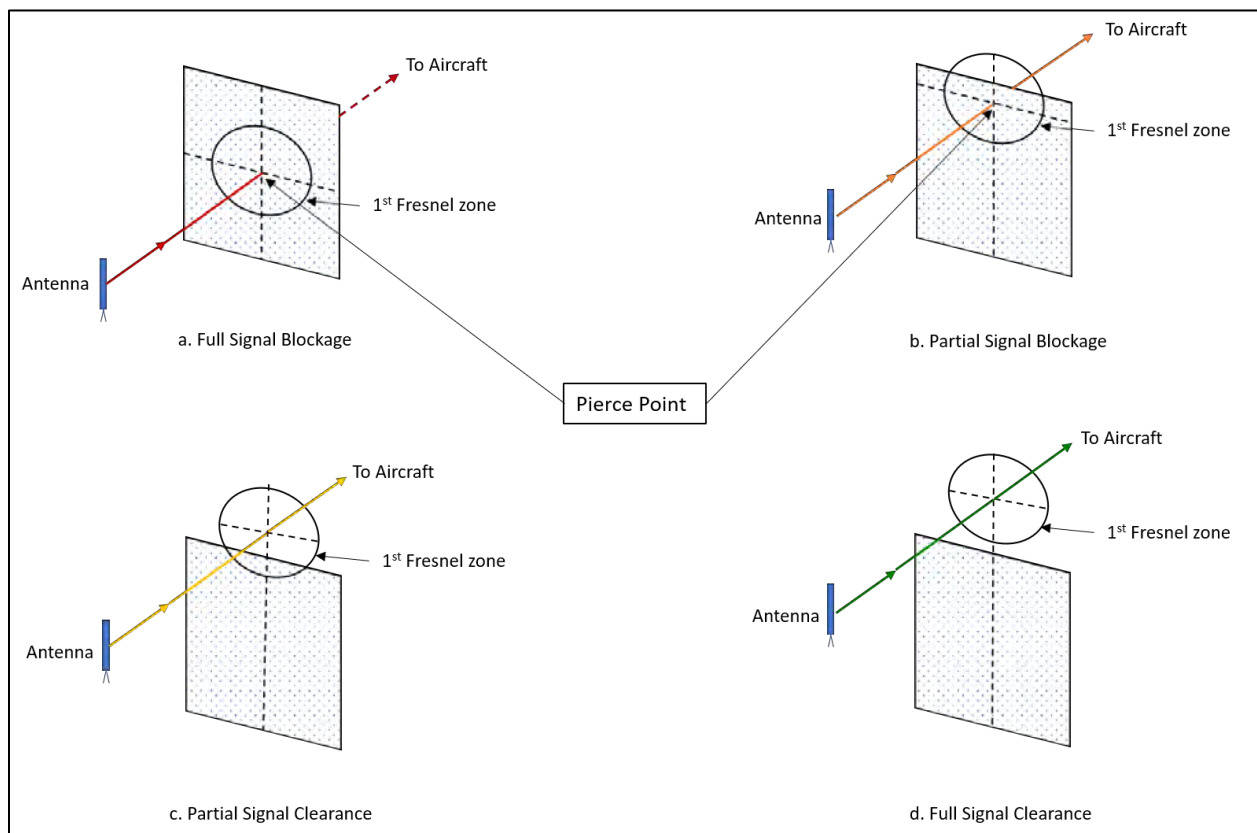


Figure C-28. Signal Blockage/Clearance Scenarios

It is important to note that Figure C-26(a) corresponds to Figure C-28(a), while Figure C-26(b) corresponds to Figure C-28(b), Figure C-26(c) corresponds to Figure C-28(c), and Figure C-26(d) corresponds to Figure C-28(d). When the direct signal is sufficiently blocked by a structure, multipath from other structures may

have a more detrimental effect on ranging accuracy. In this situation, the direct signal is attenuated by the blockage while the signal strength of multipath from other sources can be unaffected by that blockage, which effectively increases the M/D ratio.

Considering that the four scenarios in Figure C-28 could represent four static snapshots of a flight profile, the next step is to apply the information given in Figure C-26 to a dynamic case where shadowing occurs along the profile. This case is taken to demonstrate proper application of diffraction gain data to the task of estimating the impact of the signal shadowing on coverage performance. For this discussion, it is assumed that the distance from the shadowing structure to the aircraft is much greater than the distance from the shadowing structure to the DME antenna.

Figure C-29 shows the plan view for a level-run flight profile that passes through a shadowed region caused by a structure that is more than six Fresnel Zones wide. As shown in the inset of Figure C-28, the pierce-point trace shown on the vertical profile is many Fresnel Zones below the top edge of the shadowing structure. This location allows one to approximate the attenuation by considering the problem as an infinite half-plane with its boundary running parallel to the vertical axis. As discussed below, the symmetry of the shadowing geometry is used to adapt the results to that of an infinite strip having finite width. In the end, the width of the structure and nature of the vertical profile are such that full signal blockage occurs because the geometry presented is like that shown in Figure C-28(a).

Radial lines from the DME antenna have been drawn at intervals corresponding to integer values of the FKP shown on the diffraction gain plot taken from Figure C-26. Given the symmetry of the shadowing geometry (plan view), the diffraction plot is flipped along its left vertical edge, and now one is ready to estimate the signal coverage performed that would be “measured” along the flight profile. The diffraction gain data is used to determine the amount of signal attenuation that occurs in the shadowed region, thus the estimate obtained is normalized to the signal level that would be present in this region if the shadowing structure were not present. The attenuation values obtained are then included in the link budget analysis to determine if the minimum signal strength level would still be achieved in the shadowing region.

The aircraft approaches from the right side of the Figure C-29 and initially there is no signal attenuation until the aircraft is located at a position corresponding to +4 FKP on the diffraction gain plot. At this point, the constructive and destructive interference between the direct and diffracted signals becomes observable as indicated by the scalloping signatures that appear in the signal strength data until the aircraft reaches the right-side shadow region boundary (i.e., FKP = 0).

The aircraft progresses deeper into the shadowed region and the amount of signal attenuation increases until it is directly behind the center of the structure, at which

point the attenuation decreases as the aircraft exits the shadowed region. Scalloping signatures are again observed until the aircraft is well away from the left-side shadow boundary. In this case, the maximum attenuation is estimated to be about 20 dB based on the plan view portion of the analysis, which was approximated as an infinite vertical strip.

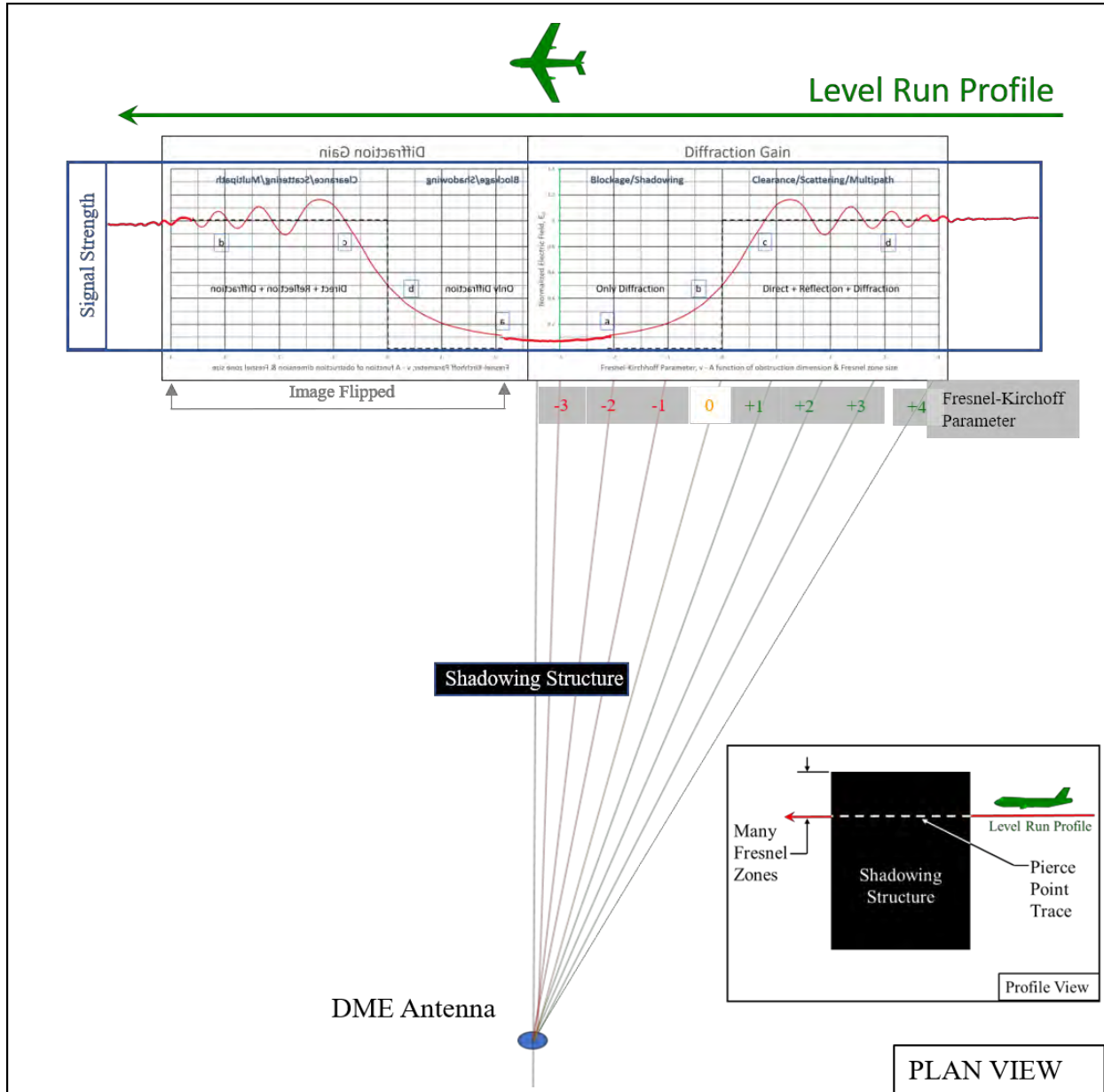


Figure C-29. Flight profile and Signal Strength Analysis, Part 1

The location of the pierce-point trace relative to the top edge of the shadowing structure will also influence the amount of attenuation that occurs. The diffraction gain data of Figure C-26 are applied in the same fashion as was explained above for the shadowing scenario depicted in Figure C-29. However, in this case, the infinite half-plane has its boundary running parallel to the horizontal axis, and the

analysis considers level-run profiles at various heights relative to the top edge of the shadowing structure as illustrated in Figure C-30. The top (i.e., highest) level run profile clears the top edge of the shadowing structure by one Fresnel Zone and the amount of signal attenuation would be negligible (≤ 1 dB).

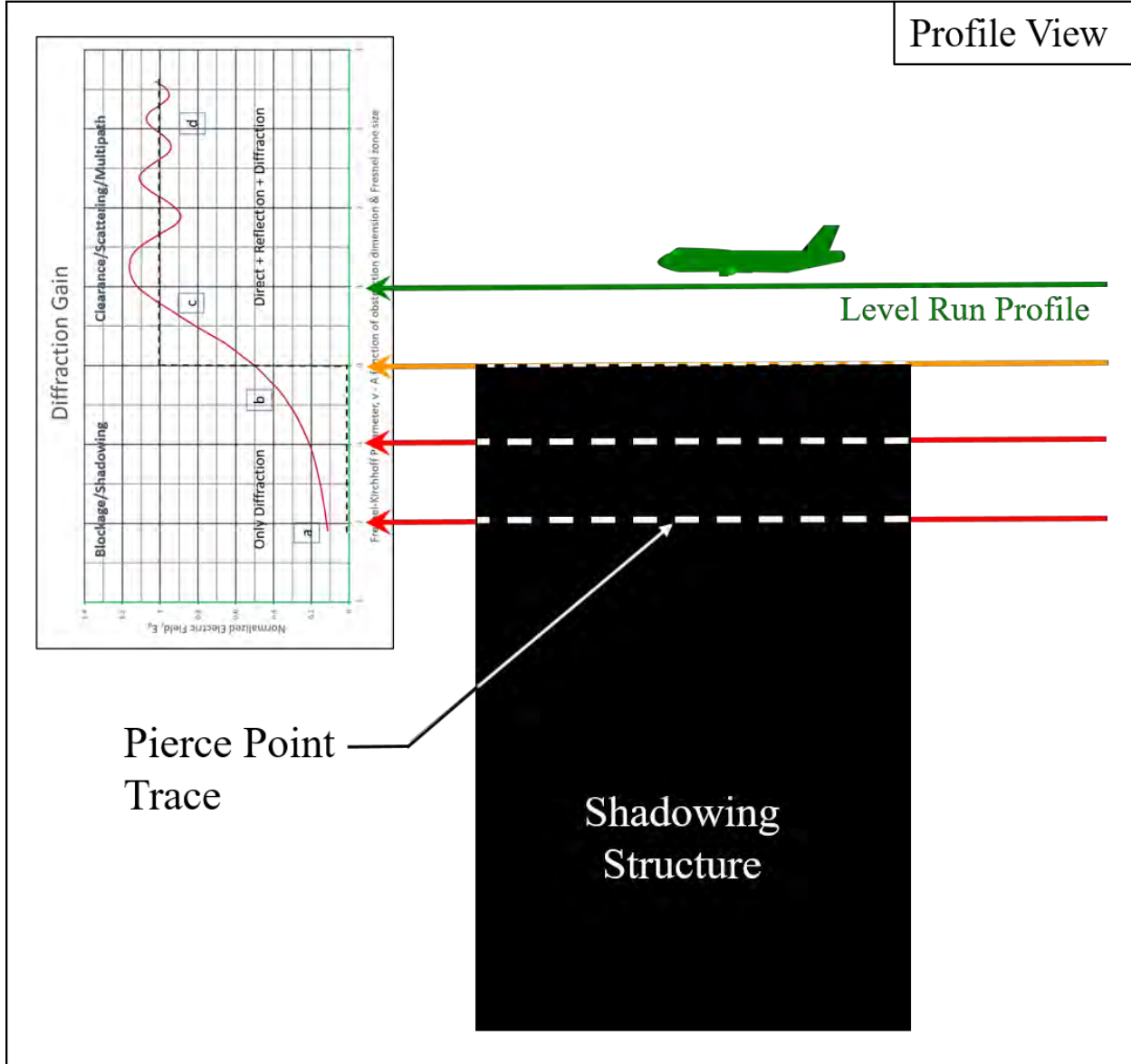


Figure C-30. Flight Profile and Signal Strength Analysis, Part 2

The height of the flight profile is decreased such that the pierce point just skims across the top edge and the next level run is performed as depicted by the orange arrow in Figure C-30. This height of this flight profile is at the boundary between partial blockage and partial clearance scenarios, and as previously mentioned, the amount of attenuation expected would be about 6 dB. The height of the next lower flight profile occurs on the boundary between partial blockage and full blockage scenarios, and the lowest profile is well within the full blockage region. When the

pierce point is well away from the horizontal edge of the shadowing structure, signal attenuation in the range of 14-20 dB would be expected, respectively for each profile.

The next step is to combine the outcomes from the above two analyses, each of which focused on estimating signal attenuation for a one-dimensional case of an infinite half plane. The combination will be done in a notional fashion, as the complexity of performing a two-dimensional analysis requires knowledge of physical optics techniques and related computation methods beyond that presented in the preceding tutorial section. This notional approach is intended to provide one the insight needed to make qualitative assessments when performing a site survey. Figure C-31 shows four zones overlaid on or about a rectangular shadowing structure. Any signal reception point behind the plate that causes the pierce point to lie within the inner most zone (i.e., red zone) will experience significant signal attenuation (≥ 20 dB). Significant attenuation occurs because the pierce point is more than a Fresnel Zone radius away from all structure edges, which causes the diffracted signal reaching the reception point to be very weak. In most cases, sufficient signal strength is unlikely to exist in this portion of the shadowed region when the dimensions of this zone exceed a few Fresnel Zones. In the rare cases where sufficient signal strength exist, the useable signal coverage distance behind the structure will be greatly reduced compared to the unobstructed case.

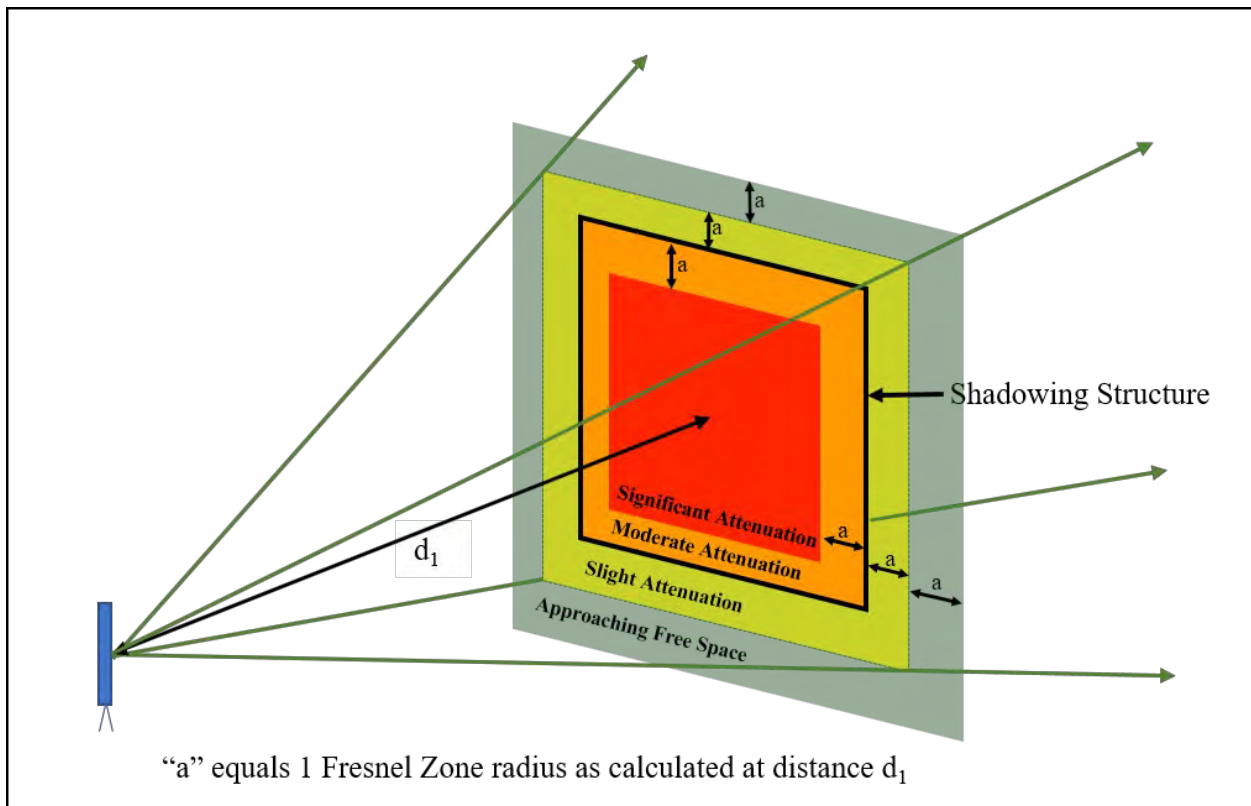


Figure C-31. Qualitative Zonal Assessment of Signal Attenuation Due to Shadowing

When the pierce point lies within the next outer zone (i.e., orange zone of Figure C-31), a partial signal blockage condition exists, and moderate signal attenuation will occur because the signal path for more the half of the LOS region will be obstructed. In many cases, sufficient signal strength is unlikely to exist in this portion of the shadowed region when the dimensions of this zone exceed a few Fresnel Zones and the signal strength in the vicinity of the structure is within about 10 dB of the minimum signal strength requirement.

When the pierce point lies within the third outer zone (i.e., yellow zone of Figure C-31), a partial signal clearance condition exists, and slight signal attenuation will occur because the signal path for more the half of the LOS region will be unobstructed. In many cases, sufficient signal strength is likely to exist in this portion of the shadowed region even when the dimensions of this zone exceed a few Fresnel Zones, provided that the signal strength in the vicinity of the structure is about 6 dB greater than the minimum signal strength requirement.

When the pierce point lies within the outer most zone (i.e., green zone of Figure C-31), a full signal clearance condition exists, and the signal strength quickly approaches that of the unobstructed case (i.e., free space condition). Minor variations in signal strength will occur until the pierce point is a few Fresnel Zones away from the nearest structure edge.

The volume of space in which signal strength may be affected by a shadowing structure can quickly be identified by adding a shadowing silhouette around the structure and performing ray tracing as shown in Figure C-32. The approach provides a basic analysis of the shadowing caused by the structure. If a more descriptive analysis is desired, ray tracing can be performed for each zone shown in Figure C-31 to detail the regions where significant, moderate, and slight attenuation effects would be expected. The mapping of the qualitative descriptors “significant”, “moderate”, and “slight attenuation” to approximate values is dependent on the dimensions of the structure in terms of number of Fresnel radii.

Siting engineers with Physical Optics or signal propagation backgrounds may have the knowledge to make such estimates, while others may elect to rely on mathematical model. The decibel (dB) values stated above should be representative of the attenuation levels when the dimensions of the structure exceed six Fresnel Zone Radii.

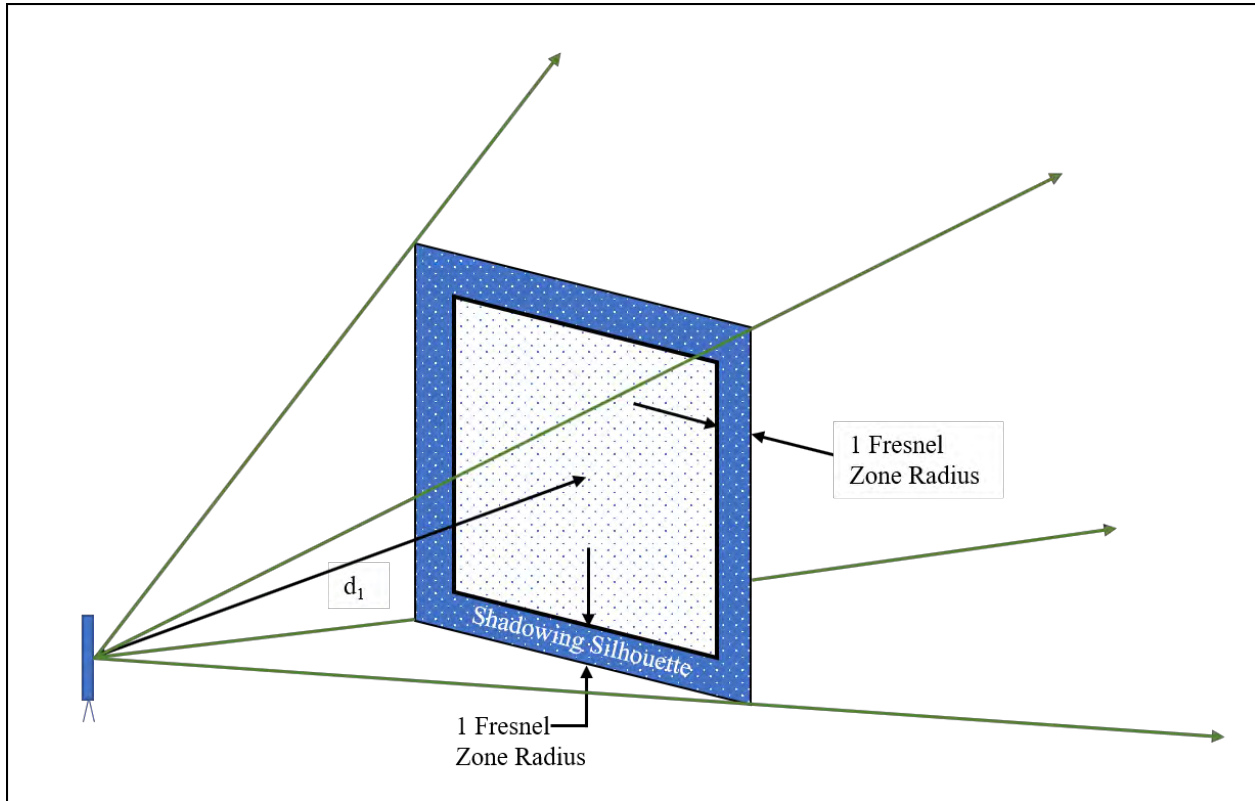


Figure C-32. Shadowing Silhouette used when Performing Ray Tracing

- ii. **Evaluating signal attenuation due to fading.** As previously stated, meeting the coverage requirement throughout the service volume requires the DME design to incorporate characteristics that provide resistance to, or sufficient control of, signal fading caused by multipath effects. Similarly, it was noted that multipath can be categorized as lateral, longitudinal, or a combination of the two.

It is important to understand how this multipath alters the signal strength and the effect these alterations have on system performance. The vector wheel concept (see Figure C-7) was used previously to illustrate qualitatively how ground reflection can add to, or subtract from, the direct signal. Both the worst-case (180°) and best-case (0°) relative phase conditions were introduced (Figure C-8 and Figure C-9). The discussion in this section will build upon this qualitative understanding by summarizing the results of a comprehensive study that was performed to characterize the signal attenuation (i.e., worst case) or amplification (i.e., best case) that can occur due to reflection of the DME radiated signal by the ground (Reference Z).

The relative phase between the direct and reflected signal (i.e., multipath) is a function of the geometry between the transmitter antenna, scatterer, and receiver antenna. When this geometry is fixed, the relative phase has a fixed value as well. When the geometry is dynamic, such as the case when the receiver antenna is mounted on an aircraft, the relative phase will vary with time. This variation with time represents the multipath arrow of the vector wheel spinning in time and thus

the signal strength cycling through maximums and minimums.

Reflection from the ground is an ever-present source of multipath and a good example to start with for illustrating fading effects. A straight-level-run flight test maneuver (i.e., a level run), or simulated flight path towards or away from a ground-based transmitting antenna, can be used for collecting signal strength data that enable the assessment of signal coverage. For example, the level run profile illustrated in Figure C-33 can be used to produce signal strength plots like that shown in Figure C-34.

The general trend of the signal strength plot shown in Figure C-34 follows what is known as the free space loss curve, which accounts for the spreading of a finite amount of transmitter power over an increasingly larger spherical surface as the signal energy propagates away from the transmitter antenna. A bias between calculated and measured signal strength data may be introduced depending on how rigorously one accounts for transmitter output power, cable losses, and antenna gain. Scattering of the radiated signal by objects in the environment can also affect the signal strength measured at any given point in space. As previously mentioned, the signal reflected from the ground will interact with the direct signal to cause fading (i.e., attenuation) and/or amplification.

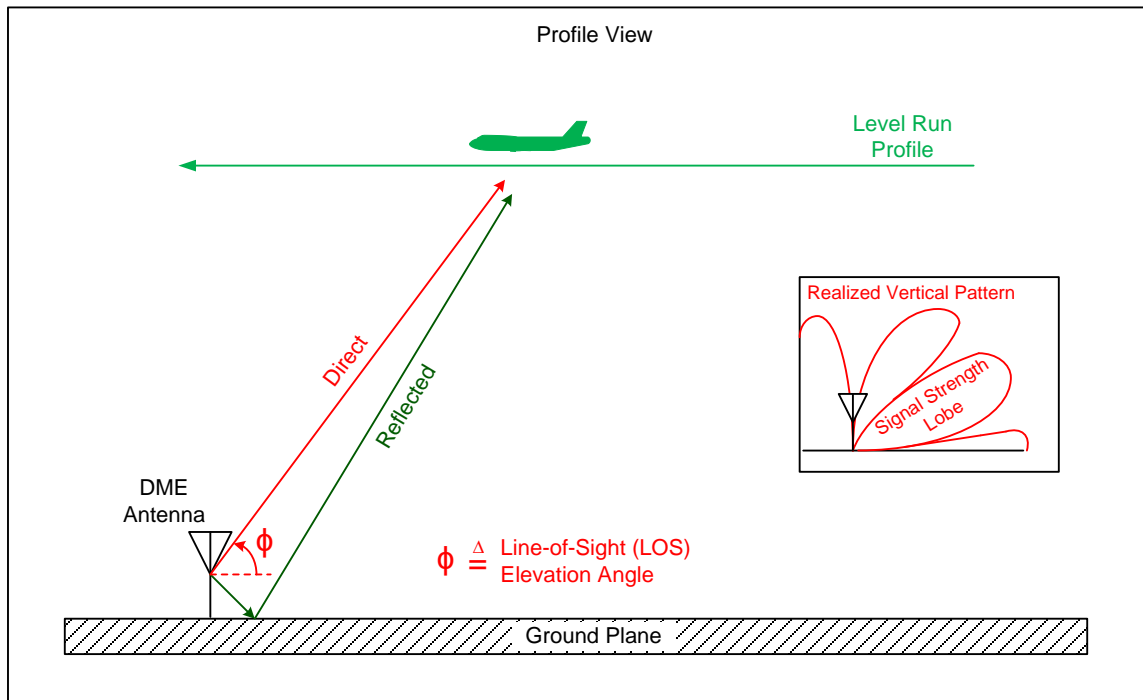


Figure C-33. Level Run Flight Measurement Profile

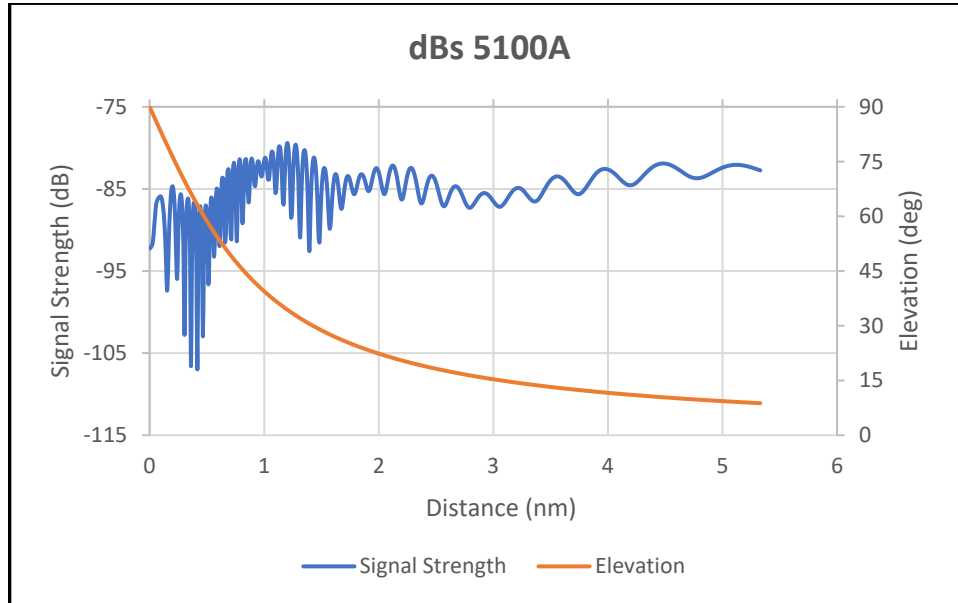


Figure C-34. Example Fading Data Produced by Level-run Flight Measurement Profile

Fading due to multipath is influenced by the surface reflectivity and roughness of the scatterers. Because of this, the aforementioned analysis in Reference Z investigated multiple earth surface conditions as well as multiple surface roughnesses to generate charts to illustrate the effect of fading. Figure C-35 shows examples of the fading analysis results for both the worst-case and best-case relative phase conditions. As the vector wheel inset shows (within Figure C-35), the ground reflection is 180 electrical degrees out-of-phase with the direct signal for the worst-case condition. This condition results in the fading data having negative values, which indicates there is an attenuation in signal strength compared to free-space conditions. Similarly, for the best-case phase condition, the vector wheel inset shows that the ground reflection is completely in-phase with the direct, which “amplifies” the SIS.

The required vertical pattern characteristics for approved DME antennas provide resistance to, or sufficient control of, signal fading caused by multipath effects for typical antenna heights and ground plane situations. This topic is discussed further in Chapter 4 of this Order and the full analysis can be found in Reference Z.

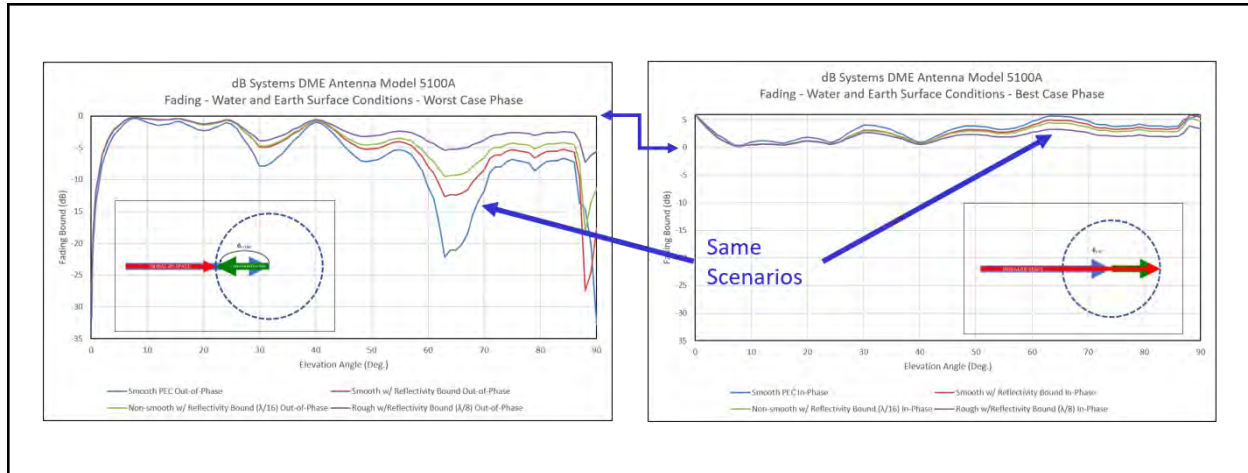


Figure C-35. Example Fading Results for Worst-Case-Phase and Best-Case-Phase Conditions

Multipath from structures in the vicinity of the DME antenna can also cause signal fading. Again, multipath from such structures can be categorized as lateral, longitudinal, or a combination of the two, which primarily affects where the multipath will be projected into the service volume. The important distinction of this situation compared to that of the ground reflection case is that the dimensions of the structure are finite unlike that of the ground plane (i.e., Earth surface) the antenna is mounted above. Among other properties, the size of a reflecting surface greatly influences the strength of the multipath, which in turn determines the depth of fading that may occur. The dimensions of a structure also influence the location and size of the multipath region that is produced. While ray tracing can be used to define the geometrical boundaries of a multipath region, additional analysis is required to evaluate the depth of signal fading (i.e., signal attenuation) that may occur within a given multipath region. One such analysis method is presented below.

Figure C-29 describes the signal attenuation caused by a shadowing structure, and the scenario illustrated will be used as a starting point for this discussion, which is outlined in Figure C-36. The shadowing scenario is presented at the top of this figure, and it details how significant signal attenuation occurs in the shadowed region behind the multipath structure. Given that the DME antenna radiates the same amount of energy in every direction, the question arises regarding where the energy radiated towards the shadowing region went. Of course, this energy was reflected back towards the antenna by the multipath structure.

Assuming that this structure does not absorb that energy (or absorbs very little of it), conservation of energy can be applied to determine (or approximate) the strength of the reflected signal within the multipath region shown in Figure C-36, as well as the strength of the diffracted signal outside of this region. The red trace shown in the figure is computed as one minus the corresponding diffraction gain shown for the shadowing scenario. That is, areas of strong signal attenuation in the shadowed region have a corresponding area of strong multipath reflections in the

opposite direction. Likewise, areas of minimal or no attenuation have corresponding areas of minimal or essentially zero diffracted signal energy.

Further, it should be realized that the relationship between these corresponding areas is in an angular sense, and that a direct signal component will also be present everywhere, except within the shadowed region. Also, the attenuation, reflection, and diffraction levels are based on a normalized electric field, thus these levels are in comparison to the field that would exist in the structure-free case.

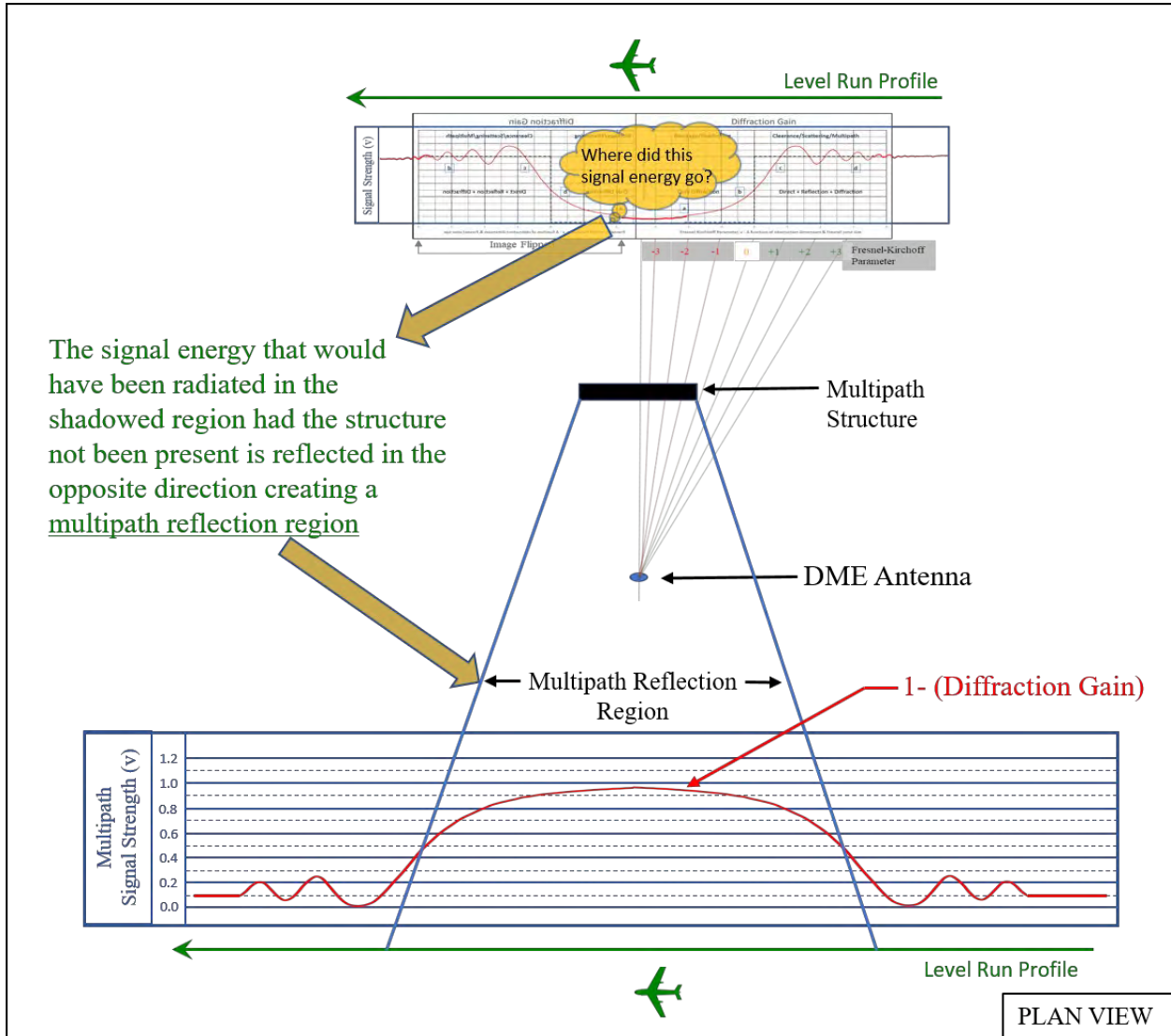


Figure C-36. Shadowing and Reflection Multipath Signal Strength Relationships

The preceding discussion is intended to give a notional understanding of the relationship between signal attenuation in a shadowed region and the strength of the signal reflected into the corresponding multipath and diffraction regions. This understanding should be sufficient to enable one to perform qualitative analysis of fading effects.

The Physical Optics technique used for calculating radiation through an electrically large aperture can be applied for calculating the multipath and diffracted signal levels as shown in Figure C-37. The multipath object is replaced by its complementary aperture, and image theory is applied to determine the location of the source, which is shown as a “DME Image Antenna” in the figure. Strong multipath signals are present in the area where a direct LOS path exists from the image antenna to the reception point, and this area is denoted as the “Multipath Reflection Region” in the figure. Outside this region, the multipath signal present is due to energy diffracted by the aperture edges and the magnitude of this signal falls off as a function of Fresnel Zone radii much like that for the knife edge diffraction case.

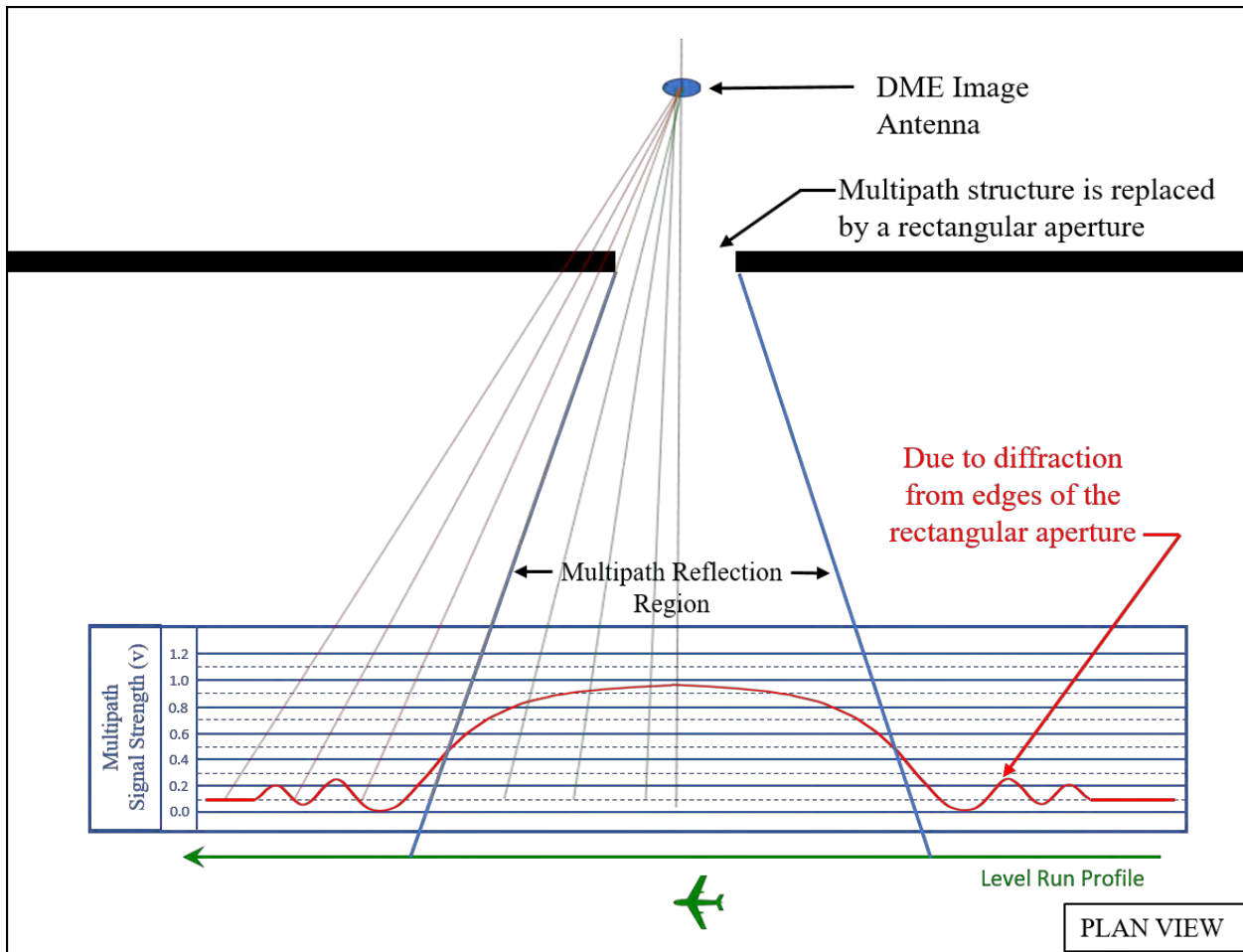


Figure C-37. Radiation Through an Electrically Large Rectangular Aperture

Like the analysis performed above in Section 5.a.i for shadowing (see Figure C-29), a qualitative zonal analysis can be performed to identify regions where significant, moderate, and slight multipath signal levels will be present. Significant multipath signal levels will produce deep fading, whereas shallow fading will be produced when slight (weak) multipath levels are present. As shown in Figure C-38, one of two approaches can be used to perform this zonal analysis. Panel a. of this figure

shows an approach that uses the real DME antenna (aka source antenna) location; four reflecting zones; Snell's law to identify reflection points within each zone; and ray tracing as described in Section 4.a.v above. The two innermost zones represent the real surface of the multipath structure, and the outer two zones are "imaginary surfaces" constructed for analytical purposes.

When the multipath structure consists of flat surfaces with dimensions exceeding six Fresnel Zone Radii, the signal strength for reflections from the innermost zone (i.e., red zone) will be a function of the incidence angle and can be computed using the equations for the Fresnel Reflection Coefficient (Γ) (Reference Z). Alternatively, a worst-case approach is to assume the structure is a Perfect Electric Conductor (PEC), and in this case, the magnitude of Γ is assumed to be one for all incidence angles. The magnitude of Γ should be reduced by 6 dB once the specular point reaches the outer edge of the second inner zone, and by 14 dB when reaching the outer edge of the third zone. It is worth noting that the multipath signal levels stated in this paragraph can be used to calculate the M/D ratio needed for making estimates of the ranging error caused by the multipath signal; they still need to be adjusted to account for the additional propagation loss that occurs due to traveling a longer path than the direct signal.

Panel b. of Figure C-38 shows an approach that uses the image DME antenna location; the complementary rectangular aperture; four aperture zones; sample pierce points within each zone; and ray tracing. Like the case above, the two innermost zones represent the aperture, and the outer two zones are "imaginary apertures" constructed for analytical purposes. The attenuation values stated in the above paragraph should be applied when the pierce point is at the corresponding reflection point as stated above.

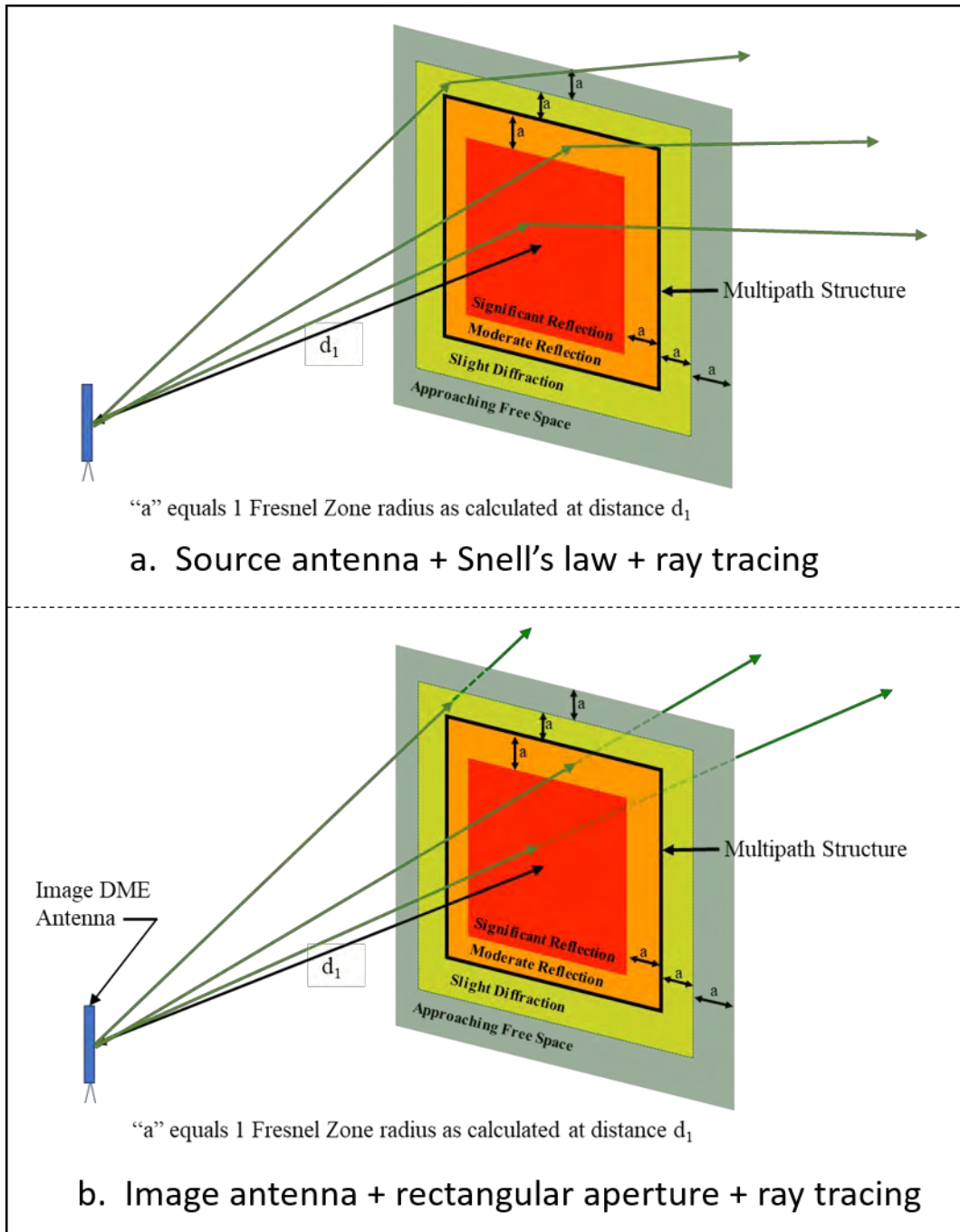


Figure C-38. Qualitative Zonal Assessment for Signal Attenuation Due to Fading

The volume of space in which signal strength may be affected by fading caused by a multipath structure can quickly be identified by adding a diffraction silhouette around the structure and performing ray tracing as shown in Figure C-39. As with the shadowing case, this approach provides a basic analysis of the fading caused by the structure, and if a more descriptive analysis is desired, ray tracing can be performed for each zone as discussed above. Also, the analysis will also identify the volume of space where ranging errors may exceed desired levels or even be out-

of-tolerance, depending on the dimensions of the structure. Conversely, outside of this volume of space, the magnitude of the multipath signals diffracted from structure edges is expected to be at least 14 dB below the direct signal (i.e., M/D ratio ≤ -14 dB). As discussed further in Section 5.b.iv, the magnitude of the resulting ranging errors are expected to be on the order of 100 feet (see Figure C-48 and Figure C-49) in most cases.

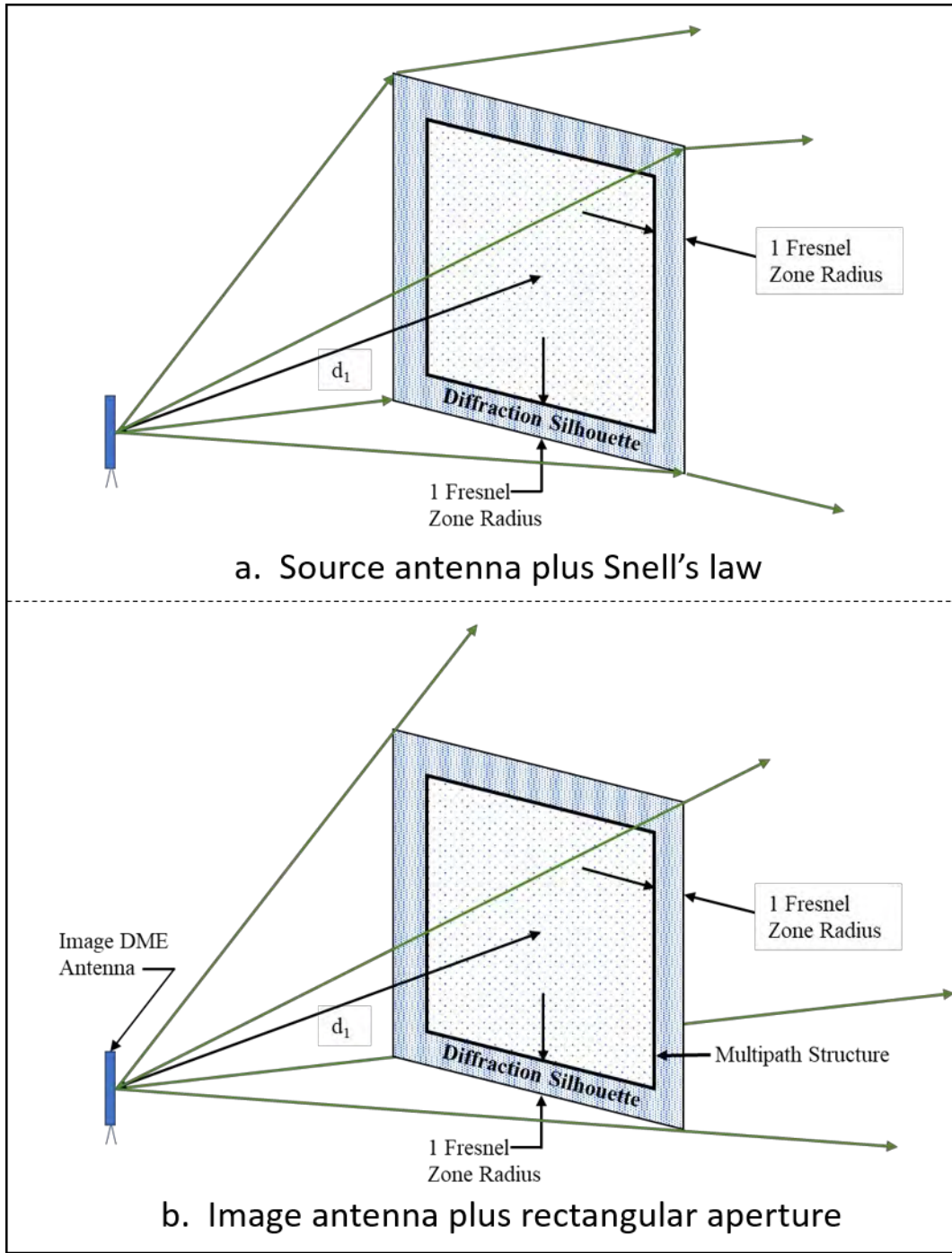


Figure C-39. Diffraction Silhouette Used When Performing Ray Tracing

- b. Evaluating ranging error due to multipath.** This section is further broken down to characterize multipath and how it affects the signal in space. The discussion includes information about how the signal in space TOA is processed and how it influences multipath error magnitudes and arrival zones. A method for determining absolute time delays is demonstrated. Finally, jitter and control of synchronous multipath effects is addressed.
- i. **Overview.** This section starts with a discussion of TOA signal processing and how multipath affects the TOA measurement. A foundational discussion follows regarding how multipath can deform the shape of the pulse used by the DME receiver for the TOA measurements and how this deformation results in ranging error. Plots of worst-case error magnitudes as a function of M/D ratio, relative phase, and relative time delay are presented along with the methodology employed to produce them. These plots are then analyzed to define relative time-delay bounds that describe early and late multipath arrival zones about the direct-signal pulse used for the TOA measurement (i.e., the TOA measurement pulse). Multipath arriving within these zones has the potential to generate measurable ranging errors, including errors with magnitudes large enough to impair operational performance in some cases.

The operational RF environment is briefly explored to illustrate multipath scenarios that can produce multipath within either the early or late multipath arrival zones that surround the TOA measurement pulse. Because the multipath arrival zones are defined relative to the TOA measurement pulse, methods for computing the absolute time-delay values needed for defining echo (multipath) ellipsoids are required. Such methods are presented, as is the importance of using a jittered interrogation signal format to control the ranging errors caused by synchronous multipath effects.

- ii. **TOA Processing and Multipath.** It is important to understand how the DME SIS is processed and how multipath is analyzed. In the absence of multipath interference, the DME pulse-pairs arrive at the reception point without deformation. When the signal is processed as illustrated in Figure C-23, the half amplitude find function processing used for the TOA determination (DME/N) outputs waveforms as shown in Figure C-40(a). This represents the processed DME signal in the SIS domain. When multipath interference is present, the DME pulse-pairs could arrive at the reception point with or without deformation. When this signal is processed as illustrated in Figure C-23, the half amplitude find function processing used for the TOA determination (DME/N) outputs waveforms as shown in Figure C-40(b).

As with Figure C-40(a), this represents the processed signal in the SIS domain. It should be noted that Figure C-40(a) and Figure C-40(b) appear similar, and in the SIS domain the receiver cannot de-construct the composite pulse into the direct and multipath signal components. Therefore, when the impact of multipath effects on the DME signal are analyzed, it is necessary to do so in the Multipath Analysis Domain. In this domain, the direct and multipath components are combined to

produce the composite signal, which is then analyzed to determine the resulting range error.

Figure C-40(d) shows how the composite pulse is made up of the direct pulse (dotted-line) and the multipath pulse (red-line). By examining how the direct and multipath signals combine to form the resultant composite pulses in the Multipath Analysis Domain, a better understanding of how multipath can impact the DME signals is gained. Therefore, the Multipath Analysis Domain will be used in this Appendix to illustrate multipath effects on the DME signal. Figure C-40(d) further shows how the half-amplitude points of the Direct and Composite Pulses (T_d Direct, T_d Composite) and how the multipath can affect the TOA. The way the multipath pulse affects the direct pulse (pulse deformation) as well as its impact on the TOA is discussed next.

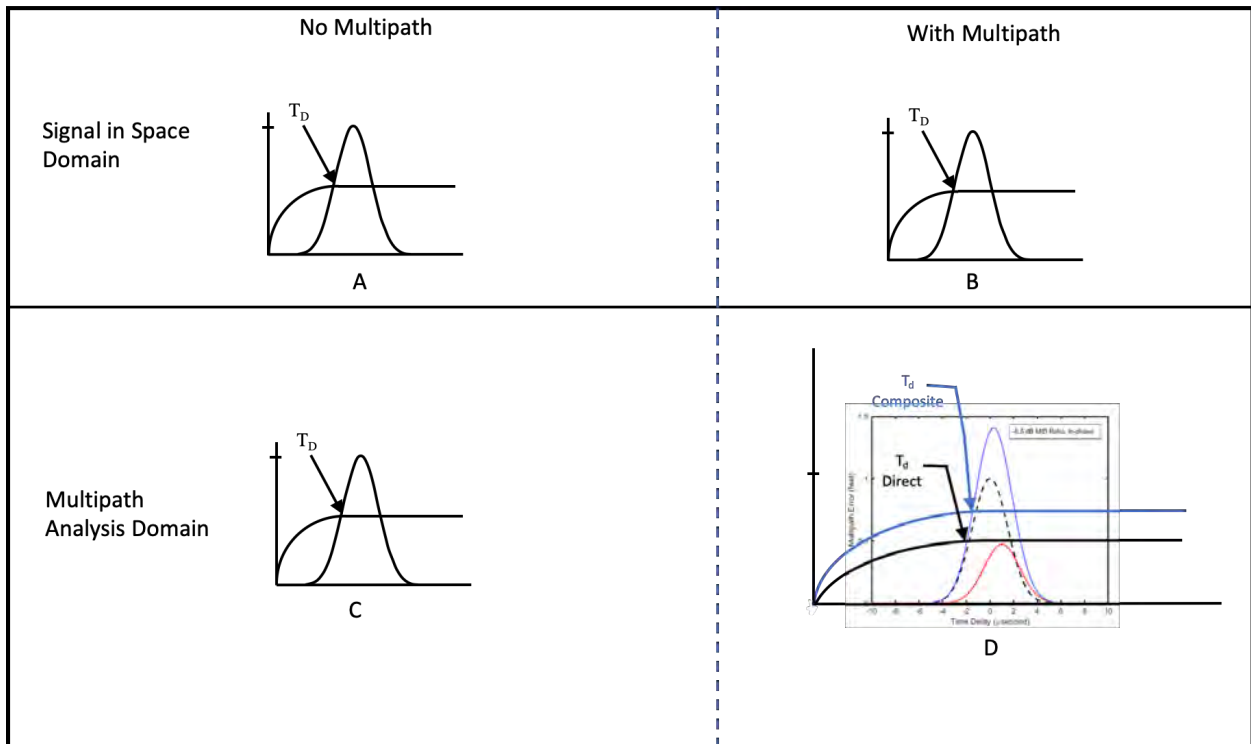


Figure C-40. TOA Processing With and Without Multipath

- iii. **Pulse Deformation Fundamentals.** This section examines when and how a multipath pulse affects the shape of the composite pulse that is used for making the TOA determination. The concept presented is applicable whether the first pulse or second pulse of the pair is used for the range measurement. This independence is achieved because the multipath pulse parameters (i.e., amplitude, phase, and arrival time) are defined relative to the direct pulse that is used for the measurement. That is, they are defined by an M/D signal ratio, relative time delay (τ), and relative phase as previously discussed.

Multipath pulses may be a result of direct pulses that are reflected from objects as

small as an outdoor equipment enclosure, or as large as a mountain range. Because they initially propagate to an intermediate location, they travel a longer propagation path from the transmitter to the receiver antenna than the corresponding direct pulses. Regardless of their amplitude or relative phase, the multipath pulses will not interfere with the direct pulses unless the multipath path pulse arrives at the receiver antenna while the direct pulse is also being received; this interference condition is depicted in Figure C-41. The discussion that follows validates this condition and provides the background necessary for quantifying the range of time-delay values that constitute a “same time” arrival.

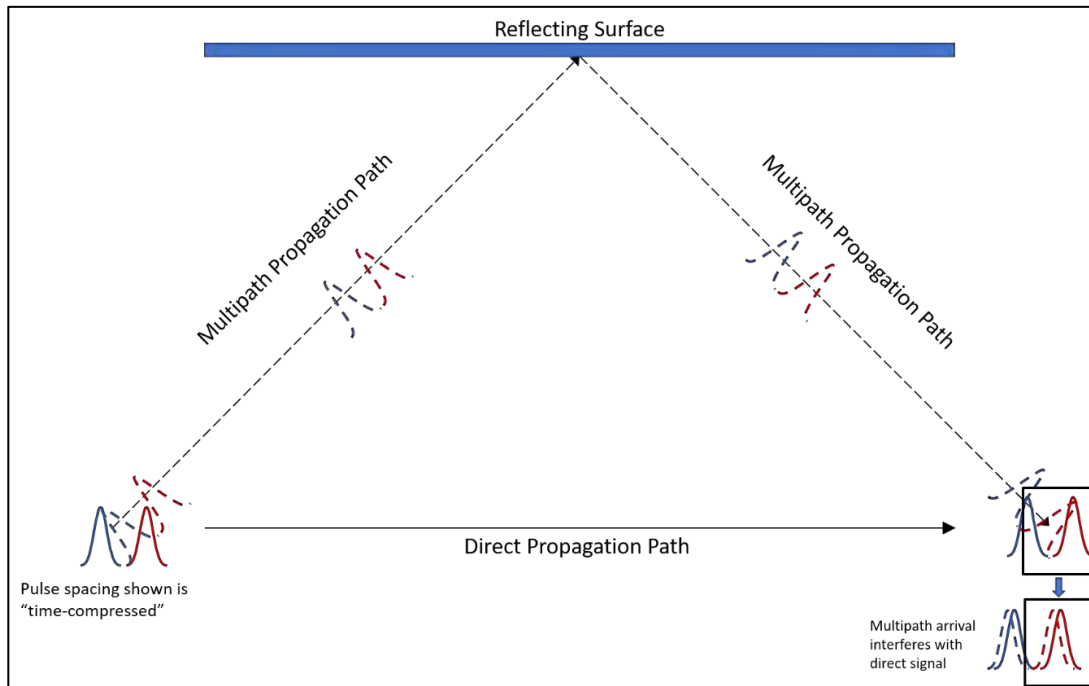


Figure C-41. Multipath Pulses From Same Reply Cycle Arriving Slightly Later than Direct Pulses

Figure C-42 illustrates the manner in which the multipath scenario of Figure C-41 results in a deformed pulse in the Multipath Analysis Domain. This scenario results from the simplest multipath case, when the multipath of the same interrogation or reply cycle arrives slightly later than the direct signal. The deformed pulse in this case results from the in-phase multipath combining with the direct signal to form the composite signal, which has a different TOA point than the direct. The way in which deformed pulses are formed is examined later in this section.

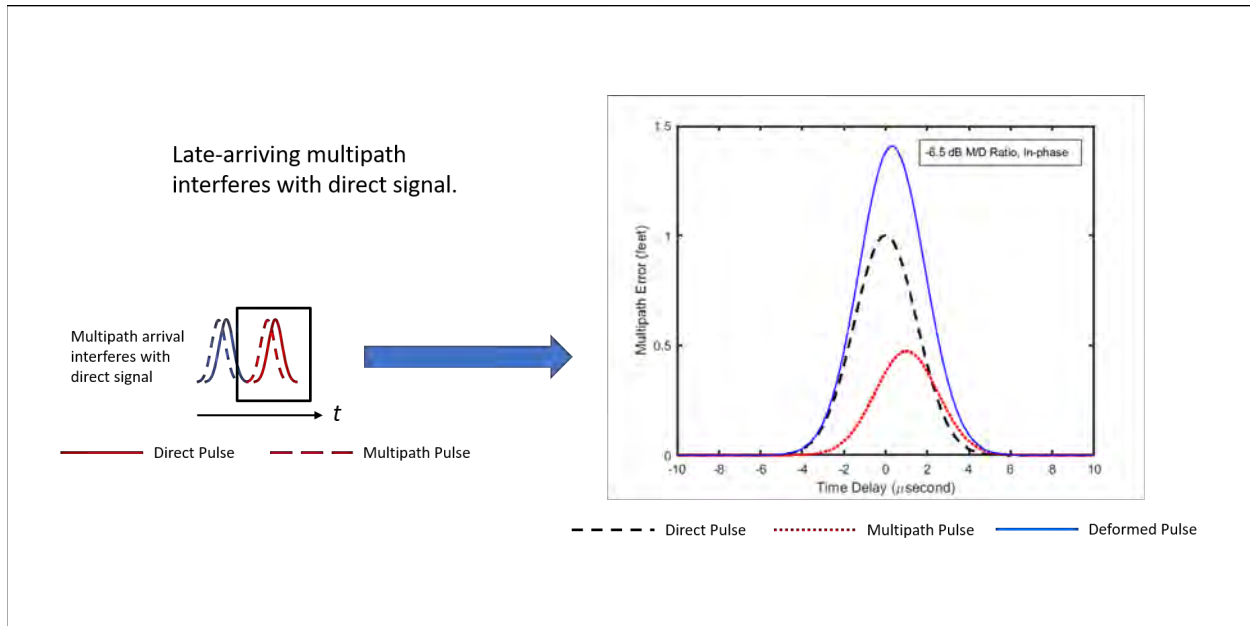


Figure C-42. Example of Pulse Deformation for Late-arrival Multipath

As previously discussed, the half-voltage point of the leading edge of the timing pulse is used for TOA determination for DME/N. The pulse used for making the TOA determination has changed over time as previously discussed in Section 4.b.ii with early generation equipment using the second pulse of the pair while modern designs use the first pulse. In either case, the way in which the composite timing pulse is deformed can change the TOA location, thus inducing ranging error due to multipath. Next, it is necessary to examine how the multipath pulse can deform a direct pulse.

Figure C-43 depicts a multipath pulse and a direct pulse. In this scenario the time delay between the two pulses is large enough that the multipath pulse does not deform the direct pulse. This is because the multipath pulse in the area to the right of point B does not have enough energy to deform the direct pulse enough to affect the location of the TOA point. This same situation is true for the area to the left of point A, which will become relevant as the discussion progresses. Because the TOA location is unchanged, this case does not induce any ranging error. In layman terms, this “no effect on ranging” condition holds true for two cases. Either the multipath pulse arrives “too early” or “too late” in time relative to the direct pulse. That is, they are two distinct pulses as far as the receiver is concerned.

While this condition may not pose a problem for range measurement, it can still cause performance problems because the pulse decoder in the receiver may reject the unaffected direct pulse due to a pulse spacing issue when the amplitude of the multipath path pulse is close (≈ 1 dB) to that of the direct. If this condition persists long enough, it can cause a receiver unlock condition, which would cause the ranging service to become unavailable until the condition ceases.

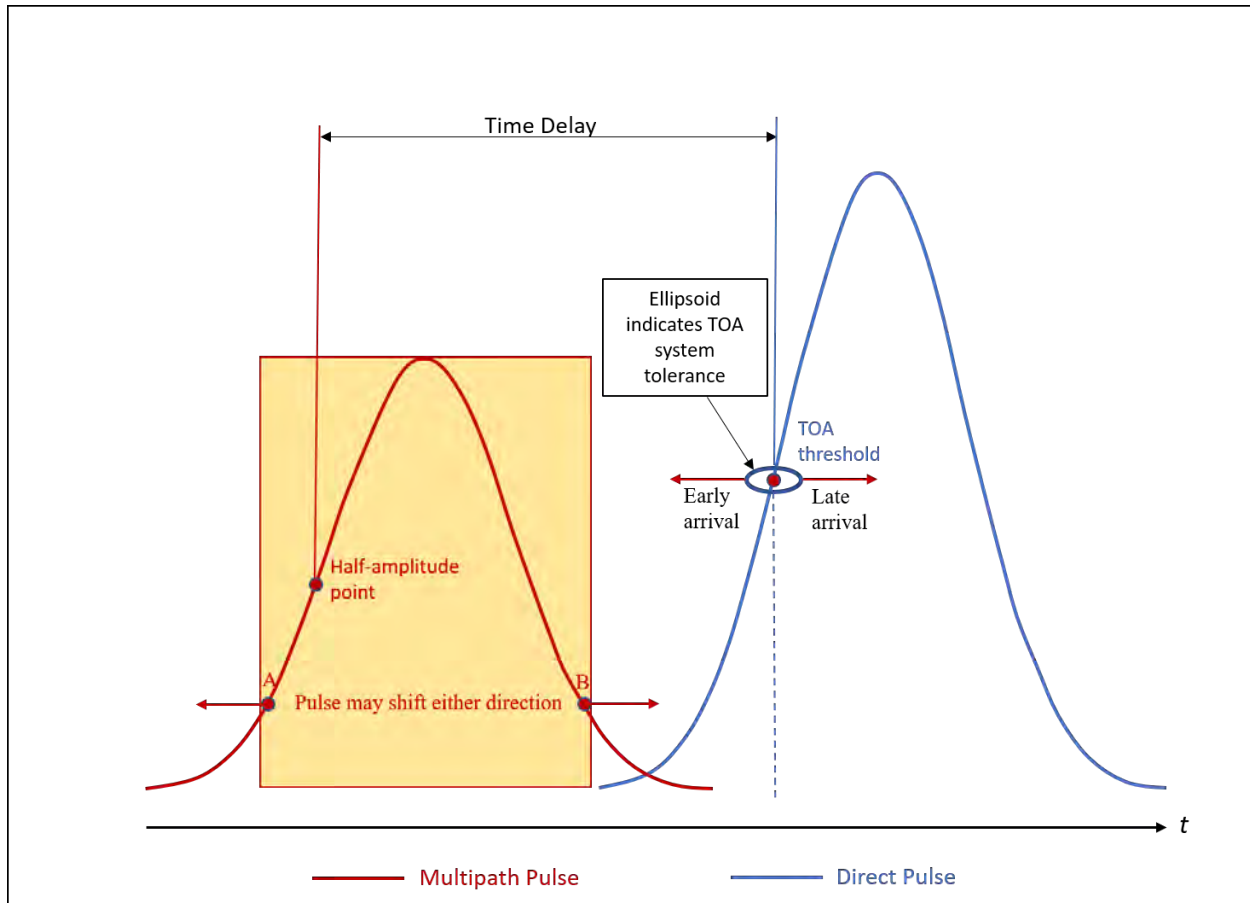


Figure C-43. Multipath Pulse and Direct Pulse Parameters

The next step is to illustrate how the TOA location shifts when the multipath pulse overlays the direct pulse. In reality, the magnitude of the multipath pulse can add to (in-phase condition) or subtract from (out-of-phase condition) the magnitude of the direct pulse. In either case, the result may be a deformed composite pulse that has a TOA location that is shifted from the direct-pulse-only TOA location. In the discussions below, the in-phase condition where the multipath pulse adds to the magnitude of the direct pulse is illustrated. The out-of-phase condition, where the magnitude of the multipath pulse is subtracted from the direct pulse, is addressed in the following subsection.

The analysis illustrating the shift in the TOA location is conducted in the Multipath Analysis Domain by moving the multipath pulse shown in Figure C-43 from left to right while the direct pulse stays fixed. Figure C-44 illustrates this progression by showing three cases as the multipath pulse moves from left to right. Figure C-44(A) depicts the multipath arriving earlier than the direct pulse. In this case, the time delay is such that the two pulses combine to create a deformed composite pulse having a TOA location noticeably shifted from that of the direct pulse. When part of the multipath pulse inside the yellow box shown in Figure C-44(A) begins to combine with the direct pulse, the magnitude of the multipath pulse adds to the magnitude of the direct pulse, resulting in a deformed pulse. Furthermore, it should

be noted that the yellow box shown in Figure C-44(A) identifies the portion of the multipath pulse that has an amplitude large enough to generate a deformed composite pulse when it is added to the direct pulse. The exact location of points A and B on the multipath pulse depends on the M/D ratio and relative phase, which is explored further in the subsections that follow.

The red and blue vertical lines at the top of Figure C-44(A) run through the half-amplitude (half-voltage) points of the deformed composite pulse and the direct pulse, respectively. These lines illustrate that the deformed composite pulse has a TOA that is shifted to the left compared with the direct pulse, which induces range error because the TOA has changed. It is important to note that the TOA will be out-of-tolerance if its location falls outside of the ellipsoid boundary (as shown at the top in Figure C-44(A)).

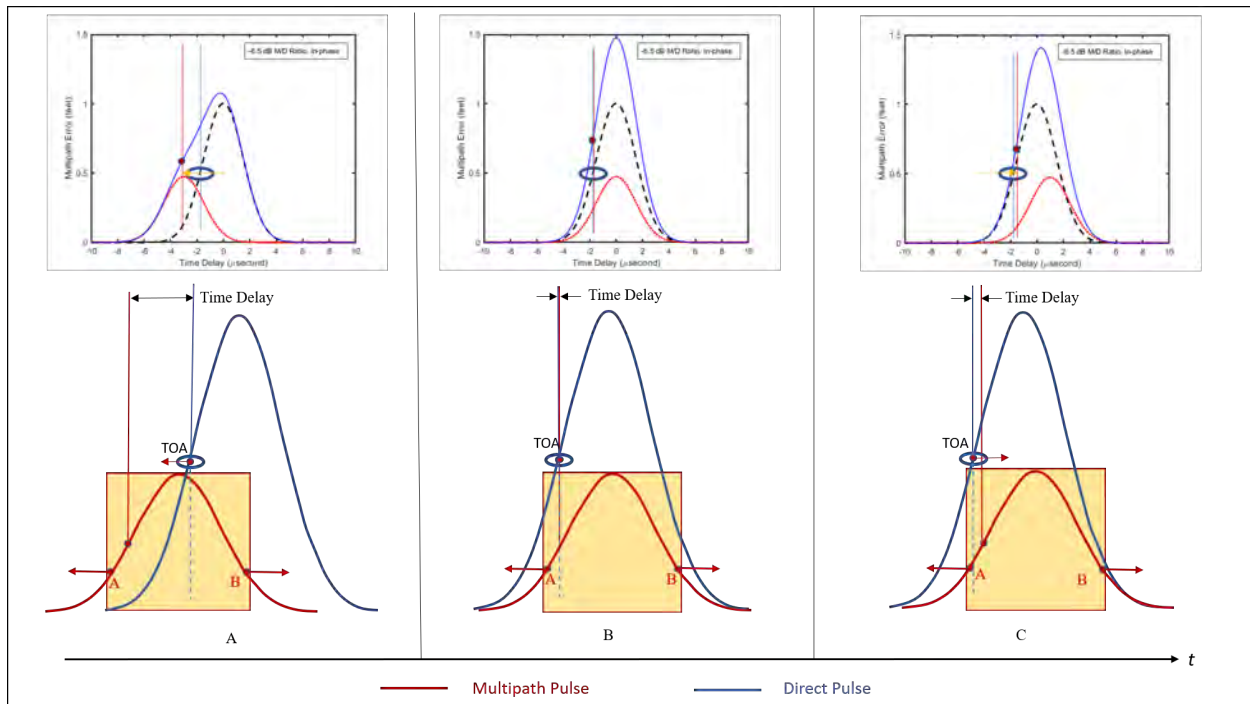


Figure C-44. Multipath Pulse Influence on Direct Pulse Time-of-arrival Threshold

As the multipath pulse continues to move to the right, it gets to a point where the multipath pulse completely overlays the direct pulse. This situation is shown in Figure C-44(B). The magnitude of the multipath pulse adds to the magnitude of the direct pulse, again creating a composite pulse. As previously explained, the red and blue vertical lines shown at the top of Figure C-44(B) run through the half-amplitude (half-voltage) points of the composite pulse and the direct pulse, respectively. These lines illustrate that, in this case, the composite pulse has a TOA that is the same as the direct pulse, which results in zero range error. That is, no deformation occurred in terms of a range error being introduced, and the effect in this case is analogous to amplification of the direct pulse. Attenuation of the direct pulse would have occurred for the out-of-phase case. It is important to note that

when the time delay is zero, a multipath pulse will not cause a range error to occur.

As the multipath pulse continues to move to the right, it gets to a point where the multipath arrives later than the direct pulse, and the time delay is just enough for the two pulses to continue to combine. As with Figure C-44(A), part of the multipath pulse inside the yellow box shown in Figure C-44(C) is still combining with the direct pulse. The magnitude of the multipath pulse adds to the magnitude of the direct pulse, resulting in a deformed composite pulse. The red and blue vertical lines shown at the top of Figure C-44(C) run through the half-amplitude (half-voltage) points of the composite/deformed pulse and the direct pulse, respectively. These lines illustrate that this deformed composite pulse has a TOA that is shifted to the right as compared with the direct pulse, which induces range error.

Based on the preceding discussion, three multipath arrival zones about the direct pulse have been developed, and these zones are classified as “early”, “late-short”, or “late-long” as illustrated in Figure C-45. Time delay is the parameter that determines if a multipath pulse will arrive within one of these three zones. Multipath that has an “early” time-delay will distort the portion of the pulse used to estimate the TOA and therefore has the potential to result in significant range error. Multipath categorized as “late-short” results in a deformed pulse, but with less range error than an “early” pulse. The “long-delay” multipath does not cause ranging errors, since it does not distort the portion of the direct-signal pulse that is processed to estimate the pulse TOA. The above characterization assumes that the magnitude of the direct pulse is larger than that of the multipath pulse.

The magnitude of the range error is a function of the M/D ratio, the TOA of the multipath relative to the direct signal (time-delay), the phase of the multipath signal relative to the direct, and the multipath scalloping frequency resulting from receiver motion in the dynamic case.

While the discussion to this point focused on describing the conditions where multipath may cause ranging error, the presence of multipath can also cause a receiver unlock condition as previously noted. The DME receiver is required to validate each pulse-pair by confirming that the pulse width and spacing fall within prescribed tolerances. Multipath having an amplitude very similar to that of the direct pulse, but arriving outside the arrival zones discussed above, can cause pulse spacing violations. Similarly, multipath arriving within these zones may cause pulse width violations, even when arriving within the “late-long” arrival zone. If any of these conditions, or a combination thereof, persists long enough, it can cause a receiver unlock condition, which would cause the ranging service to become unavailable until the condition ceased.

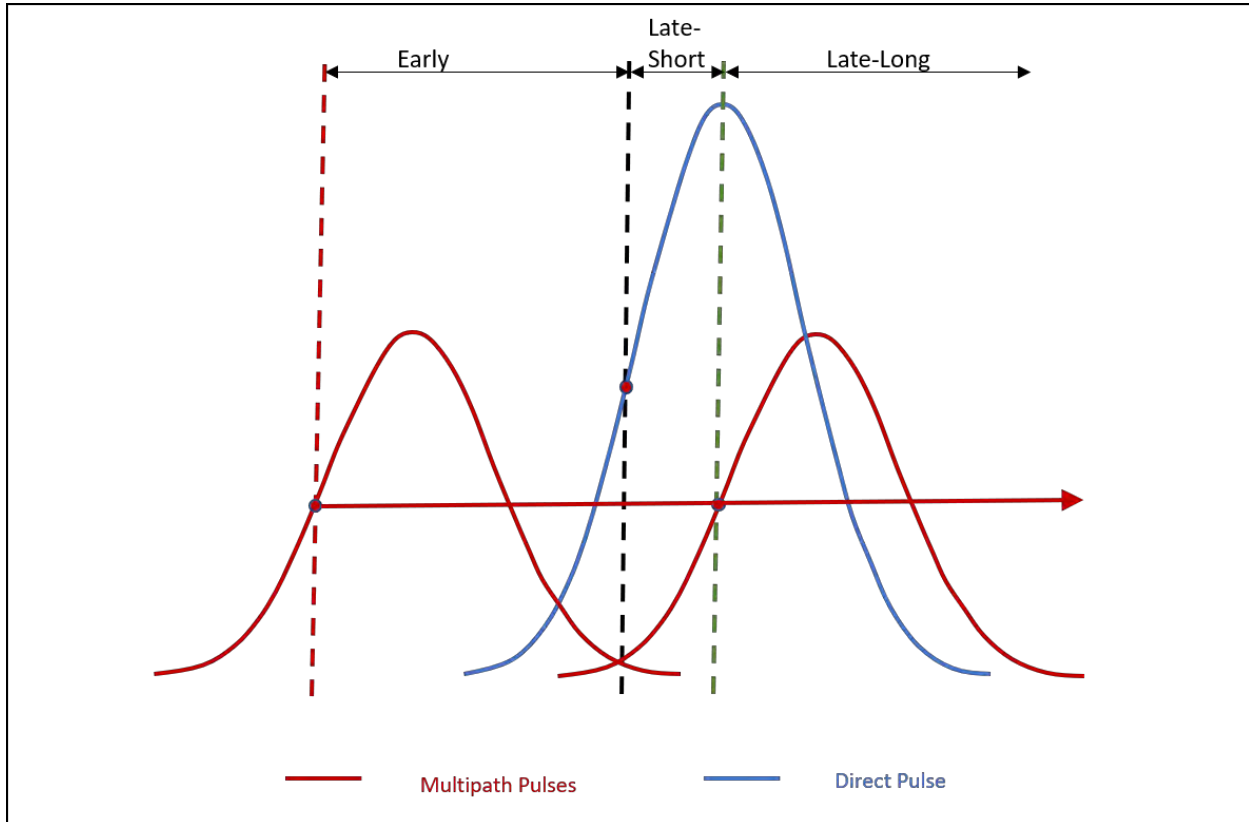


Figure C-45. Early and Late Multipath Pulse to Direct Pulse Timing Regions

- iv. **Characterization of Multipath Error Magnitudes.** Figure C-46 quantifies the range error (aka multipath error) caused by an in-phase multipath pulse with a -6.5 dB M/D ratio as a function of time delay. As defined earlier, time delay is the difference between the TOA of the multipath signal relative to the TOA of the direct path signal, where a positive value indicates that the multipath arrives later in time. For DME/N, the TOA is the time that corresponds to the half-voltage point on the leading-edge of the pulse. The span of time delay values selected ensures that the multipath pulse is initially positioned at the start of the “early” arrival zone and then progressed through to the end of the “late-long” arrival zone.

In addition to the data plot, Figure C-46 provides pulse deformation snapshots at 1 μ s intervals to illustrate how the multipath and direct pulses combine to create the resulting deformed composite pulse. At a time delay of -6 μ s, the corresponding snapshot shows that the trailing tail of the early-arriving multipath pulse (shown in red) approaches the leading tail of the direct pulse (shown in black), but is not close enough to affect the TOA. Note that the composite pulse (shown in blue) is the addition of the in-phase multipath and direct pulses. As the multipath moves toward the direct pulse, it is easily observed that the TOA measured by the receiver moves to the left, significantly influencing the multipath distance error. The steep climb in range error at -4 μ s is a result of the multipath reaching an amplitude that matches the half-voltage point of the direct signal, which triggers a very early TOA

determination. At 0 μs , the multipath pulse directly overlays the direct pulse, resulting in an unaffected TOA, as expected. As the multipath pulse continues past the direct pulse (late arrival), the TOA moves to the right, but to a significantly less degree than that of the early-arriving pulse. At approximately 4 μs late arrival for the multipath pulse, the TOA is no longer affected and the multipath distance error is zero. A similar process is noted for Figure C-47, except in this case the out-of-phase multipath pulse is subtracted from the direct pulse.

In both cases, the magnitude of the range error for an early arriving multipath pulse is significantly more than that for the corresponding late arrival multipath pulse. This observation provides insight into why the use of the second pulse of the pair is more susceptible to multipath error than when the first pulse is used. Furthermore, not only is the error greater in magnitude, but the potential for error exists for a wider span of time delay values.

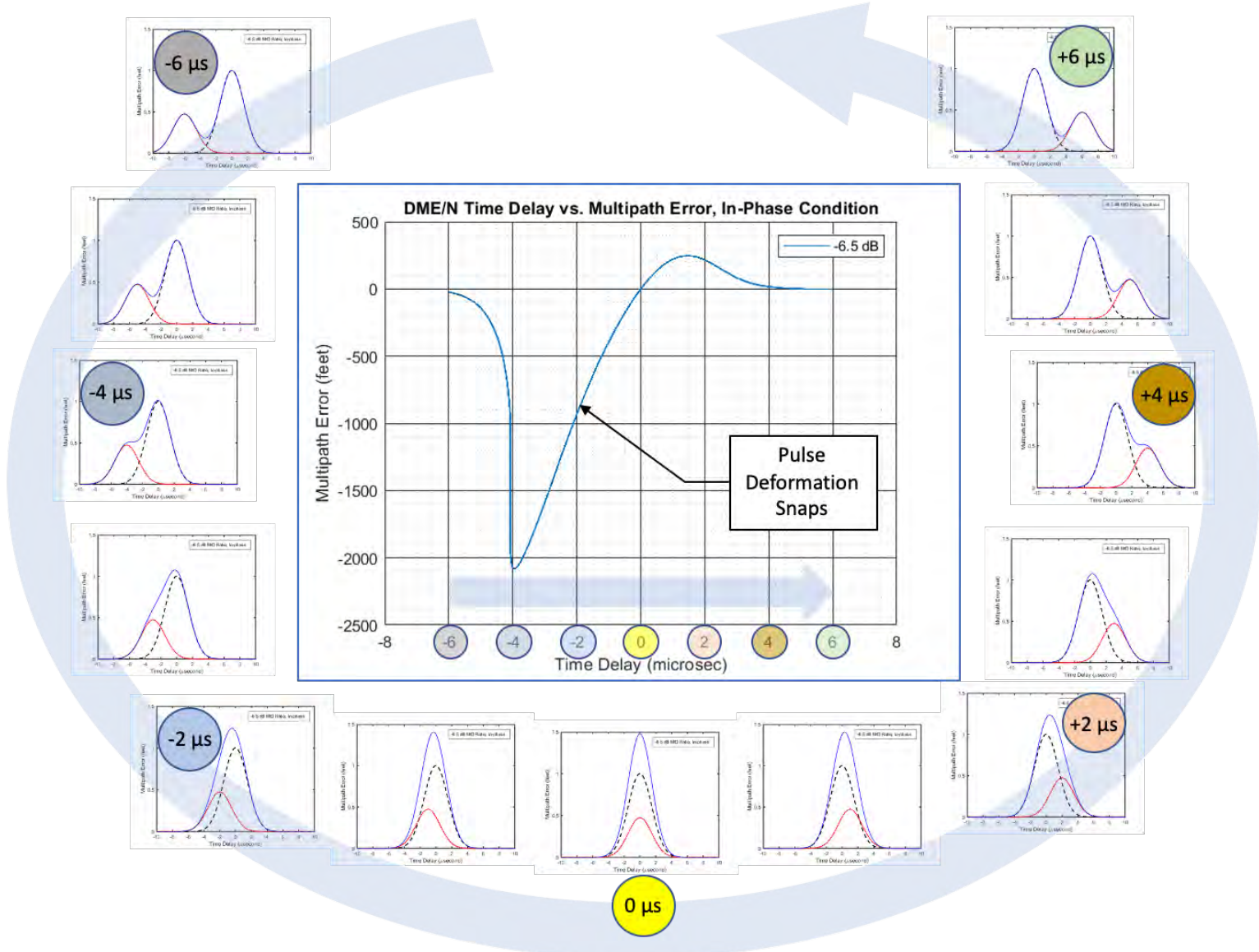


Figure C-46. Pulse Deformation Snapshots In-phase for an M/D Ratio of -6.5 dB

Figure C-46 and Figure C-47 quantify the range error caused by a multipath pulse with a -6.5 dB M/D ratio as a function of time delay, for both the in-phase and out-of-phase cases respectively. The pulse deformation snapshots provided in these figures show how the direct and multipath pulses combine to create a deformed composite pulse. Similarly, Figure C-48 and Figure C-49 show the multipath distance error resulting from deformed pulses for both in-phase and out-of-phase conditions. The M/D ratios in these figures vary from -6.5 dB to -20 dB.

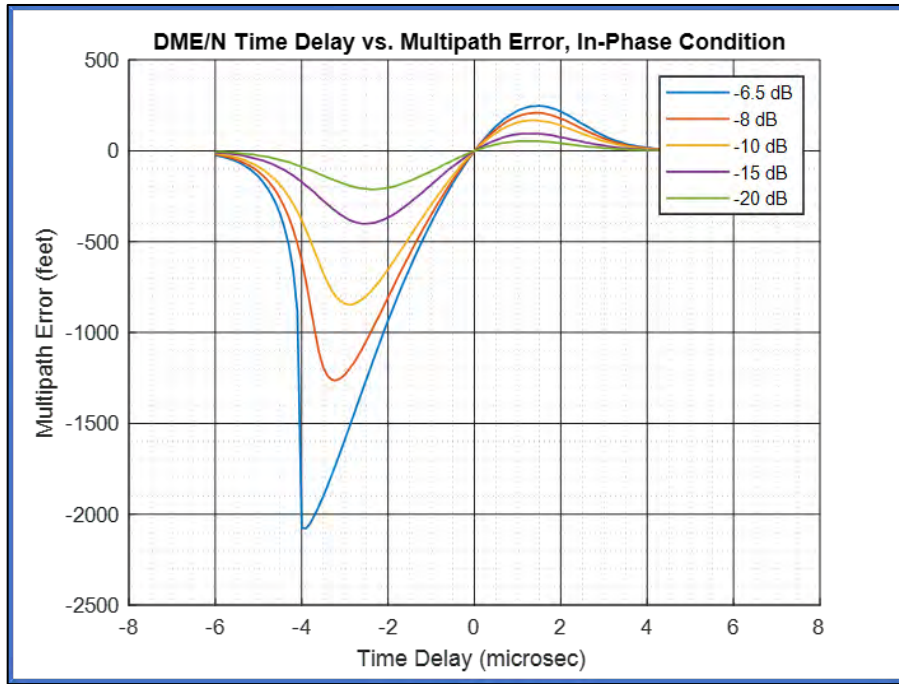


Figure C-48. DME/N Error versus Relative τ -delay, M/D Ratio, In-phase Case

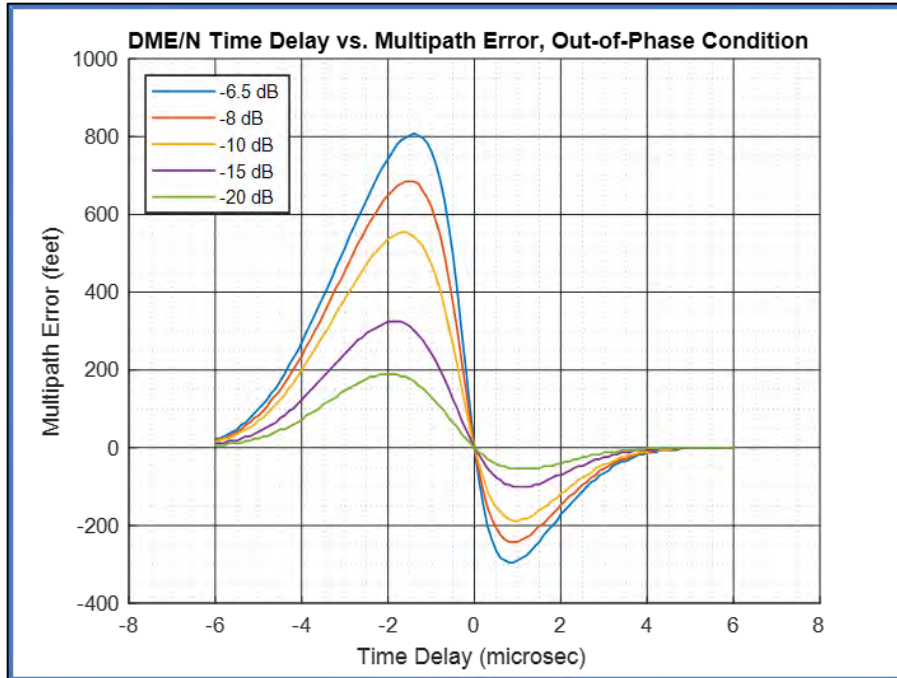


Figure C-49. DME/N Error versus Relative τ -delay, M/D Ratio, Out-of-phase Case

It is important to note that Figure C-48 and Figure C-49 illustrate curves with a range of M/D ratios from -20 dB to -6.5 dB for analytical purposes. Paragraph 2.2.14.a in RTCA DO-189 states: “...the interrogator shall operate normally, including decoding and ranging accuracy in the presence of echo or multipath conditions where the reflected signal level is not greater than -10 dB with respect to the desired signal.” Thus, when the results of a fading or error analysis yield a M/D ratio greater than -10 dB, it should be realized that this situation is likely problematic from a performance perspective. In this case, further action may be required to mitigate the impact and the action required will depend on the particulars of the situation (i.e., consider a different antenna location or change in new construction plan.).

- v. **Defining Multipath Arrival Zones.** As noted earlier, the yellow boxes shown in Figure C-44 identify the portion of the multipath pulse that has an amplitude large enough to generate “measurable” range error, and that the exact location of points A and B on the multipath pulse depends primarily on the M/D ratio when worst-case conditions prevail in terms of relative phase. Building upon this information, the results presented in Figure C-48 and Figure C-49 can be used to define the location of these points as a function of M/D ratio, provided that a suitable threshold value has been established for what constitutes a “measurable” range error. Once such a threshold has been established, time-delay thresholds for the multipath arrival zones can be determined.

The accuracy requirement stated in FAA-E-2996, “Performance Specification for Distance Measuring Equipment (DME),” were used to establish a suitable range error threshold. Paragraph 3.2.4.4 (Accuracy) of FAA-E-2996 states “The

transponder shall not contribute more than $\pm 0.5 \mu\text{s}$ (75 meters (250 feet)) to the overall system error budget.” A conservative approach is to use 10% of $0.5 \mu\text{s}$ (50 nanoseconds, or approximately 50 feet) as the threshold, then use this threshold to determine the times at which the multipath begins to influence the direct pulse TOA (i.e., cause measurable error). The DME/N multipath error plots shown in Figure C-48 and Figure C-49 were used to determine the early, late-short, and late-long zones for the in-phase and out-of-phase multipath with a minimum M/D ratio of -20 dB and maximum M/D ratio of -6.5 dB.

An illustration of the in-phase multipath arrival zone for an M/D ratio of -6.5 dB is shown in Figure C-50. The red horizontal lines are drawn at the multipath error threshold of ± 50 feet. The -6.5 dB M/D ratio trace, shown in blue, first crosses the 50 feet error line at approximately $-5.6 \mu\text{s}$, and this marks the beginning of the Early zone. The Early zone continues until the multipath pulse coincides with the direct pulse, which is indicated by a time delay of $0 \mu\text{s}$. This also marks the beginning of the Late-Short zone, which persists until the multipath again crosses the 50 feet multipath error at $3.3 \mu\text{s}$. The Late-Long zone indicates that the multipath no longer affects the direct pulse TOA. The same approach is used to determine the early ($-4.5 \mu\text{s}$) and late arrival zones ($1.6 \mu\text{s}$) for in-phase multipath having an M/D ratio of -20 dB (Figure C-51). Applying this same procedure also results in the early ($-5.5 \mu\text{s}$) and late arrival zones ($3.2 \mu\text{s}$) for out-of-phase multipath having an M/D ratio of -6.5 dB (Figure C-52). Finally, the last application yields early ($-4.5 \mu\text{s}$) and late arrival zones ($1.5 \mu\text{s}$) for out-of-phase multipath having an M/D ratio of -20 dB (Figure C-53).

The results are summarized in Figure C-54, depending on the M/D ratio, the multipath pulse can affect the thresholding point of the direct pulse when arriving as early as $5.6 \mu\text{s}$ before the direct pulse arrival, or as late as $3.3 \mu\text{s}$ after the direct pulse arrival.

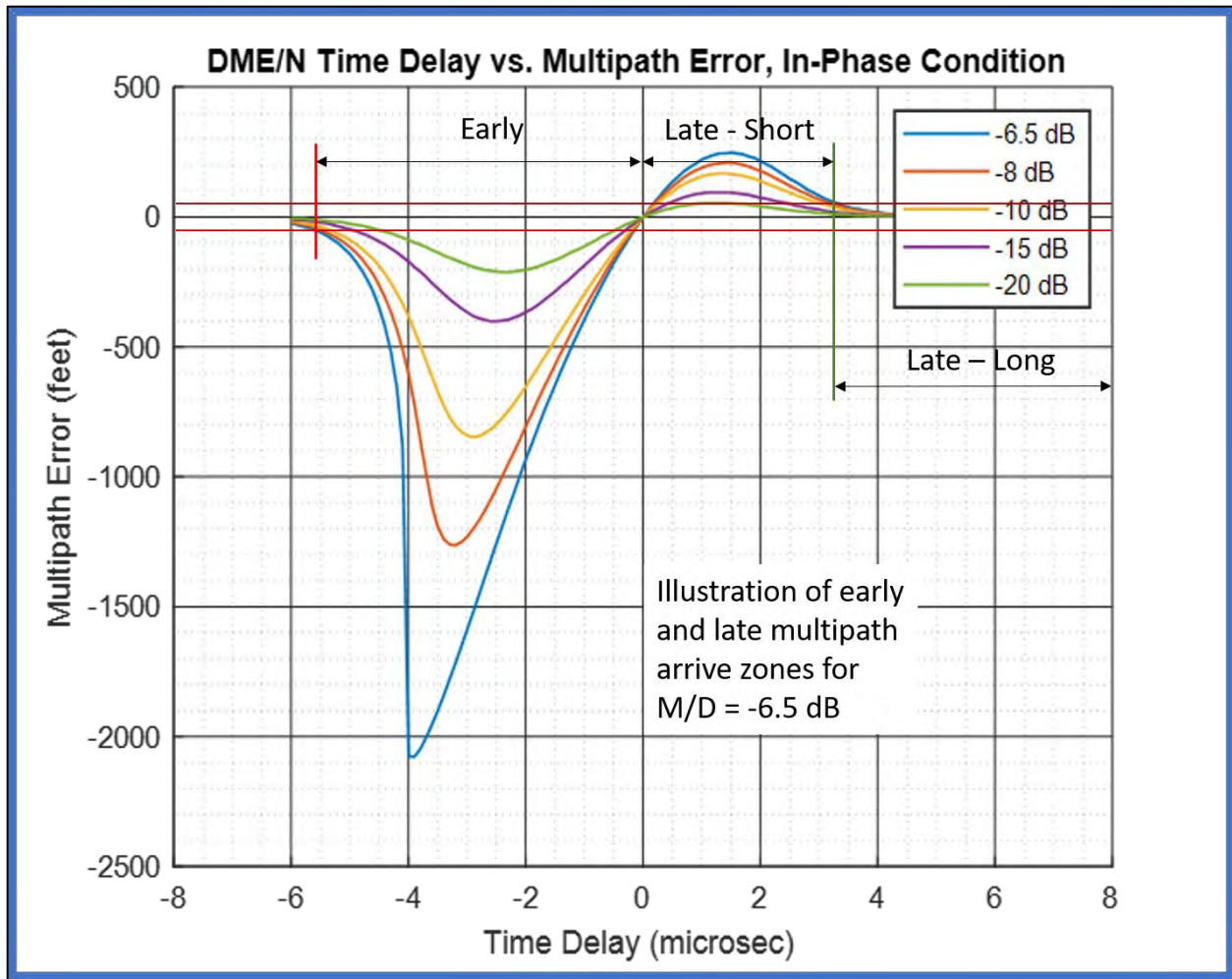


Figure C-50. In-phase Multipath Arrival Zones with Indications for -6.5 dB M/D Ratio

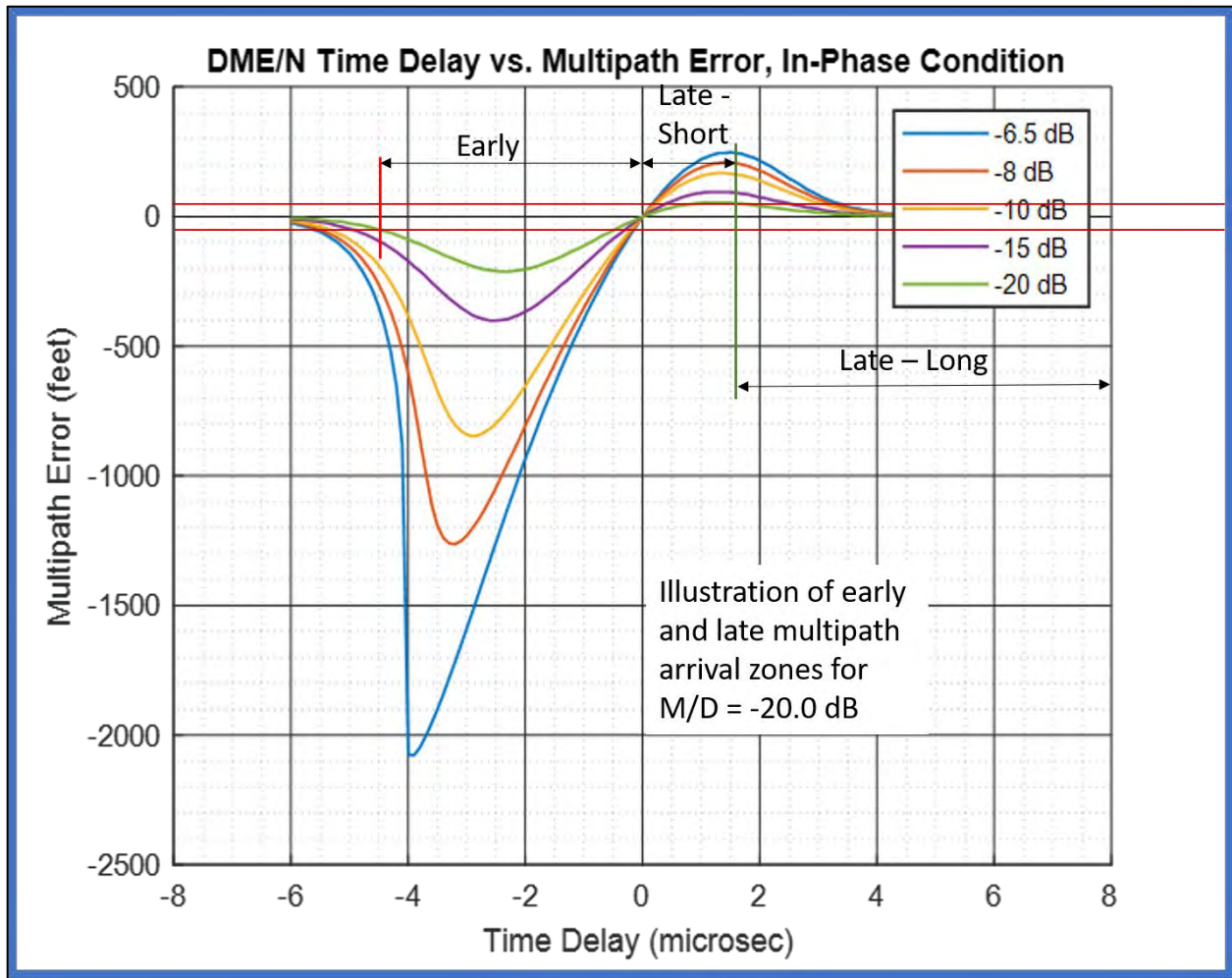


Figure C-51. In-phase Multipath Arrival Zones with Indications for -20 dB M/D Ratio

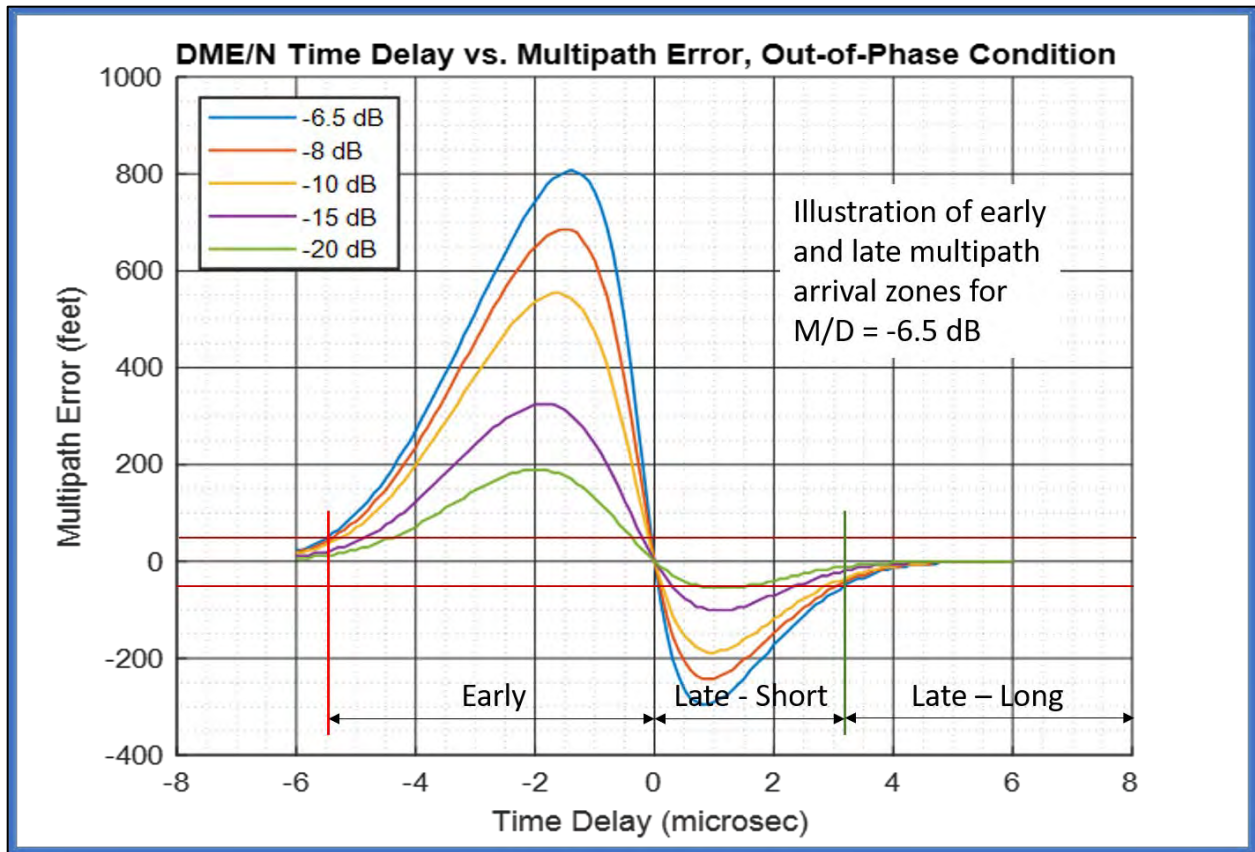


Figure C-52. Out-of-phase Multipath Arrival Zones with Indications for -6.5 dB M/D Ratio

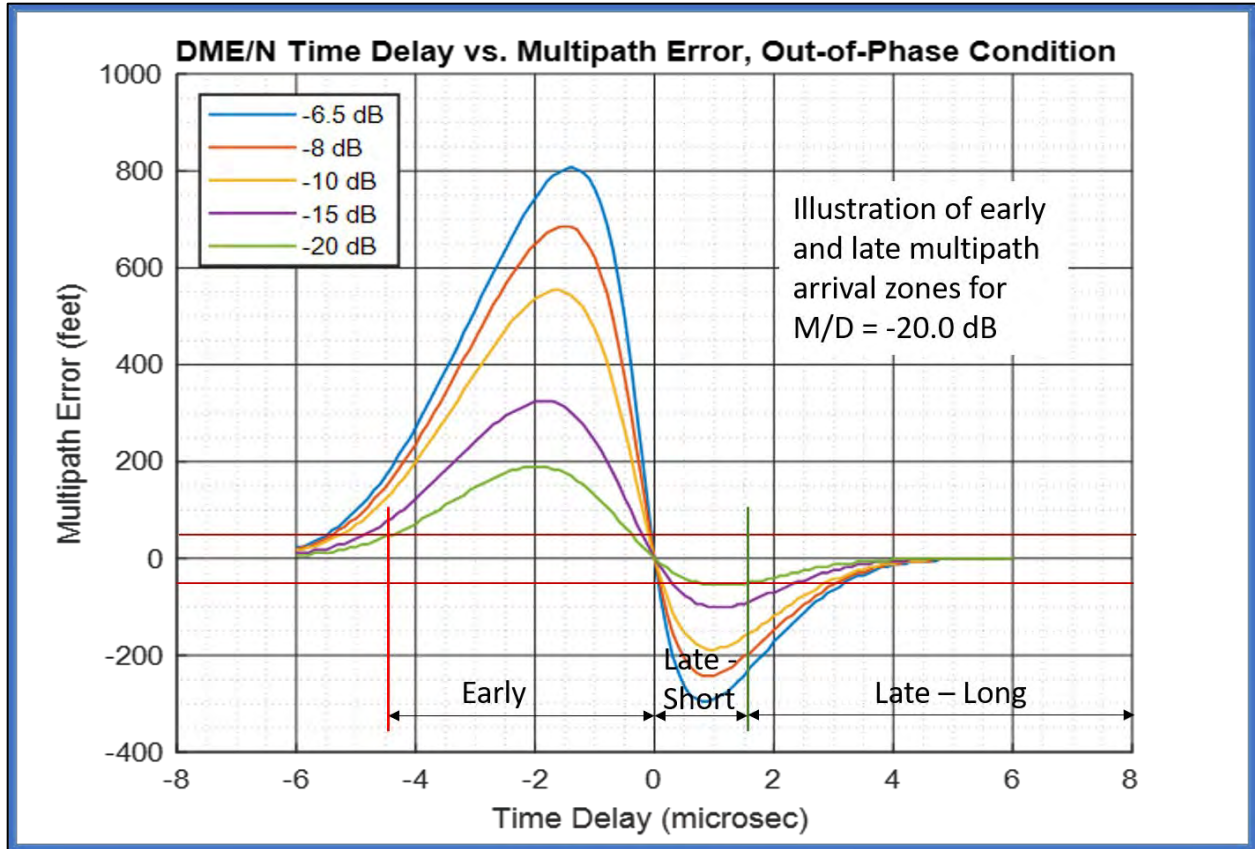


Figure C-53. Out-of-phase Multipath Arrival Zones with Indications for -20 dB M/D Ratio

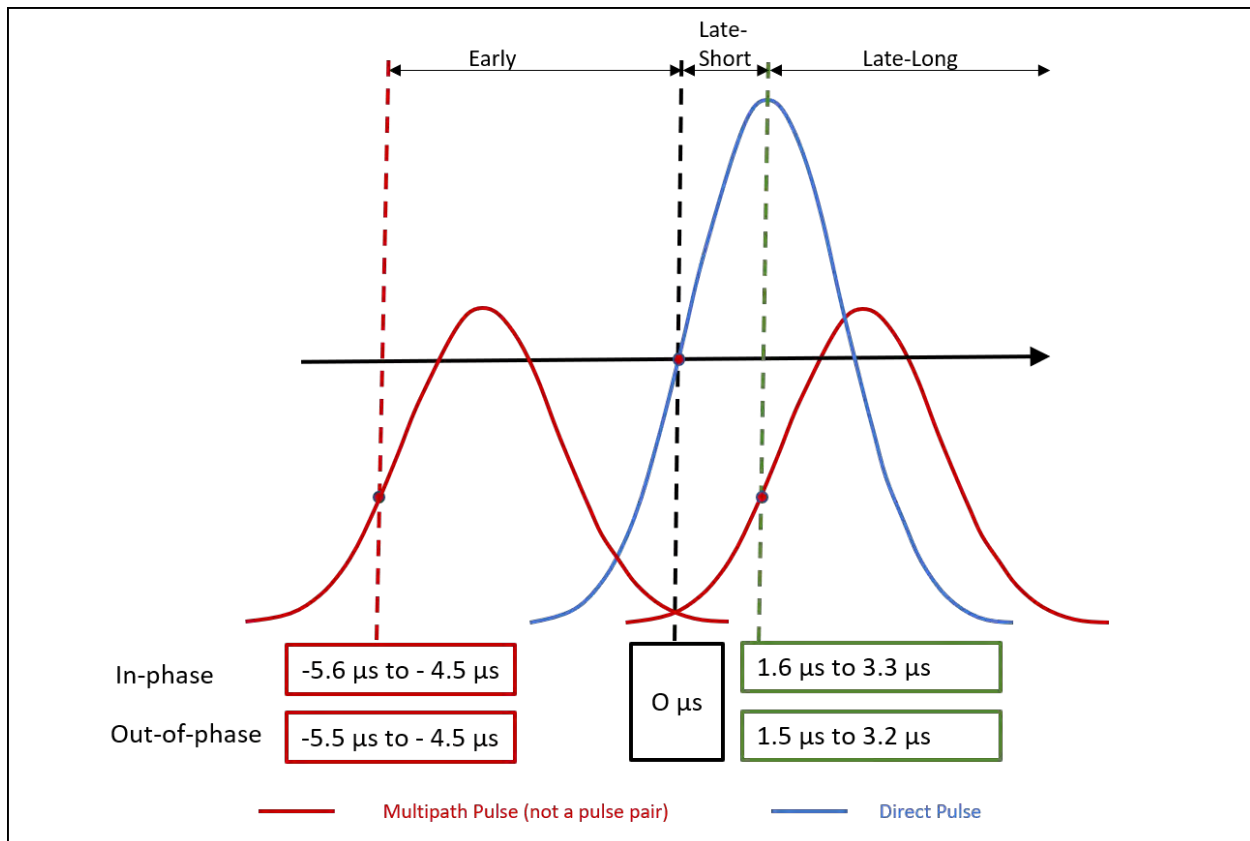


Figure C-54. Early and Late Arrival Zone Summary for -6.5 dB and -20 dB M/D Ratios

Now that the early arrival, late-short arrival, and late-long arrival zones have been identified, the scattering geometry and mechanisms that produce the multipath in an operational RF environment will be examined.

- vi. **Examination of the Operational RF Environment.** This section examines the operational RF environment from a transponder (i.e., ground equipment) perspective. As illustrated in Figure C-55, the transponder services multiple DME-equipped aircraft; these aircraft are at different distances and/or elevation angles from the transponder, and the orientation of their flight paths relative to the transponder varies. The transmission of interrogations from an aircraft (i.e., DME interrogator) to a transponder is referred to as the downlink, while the transmission of replies from a transponder to an aircraft (i.e., DME interrogator) is referred to as the uplink. Both the uplink and downlink provide a constantly changing RF environment, primarily because the aircraft are in motion.

The top portion of Figure C-56 shows an example downlink sequence that is received by a transponder. It should be noted that the interrogation pulse-pairs arrive at the transponder with different signal amplitudes and that the interrogation sequence for each individual aircraft is “jittered”. The amplitudes vary because of factors such as the aircraft being at different distances from the transponder; the aircraft being at different elevation angles, variations in power transmitted by the interrogators and implementation losses, and differences in propagation loss due to

environmental effects (e.g., rain, signal fading, signal shadowing). Overlapping pulse-pairs may be present due to garble or multipath effects.

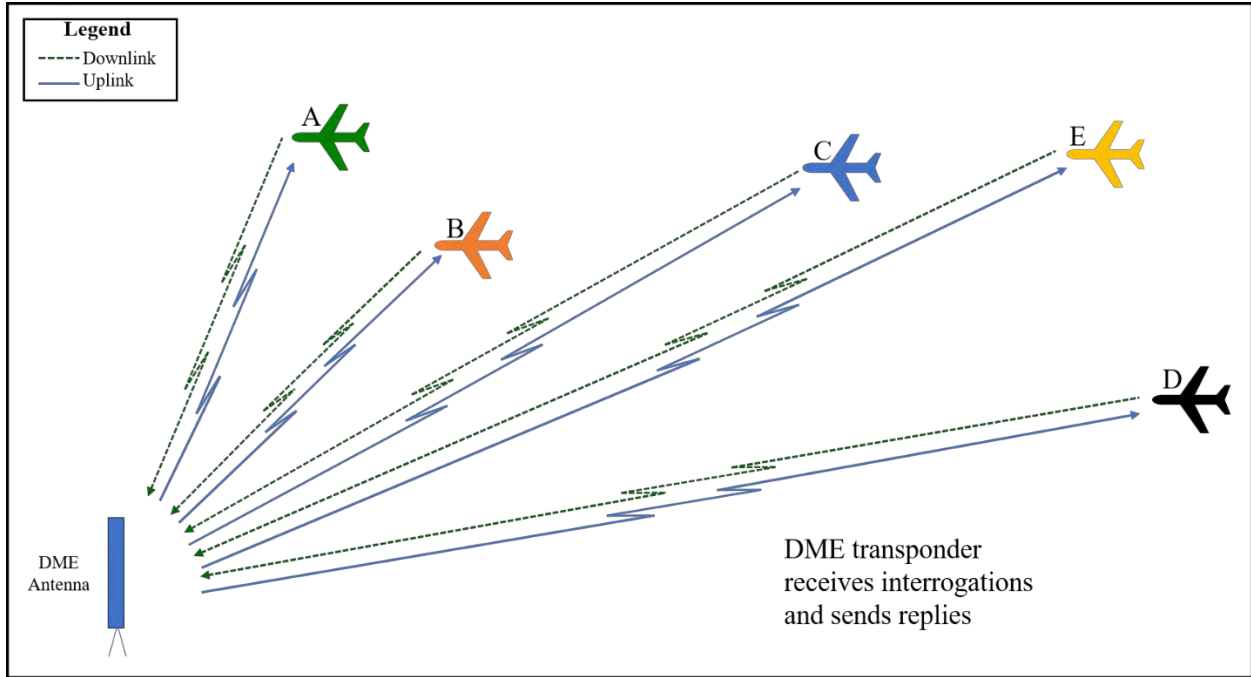


Figure C-55. DME Transponder Receives and Replies to a Sequence of Aircraft Interrogations

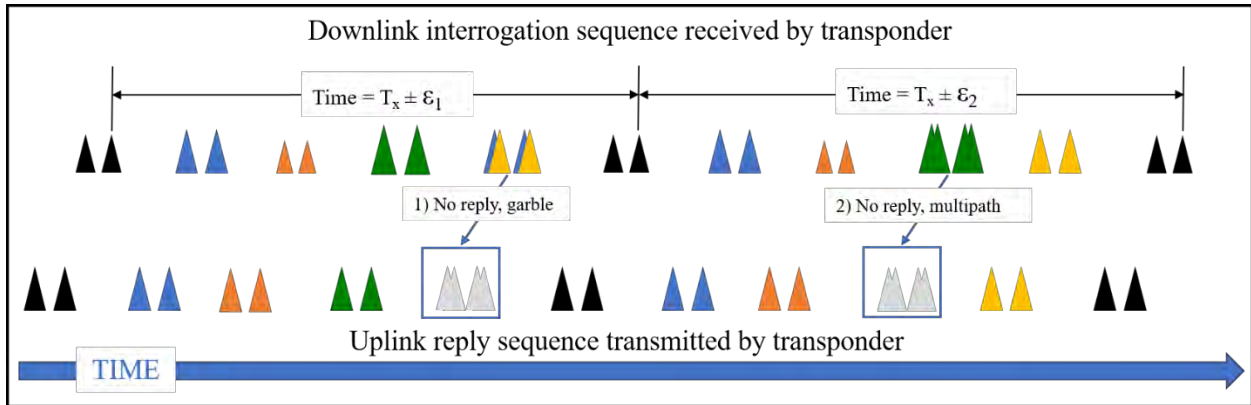


Figure C-56. Downlink and Uplink Sequences

While there is a transmission suppression bus on the aircraft to prevent equipment operating in the same band from transmitting at the same time, there is no such mechanism to coordinate the transmission of DME interrogations between aircraft. Thus, the reception of interrogations from two aircraft may occasionally arrive at the transponder antenna very close in time, overlap of the pulse-pair occurs, and the result is effectively a distorted composite pulse-pair. This phenomenon is known as garble, and an example is illustrated by case 1 in Figure C-56. As previously discussed, multipath may also result in a deformed composite pulse-pair as illustrated by case 2 in Figure C-56.

Minimum interrogation rates must be achieved to satisfy certain performance and guidance quality requirements, and this interval is denoted as T_x in Figure C-56. This figure also shows that the interrogation interval is altered slightly in a random fashion (i.e., $\pm \epsilon_1$, $\pm \epsilon_2$), which is commonly referred to as being “jittered.” A jittered interrogation interval is used to mitigate the impact of synchronous error mechanisms. One such mechanism is discussed in Sections 5.b.vii and Section 5.b.viii, and additional information about jitter is provided in Section 5.b.ix.

The bottom portion of Figure C-56 shows an example uplink sequence that is transmitted by a transponder. The reply pulse-pairs are transmitted a fixed-delay time after the reception of a validated interrogation pulse-pair and have a constant amplitude at the transponder antenna input. The uplink reply sequence is a delayed version of the jittered interrogation sequence, except for an occasional “missing” reply due to the rejection of interrogation pulse-pairs tainted by garble or multipath. While the fixed-delay provides the time necessary to accomplish TOA determination and pulse-pair validation by the receiver, it also results in the protection from synchronous errors provided by jitter to be passed along to the uplink.

While the amplitude of the reply signal arriving at the interrogator does not vary due to distance and elevation angle considerations as in the case of the transponder, amplitude variations will still occur due to signal fading and shadowing. Overlapping pulse-pairs due to multipath effects may also be present.

It is important to note that the interval between the uplink pulse-pairs shown in Figure C-56 is greater than the fixed delay. Upon validating an interrogation pulse-pair, the transponder receiver is disabled for a period of time. In early equipment designs, the disabling was accomplished by using a blanking gate (aka dead time gate), thus this time has become known as the blanking or dead gate time. This time is on the order of $60 \mu\text{s}$ (for X-channel), which would be the minimum value for the interval between the pulse-pairs because the next interrogation pulse-pair is likely received some short time after the transponder receiver is again enabled. Traffic load is another factor that would affect this interval. Similar considerations apply to the interval between interrogation pulse-pairs.

- vii. **Determining Absolute Time Delays.** The discussion in this section, as well as the two that follow, demonstrates how jitter can mitigate synchronous error mechanisms and provides insight into the amount of jitter required to do so effectively. While this is a system design concept topic, it is taken herein to show how jitter mitigates the occurrence of synchronous multipath effects, and thus the ranging error that could result from such effects. The discussion in this section and the next assume jitter is not used, and the last section illustrates how jitter provides mitigation. This multi-section discussion starts with examining multipath effects given the operational RF environment, then methods for computing absolute time-delay values are presented. The concept of echo/multipath ellipsoid families is introduced and the discussion concludes with a tutorial on the application of jitter to mitigate synchronous multipath effects.

Figure C-55 illustrates that the DME transponder receives interrogations and sends replies to many aircraft in the airspace, and the resulting RF environment is a continuous sequence of uplink and downlink pulse-pairs as shown in Figure C-56. Figure C-57 builds upon these concepts and demonstrates how multipath pulses resulting from interrogations from and replies to one aircraft can affect the direct signals from/to another aircraft. In this figure, an interrogation from Aircraft A (Green) is shown as the first one to be received by the transponder. This interrogation is followed by the interrogations from the Aircraft B (Orange), Aircraft C (Blue), and Aircraft D (Black) respectively as shown in the interrogation sequence presented in the top block of Figure C-57. The fixed reply delay results in an uplink sequence that is simply a delayed version of the downlink sequence with the replies being sent in the same sequence in which they were received.

Consider a scenario where Aircraft C (Blue) has interrogated the transponder; Aircraft B has interrogated the transponder 1 reply cycle earlier; and Aircraft A has interrogated 2 reply cycles earlier. In this scenario, the signal in space at Aircraft C (Blue) will consist of the replies to the interrogations in the same sequence. The relative TOA of these replies for the case of early, late-short, and late-long arrival multipath are as shown in the lower block of Figure C-57, and assume that first pulse timing is used. It is noted that early arrival pulses do not apply for replies to the interrogation from the Aircraft C (Blue), and again, this statement assumes first pulse timing is used. However, depending on the multipath environment, the interrogation from Aircraft B (orange), one reply cycle earlier, can result in the presence of early, late-short, and late-long arrival pulses. The relative time delays for early, late-short, and late-long arrival multipath for this scenario are as shown in the lower block of the figure. In a similar manner, the replies to the interrogation from Aircraft A, two reply cycles earlier, are also shown in the block. The illustration attempts to capture the differences in the absolute time delays and the magnitude of the received signals. The echo ellipsoid number come into play in the next section.

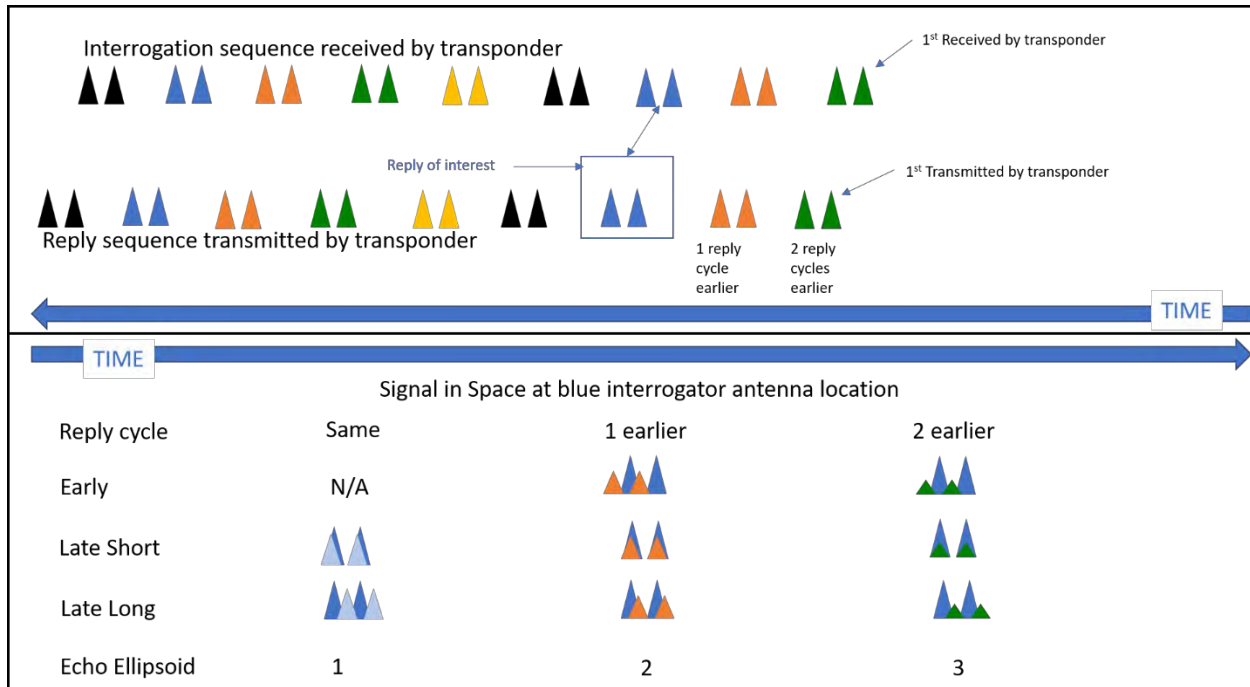


Figure C-57. Multipath TOA Relative to Direct Pulse Scenarios for First Pulse Timing

Based on the discussion regarding Figure C-57, multipath interference can be enumerated into the following types:

1. First pulse of same reply interfering with first pulse of user aircraft reply;
2. First pulse of same reply interfering with second pulse of user aircraft reply;
3. Second pulse of earlier reply interfering with first pulse of user aircraft reply;
4. First pulse of earlier reply interfering with first pulse of user aircraft reply;
5. Second pulse of earlier reply interfering with second pulse of user aircraft reply;
6. First pulse of earlier reply interfering with second pulse of user aircraft reply;
7. Etc., the above cases are sufficient for the purposes of this discussion.

For the first type of multipath interference listed above, the absolute time delay and relative time delay values are the same. Therefore, no further computation is required for this type of multipath interference. Next, prerequisite background information will be provided to lay the groundwork necessary for understanding how the absolute time delay is computed for the remaining cases.

It should be noted that the reply delay values shown in Figure C-54, as well as the cases illustrated in the bottom panel of Figure C-57, are relative time-delay values; that is, the delay time is relative to the arrival of the direct pulse that is used for making TOA determinations. While this is ultimately the time-related parameter that influences the magnitude of the range error that results, it should be realized that a specific relative time-delay value can be generated by more than one absolute time-delay scenario. In the context of this discussion, absolute time delay is the difference in the propagation time of the multipath pulse and propagation time for the direct pulse, where the propagation time is the time required for the pulse to

travel from the transmitter antenna to the receiver antenna.

This mapping of multiple absolute time-delay values to one relative time-delay value is an inherent characteristic of periodic waveforms, and it should be noted that the absolute time-delay value is proportional to the length of the propagation path. Furthermore, such path lengths can be defined as some integer number of wavelengths plus a fractional portion of a wavelength (i.e., $x\lambda + 0.y\lambda$). Generally, the fractional portion (i.e., $0.y\lambda$) is directly observable by the receiver, and there is ambiguity regarding the integer portion (i.e., $x\lambda$); that is, does “x” equal 5, 10, or 25?

This concept can be adapted to the analysis of uplink DME multipath effects by expressing the absolute time delay as “ $a\lambda + b\lambda + 0.c\lambda$ ”. In this case, the “ $a\lambda$ ” is that portion of the propagation path that accounts for the reply cycle that generated the multipath (i.e., same cycle, 1 earlier, and so on). The “ $b\lambda + 0.c\lambda$ ” accounts for that portion of the propagation path that generates the relative time delay, and finally, “ $0.c\lambda$ ” determines the relative phase. This adapted concept is applied via timing diagrams to illustrate how absolute time-delay values can be computed for the various types of multipath interference.

Figure C-58 provides general guidance on how to interpret the timing diagrams that follow, including the various propagation path components that come into consideration. As illustrated, the exercise in each case is to determine how much earlier in time does the direct and multipath signal have to leave the transponder antenna so as to arrive at the user aircraft antenna at the same time. The top box of Figure C-58 provides a two-dimensional depiction of the first pulse of an earlier reply cycle interfering with the second pulse of the user aircraft reply. This depiction is then flattened into one dimension showing the time components that determine the length of the multipath propagation path needed to make the interference occur. This concept will now be applied to each of the remaining multipath types to illustrate how the absolute time-delay values can be computed.

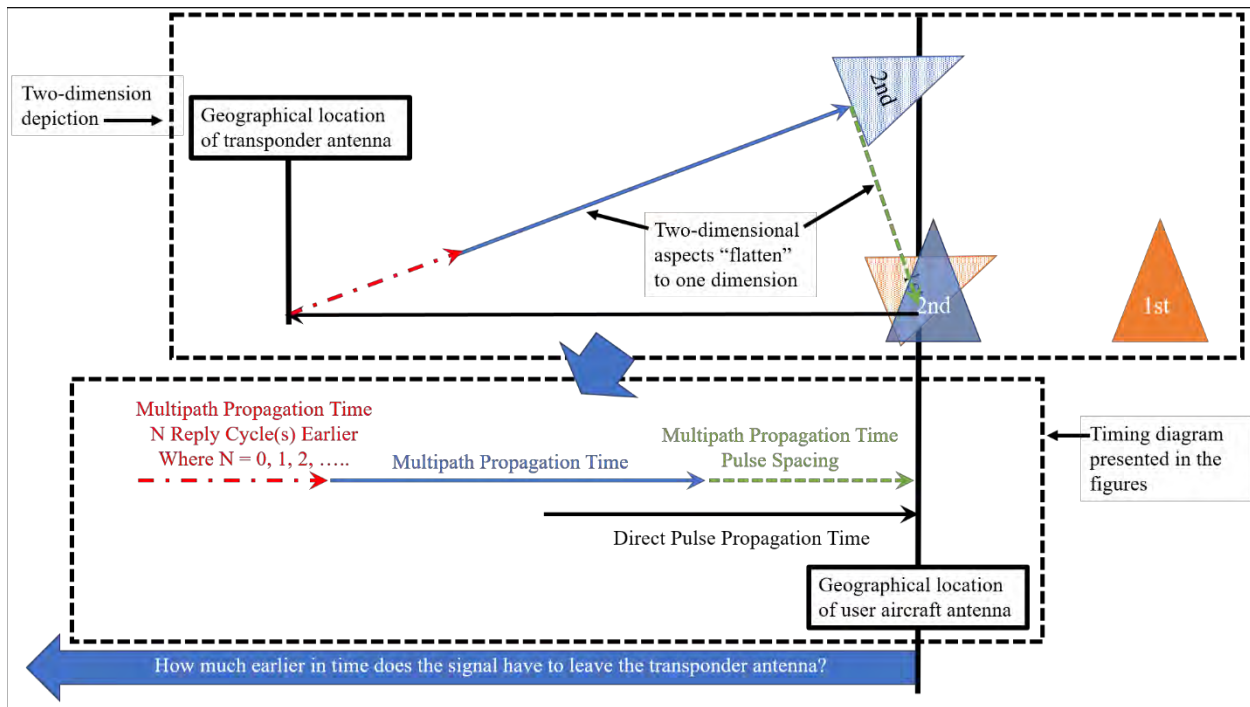


Figure C-58. Interpretation of Time Diagram for Computing Absolute Time-delay Values

The second type of interference listed above occurs when the second pulse is used for TOA measurements, and during the same reply cycle, the first pulse multipath interferes with the second pulse timing measurement (see Figure C-59). Similarly, the third and fourth multipath interference types are illustrated in Figure C-60 and Figure C-61, and the fifth and sixth multipath interference types are illustrated in Figure C-62 and Figure C-63. Note that these figures work together to show how early and late multipath affects the direct signal by introducing an absolute time delay in the TOA measurement, thereby affecting the ranging accuracy.

The absolute time-delay computations for each of the multipath interference types were developed and illustrated in Figure C-59 through Figure C-63. An overview is provided below regarding how these computations were developed for the multipath interference type 2 and type 3 scenarios. This overview should provide sufficient insight into how the computations for the remaining three multipath interference types were developed (see Figure C-61 through Figure C-63).

In the multipath interference type 2 scenario, the multipath pulses travel a slightly longer path and arrive a little later than the direct pulses. In Figure C-59, the first multipath pulse is shown arriving at exactly the same time as the second direct pulse. This results in no timing error. If the multipath pulses arrive a little earlier, the TOA will shift to the left, resulting in an early arrival measurement. Likewise, if the multipath pulses arrive a little later, the TOA will shift to the right, resulting in a late arrival measurement. Recall that TOA errors have a greater magnitude when the multipath arrives early.

In the multipath interference type 3 scenario where the second pulse of the earlier reply interferes with the first pulse of the user aircraft reply, how the absolute time delay is computed is shown in Figure C-60. The top of Figure C-60 shows an “Expanded TOA Pulse Reference Frame”. This reference frame illustrates and facilitates analysis of the absolute time delay. In this reference frame, time delay is generally defined by Equation 14 and Equation 16. It is important to note that the time delays are referenced from the half amplitude point of the leading edge of the pulse and not by the peak of the pulse. This is shown in Figure C-60 in the lower right-hand corner. In this part of the figure, the relative time delay between the multipath pulse and the direct pulse (T_{rd}) is introduced and accounted for, which further adds to the definition of time delay. This accounts for the early arrival, late-short arrival, and late-long arrival zones discussed above in Figure C-54. The fully evolved equation for time delay is shown in Equation 17.

$$\text{Time Delay} = T_{er} - T_{ua} \quad \text{Equation 14}$$

Where:

T_{er} = Early Reply Propagation Time, and
 T_{ua} = User Aircraft Propagation Time.

Note $T_{ua} = d/v$

Where:

d = The distance between the transponder and aircraft ellipsoid foci (See Figure C-17),
 and
 v = Velocity of propagation.

$$\text{Note that : } T_{er} = T_{rc} + T_{ua} + T_{ps} \quad \text{Equation 15}$$

Where:

T_{er} = Early Reply Propagation Time,
 T_{rc} = Variable Reply Spacing Time,
 T_{ua} = User Aircraft Propagation Time, and
 T_{ps} = Pulse Spacing Time.

$$\text{Therefore, Time Delay} = T_{rc} + T_{ps} \quad \text{Equation 16}$$

Where:

T_{rc} = Variable Reply Spacing Time, and
 T_{ps} = Pulse Spacing Time.

$$\text{Time Delay} = T_{rc} + T_{ps} + T_{rd} \quad \text{Equation 17}$$

Where:

T_{rc} = Variable Reply Spacing Time,

T_{ps} = Pulse Spacing Time, and

T_{rd} = Relative Time Delay between the Multipath Pulse and the Direct Pulse.

How the absolute time delays are calculated for the remaining multipath interference types is illustrated in Figure C-61, Figure C-62, and Figure C-63.

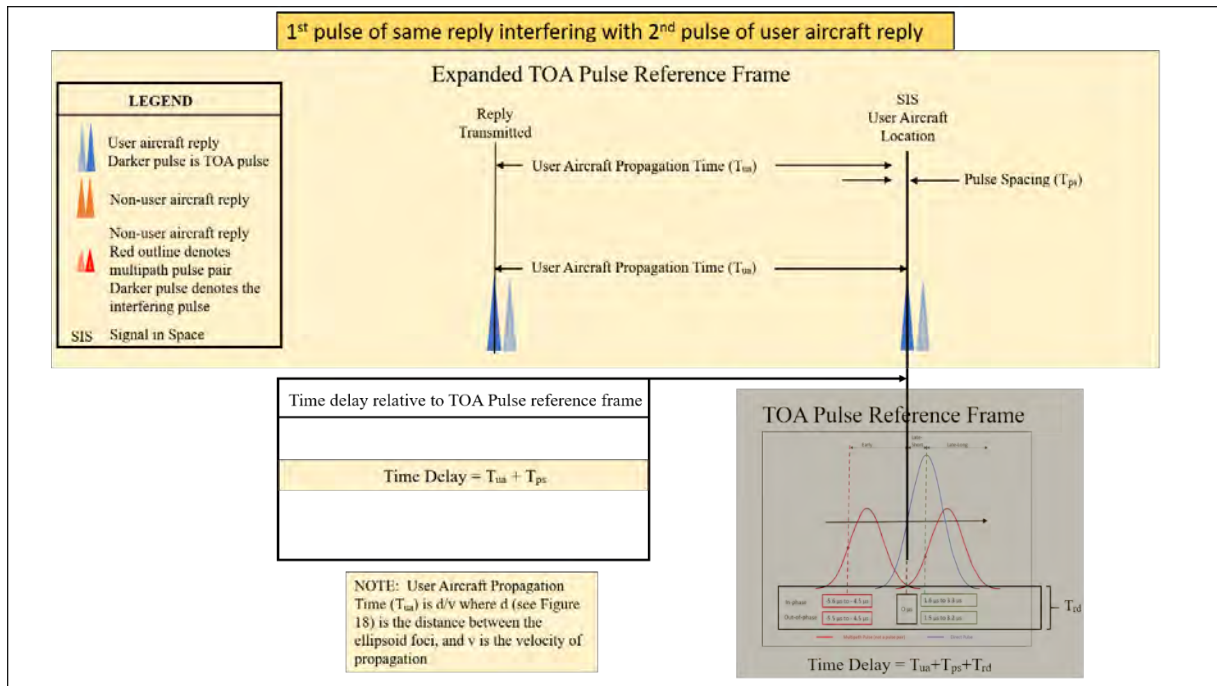


Figure C-59. Multipath Case – 1st Pulse of Same Reply Interfering with 2nd Pulse of User Aircraft Reply

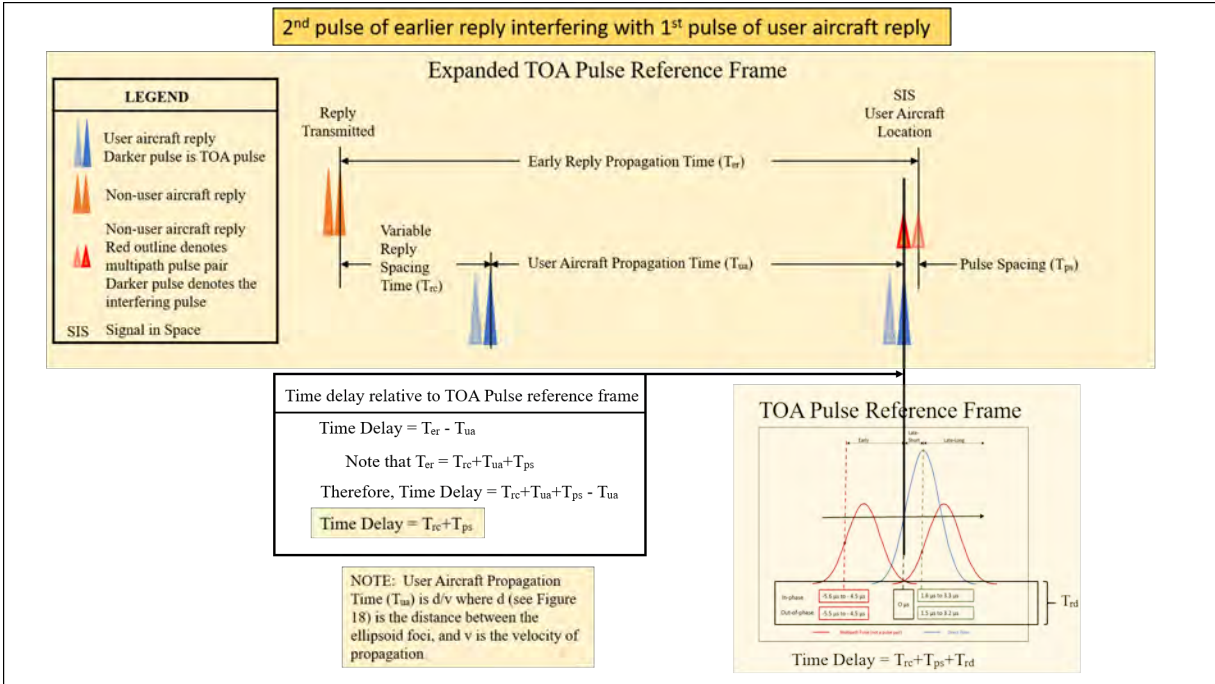


Figure C-60. Multipath Case – 2nd Pulse of Earlier Reply Interfering with 1st Pulse of User Aircraft Reply

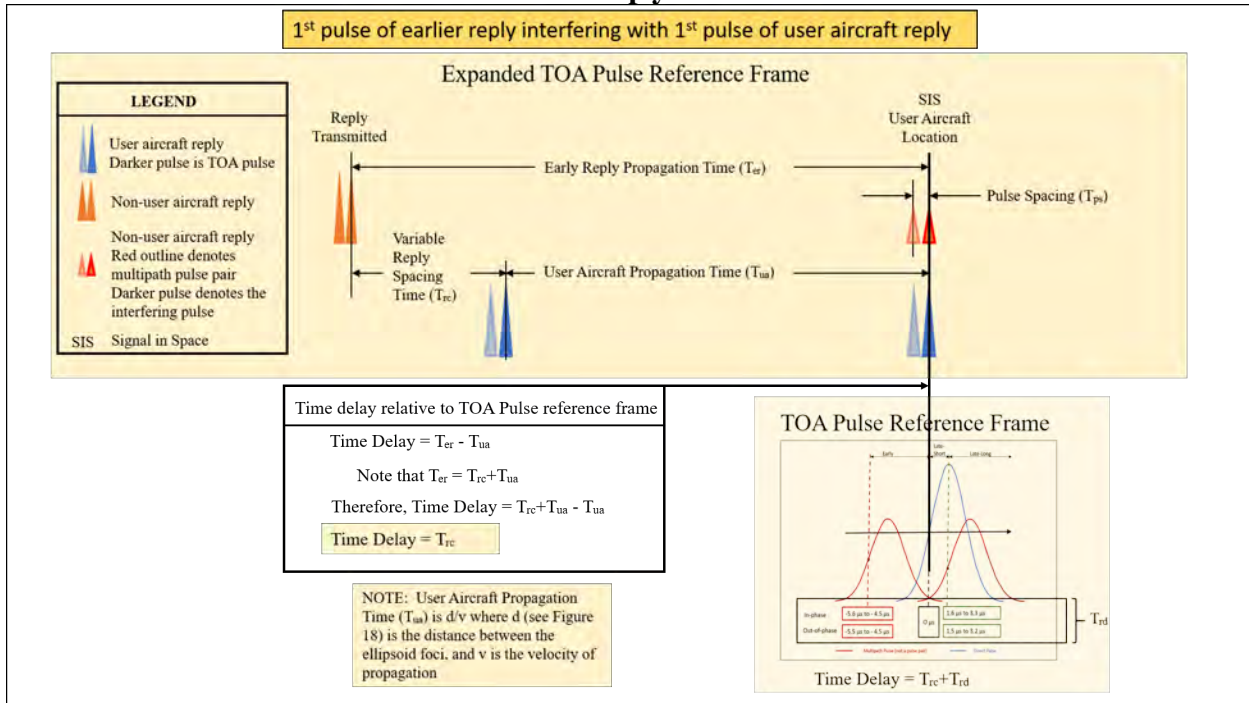


Figure C-61. Multipath Case – 1st Pulse of Earlier Reply Interfering with 1st Pulse of User Aircraft Reply

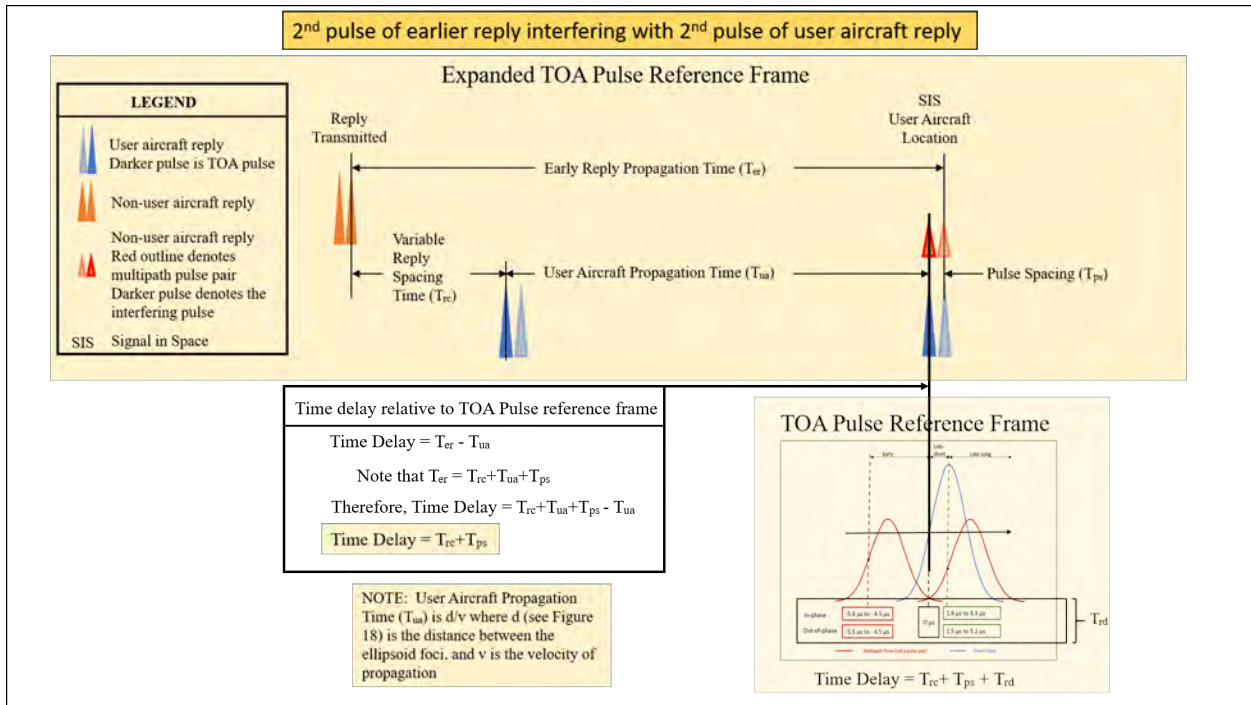


Figure C-62. Multipath Case – 2nd Pulse of Earlier Reply Interfering with 2nd Pulse of User Aircraft Reply

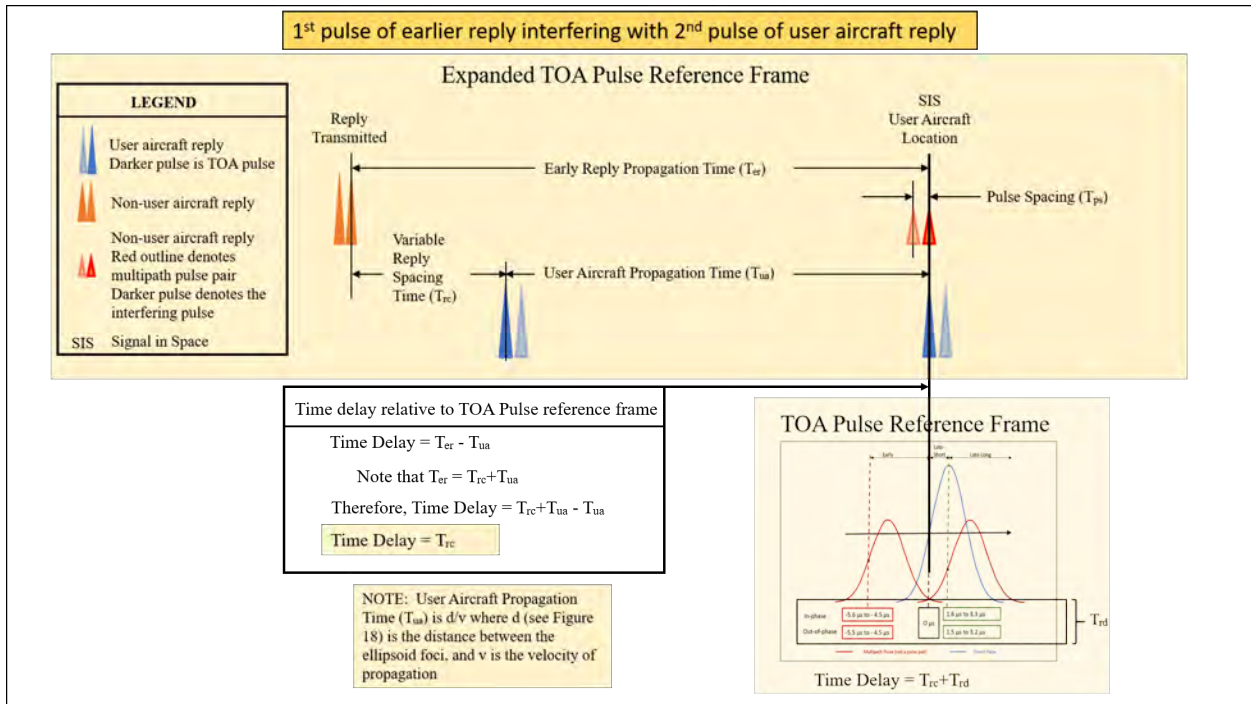


Figure C-63. Multipath Case – 1st Pulse of Earlier Reply Interfering with 2nd Pulse of User Aircraft Reply

- viii. **Echo (Multipath) Ellipsoid Families.** Figure C-64 illustrates a snapshot in time of the Echo (multipath) ellipsoid families (i.e., the multipath source locations of concern) that would be responsible for the multipath scenarios that were discussed in Section 7. Based on the instantaneous geometry of Aircraft B with respect to the transponder antenna, three echo ellipsoids are drawn. It should be noted that the location, size, and shape of these echo ellipsoids change as the location of the aircraft of interest (Aircraft B) changes. Therefore, given the dynamics of the situations, a multipath object having large dimensions normally must be present to cause the multipath interference to persist long enough to have a detrimental effect beyond elevating the noise floor. This particular snapshot is discussed below.

In the first scenario, Aircraft B interrogates the DME transponder and receives a reply. Reflections from objects located on Echo Ellipsoid 1 in Figure C-64 create uplink multipath from that same interrogation reply that interferes with the received direct pulse-pair for Aircraft B. This scenario matches interference types 1 and 2 listed in Section 5.b.vii, and type 2 interference is illustrated in Figure C-59. It should be realized that the specific type of interference caused depends on which pulse of the pair is used for TOA determination.

In the second scenario, Aircraft A interrogates the DME transponder and then receives a reply. This reply propagates outward and is reflected from objects located in the environment, but only reflections from those objects located on Echo Ellipsoid 2 in Figure C-64 create multipath of interest to this discussion. Aircraft B then interrogates the DME transponder and receives a reply. However, the multipath resulting from the reply to Aircraft A, which is reflected from objects located in Echo Ellipsoid 2, reaches Aircraft B within the same TOA window as the reply to Aircraft B. Referring to Section 5.b.vii, this scenario matches multipath interference types 3 through 6, which are illustrated in Figure C-60 through Figure C-63. Again, it should be realized that the specific type of interference caused depends on which pulse of the pair is used for TOA determination.

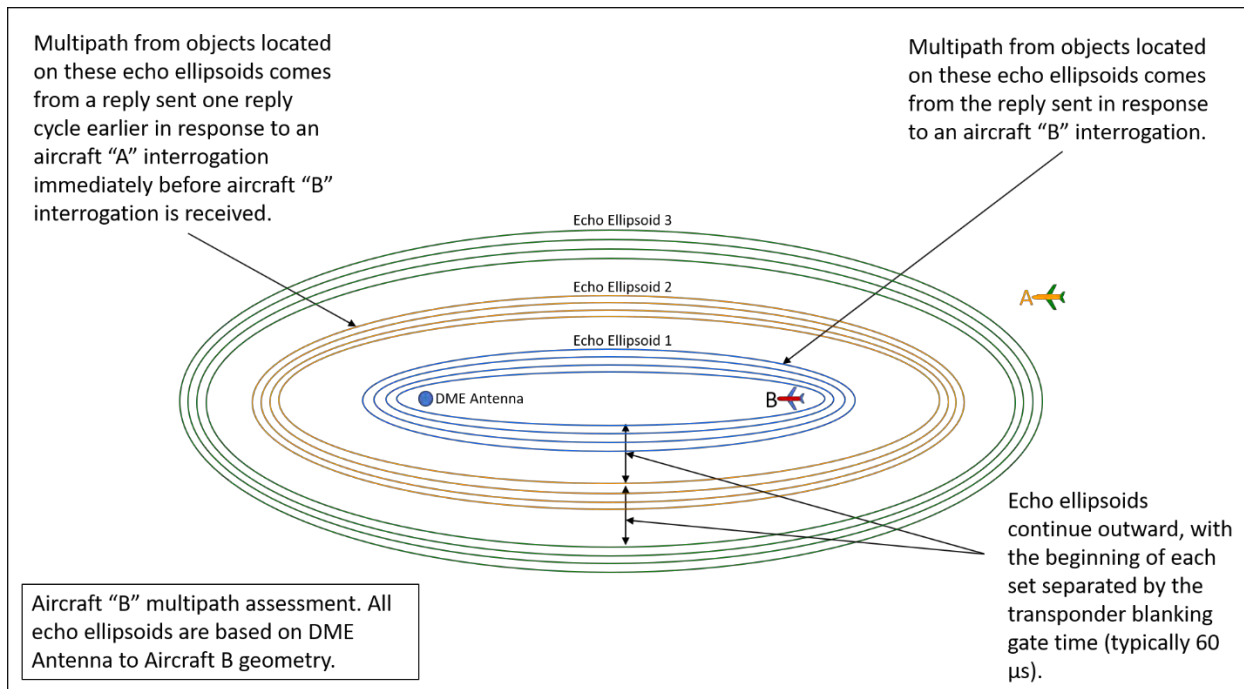


Figure C-64. Uplink Echo Ellipsoids Based on Aircraft B Geometry

In the preceding discussion, multipath scenarios for two echo ellipsoids (1 and 2) were examined above. As shown in Figure C-58, the number of reply cycles that occurs between the broadcast of the multipath pulse-pair and the direct pair is a parameter used in computing the absolute time delay. Taking the second scenario as an example, the time in between these two replies (aka the reply cycle) is influenced by the following: (1) the transponder receiver blanking time; and (2) the time between when the receiver is re-enabled and the interrogation from Aircraft A is received by the transponder. It should be noted that the second component of the reply cycle time decreases as traffic loading increases and is ignored in the following discussion for simplicity reasons, but the concept remains the same. Furthermore, a blanking gate time of 60 μ s is assumed for the purposes of discussion.

A blanking gate delay of 60 μ s between echo ellipsoids corresponds to a distance of approximately 59,000 feet, or 9.71 nmi. Multipath that is delayed three cycles has a path length of tens of miles, which indicates a large time delay. As the multipath travels a longer path, with longer time delays, the M/D ratio also decreases. Additionally, as objects that produce reflections get farther away from the aircraft, they also become a smaller fraction of the Fresnel Zone. The echo ellipsoids could continue with a third (as shown in Figure C-64), fourth, and fifth family of ellipsoids, but will generally cease to affect the direct signal because: 1) There is no unobstructed path to illuminate the scatterer, and 2) Curvature of the earth adversely affects multipath propagation. That said, the multipath in echo ellipsoid regions far from the aircraft may cause noise-like effects on the received signal, with an exception being when large mountains are present. In this case, the mitigation of synchronous multipath effects is an important aspect of the DME

system concept, and jitter is a means for accomplishing such mitigation.

- ix. **Jitter and Mitigation of Synchronous Multipath Effects.** The discussion in Section 5.b.viii above led to the conclusion that Echo Ellipsoid 1 is the only area between the DME antenna and the aircraft that may be likely to cause multipath interference, except when mountainous terrain is present. Not only are areas beyond this ellipsoid physically unlikely to cause reflections due to geometrical considerations, but another mechanism is also in place to prevent synchronous multipath effects from objects beyond this region.

Previously when discussing the top portion of Figure C-56 (i.e., downlink), it was noted that the interrogation sequence for each individual aircraft is “jittered,” and that while the fixed-delay provides the time necessary to accomplish TOA determination and pulse-pair validation by the transponder receiver, it also results in the protection from synchronous errors provided by jitter to be passed along to the uplink. That is, DME transponder replies are indirectly jittered, or randomized, preventing synchronous multipath interference. Figure C-65 shows a reply sequence that has been transmitted by the transponder. Note that the top row reflects that the timing between consecutive replies is not synchronous, but has instead been randomized. The smaller pulses outlined in red indicate synchronous multipath from the same reply cycle for the aircraft of interest.

The second line shows multipath from a reply to a different aircraft that happened one reply cycle earlier. The multipath is not only jittered, but also is decreased in magnitude due to the much greater propagation path length. Similarly, the third line shows multipath from two reply cycles earlier wherein the multipath is further reduced in magnitude and has also been randomized.

The composite SIS is shown on the bottom line. Since replies to other aircraft are asynchronous, as well as having reduced amplitudes, the interference from this type of multipath tends to not cause ranging errors.

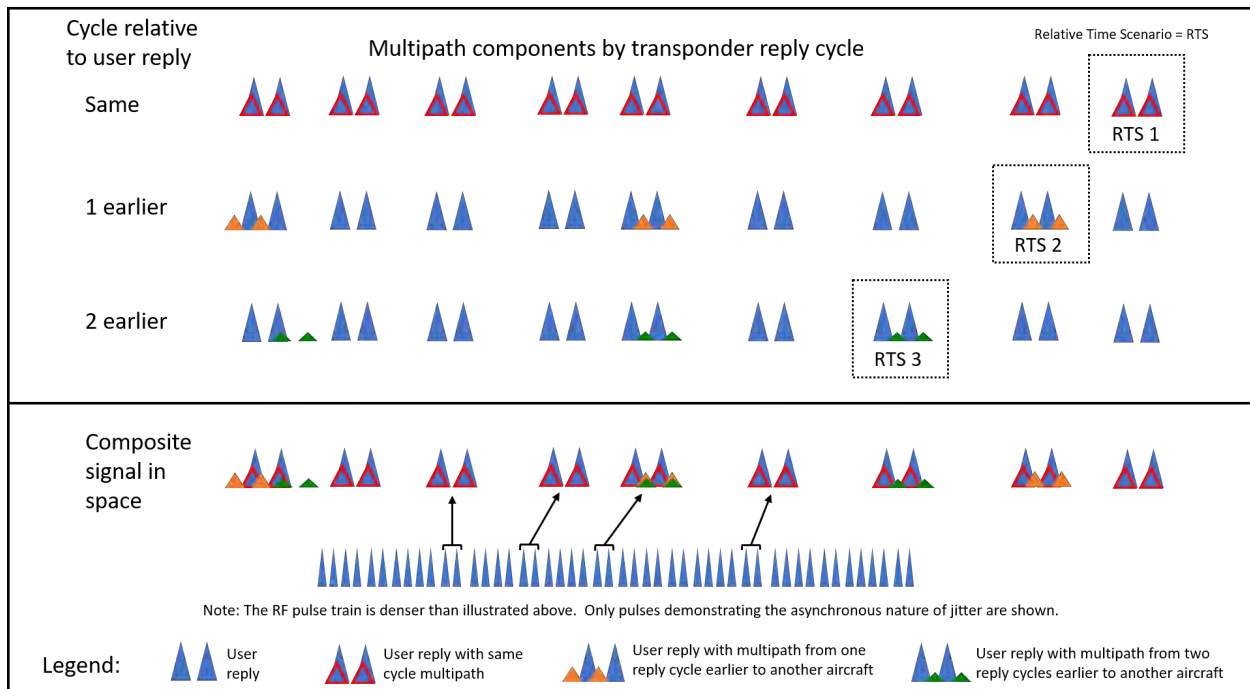


Figure C-65. Interrogation Replies are Jittered (Asynchronously) to Prevent Multipath Interference

The block around the DME side of Echo Ellipsoid 1 in Figure C-66 shows the area surrounding the DME antenna that is of primary concern for siting. Reflections from this ellipsoid are synchronous and therefore have the most potential for interference; however, objects must be relatively close to the antenna for problems to occur. When the aircraft is not close to the DME, the objects that are also farther away must be quite large to cover one Fresnel Zone, and they have to be higher so that the multipath is able to travel vertically into the service volume (see Figure C-16). Recall that Snell's Law (angle of incidence equals angle of reflection) is applicable to the vertical angle, so it is difficult if not impossible for the specular reflection to reach the aircraft. It is also unlikely that there would be no interfering objects and terrain that prohibit the reflecting object from being illuminated when the aircraft is not close to the DME.

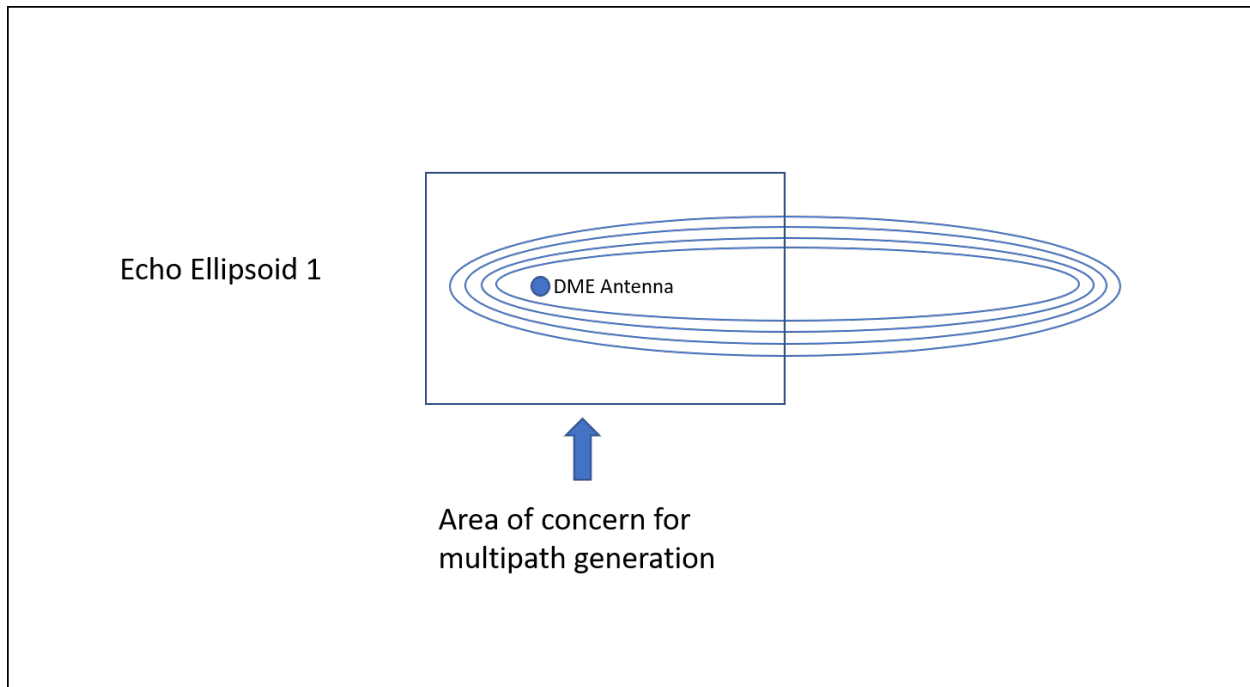


Figure C-66. Multipath Object Locations of Interest within Echo Ellipsoid 1

- x. **Example Application.** In practice, the siting engineer will survey a potential transponder antenna location and large structures may be observed nearby and noted. For example, if a tall, large building is located at a distance of 5,000 feet from a potential DME antenna site as shown in Figure C-67, multipath and shadowing from the building will result as illustrated in Figure C-15. For this example, it is assumed that the building is tall enough to penetrate through the subtending angle of the DME OCA (see Figure C-25). In such a case, the technique shown in the top panel of Figure C-39 is applied to identify the volume of space that may be affected by multipath from the larger illuminated side of the building. The result of this application is shown in Figure C-67 as well. The shaded region in this figure shows where the reflection multipath region exists (plan view), which is bordered on both sides by a diffraction multipath region.

The signal strength of the multipath is estimated by determining how the dimensions of the building side compare to the first Fresnel Zone. Two one-dimensional analyses are performed to assess the horizontal and vertical building dimensions individually. The results of these two analyses are combined to formulate a conclusion regarding how multipath affects the SIS within the region being analyzed. The examination of the horizontal dimension is addressed first for the purpose of demonstrating the analysis process. In some cases, it may be more efficient to conduct the vertical dimension analysis first. Experience in performing site surveys is the best means of developing the judgement necessary to select which dimension is assessed first. The selection is not a matter of right or wrong, but one of efficiency.

As shown in Figure C-67, the radius of the First Fresnel Zone is computed to be

approximately 71 feet, which is the dimension in the direction normal to the radial direction of the signal as it propagates outward from the DME antenna. Because the building side is not normal to the direction of signal propagation, the projection of the first Fresnel Zone onto this side must be calculated. The horizontal projection (i.e., plan view) calculation is shown in the inset of Figure C-67.

The 176-foot value for the projection is 24 feet shorter than the 200-foot length of this building side. This difference means that the LOS point shown at the center of the building in Figure C-67 can move 12 feet either to the right or to the left before one end of the Fresnel projection will move off the building. This results in a 24-foot-wide area in the center of the building for which the projection of the first Fresnel Zone may be entirely on the building side. This area is indicated by the orange rectangle shown on the multipath signal strength plot (see Figure C-67).

The magnitude of multipath signal strength in this area will approach a value of one, which indicates it will be comparable to the signal strength of the direct signal within the multipath region. In this case, the multipath signal will be slightly less than the direct signal because it travels a longer propagation path than the direct signal to reach the receiver antenna. Outside this central region, the projection of the first Fresnel Zone will not be entirely on the building side, thus the multipath signal strength decreases as illustrated. Once outside the diffraction regions shown in Figure C-67, the signal scattered by the building is too weak to have a measurable effect on the SIS.

The result of the multipath signal strength analysis indicates that M/D ratios causing both measurable ranging errors and fading effects are likely. To assess the effect on accuracy, the results of Figure C-54 are applied by determining where time-delays of less than $3.3 \mu\text{s}$ (i.e., Late-short Arrival Zone) occur within the multipath region. This analysis begins with determining the time delays at receiver locations Rx₁, Rx₂, and Rx₃ (which are located at distances d_1 , d_2 , and d_3 from the antenna site, respectively). These time delays can be computed for each location to ascertain if they fall within the $3.3 \mu\text{s}$ boundary of the Late-short Arrival Zone.

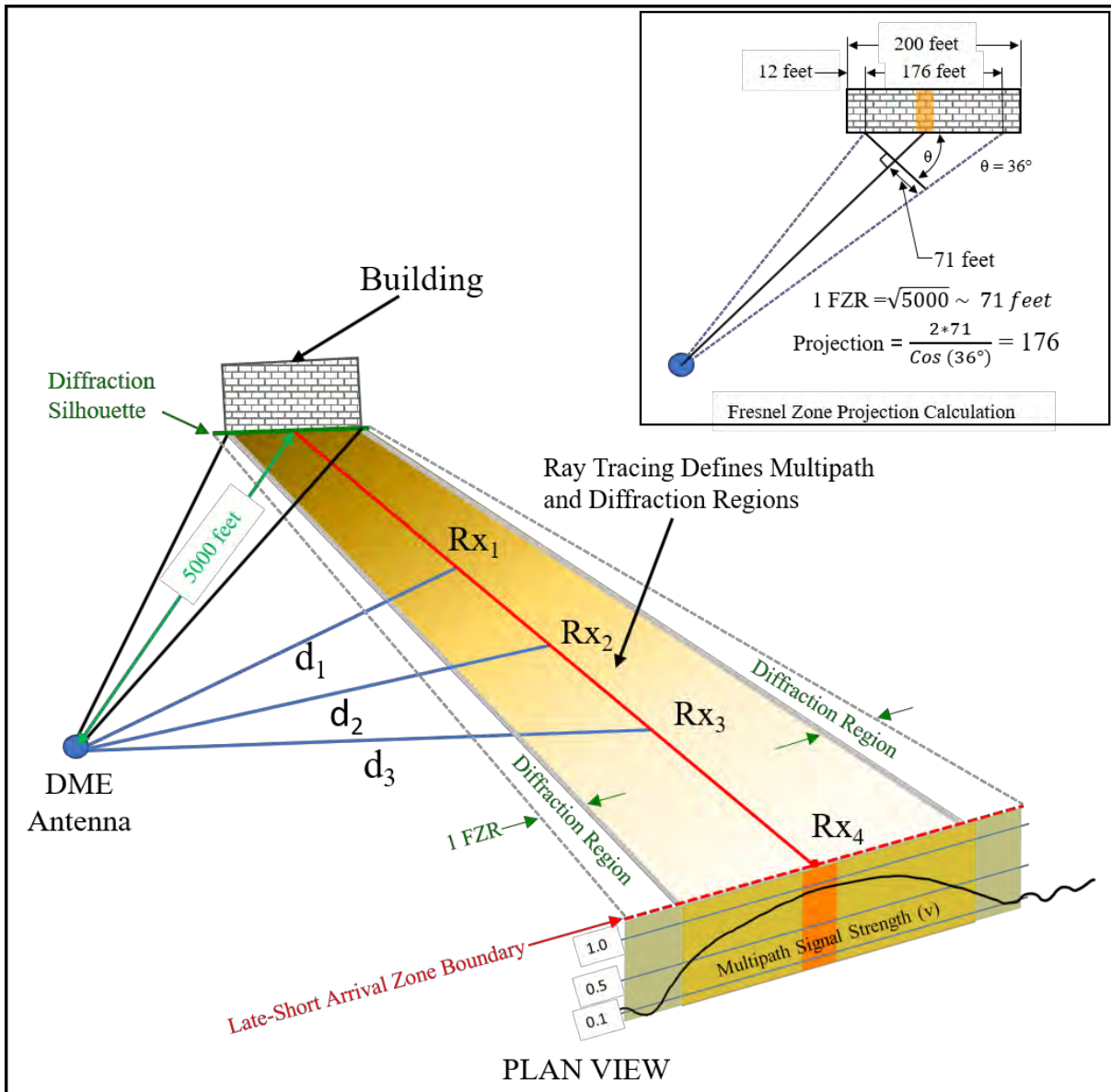


Figure C-67. Plan View Showing a Building Near a Potential DME Antenna Site

Consider a scenario where the building shown in Figure C-67 is located at a distance of 5,000 feet from the DME and at an angle of 45° (i.e., $\theta_2 = 45^\circ$) from a line between the DME and receiver point 2 (Rx₂), as shown in Figure C-68. Assuming the distance between the DME and Rx₂ is 10 nmi (60,760 feet), the time delay for the multipath signal arriving at Rx₂ can be computed using Equation 9 and then Equation 7 as shown below:

$$R = \sqrt{r^2 + d^2 - 2rd\cos(\theta)} = \sqrt{5000^2 + 60760^2 - 2(5000)(60760)\cos(45^\circ)} = 57,334 \text{ ft}$$

$$\text{Time delay, } t = \frac{r + R - d}{c} = \frac{5000 + 57334 - 60760}{9.84 \times 10^8} \approx 1.6 \mu\text{s}$$

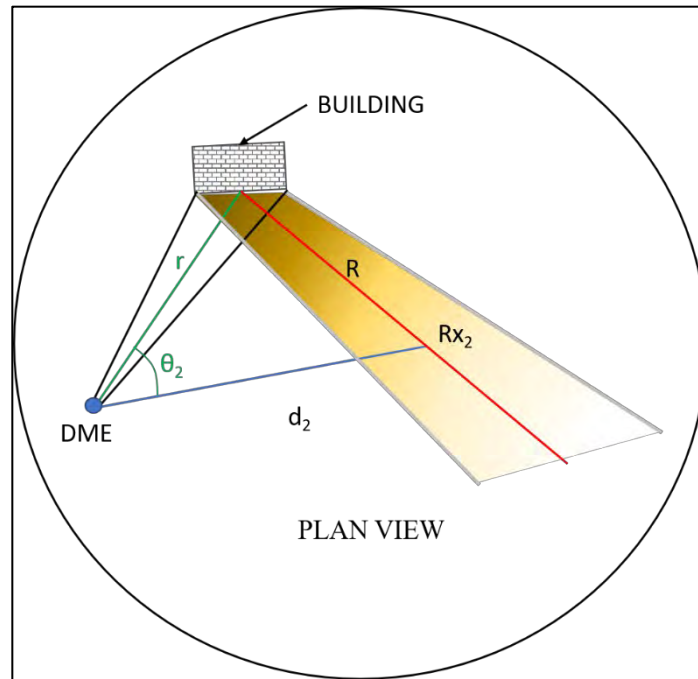


Figure C-68. Time Delay Calculations Scenario

In a similar manner to the calculations above, the time delay for Rx_1 at 8 nmi and Rx_3 at 12 nmi can also be computed to give $1.56 \mu s$ and $1.65 \mu s$, respectively. The time-delay values for these three locations fall well within the Late-Short Arrival Zone, thus measurable or even out-of-tolerance range errors are possible within this portion of the multipath region given the results of the multipath signal strength analysis. The process continues by moving the receiver location farther away from the building until a location is found where the time-delay value is approximately $3.3 \mu s$. This location identifies the geographical area corresponding to the end of the Late-Short Arrival Zone and is illustrated as location Rx_4 in Figure C-67. Measurable signal fading effects and receiver unlock conditions may still occur beyond this location.

An analysis comparing the vertical dimension of this building side to the first Fresnel Zone is performed in a similar fashion. However, in this case, the objective is to determine a scaling factor that is to be applied to the estimated multipath signal strength determined in the prior step (see Figure C-67). Figure C-69 shows three scenarios that may be encountered where the building height is varied to create the scenarios for this example.

In scenario “a” of Figure C-69, the vertical projection of the first Fresnel Zone lies completely on the building side. As shown in the front view portion of this figure, the projection will normally “creep up” slightly as the reflection point migrates across the building from the near side to the far side. It should be observed that the vertical projection of the first Fresnel Zone remains entirely on the building surface in this scenario. Given this observation, a vertical profile factor of 1.0 would be used. In this case, the multipath signal strength estimate shown in Figure C-67 is

used without any scaling applied. Observations like those shown for scenarios “b” and “c” would indicate the use of a scaling factor of 0.5 and 0.1, respectively.

This process is repeated for the smaller (or remaining) illuminated sides, then also for the shadowing case. The results from all analyses conducted are used to formulate a conclusion regarding the suitability of the antenna site under consideration.

The following closing thoughts are offered for consideration:

1. It should be realized that the same observations noted above could have resulted for a building having the same height in all three scenarios, but the building is either elevated or lowered relative to the antenna site due to terrain height differences.
2. Furthermore, given the small subtending angle shown in Figure C-25, there generally is negligible difference between the dimension of the first Fresnel Zone radius and its vertical projection onto a building side or multipath object.
3. An alternative analysis can be performed where the elevation angle that produces scenario “c” of Figure C-69 is determined, then used to define the vertical plane above which the effects of multipath will be negligible.
4. The process described above can be used to identify areas to be investigated thoroughly by modeling or site testing using a mobile DME (see sections below), particularly when the multipath object has a complex shape, non-metallic surface, and/or rough surface, as well as when multiple objects are present within the DME OCA.
5. It should be realized that the magnitude of ranging errors and the depth of signal fades experienced depends on the amount of time it takes the receiver (i.e., DME equipped aircraft) to pass through a multipath region. For a flight path that runs perpendicular to the red line shown in Figure C-67, this time may be very short for turbine aircraft, particularly if the path taken is not far from the multipath source. In this case, the magnitude of ranging errors and the depth of signal fades experienced may be operationally acceptable, or even negligible, because of the short exposure time. Conversely, a flight path running parallel to the red line shown in Figure C-67 results in a longer exposure time, which may result in out-of-tolerance conditions being experienced and/or a receiver unlock condition.

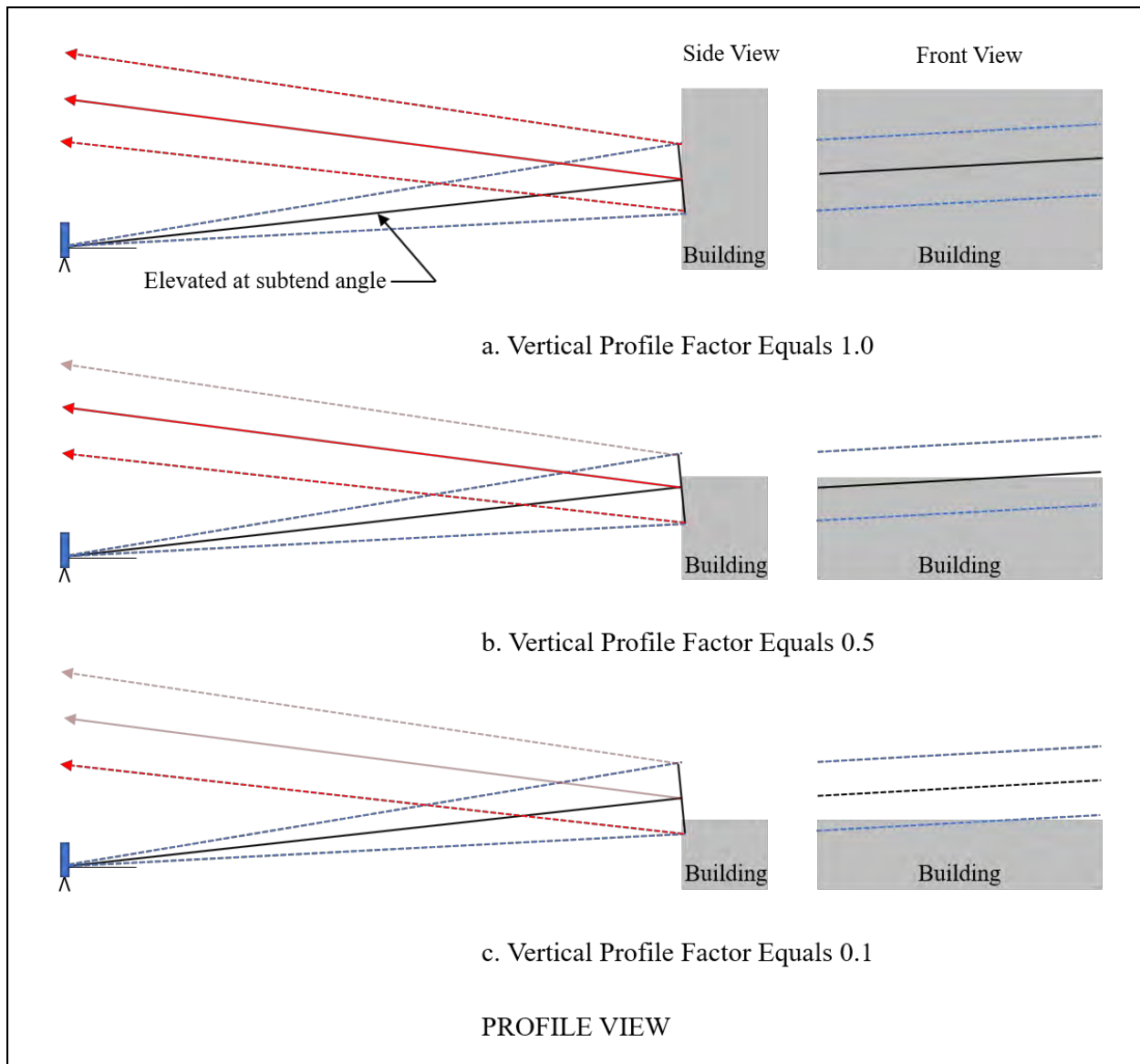


Figure C-69. Determining Vertical Profile Factor

- c. When Modeling May Be Required.** DME multipath modeling software is available. When the software is properly utilized, it can predict the effect that various siting conditions have on the performance of a DME facility. This modeling software is useful in predicting DME signal disturbance in many cases. One case in which this software is useful is when a new DME is to be sited in challenging conditions like mountainous terrain. The second case in which this software is useful is when there is a proposal of new construction near an existing DME and an analysis needs to be conducted to see if the new construction will impact the DME SIS. The third case would be to utilize the software to compare the performance achieved by the use of different antenna models. A fourth case would be when it becomes necessary to investigate changing the transponder antenna location to optimally adjust the multipath time delay in order to minimize the impact that a structure has on the DME SIS – that is, avoid time-delay

values that result in maximum ranging error. Additional information regarding multipath models can be found in Chapter 5, Chapter 6, and Appendix F.

- d. Siting Testing Using Mobile DME.** Mobile DME systems are also available. These systems can be utilized by siting engineers to provide a facility/signal to be used at a proposed site or to provide an interfering signal to test an operational installation. When used as a proposed facility/signal the mobile unit can be modified (physical position or operational parameter) to directly assess the effect of a proposed site. The mobile unit can also be used as a potential interference source as a way to assess operational site irregularities. A fully operational mobile DME can be deployed quickly, and can be utilized to verify if a particular DME siting location will provide an acceptable DME SIS. Once operational, FAA flight check can be utilized to evaluate the SIS and determine if it is within the evaluation tolerances.

Appendix D. Antenna Performance

1. Overview

The purpose of this appendix is to provide the performance characteristics of the following currently fielded DME antennas: dBS 5100A, dBS 5100A/7°, dBS 510A, dBS 540; and dBS 900E TACAN (DME mode). Topics addressed include electrical, physical, and vertical pattern characteristics, as well as available horizontal pattern options and signal fading performance. The appendix concludes with the presentation of absolute gain comparison plots and related discussion. The vertical pattern data for the dBS 510A was provided courtesy of dB Systems, Inc., at no cost to the FAA or Ohio University (OU). The remaining vertical pattern data was provided by the FAA as Government Furnished Information. The performance information presented herein is publicly available from the dB Systems, Inc. website, www.dbsant.com.

Prior to developing this appendix, a study was performed to characterize the signal attenuation (i.e., worst-case) or amplification (i.e., best-case) that can occur due to reflection of the DME radiated signal by the ground (Reference Z). During this study, the fading performance of the dBS 900E TACAN central array was characterized because it is a real antenna design having vertical pattern characteristics that provide significant resistance to signal fading caused by ground reflections. That is, the awareness of such resilient performance from a realizable antenna is noteworthy. In this case, it was envisioned that the dBS 900E TACAN central array would then be housed in a conventional DME antenna radome and that the same methods used to generate uni-directional and bi-directional horizontal patterns could be applied in this case as well.

2. Antenna Overviews

- a. **DME Antenna Models Overview.** The dB Systems, Inc. antenna models dBS 5100A, dBS 5100A/7°, dBS 510A, dBS 540, and dBS 900E are dipole arrays consisting of 8, 10, 14, or 16 elements providing main lobe gains ranging from 8 dBi to >13 dBi. The horizon gains are between 6 dBi and >11dBi depending on the model, except for the dBS 900E which has a horizon gain of ≥ 3 dBi.

The antennas are available with omni-directional, uni-directional (90°, 180°, or 210° Half Power Beam Width (HPBW)), or bi-directional (50° each lobe) horizontal pattern options, with the exception of the dBS 540, which is available only as an omni-directional model. Some models radiate an above-the-horizon null-filled pattern that minimizes the radiated cone of silence. Each of these antennas handles an input power up to at least 5,000W at 3% pulse duty cycle (dBS 900E at 4% duty cycle), except each dBS 510 model which handles an input of 10,000W at 3% duty cycle. Each antenna model operates over the entire frequency range with an input impedance of 50 ohms and Voltage Standing Wave Ratio (VSWR) of less than 2.0-2.5:1, except the dBS 900E which has a $VSWR \leq 1.8:1$. The VSWR ratings assume measurement at the end of a low loss cable not exceeding 5 feet in length. The antennas provide vertically polarized coverage with the main beam ranging from $2 \pm 1^\circ$ to $7 \pm 1^\circ$ of radiation tilted upward to minimize ground reflections.

The array within each antenna model is enclosed and effectively weatherproofed within a fiberglass radome for prolonged trouble-free use under severe environmental conditions.

Mounting is made by means of an integral base flange with 6 each mounting bolt holes. All RF input/output ports are Type N receptacles. Most arrays have two integral monitor probes (optional on the dBs 540, and not available on the dBs 510A-L, dBs 5100A-L, and dBs 5100A/7° Without Monitor Probes) which constantly sample the RF signal delivered to the antenna.

Obstruction light power is fed through the array and a provision is made for mounting an obstruction light and/or lightning arrestor at the top of the array. Lightning rod kit, obstruction light, pipe adapter (with or without cover), and plate adapter (wall mount) are available as optional items. Each of these DME antennas has been designed for ruggedness, light weight, minimum size, long life, and in accordance with FAA-E-2754 and FAA-G-2100 (common outdoor operating conditions) (see Table D-1).

Table D-1. DME Environmental Specification for dBs Antennas

	Elevation (feet)	Wind Velocity (mph)	Ice Loading	Temperature °C (°F)	Solar Radiation W/m ² (BPH)	Relative Humidity (%)
Specifications	-300 to +10,000 As defined in FAA-G- 2100H, 3.2.1.1.2 (a)	0 to 100 As defined in FAA-G- 2100H, 3.2.1.1.2 (b)	As defined in ASCE Manual 74	-32 to 43 (-25 to 110) As defined in Table C-1 of MIL-STD- 810G; Conditions defined as BASIC in the Climatic Category.	0 to 1120 (0 to 355) As defined in Table C-1 of MIL-STD- 810G; Conditions defined as BASIC in the Climatic Category.	14 to 100 As defined in Table C-1 of MIL- STD-810F; Conditions defined as BASIC in the Climatic Category.
dBs Antennas	Compliance with FAA- G-2100C, Environment III stated, except for 510A (FAA- G-2100) 900E no statement regarding compliance	0 to 100 Note: Up to 180 with HS version	Deicing Version Up to ½ inch radial ice	-50 to +70	No info	5 to 100

Note that a marine version of these antennas is available as an optional upgrade as well. The RF transmission assembly is completely sealed and weatherproofed to protect in harsh environments such as salt water, extreme humidity, wind, sand, snow, and ice.

The dBs antennas described below are high performance, full service, all band antennas that are designed specifically for use as DME antennas. The characteristics for the group of antennas are presented in two high-level groups: electrical and physical. The electrical characteristics that are covered include frequency range, polarization, impedance, power handling capability, main beam elevation location, circularity, VSWR, main beam gain, and horizon gain. The physical characteristics that are covered include the number of array radiators, number of monitor ports, environmental conditions, size, weight, radome size, and de-icing capability. Additional characteristics and optional equipment can be found on the specification sheets on the dB Systems, Inc. website.

Table D-2 lists the characteristics that are common to all dBs antenna models that are designed to radiate the DME signal within the FAA specified service volume requirements.

In the sections to follow, the dBs 5100, dBs 5100A/7°, and dBs 510 DME antenna models will be summarized with two Tables that list the characteristics that are common and unique among the different configurations within each model. Additionally, a description of available horizontal patterns within each antenna model will be given. Note that there is only one model type available for the dBs 540 DME antenna and the dBs 900E TACAN antenna.

Each dBs DME antenna model description will include a Figure for the vertical pattern and a Figure for the signal fading performance (Earth Only, Non-smooth ($\lambda/16$) in-phase and out-of-phase).

Finally, an attachment provides master signal fading performance plots for each antenna model, including a plot for Water and Earth surface conditions, a plot for Earth Only surface conditions, and a plot for Water Only surface conditions. Each plot has a total of eight data traces for smooth PEC, smooth, non-smooth, and rough ground, and for in-phase and out-of-phase ground reflections.

Table D-2. Characteristics Common to dBs DME Antenna Models

<i>Antenna Model</i>	<i>Electrical Characteristics</i>			<i>Physical Characteristics</i>	
	<i>Freq Range</i>	<i>Polarization</i>	<i>Impedance</i>	<i>Monitor Ports</i>	<i>Environmental</i>
dBs 5100A dBs 5100A/7° dBs 510A dBs 540 dBs 900E	960-1215 MHz	Vertical	50Ω	2* * Note – Monitor Ports are not provided in L (Lightweight) models or antenna models specified as such.	Meets FAA-G-2100 (common outdoor operating conditions), and FAA-E-2754

- b. dB Systems 5100A.** The dBs 5100A DME antenna utilizes a collinear 10 element dipole phased array that provides main lobe gains ranging from 9 dB to > 13 dB, and horizon gains between 7 dB and > 11 dB (depending on the model). These antennas are available in omni-directional, uni-directional, and bi-directional horizontal patterns. Only the omni-directional version of this antenna has options for High Strength (denoted as HS) for wind loading up to 180 miles per hour (mph), Lightweight (denoted as L), and deicing.

The dBs 5100A antennas handle an input power up to 5,000W at 3% pulse duty cycle and operate over the entire frequency range with an input impedance of 50 ohms and VSWR of less than 2.5:1. The antennas provide vertically polarized coverage with the main beam tilted 3° upward to minimize ground reflections (longitudinal multipath).

Antenna characteristics (both physical and electrical) are presented in the following hierarchical order. Table D-3 lists characteristics that are common to the different configurations of the dBs 5100A antenna model, and Table D-4 lists characteristics that are unique to each configuration of the dBs 5100A antenna model.

Table D-3. Characteristics Common to Configurations of the dBs Antenna Model - dBs 5100A

Antenna Models	Electrical Characteristics					Physical Characteristics		
	Freq Range	Power Handling Capability	Polarization	Impedance	Main Beam Elevation Location	Array	Monitor Ports	Environmental
dBs 5100A (all model versions)	960-1215 MHz	Up to 5 KW peak RF power at 3% duty cycle	Vertical	50Ω	Between 3° ± 1° above horizon	10 active radiator assemblies with RF choke assemblies on each end	2* * Note – Monitor Ports are not provided in L (Lightweight) models or antenna models specified as such.	Meets FAA-G-2100 (common outdoor operating conditions), and FAA-E-2754

Table D-4. Characteristics Unique to Configurations of the dBs Antenna Model - dBs 5100A

Antenna	Type	Electrical Characteristics				Physical Characteristics			
		Circularity	VSWR	Gain Main Beam	Gain Horizon	Size (inches)	Weight (lbs.)	Radome Size (inches)	Deicing
dBs 5100A	Omni-Directional	± 1 dB max on the horizon	Not greater than 2:1	9 dB/iso	7 dB/iso	77.8	22	3.25 Diameter	No
dBs 5100A-BD	Bi-Directional	50° nominal each lobe	Not greater than 2:1	> 13 dB/iso	> 11 dB/iso	80	37.7	15 width 7 depth	No
dBs	Uni-	180° nominal	Not greater	> 12	> 9 dB/iso	77.8	38	6.25 diameter	No

Antenna	Type	Electrical Characteristics				Physical Characteristics			
		Circularity	VSWR	Gain Main Beam	Gain Horizon	Size (inches)	Weight (lbs.)	Radome Size (inches)	Deicing
5100A-D/180° HPBW	Directional	HPBW; Nominal front-to-back ratio > 10 dB	than 2.5:1	dB/iso					
dBs 5100A-D/90° HPBW	Uni-Directional	90° nominal HPBW	Not greater than 2.5:1	> 13 dB/iso	> 11 dB/iso	77.8	38	6.25 diameter	No
dBs 5100A-HS	Omni-Directional	± 1 dB max on the horizon	Not greater than 2:1	9 dB/iso	7 dB/iso	77.8	24	3.25 Diameter	No
dBs 5100A-HS Deicing	Omni-Directional	± 1 dB max on the horizon	Not greater than 2:1	9 dB/iso	7 dB/iso	77.8	22	3.25 Diameter	Yes
dBs 5100A-HS/210°	Uni-Directional	210° nominal HPBW; Nominal front-to-back ratio ~ 6 dB	Not greater than 2.5:1	> 12 dB/iso	> 9 dB/iso	77.8	25	3.25 Diameter	No
dBs 5100A-L	Omni-Directional	± 1 dB max on the horizon	Not greater than 2:1	9 dB/iso	7 dB/iso	75.25	12.5	3.25 Diameter	No

- i. **Vertical Pattern.** The dBs 5100A DME antenna model has a vertical pattern shown in Figure D-1. Refer to the annotated vertical pattern of Figure 4-1 to understand the key terms and performance characteristics used with antenna vertical patterns. These terms and characteristics can be used to compare differences among DME antennas. The antenna vertical pattern specifications listed below are taken from the manufacturer product specification sheet. The specification sheet as well as additional information can be found at <https://www.dbsant.com/antenna-type/dme-antenna/>.

The important characteristics of the dBs 5100A vertical pattern are:

1. The peak gain: Approximately 3° above the horizon.
2. Width of primary lobe: The width of the primary lobe is not less than 6° at the half-power points.
3. Gain at horizon: The gain at horizon is greater than 6 dB below the peak gain.
4. Slope at horizon: The radiation pattern slope at the horizon influences the fading performance at very low elevation angles. A steeper slope will give an improved multipath to direct ratio. The slope for this antenna is 1 dB/° (0.1v/v/°) minimum.
5. Sidelobes below horizon: The power gain between 10° and 50° below horizon is lower than the power gain at the peak of the major lobe by at least 12 dB.
6. Shoulders: The power gain between 6° and 40° above horizon does not pass below a straight line joining the points of co-ordinates (+6°, -15 dB) and (+40°, -25 dB) with values referenced to the peak of the major lobe above its horizon.

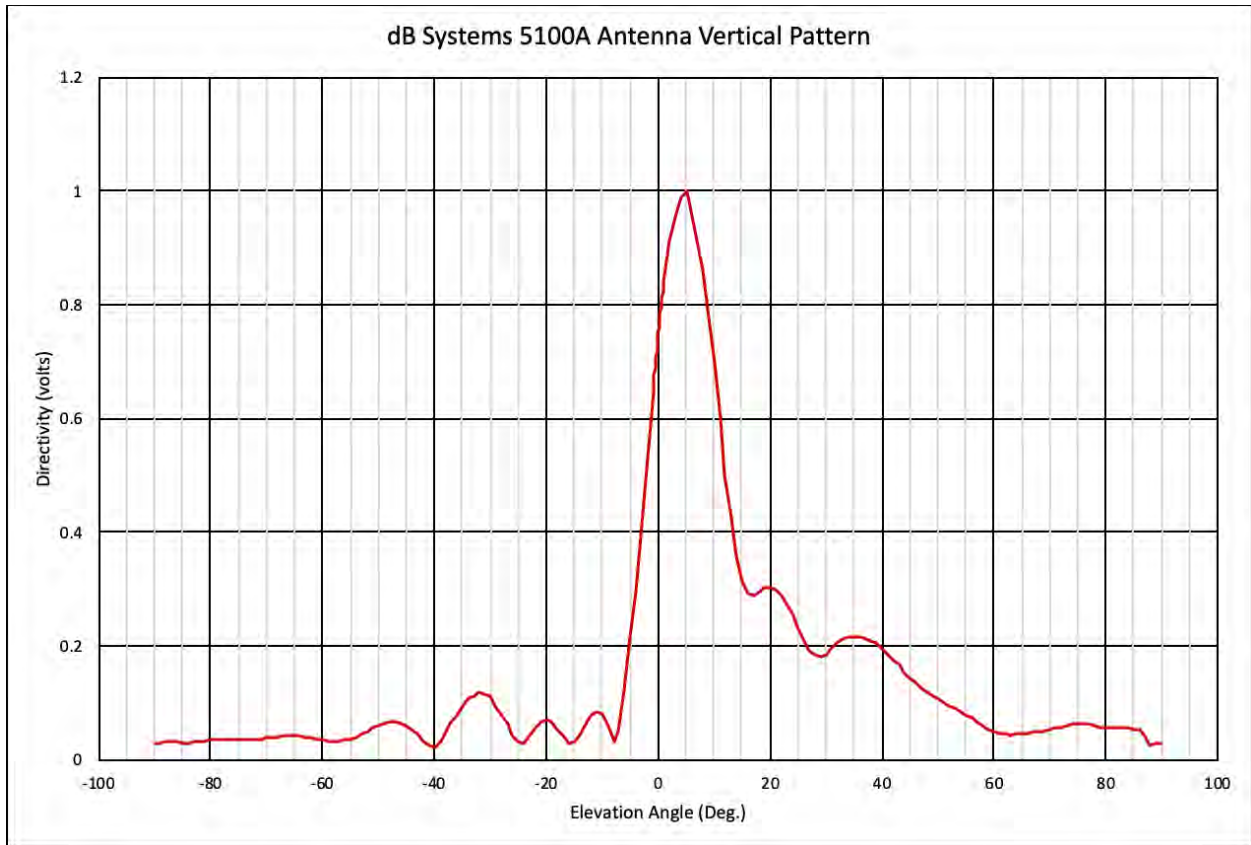
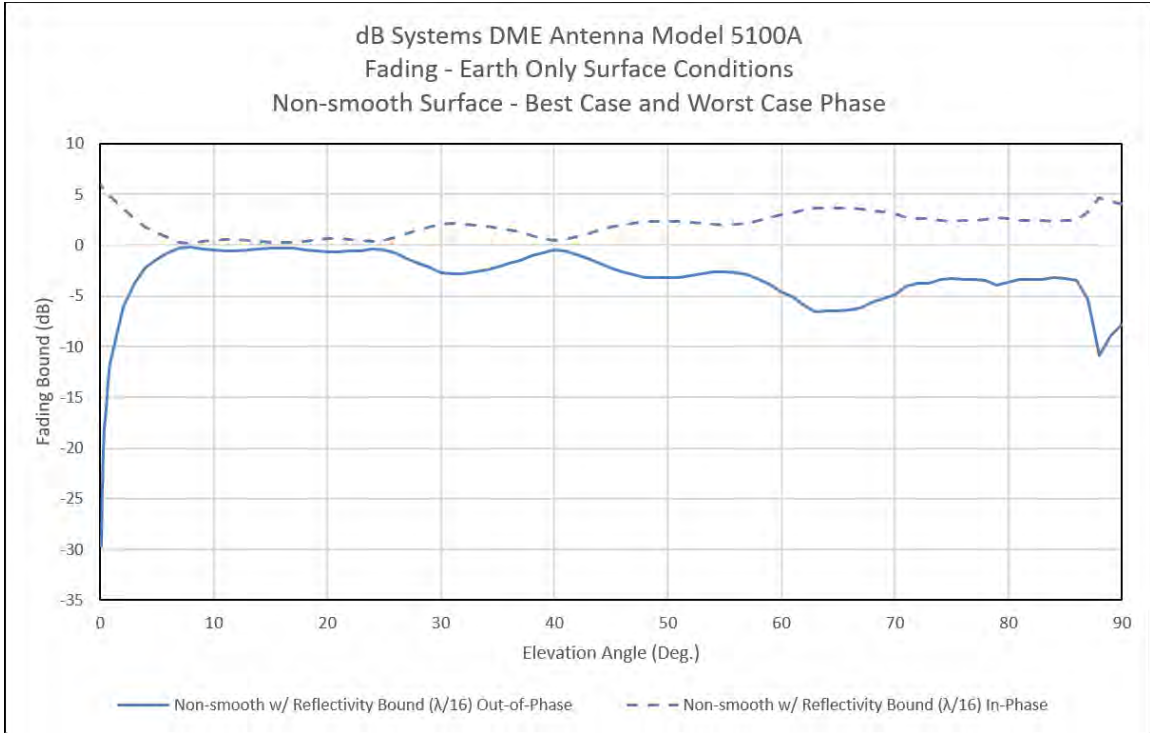


Figure D-1. dBs 5100A Directivity vs. Elevation Angle

a) Signal Fading Performance

A detailed DME signal fading analysis was conducted by OU (Reference Z). Information regarding signal fading is also provided in Chapter 3 and Chapter 4 of this Order. These sections describe how multipath can cause constructive (in-phase) and destructive (out-of-phase) interference. Figure D-2 shows best-case and worst-case fading effects using typical earth surface conditions for the dBs 5100A DME antenna.



**Figure D-2. dBs Antenna Model 5100A Fading Analysis
Best Case/Worst Case Phase - Earth Only Surface Conditions**

- ii. **Horizontal Patterns.** The dBs 5100A DME antenna model is available in omni-directional, uni-directional, and bi-directional horizontal patterns. Refer to the annotated horizontal patterns of Figure 4-2, Figure 4-3, and Figure 4-4 to understand the key terms and performance characteristics used with antenna horizontal patterns. These terms and characteristics can be used to compare differences among DME antennas. The antenna horizontal pattern specifications listed below are taken from the manufacturer product specification sheet. The specification sheet as well as additional information can be found at <https://www.dbsant.com/antenna-type/dme-antenna/>.

The important characteristics of the dBs 5100A horizontal pattern are:

1. Omni-directional: Circularity of ± 1 dB max on the horizon.
2. Uni-directional: Available with 90°/180°/210° nominal beam widths (i.e., HPBW).
3. Bi-directional: Available with 50° nominal beam width (i.e., HPBW).

- c. **dB Systems 5100A/7°.** The dB Systems, Inc. 5100A/7° DME antenna utilizes a collinear 10 element dipole phased array that provides main lobe gains ranging from 9 dB to > 12 dB, and horizon gains between 4 dB and > 6 dB (depending on the model). These antennas are available in omni-directional and uni-directional horizontal patterns. Only the omni-directional version of this antenna has an option to have the monitor probes removed.

The dBs 5100A/7° antennas handle an input power up to 5,000W at 3% pulse duty cycle and operate over the entire frequency range with an input impedance of 50 ohms and VSWR of less than 2.5:1. The antennas provide vertically polarized coverage with the main beam tilted 7° upward to further minimize ground reflections (longitudinal multipath).

Antenna characteristics (both physical and electrical) are presented in the following hierarchical order. Table D-5 lists characteristics that are common to the different configurations of the dBs 5100A/7° antenna model, and Table D-6 lists characteristics that are unique to each configuration of the dBs 5100A/7° antenna model.

Table D-5. Characteristics Common to Configurations of the dBs Antenna Model - dBs 5100A/7°

Antenna	Type	Electrical Characteristics					Physical Characteristics					
		Freq Range	Power Handling Capability	Polarization	Impedance	Main Beam Elevation Location	Array	Monitor Ports	Size (inches)	Radome Size (inches)	Deicing	Environmental
dBs 5100A-D/7° (all model versions)	Uni-Directional	960-1215 MHz	Up to 5 KW peak RF power at 3% duty cycle	Vertical	50Ω	Between 7° ± 1° above horizon	10 active radiator assemblies with RF choke assemblies on each end	2* * Note – Monitor Ports are not provided in antenna models specified as such.	77.8	3.25 diameter	No	Meets FAA-G-2100 (common outdoor operating conditions), and FAA-E-2754

Table D-6. Characteristics Unique to Configurations of the dBs Antenna Model - dBs 5100A/7°

Antenna	Type	Electrical Characteristics				Physical Characteristics
		Circularity	VSWR	Gain Main Beam	Gain Horizon	Weight (lbs.)
dBs 5100A-D/7° Main Beam, 90° HPBW	Uni-Directional	90° nominal HPBW	Not greater than 2.5:1	> 12 dB/iso	> 6 dB/iso	38
dBs 5100A/7°	Omni-Directional	± 1 dB max on the horizon	Not greater than 2:1	9 dB/iso	4 dB/iso	22
dBs 5100A/7° without monitor probes	Omni-Directional	± 1 dB max on the horizon	Not greater than 2:1	9 dB/iso	4 dB/iso	22

- i. **Vertical Pattern.** The dBs 5100A/7° DME antenna model has a vertical pattern shown in Figure D-3. Refer to the annotated vertical pattern of Figure 4-1 to understand the key terms and performance characteristics used with antenna vertical patterns. These terms and characteristics can be used to compare differences among DME antennas. The antenna vertical pattern specifications listed below are taken from the manufacturer product specification sheet. The specification sheet as well as additional information can be found at <https://www.dbsant.com/antenna-type/dme-antenna/>.

The important characteristics of the dBs 5100A/7° vertical pattern are:

1. The peak gain: Approximately 7° above the horizon.
2. Width of primary lobe: The width of the primary lobe is not less than 6° at the half-power points.
3. Gain at horizon: The gain at horizon is greater than 6 dB below the peak gain.
4. Slope at horizon: The radiation pattern slope at the horizon influences the fading performance at very low elevation angles. A steeper slope will give an improved multipath to direct ratio. The slope for this antenna is 1 dB/° (0.1v/v/°) minimum.
5. Sidelobes below horizon: The power gain between 10° and 50° below horizon is lower than the power gain at the peak of the major lobe by at least 12 dB.
6. Shoulders: The power gain between 6° and 40° above horizon does not pass below a straight line joining the points of co-ordinates (+6°, -15 dB) and (+40°, -25 dB) with values referenced to the peak of the major lobe above its horizon.

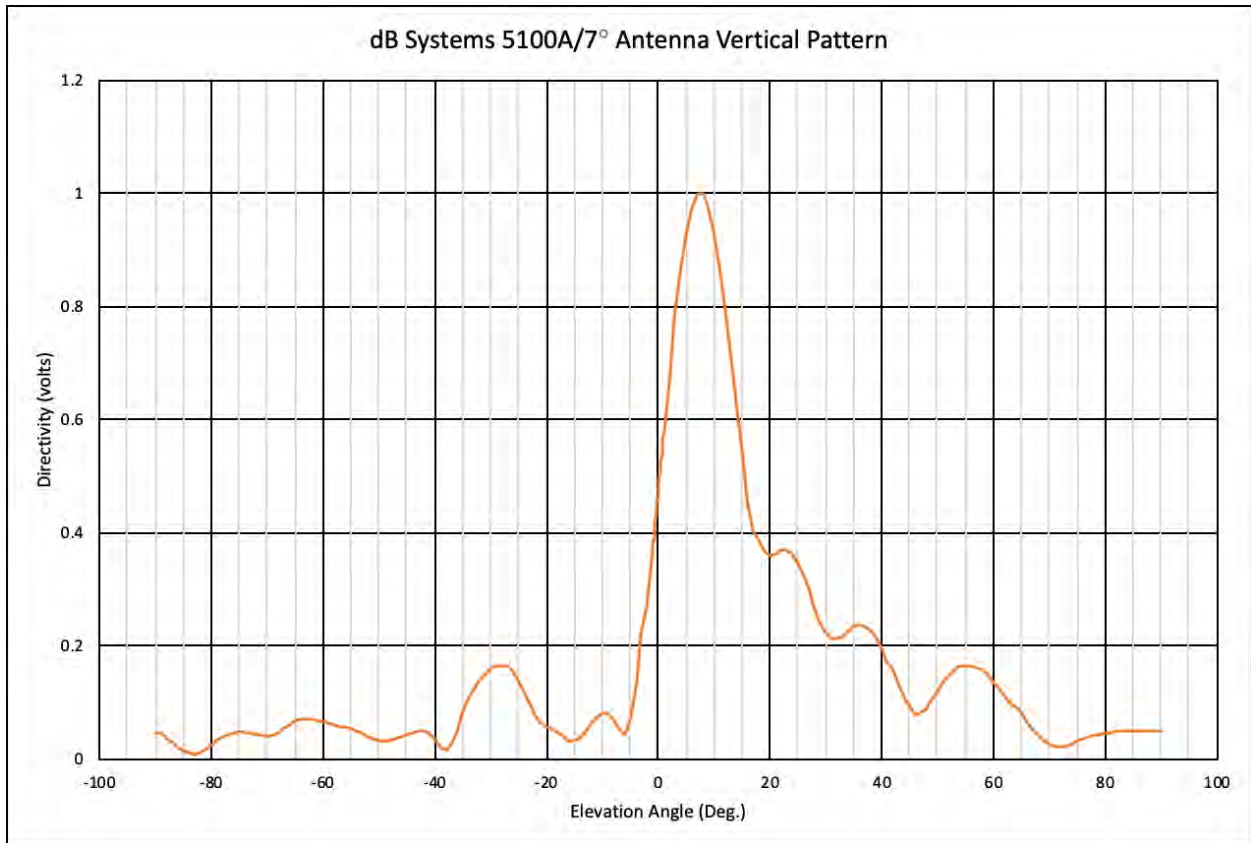


Figure D-3. dBs 5100A/7° Directivity vs. Elevation Angle

a) Signal Fading Performance

A detailed DME signal fading analysis was conducted by OU (Reference Z). Information regarding signal fading is also provided in Chapter 3 and Chapter 4 of this Order. These sections describe how multipath can cause constructive (in-phase) and destructive (out-of-phase) interference. Figure D-4 shows best-case and worst-case fading effects using typical earth surface conditions for the dBs 5100A/7° DME antenna.

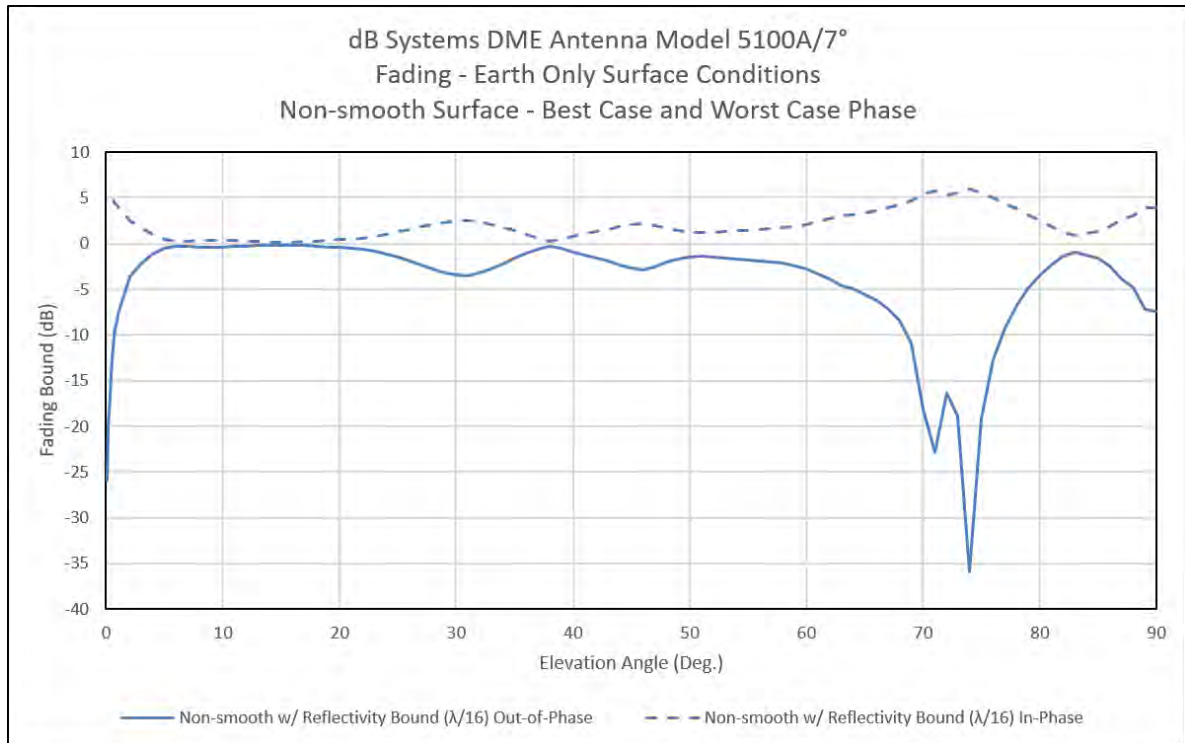


Figure D-4. dBs Antenna Model 5100A/7° Fading Analysis

- ii. **Horizontal Patterns.** The dBs 5100A/7° DME antenna model is available in omni-directional and uni-directional horizontal patterns. Refer to the annotated horizontal patterns of Figure 4-2, Figure 4-3, and Figure 4-4 to understand the key terms and performance characteristics used with antenna horizontal patterns. These terms and characteristics can be used to compare differences among DME antennas. The antenna horizontal pattern specifications listed below came from the manufacturer product specification sheet. The specification sheet as well as additional information can be found at <https://www.dbsant.com/antenna-type/dme-antenna/>.

The important characteristics of the dBs 5100A/7° horizontal pattern are:

1. Omni-directional: circularity of ± 1 dB max on the horizon.
2. Uni-directional: Available with 90° nominal beam width (i.e., HPBW).

- d. **dB Systems 510A.** The dB Systems, Inc. 510A DME antenna utilizes 8 elements and other components that provide main lobe gains ranging from 8 dB to 12 dB, and horizon gains between 6 dB and 10 dB (depending on the model). These antennas are available in omni-directional, uni-directional, and bi-directional horizontal patterns. Only the omni-directional version of this antenna has options for High Strength (denoted as HS) for wind loading > 100 mph, and Lightweight (denoted as L).

The dBs 510A antennas handle an input power up to 10,000W at 3% pulse duty cycle and operate over the entire frequency range with an input impedance of 50 ohms and VSWR of less than 2:1. The antennas provide vertically polarized coverage with the

main beam tilted between 2° and 5° upward to minimize ground reflections (longitudinal multipath).

Antenna characteristics (both physical and electrical) are presented in the following hierarchical order. Table D-7 lists characteristics that are common to the different configurations of the dBs 510A antenna model, and Table D-8 lists characteristics that are unique to each configuration of the dBs 510A antenna model.

Table D-7. Characteristics Common to Configurations of the dBs Antenna Model - dBs 510A

Antenna	Electrical Characteristics					Physical Characteristics			
	Freq Range	Power Handling Capability	Polarization	Impedance	Main Beam Elevation Location	Array	Monitor Ports	Deicing	Environmental
dBs 510A (all model versions)	960-1215 MHz	Up to 10 KW peak RF power at 3% duty cycle	Vertical	50Ω	Between 2° and 5° above horizon	8 active radiator assemblies with RF choke assemblies on each end	2* * Note – Monitor Ports are not provided in L (Lightweight) models or antenna models specified as such.	No	Meets FAA-G-2100 (common outdoor operating conditions), and FAA-E-2754

Table D-8. Characteristics Unique to Configurations of the dBs Antenna Model - dBs 510A

Antenna	Type	Electrical Characteristics				Physical Characteristics		
		Circularity	VSWR	Gain Main Beam	Gain Horizon	Size (inches)	Weight (lbs.)	Radome Size (inches)
dBs 510A	Omni-Directional	± 1 dB max on the horizon	Not greater than 2:1	8 dB/iso	6 dB/iso	77.8	21	3.25 diameter
dBs 510A-BD	Bi-Directional	50° nominal each lobe	Not greater than 2:1	12 dB/iso	10 dB/iso	80	35.7	15 width 7 depth
dBs 510A-D, 90° HPBW	Uni-Directional	90° nominal HPBW	Not greater than 2.5:1	12 dB/iso	10 dB/iso	77.8	38	6.25 diameter
dBs 510A-HS	Omni-Directional	± 1 dB max on the horizon	Not greater than 2:1	8 dB/iso	6 dB/iso	77.8	21	3.25 diameter
dBs 510A-L	Omni-Directional	± 1 dB max on the horizon	Not greater than 2:1	8 dB/iso	6 dB/iso	64	10.2	3.25 diameter

- i. **Vertical Pattern.** The dBs 510A DME antenna model vertical pattern is shown in Figure D-5. Refer to the annotated vertical pattern of Figure 4-1 to understand the key terms and performance characteristics used with antenna vertical patterns. These terms and characteristics can be used to compare differences among DME antennas. The antenna vertical pattern specifications listed below are taken from the manufacturer product specification sheet. The specification sheet as well as additional information can be found at <https://www.dbsant.com/antenna-type/dme-antenna/>.

The important characteristics of the dBs 510A vertical pattern are:

1. The peak gain: Approximately 5° above the horizon.
2. Width of primary lobe: The width of the primary lobe is not less than 10° at the half-power points.
3. Gain at horizon: The gain at horizon is greater than 6 dB below the peak gain.
4. Slope at horizon: The radiation pattern slope at the horizon influences the fading performance at very low elevation angles. A steeper slope will give an improved multipath to direct ratio. The slope for this antenna is $0.44 \text{ dB}/^\circ$ ($0.5 \text{ v}/\text{v}/^\circ$) minimum.
5. Sidelobes below horizon: The power gain between 6° and 50° below horizon is lower than the power gain at the peak of the major lobe by at least 8 dB.
6. Shoulders: The power gain between 6° and 15° above horizon shall be greater than a level which is 20 dB below the power gain at the peak of the major lobe above its horizon. The power gain between 15° and 45° above horizon shall be greater than a level which is 30 dB below the power gain at the peak of the major lobe above its horizon.

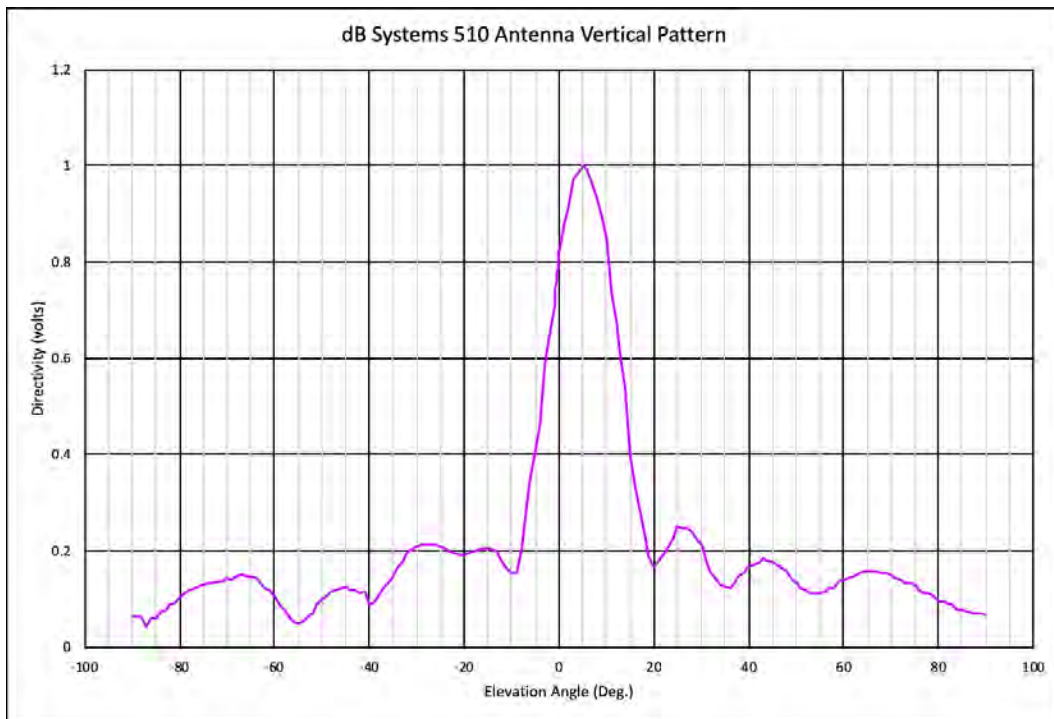


Figure D-5. dBs 510A Directivity vs. Elevation Angle

a) Signal Fading Performance

A detailed DME signal fading analysis was conducted by OU (Reference Z). Information regarding signal fading is also provided in Chapter 3 and Chapter 4 of this Order. These sections describe how multipath can cause constructive (in-phase) and destructive (out-of-phase) interference. Figure D-6 shows best-case and worst-case fading effects using typical earth surface conditions for the dBs 510A DME antenna.

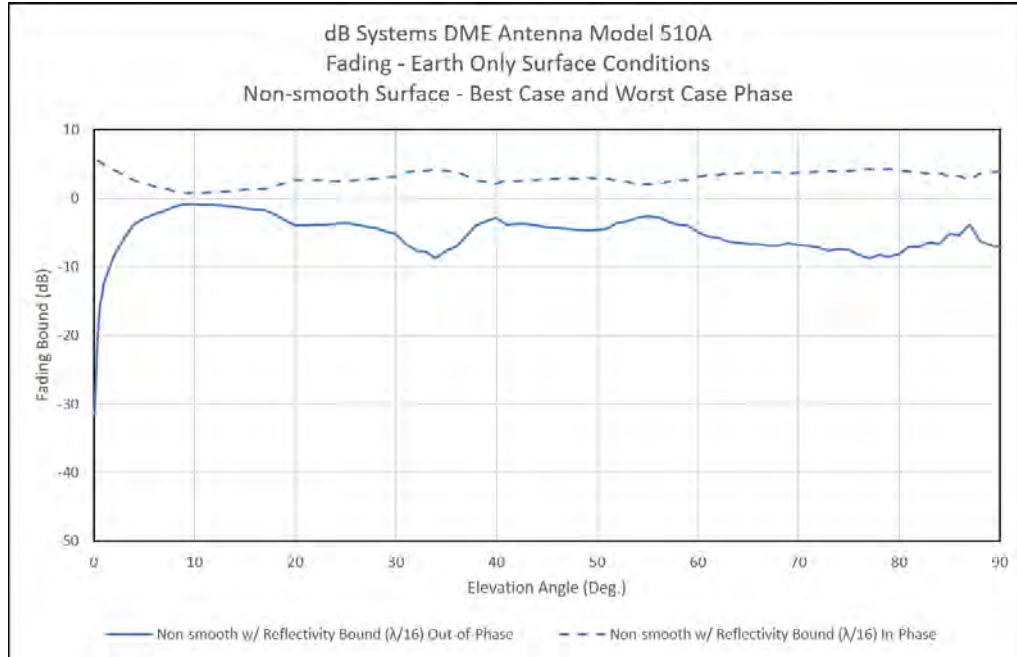


Figure D-6. dBs Antenna Model 510A Fading Analysis

- ii. **Horizontal Patterns.** The dBs 510A DME antenna model is available in omni-directional, uni-directional, and bi-directional horizontal patterns. Refer to the annotated horizontal patterns of Figure 4-2, Figure 4-3, and Figure 4-4 to understand the key terms and performance characteristics used with antenna horizontal patterns. These terms and characteristics can be used to compare differences among DME antennas. The antenna horizontal pattern specifications listed below are taken from the manufacturer product specification sheet. The specification sheet as well as additional information can be found at <https://www.dbsant.com/antenna-type/dme-antenna/>.

The important characteristics of the dBs 510A horizontal pattern are:

1. Omni-directional: Circularity of ± 1 dB max on the horizon.
2. Uni-directional: Available with 90° nominal beam width (i.e., HPBW).
3. Bi-directional: Available with 50° nominal beam width (i.e., HPBW).

- e. **dB Systems 540.** The dB Systems, Inc. 540 DME antenna utilizes a collinear 16 element dipole phased array that provides main lobe gain >12 dB, and horizon gain of 9 dB. This antenna is only available in an omni-directional horizontal pattern.

The dBs 540 antenna handles an input power up to 5,000W at 3% pulse duty cycle and operates over the entire frequency range with an input impedance of 50 ohms and VSWR of less than 2:1. The antenna provides vertically polarized coverage with the main beam tilted 2° upward to minimize ground reflections (longitudinal multipath).

Table D-9 lists the physical and electrical characteristics of the dBs 540 antenna model.

Table D-9. Characteristics of the dBs Antenna Model - dBs 540

Antenna	Type	Electrical Characteristics									Physical Characteristics						
		Circularity	Freq Range	Power Handling Capability	Polarization	Impedance	VSWR	Gain Main Beam	Gain Horizon	Main Beam Elevation Location	Array	Monitor Ports	Size (inches)	Weight (lbs.)	Radome Size (inches)	Deicing	Environmental
dBs 540	Omni-Directional	± 1 dB max on the horizon	960-1215 MHz	Up to 5 KW peak RF power at 3% duty cycle	Vertical	50Ω	Not greater than 2:1	>12 dB/iso	9 dB/iso	Between 2° ± 1° above horizon	16 active radiator assemblies with RF choke assemblies on each end	Optional; 2	137	30	3.25 diameter	No	Meets FAA-G-2100 (common outdoor operating conditions), and FAA-E-2754

- i. **Vertical Pattern.** The dBs 540 DME antenna model has a vertical pattern shown in Figure D-7. Refer to the annotated vertical pattern of Figure 4-1 to understand the key terms and performance characteristics used with antenna vertical patterns. These terms and characteristics can be used to compare differences among DME antennas. The antenna vertical pattern specifications listed below is taken from the manufacturer product specification sheet. The specification sheet as well as additional information can be found at <https://www.dbsant.com/antenna-type/dme-antenna/>.

The important characteristics of the dBs 540 vertical pattern are:

1. The peak gain: Approximately 2° above the horizon.
2. Width of primary lobe: The width of the primary lobe is not less than 4° at the half-power points.
3. Gain at horizon: The gain at horizon is greater than 6 dB below the peak gain.
4. Slope at horizon: The radiation pattern slope at the horizon influences the fading performance at very low elevation angles. A steeper slope will give an improved multipath to direct ratio. The slope for this antenna is 2 dB/° (0.1v/v/°) minimum.

5. Sidelobes below horizon: The power gain between 10° and 30° below horizon is lower than the power gain at the peak of the major lobe by at least 12 dB.
6. Shoulders: The power gain between 6° and 40° above horizon does not pass below a straight line joining the points of co-ordinates (+6°, -15 dB) and (+40°, -25 dB) with values referenced to the peak of the major lobe above its horizon.

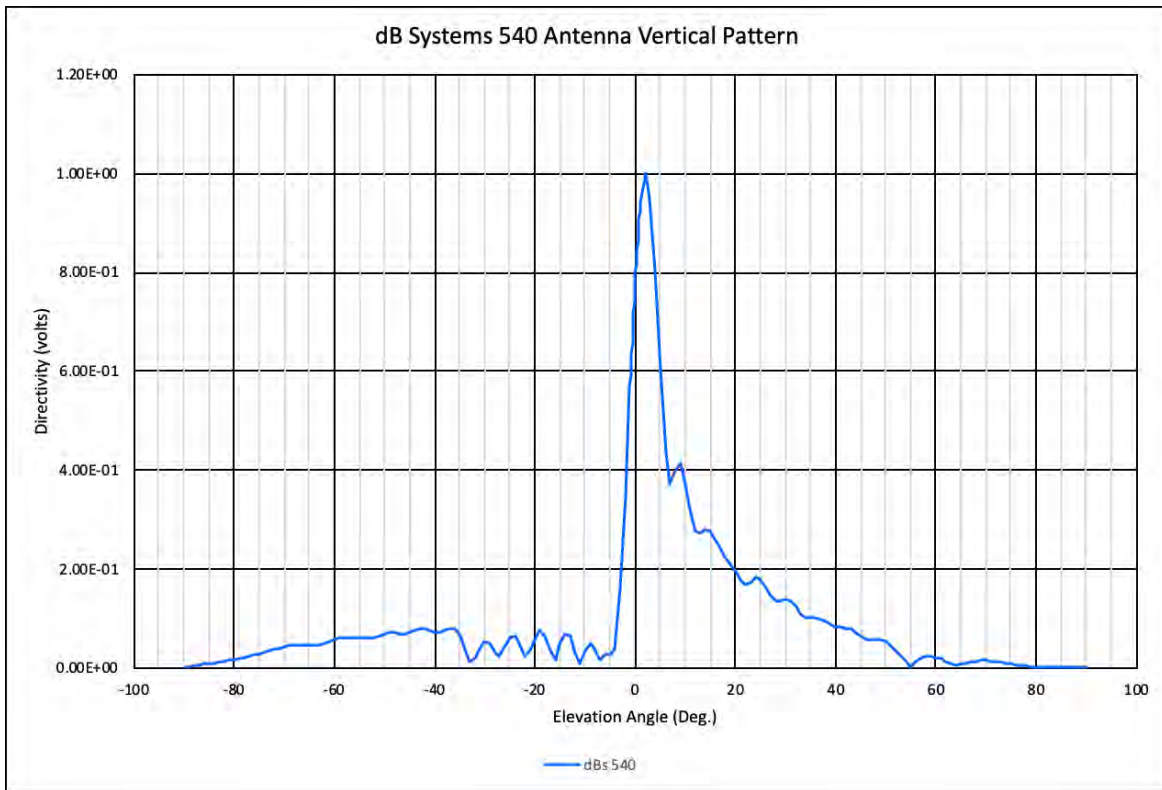


Figure D-7. dBs 540 Directivity vs. Elevation Angle

a) Signal Fading Performance

A detailed DME signal fading analysis was conducted by OU (Reference Z). Information regarding signal fading is also provided in Chapter 3 and Chapter 4 of this Order. These sections describe how multipath can cause constructive (in-phase) and destructive (out-of-phase) interference. Figure D-8 shows best-case and worst-case fading effects using typical earth surface conditions for the dBs 540 DME antenna.

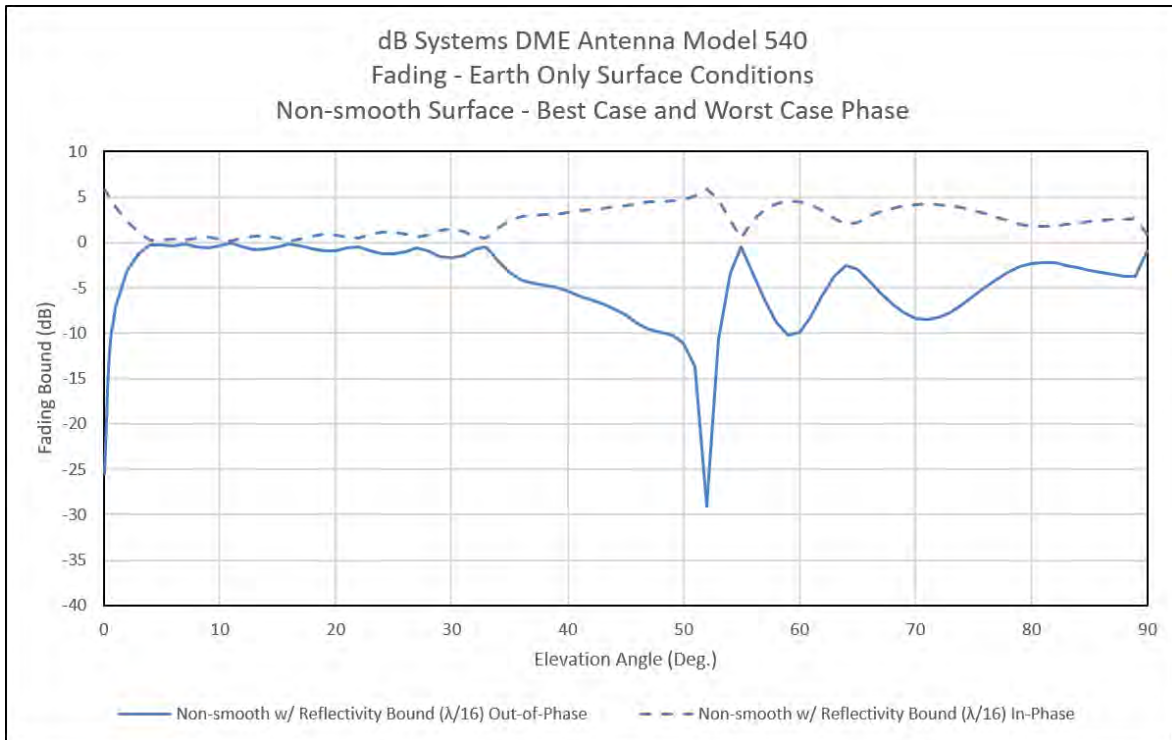


Figure D-8. dBs Antenna Model 540 Fading Analysis

- ii. **Horizontal Patterns.** The dBs 540 DME antenna model is only available in an omni-directional horizontal pattern. Refer to the annotated horizontal pattern of Figure 4-2 to understand the key terms and performance characteristics used with antenna horizontal patterns. These terms and characteristics can be used to compare differences among DME antennas. The antenna horizontal pattern specifications listed below are taken from the manufacturer product specification sheet. The specification sheet as well as additional information can be found at <https://www.dbsant.com/antenna-type/dme-antenna/>.

The important characteristic of the dBs 540 horizontal pattern is:

1. Omni-directional: circularity of ± 1 dB max on the horizon.

- f. **dB System 900E DME.** As mentioned in the overview section above, a study was performed to characterize the signal attenuation (i.e., worst-case) or amplification (i.e., best-case) that can occur due to reflection of the DME radiated signal by the ground. During this study, the fading performance of the dB Systems Model 900E TACAN central array was characterized because it is a real antenna design having vertical pattern characteristics that provide significant resistance to signal fading caused by ground reflections. That is, the awareness of such resilient performance from a realizable antenna is noteworthy. In this case, it was envisioned that the dBs 900E TACAN central array would then be housed in a conventional DME

antenna radome and that the same methods used to generate uni-directional and bi-directional horizontal patterns could be applied in this case as well.

The dBs 900E DME antenna utilizes a collinear 14 element cylindrical dipole phased array that provides main lobe gain >9 dB, and horizon gain of >3 dB.

The dBs 900E antenna handles an input power up to 5,000 W at 4% pulse duty cycle and operates over the entire frequency range with an input impedance of 50 ohms and VSWR of less than 1.8:1. The antennas provide vertically polarized coverage with the main beam tilted approximately 7° upward.

Table D-10 lists the physical and electrical characteristics of the dBs 900E antenna model.

Table D-10. Characteristics of the dBs Antenna Model - dBs 900E

Antenna	Type	Electrical Characteristics									Physical Characteristics						
		Circularity	Freq Range	Power Handling Capability	Polarization	Impedance	VSWR	Gain Main Beam	Gain Horizon	Main Beam Elevation Location	Array	Monitor Ports	Size (inches)	Weight (lbs.)	Radome Size (inches)	Deicing	Environmental
dBs 900E	TACAN, High Vertical Aperture	N/A	1X - 126X; 1Y - 126Y; 962 - 1213 MHz	Up to 5 KW peak RF power at 4% duty cycle (200W Average)	Vertical	50Ω	Not greater than 1.8:1	≥ 9 dB/iso	≥ 3 dB/iso	Between 5° to 7° above horizon, typically 7°	14 Element, Co-linear, cylindrical Dipole Array	Yes	118	600	36 diameter	No	Meets FAA-G-2100 (common outdoor operating conditions), and FAA-E-2754

- i. **Vertical Pattern.** The dBs 900E DME antenna model has a vertical pattern shown in Figure D-9. Refer to the annotated vertical pattern of Figure 4-1 to understand the key terms and performance characteristics used with antenna vertical patterns. These terms and characteristics can be used to compare differences among DME antennas. The antenna vertical pattern specifications listed below came from the manufacturer product specification sheet. The specification sheet as well as additional information can be found at <https://www.dbsant.com/antenna-type/tacan-antennas/>.

The important characteristics of the dBs 900E vertical pattern are:

1. The peak gain: Between 5° and 7° above the horizon.
2. Width of primary lobe: The width of the primary lobe is not less than 5° at the half-power points, per FAA-E-2828a.
3. Gain at horizon: The gain at horizon is greater than 6 dB below the peak gain.
4. Slope at horizon: The radiation pattern slope at the horizon influences the fading performance at very low elevation angles. A steeper slope will give an improved multipath to direct ratio. The specification sheet says the slope for this antenna is $\geq (0.2v/v^\circ)$ minimum.
5. Sidelobes below horizon: The power gain between 10° and 50° below horizon is lower than the power gain at the peak of the major lobe by at least 16 dB.
6. Shoulders: The power gain between 6° and 20° above horizon shall be greater than a level which is 15 dB below the power gain at the peak of the major lobe above its horizon. The power gain between 20° and 50° above horizon shall be greater than a level which is 25 dB below the power gain at the peak of the major lobe above its horizon.

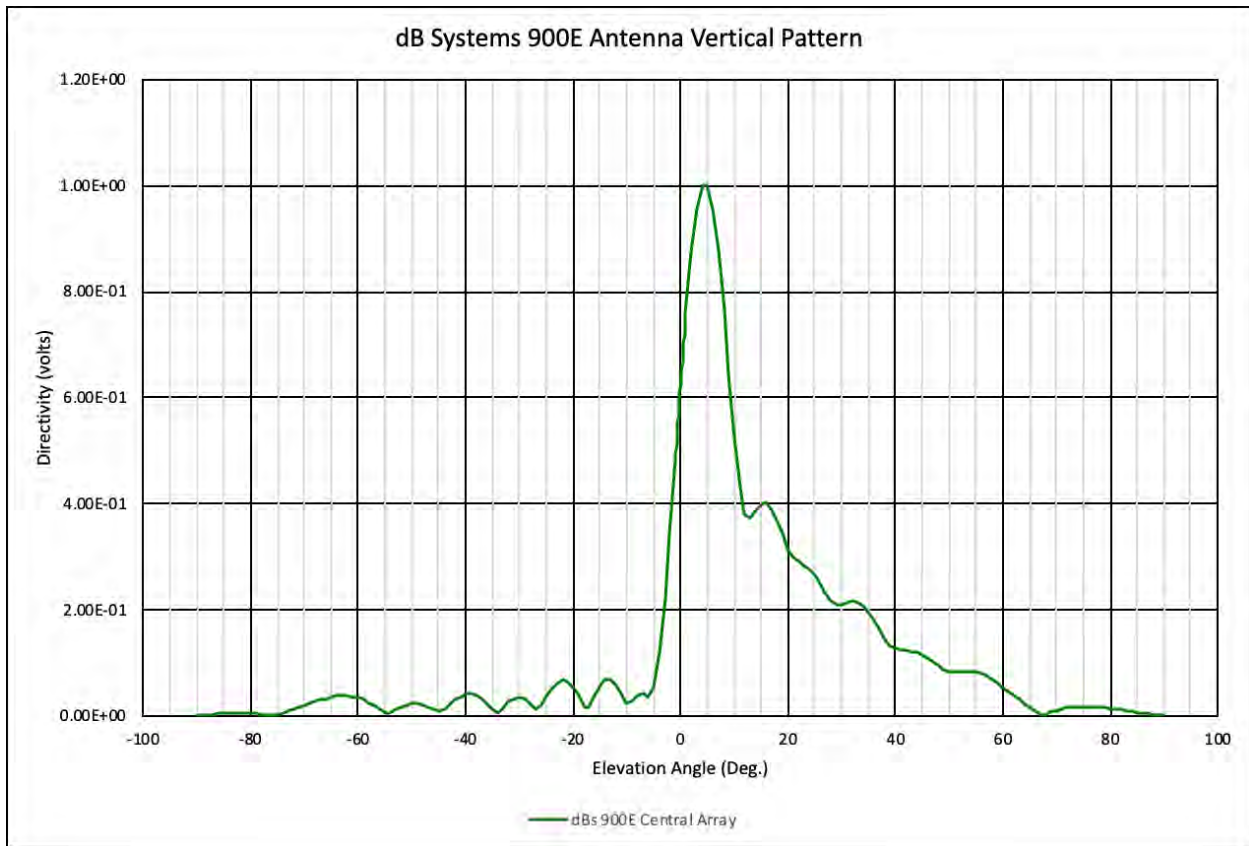


Figure D-9. dBs 900E Directivity vs. Elevation Angle

a) Signal Fading Performance

A detailed DME signal fading analysis was conducted by OU (Reference Z). Information regarding signal fading is also provided in Chapter 3 and Chapter 4 of

this Order. These sections describe how multipath can cause constructive (in-phase) and destructive (out-of-phase) interference. Figure D-10 shows best-case and worst-case fading effects using typical earth surface conditions for the dBs 900E antenna.

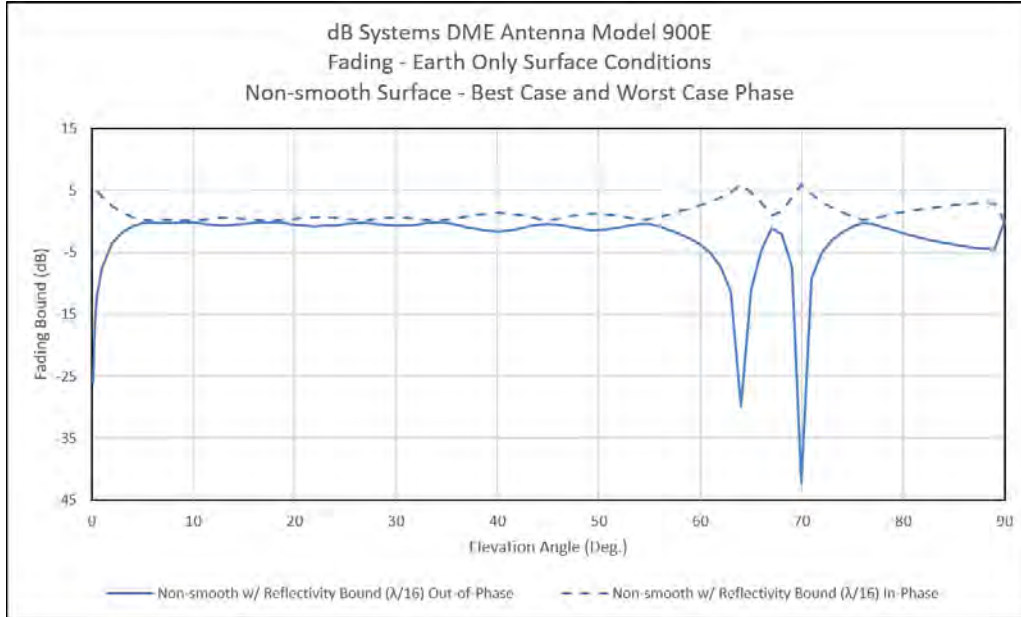


Figure D-10. dBs Antenna Model 900E Fading Analysis

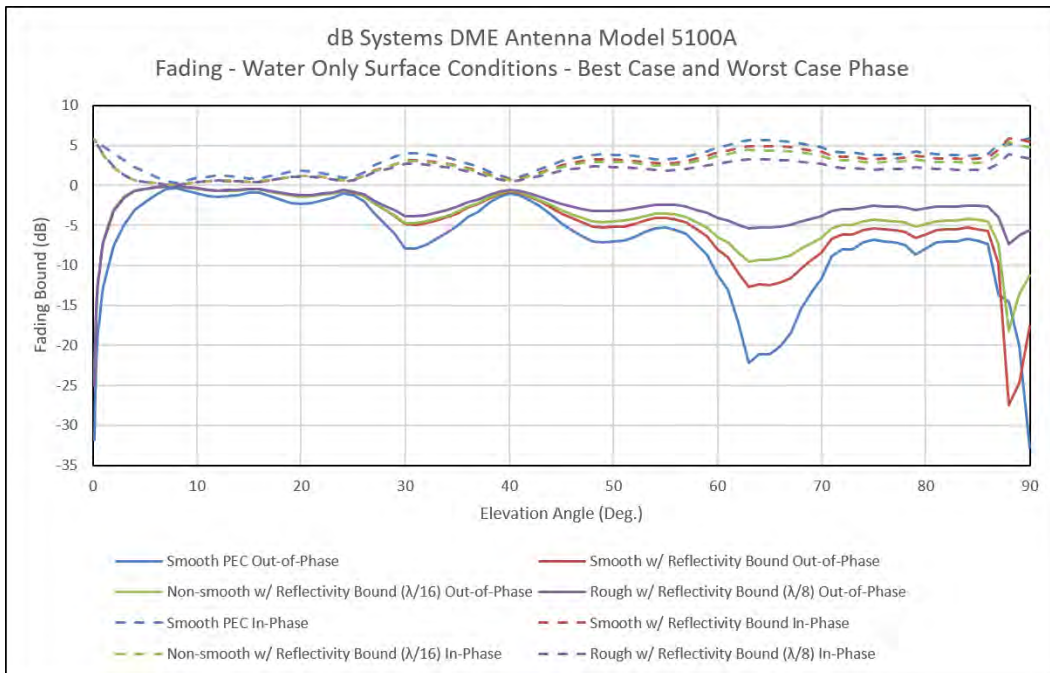
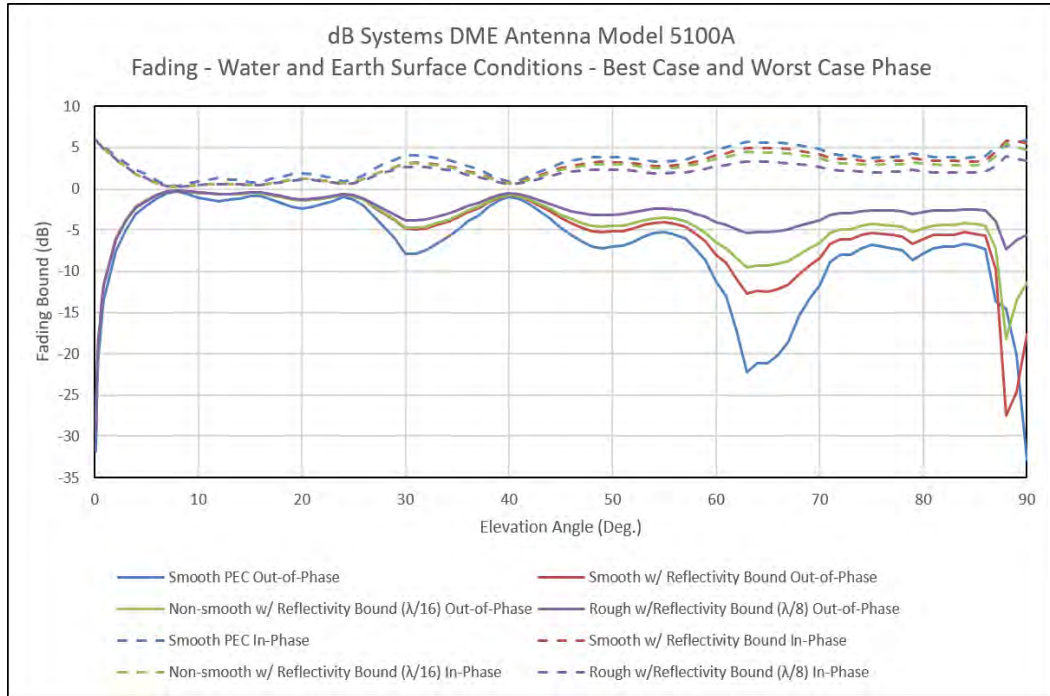
- ii. **Horizontal Patterns.** As previously noted, the dBs 900E DME antenna model could be manufactured to provide omni-directional, uni-directional, and bi-directional horizontal patterns. Refer to the annotated horizontal patterns of Figure 4-2, Figure 4-3, and Figure 4-4 to understand the key terms and performance characteristics used with antenna horizontal patterns. These terms and characteristics can be used to compare differences among DME antennas. The antenna horizontal pattern specifications listed below came from the manufacturer product specification sheet. The specification sheet as well as additional information can be found at <https://www.dbsant.com/antenna-type/tacan-antennas/>.

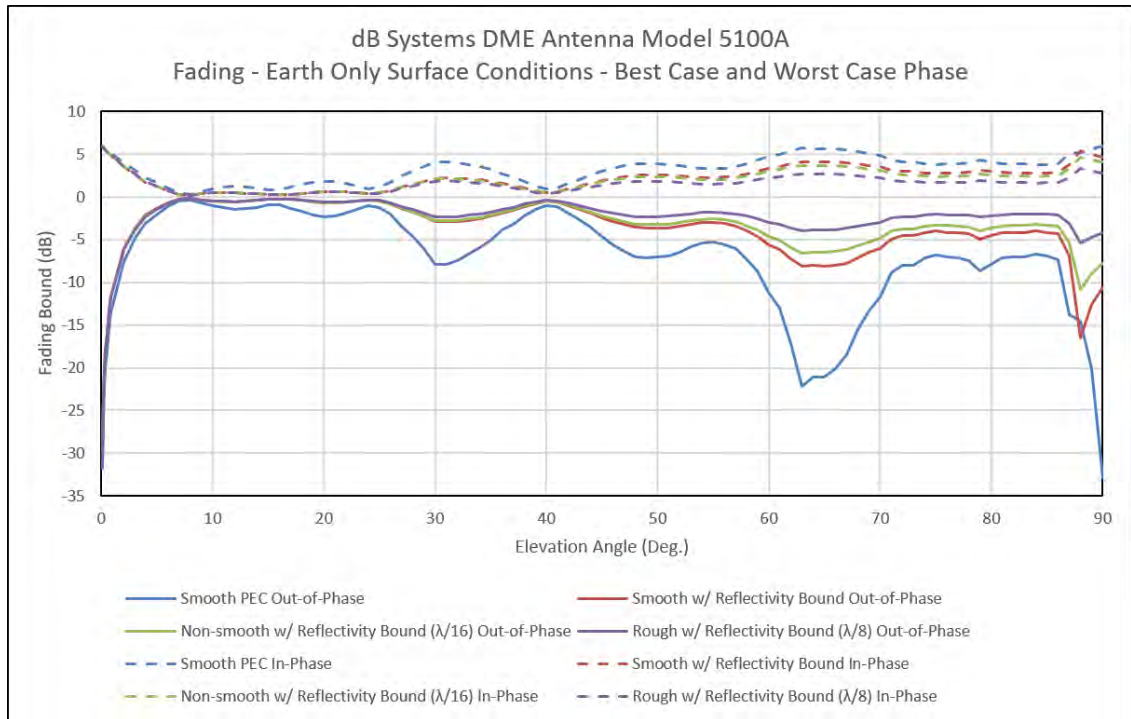
The important characteristic of the dBs 900E horizontal pattern is:

1. **Omni-directional:** Based on the actual performance of the dBs 900E TACAN antenna central array, the power density measured over all azimuth angles shall not vary by more than ± 1 dB, per FAA-E-2828a.

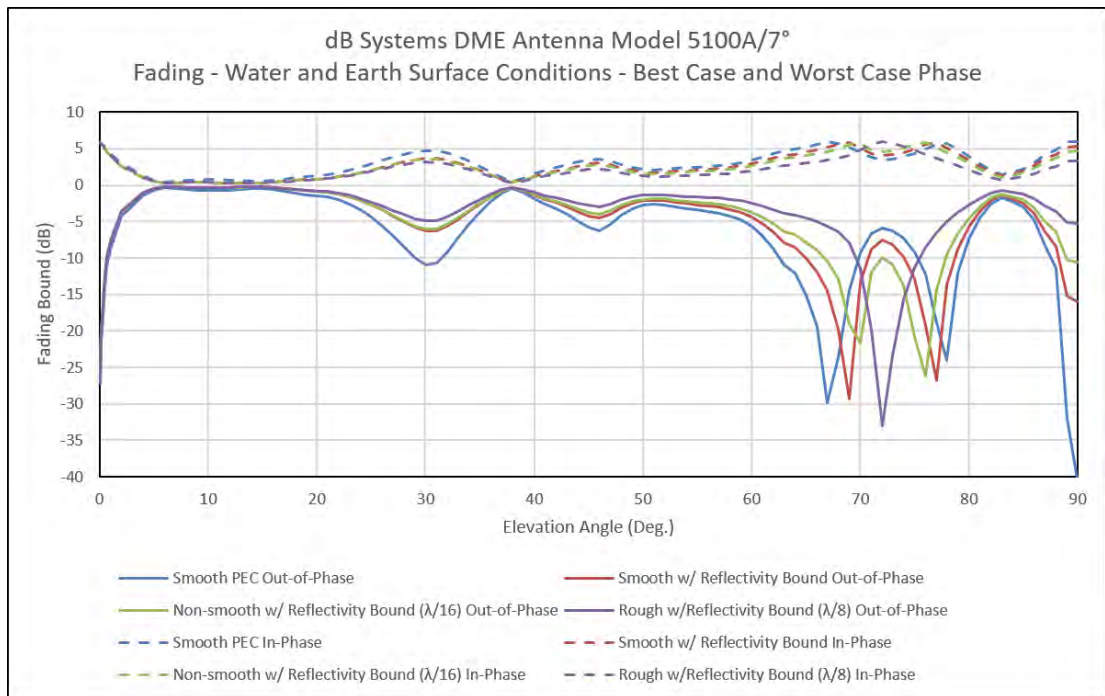
ATTACHMENT
AVAILABLE FADING DATA PLOTS

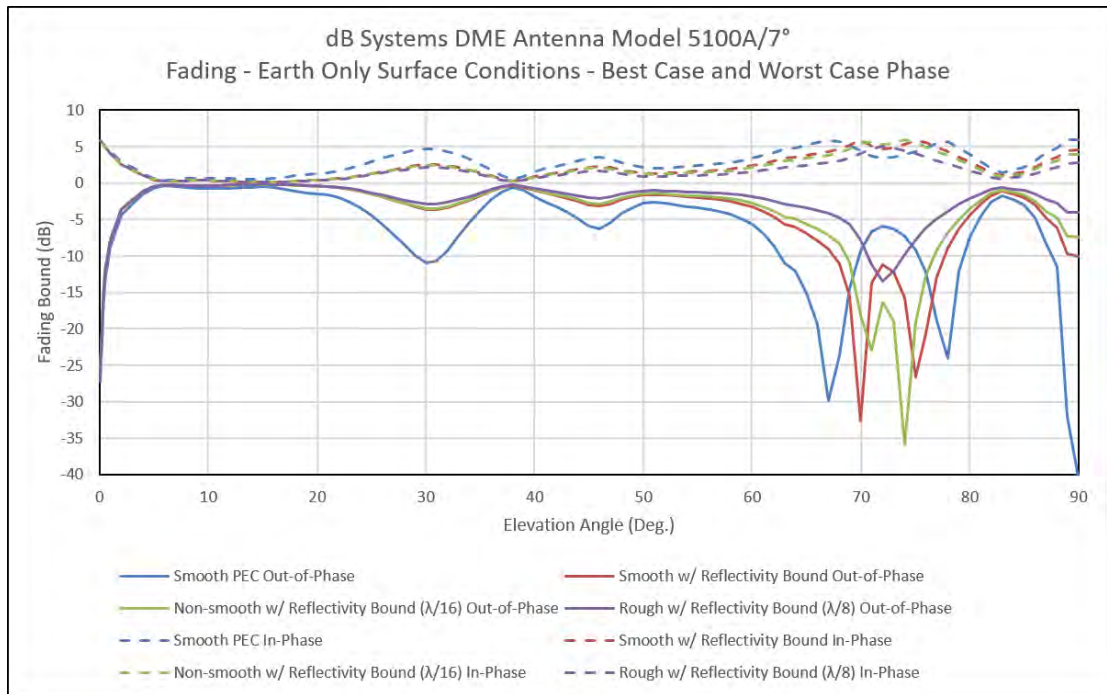
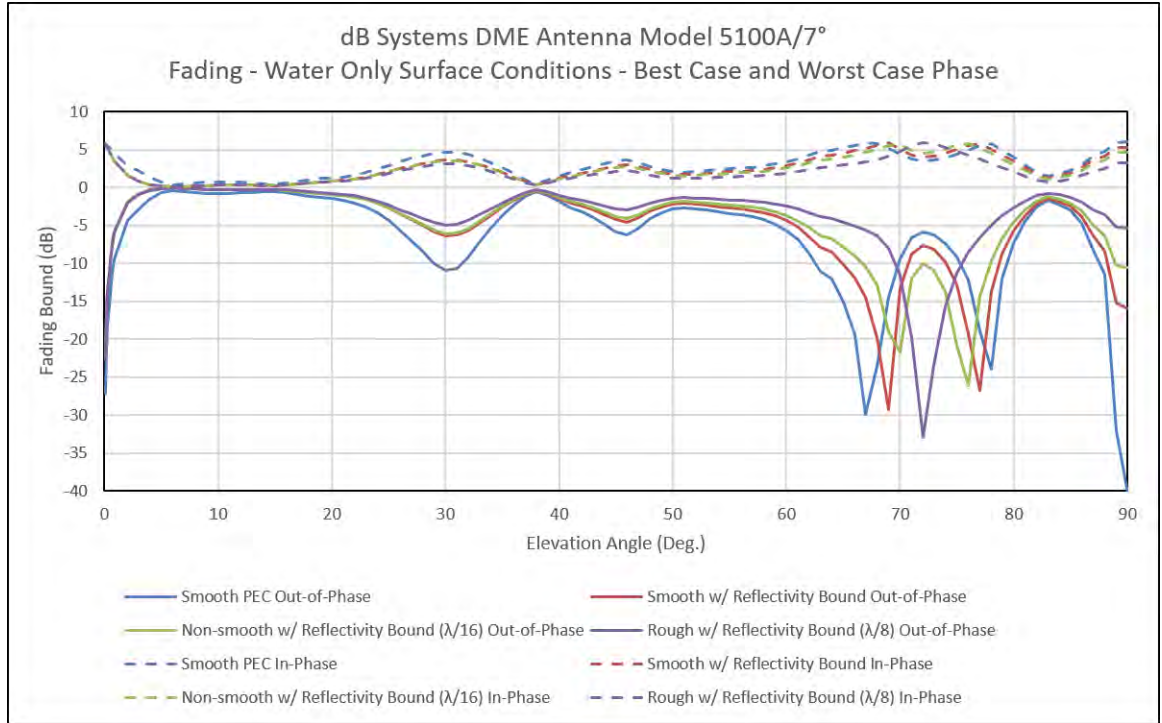
1. dBs 5100A



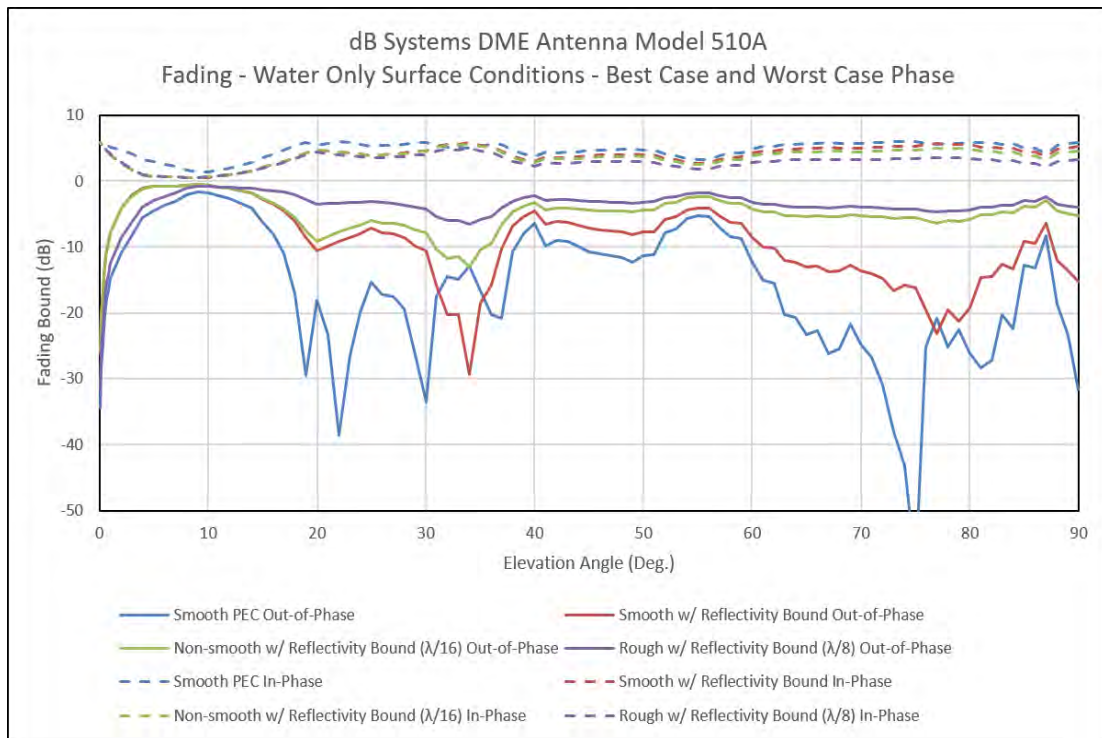
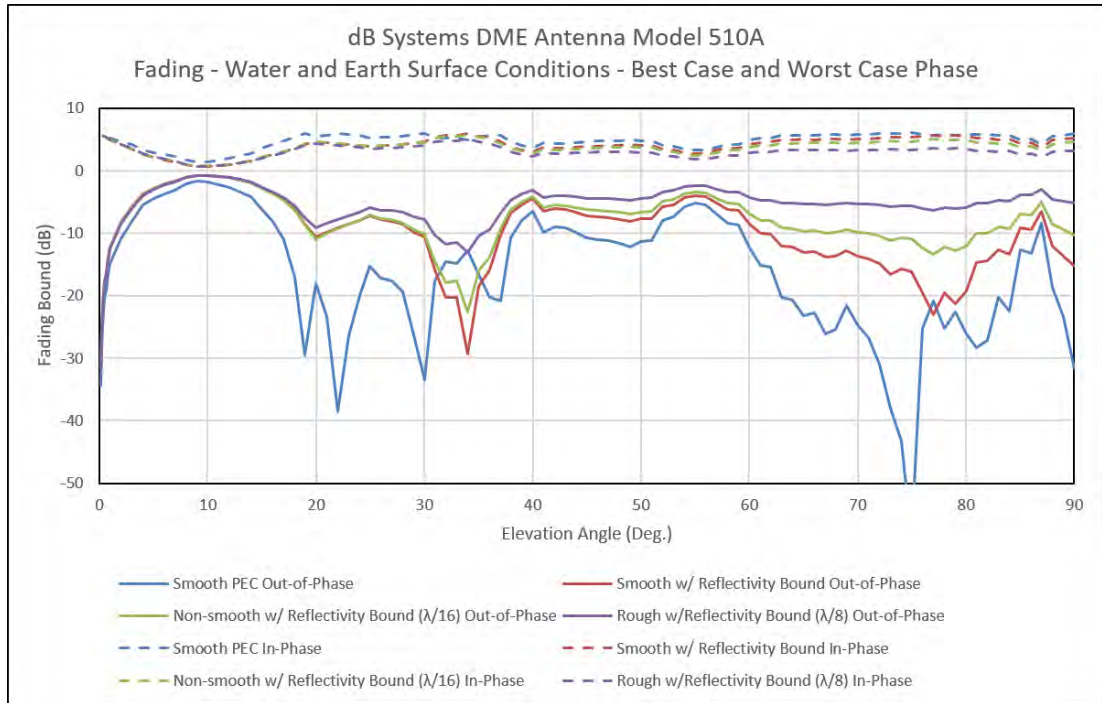


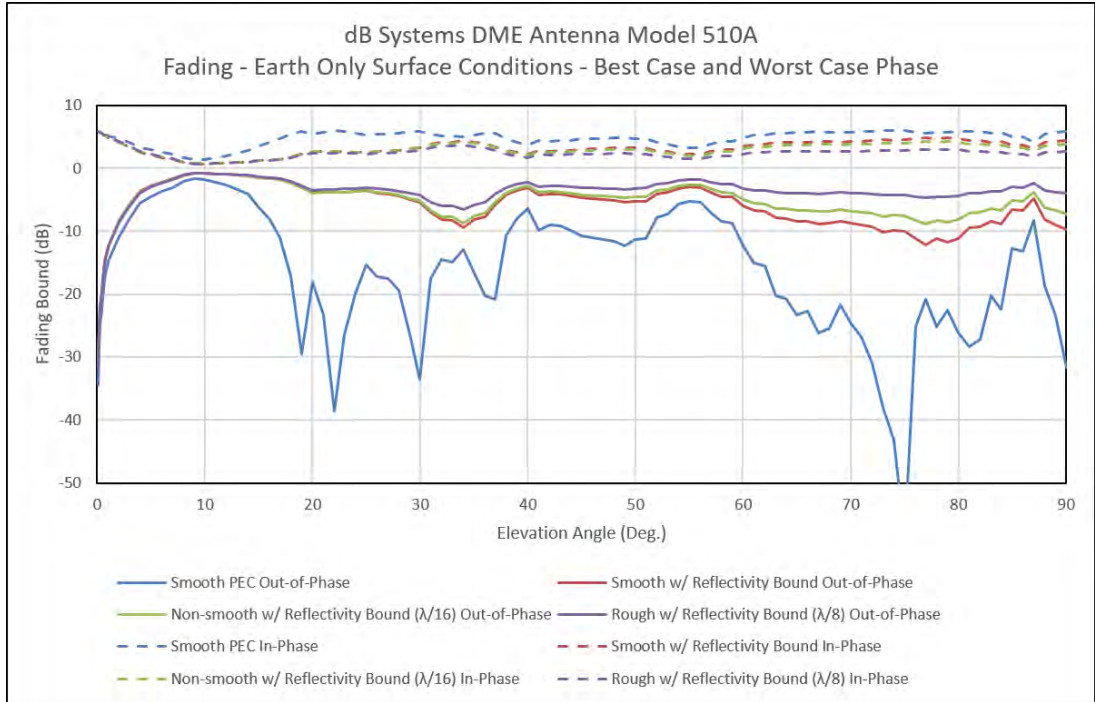
2. dBs 5100A/7°



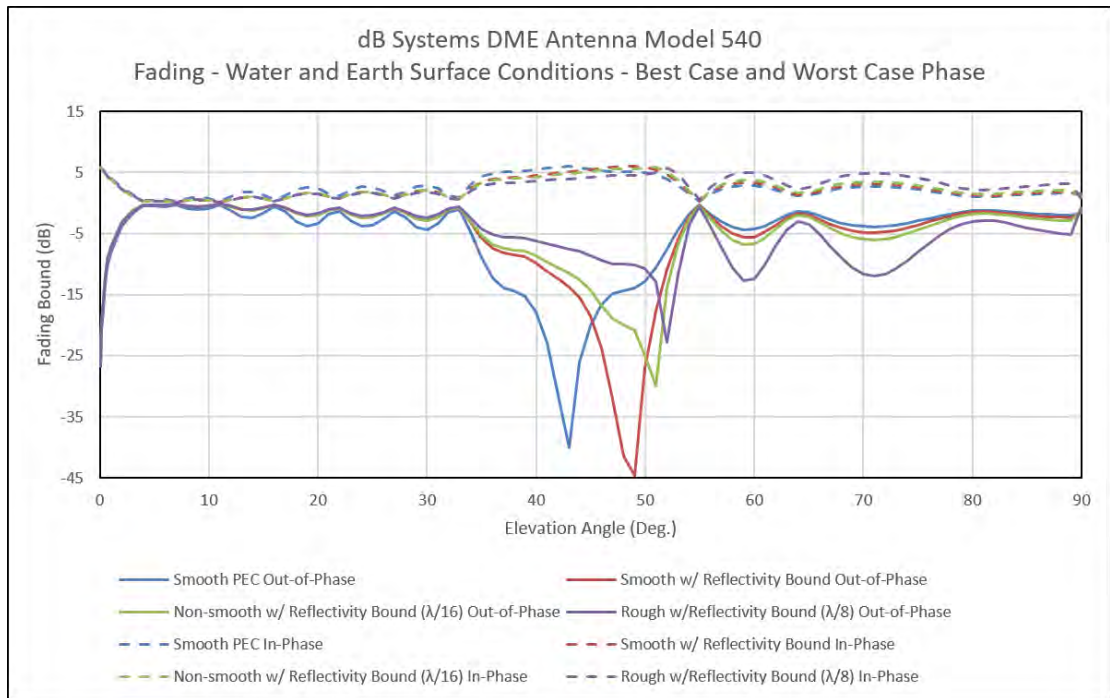


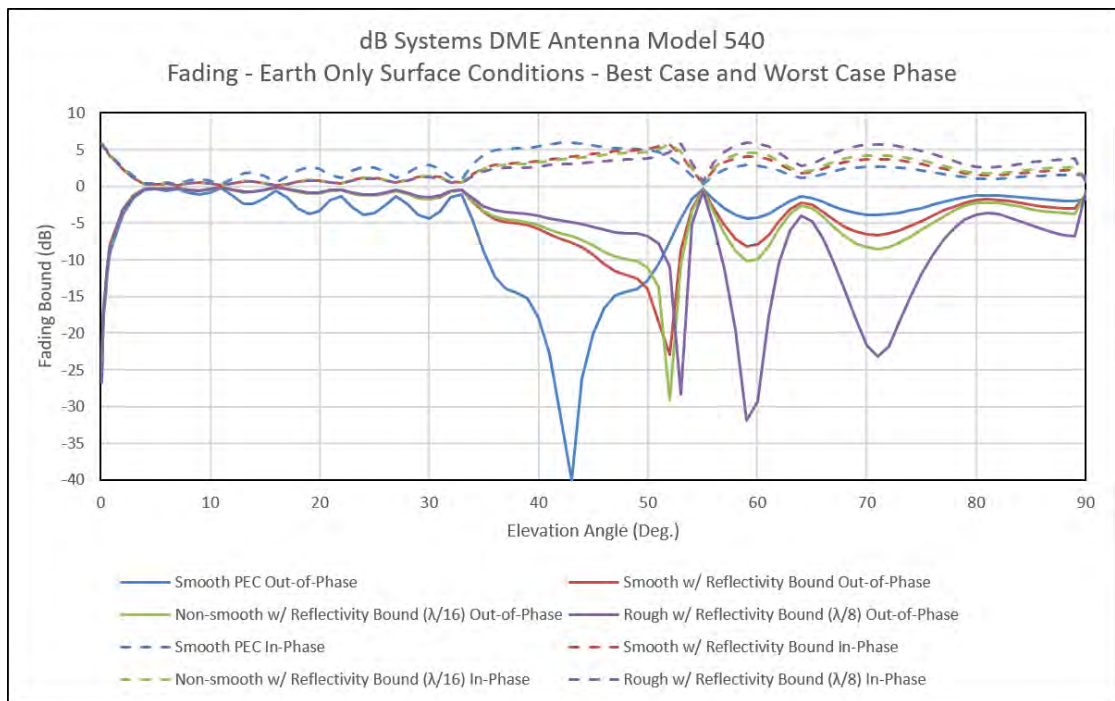
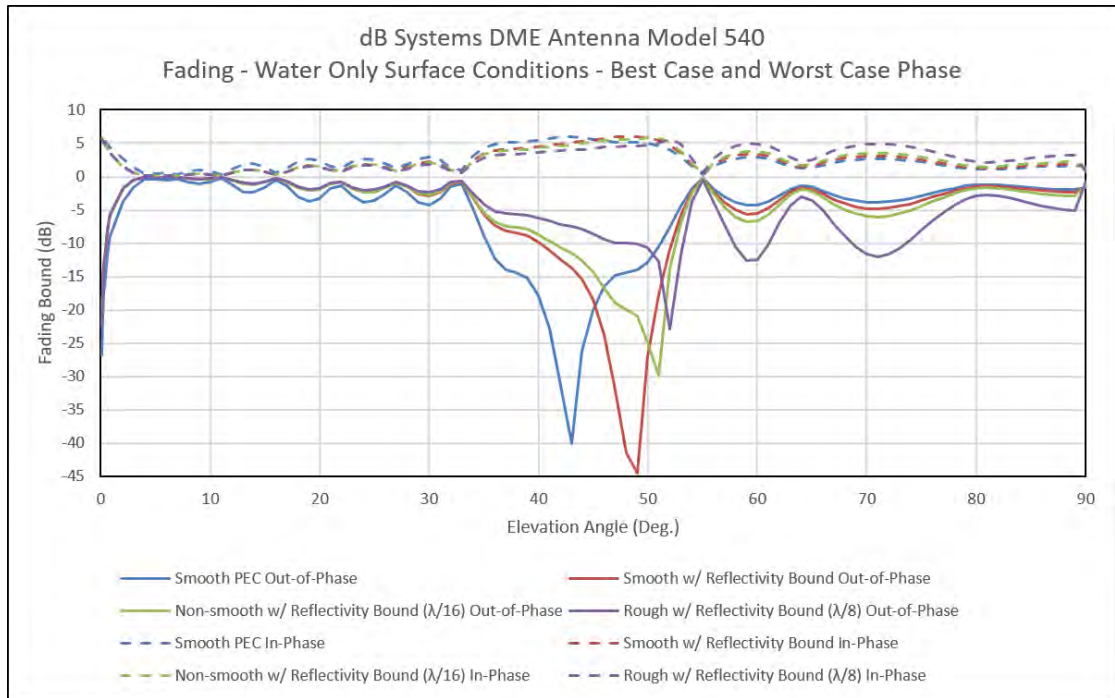
3. dBs 510A



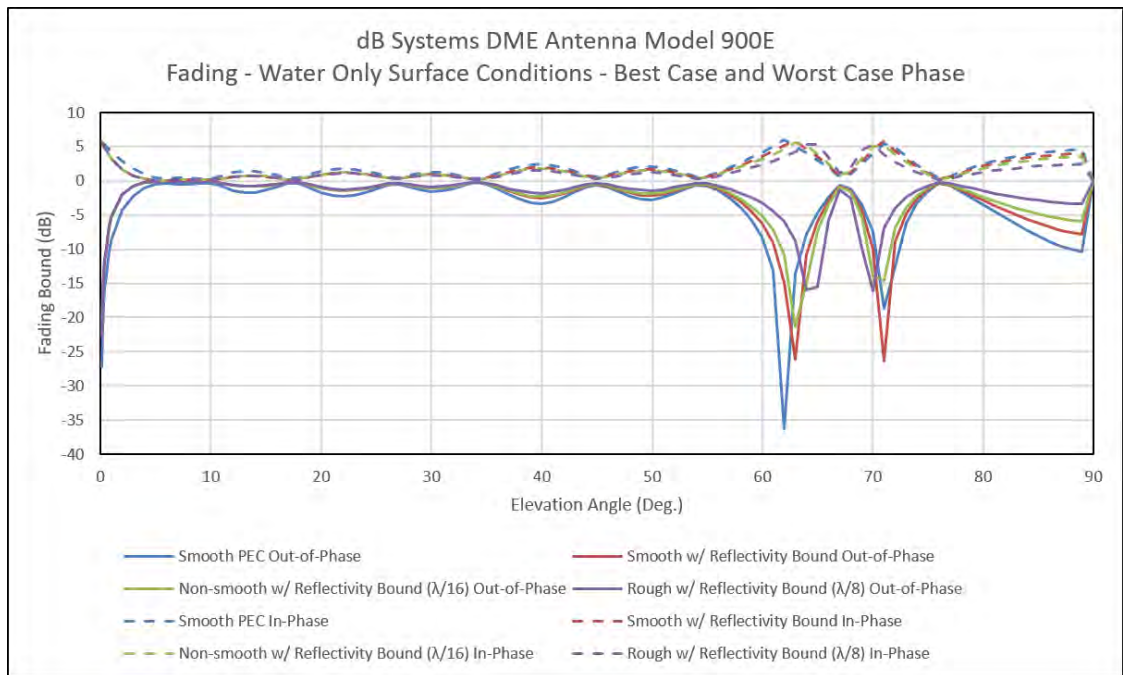
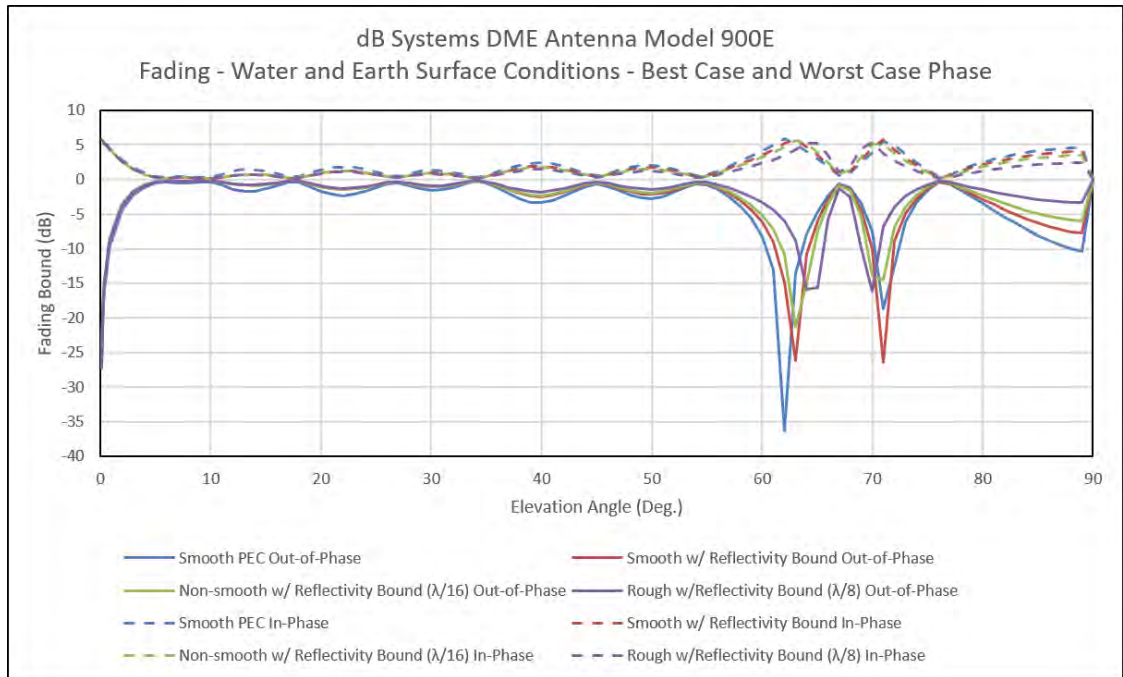


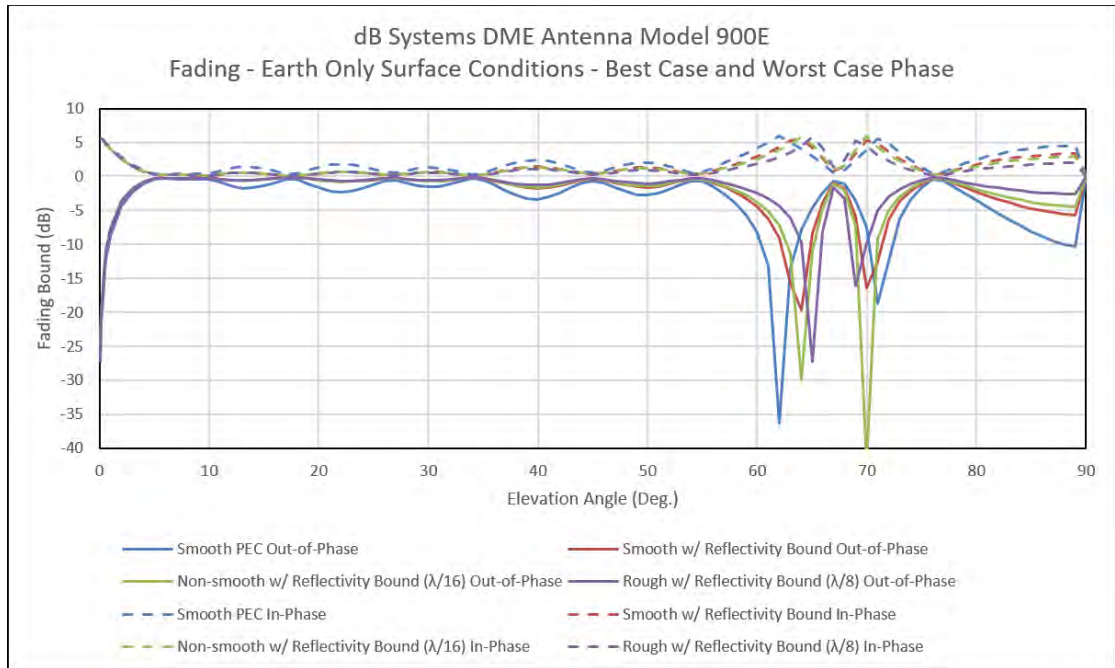
4. dBs 540





5. dBs 900E





Appendix E. Echo Location

1. Introduction

The DME Siting Order is expected to primarily be used during the initial siting of a new facility. It may also be used when proposed changes to a facility are being planned. Using the guidelines of the Order, Signal-in-Space (SIS) analysis is expected to result in one of three outcomes:

1. The site meets the most basic siting requirements and installation is approved;
2. Some of the basic requirements are not met and a more rigorous analysis is conducted; or
3. Analysis determines the site is not acceptable.

The analysis is based on observations of the environment around the site. Even the best effort to identify possible multipath reflecting objects is likely to occasionally miss a significant object, or the analysis did not correctly identify the impact. At challenging sites, a temporary DME may also be installed to “test” coverage. Subsequent flights by Flight Inspection (FI) or pilots may indicate problems. Common problems are lack of signal strength, dropped track, or range error. Lack of signal strength is most commonly due to signals being attenuated or blocked. Dropped track is generally caused by multipath or lack of signal strength. Smaller range errors are due to multipath, while larger range errors are caused by a combination of multipath with the direct path being blocked.

The technique described in this appendix can be used to identify the location of reflecting surfaces that can cause multipath. It does not take into account the actual Radio Frequency (RF) propagation effects. Refer to Chapter 3 and Appendix C of this Order to find more details on RF propagation and the complexities of multipath.

2. Background

Other sections of this document describe the technical information needed to understand how various objects, conditions, and signal propagation may impact a proposed installation. Important in that analysis is to determine the magnitude of any issues, and if the magnitude of the problem is large enough to be a concern. The purpose of this appendix is to provide techniques that can be applied to identify the cause of an unexpected error or gap in signal coverage observed during a flight test or inspection. In order to locate the multipath source, it is important to have a basic understanding of multipath.

There are two types of multipath: longitudinal and lateral. Longitudinal multipath occurs along the path from transmitter to aircraft. It causes an expected effect called fading and produces vertical nulls in the antenna radiation. The reflecting source is generally the counterpoise and/or the earth surface surrounding the facility. Since the direct and reflected path lengths are similar, ranging errors tend to be small and operationally insignificant. See discussion regarding multipath in Chapter 4 (Figure 4-31).

Lateral multipath occurs when the transmitted signal is reflected by an object. Figure E-1 below shows the basic concept. The object may be man-made (e.g., a building) or natural

(e.g., terrain). The direct path signal will always be received at the aircraft before the reflected signal. It is possible the direct signal will be attenuated or blocked and only the reflected signal received in certain areas. The reflecting surface must be illuminated by a signal from the transmitter, the angle of the reflecting object must be correct, and the path from the reflector to the receiver must be clear. It is possible both types of multipath will exist at the same time.

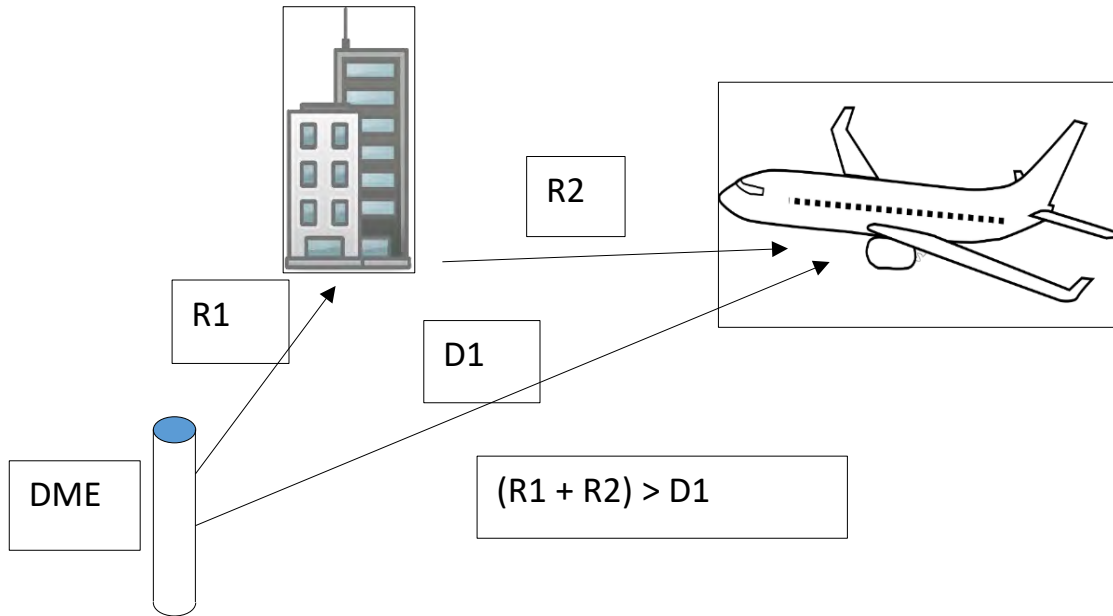


Figure E-1. Multipath Overview

Effects of multipath are dependent on actual multipath delays. Figure E-2 below shows several delay ranges. Ideal pulse-pairs are shown to explain general concepts. In real world observations, the direct path signal and multipath pulse-pairs will be combined based on delay, phase, and relative amplitudes. The combined pulses may not even look like a DME pulse. Waveform “Original” is a typical pulse-pair and represents the direct path signal.

Waveform “Delay 1” shows a multipath delay which causes the multipath pulse-pair to overlap the direct pulse-pair. The overlap occurs on both the first and second pulse of the pair. Depending on the actual delay, phase, and relative amplitudes, it is possible to distort the combined pulses such that the receiver determines it is not a valid pulse or creates a timing error.

Waveform “Delay 2” shows the first pulse of multipath pulse-pair occurring between the first and second pulse of the direct pulse-pair. The second pulse of the multipath pulse-pair occurs after the second pulse of the direct pulse-pair. Waveform “Delay 4” is similar to “Delay 2” except the first pulse of multipath pulse-pair now occurs after the second pulse of the direct pulse-pair. In each case, the multipath has no impact on proper DME operation.

Waveform “Delay 3” shows the first pulse of the multipath pulse-pair occurring during the second pair of the direct pulse-pair. Like “Delay 1”, the effect is a mixing of the two pulses. Airborne interrogators approved after 1989 must use the first pulse of the pair to determine range therefore it is not expected to cause a range error. It is still possible to distort the pulse so that it is not decoded as a valid pulse. If not decoded as a valid pulse, the pulse-pair will not be decoded. The pulse-pairs shown are for X-channel spacing of 12 μ s. If the DME is operating on Y-channel, pulse spacing will be 36 μ s and delays required to cause a problem will also change.

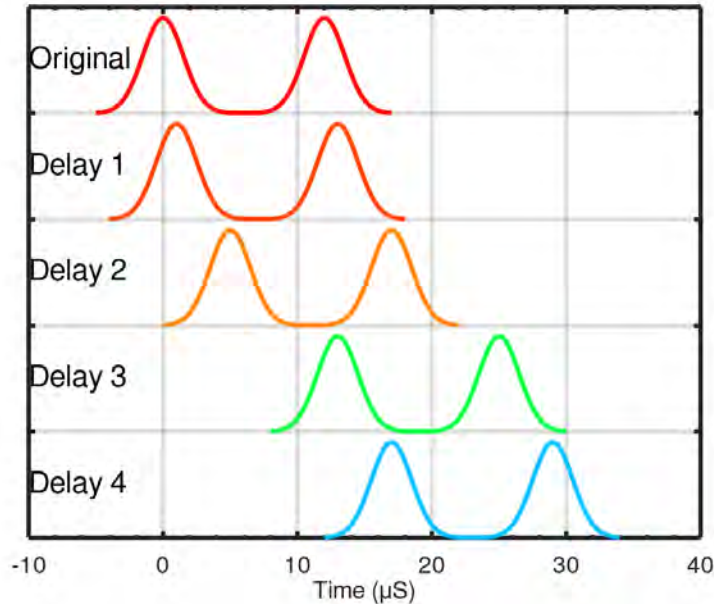


Figure E-2. Examples of Multipath Delay (Big Picture)

As mentioned above, combining the direct and multipath pulses can produce pulses that do not look like the typical DME pulse. Figure E-3 below shows two examples of a single pulse with multipath. The dashed line shows an ideal pulse. The dotted red line shows a multipath pulse which is delayed 4 μ s and attenuated below the direct pulse by 6.5 dB. The solid blue line is the resulting waveform when the two waveforms are combined. Figure E-3 shows the waveforms when signals are in-phase, and Figure E-4 shows out-of-phase. At DME frequencies, the wavelength is approximately 1 foot. Changing from in-phase to out-of-phase only requires a small change in the difference in propagation distances between the direct and delayed pulses.

It is important to understand that the combined pulse shape may be continually changing in the overlap region. Figure E-3 also shows how the width of the combined pulse at the half amplitude can be changed. For more details on the effect of multipath on pulse shape and processing impacts refer to Appendix C.

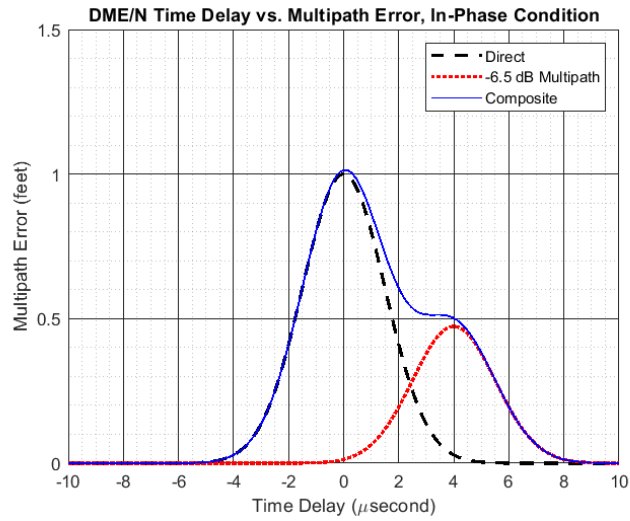


Figure E-3. Combined Pulse (In-phase)

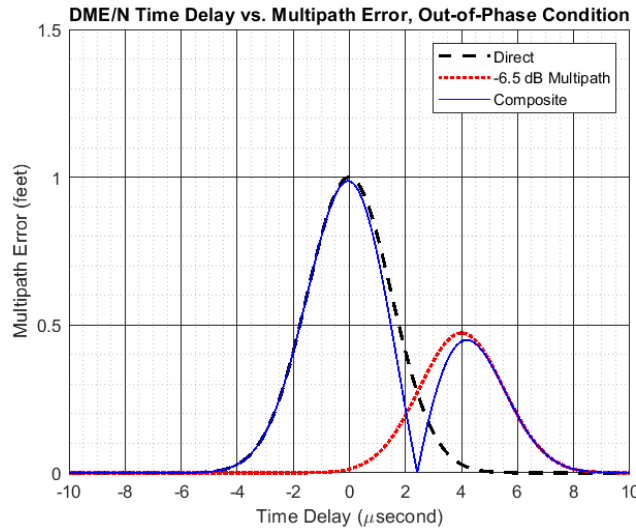


Figure E-4. Combined Pulse (Out-of-phase)

Multipath delay is generated by a difference in propagation path between the direct path and the reflected rays. An ellipsoid can be generated which defines all locations which satisfy the geometric locations that can produce the desired delay. The ellipsoid is often referred to as an echo ellipsoid. Only those points on the surface of the ellipsoid that intersect a reflecting surface are of interest. Terrain, earth curvature, and man-made structures need to be considered. Programs currently exist which are capable of defining the ellipsoidal surface in terms of latitude, longitude, and Mean Sea Level (MSL) altitude. The information is then used as an input to applications like Google Earth which are able to display the 3D surface on a terrain map.

Displaying the 3D ellipsoidal surface on a 2D surface requires the addition of many lines. These additional lines better define the shape, but also make it more difficult to identify

possible sources of reflections. It is possible to replace the ellipsoid (3D) with an ellipse (2D). Figure E-5 below shows a vertical plane through an ellipsoid. The ellipsoid is drawn such that the central axis goes through the transmitting antenna and aircraft. It is shown rotated in the vertical plane. Rotation is due to difference in transmitter antenna height and aircraft height. Height of the transmitting antenna is defined as the MSL elevation of the facility plus the antenna height above the facility elevation. Aircraft height is defined as MSL altitude.

A plane through the ellipsoid that also passes through the central axis will always be defined by an ellipse. The ellipse is defined by the same semi-major axis, semi-minor axis, and eccentricity of the ellipsoid. The curved line represents the vertical geodetic datum reference (i.e., 0 MSL). The irregular line represents the terrain defined in terms of MSL and is plotted with respect to the vertical datum reference. The solid vertical line shows the point where the ellipsoid no longer intersects with the terrain. The area to the right of the line shows the ellipsoid is above the terrain and unlikely to be the location of a reflector. It is still possible for very tall structures or lower structures on higher terrain to act as multipath reflectors. The area to the left of the line shows where a reflecting surface could cause multipath. In order to produce the desired delay, only those locations where the ellipsoid intersects the terrain are of interest. The dashed line is a slice through the ellipsoid which is perpendicular to the central axis of the ellipsoid. The box in the lower left corner shows this slice.

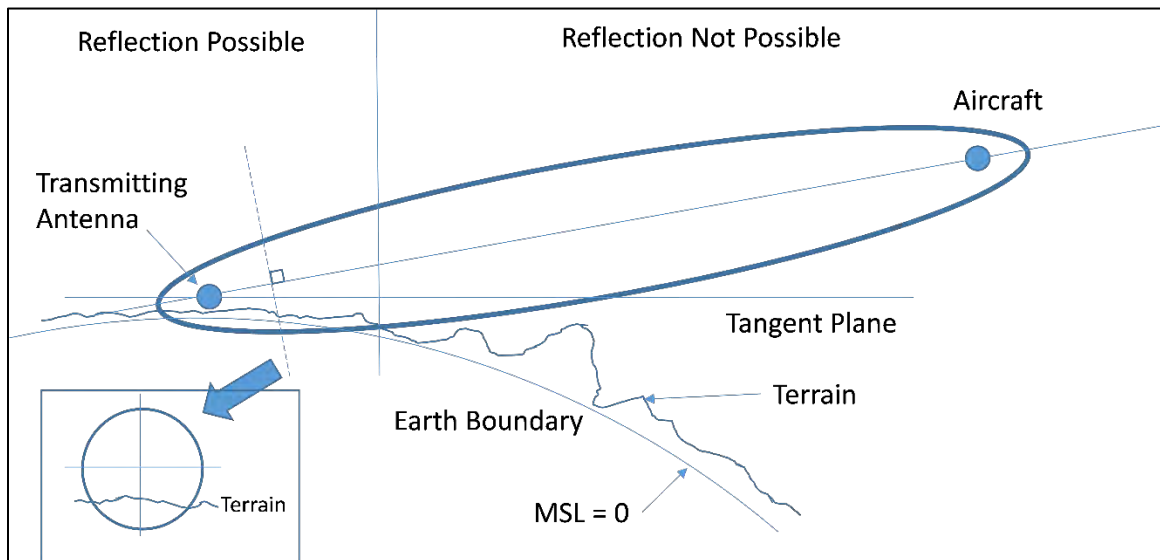


Figure E-5. Ellipsoid Overview

Figure E-6 below shows a slice through the ellipsoid (dashed line in the previous figure). The slice is perpendicular to the axis between the transmitter and aircraft and is circular. The size will vary as a function of location along the ellipsoid axis. In order for terrain or a man-made structure plus terrain to be a possible reflecting source it must be located on the circle. It is the only realizable point which will have the correct geometric relationship to produce the desired multipath delay. The point is represented by a blue star. The ellipse method will define the point of interest as the red star. If both points were plotted on a map,

the ellipse point would always be farther from the ellipse centerline than the ellipsoid point.

Changes in distance between the transmitter and aircraft plus vertical rotation of the ellipsoid will cause the difference to vary. In all cases, the ellipse method will contain the reflecting surface. The area shown in red is not likely to include a multipath reflector as it is expected to be above the surface of the earth.

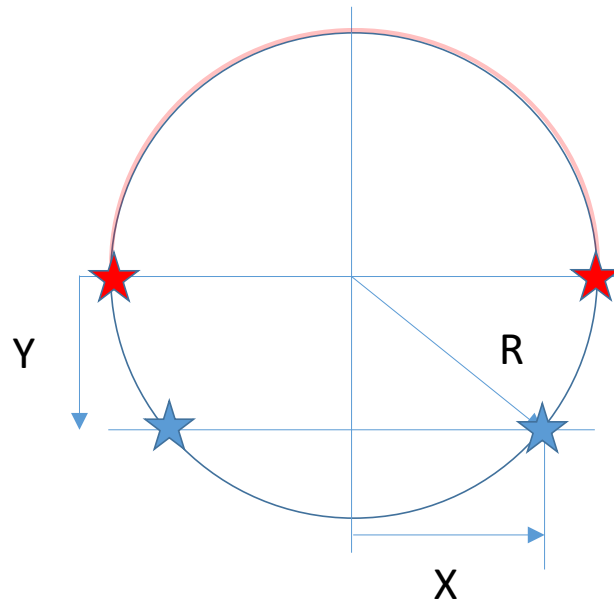


Figure E-6. Vertical Slice through an Ellipsoid

Using an ellipse instead of an ellipsoid does simplify the analysis, but also introduces errors which needs to be considered. The errors are the difference in perpendicular distance from the centerline to the ellipse or ellipsoid. The errors will vary as a function of distance along the path from transmitter to aircraft, the actual distance from transmitter to reported multipath location, pulse delay, and vertical angle of the ellipsoid. This error will influence the area inside the ellipse that needs to be considered when searching for a reflecting source. Unfortunately, it is not a single value.

Figure E-7 shows the difference between using the ellipse method and the ellipsoid method. The X-axis is horizontal distance from the transmitter to the analysis point. The Y-axis shows the difference in the perpendicular distance from ellipse center axis between ellipse (R value from above) and the width of the ellipsoid as it intersects the earth (X value from above). Due to the large combination of variables, the results have been grouped into series. Each series uses a constant pulse delay while the distance between the transmitter and the reported multipath location and elevation angle are varied. Pulse delay values included 1, 3, 5, 12, and 36 μ s. Ellipsoid rotation angle included 0°, 2°, and 4°. The distance between the transmitter and reported multipath location was varied from 1 to 20 nmi. Each color grouping includes a series.

These are important observations from Figure E-7:

1. The large negative or downward spikes are occurring when the analysis point (distance from transmitter) is approaching the reported multipath location.
2. The errors tend to be larger as the pulse delay values decrease (red = 1 μ s, orange = 3 μ s, green = 5 μ s).
3. When considering the region from 0 to 3 nmi from the transmitter, the difference is less than 200 feet.

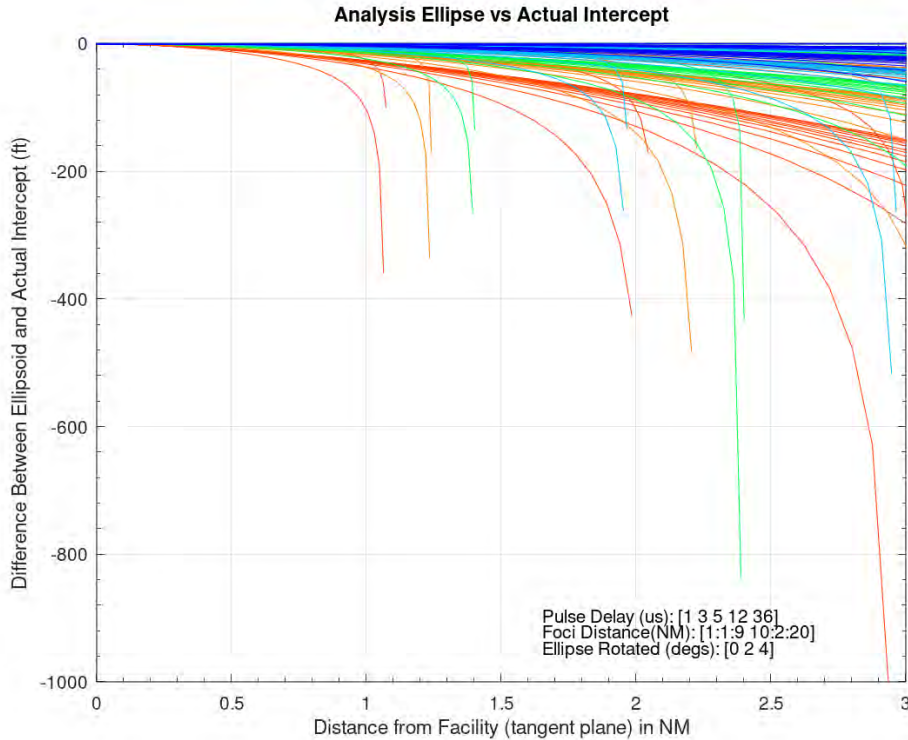


Figure E-7. Difference in Distance to Ellipse vs Ellipsoid Intersection with Terrain

3. Limiting the Area of Consideration (AOC)

There are practical limits on the location of the reflecting surface. The reflecting surface must be illuminated by a signal from the transmitter, the angle of the reflecting object must be correct, and the path from the reflector to the receiver must be clear of blockages. As the distance from the transmitter to the reflecting surface increases, the signal spreads. This means the reflecting object must also increase in size to reflect the same energy as at a closer point. In order for the multipath to be an operational issue, the correct geometry must also exist for a duration long enough to impact DME receiver tracking otherwise it is seen as noise. Direction of flight is therefore a factor. An aircraft flying by a facility is constantly changing the geometry except for certain cases. If the reflecting surface is behind the facility relative to the aircraft position, the geometry will be less sensitive to position change and the problem can exist for a longer duration. Aircraft flying an approach will be more likely to maintain areas of correct geometry for longer durations.

There is no magic number for area of consideration around a facility to identify a reflecting surface. Refer to Appendix C to better understand all the variables. To aid in visualizing the impact of the numerous variables, a series of ellipses defining locations of possible reflecting surfaces for various ellipse parameters are shown.

Figure E-8 shows how the ellipse changes when the pulse delay is varied while maintaining the distance from the transmitter to the observed multipath location is held constant. The asterisk (*) is the transmitter position while plus sign (+) is the observed multipath location. The dotted lines show ranges rings around the transmitter. Rings are at 1, 2, 3, 4, and 5 nmi. As the pulse delay increases, the size of the ellipse also increases. If the measured pulse delay is not correct, it will change the size of the ellipse. This means when using the ellipse to locate a possible reflecting source, it will be necessary also look on both sides of the ellipse

Ellipse Variation as Function of Multipath Delay (Constant Range DME to Aircraft)

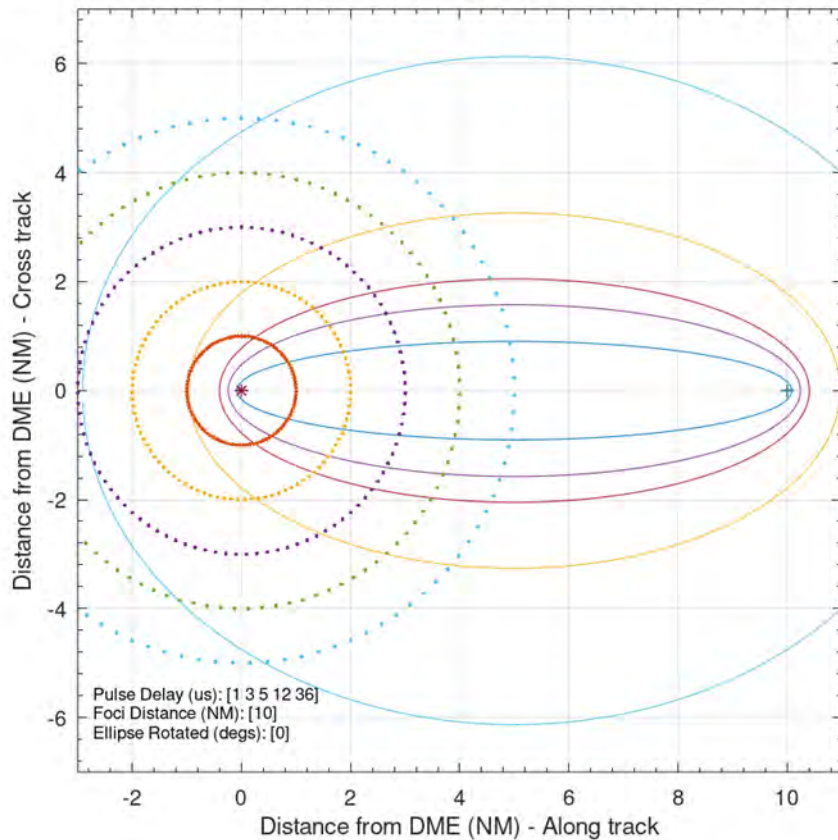


Figure E-8. Ellipse Variation as Function of Pulse Delay Variation

Figure E-9 below shows how the ellipse changes when the distance from the transmitter to the observed multipath location is varied while maintaining the reply delay constant. The asterisk (*) is the transmitter position while plus sign (+) is the observed multipath location. The dotted lines show ranges rings around the transmitter. Rings are at 1, 2, 3, 4, and 5 nmi. As the distance from the transmitter to the observed multipath location increases, the

size of the ellipse lengthens, but the various ellipses near the transmitter almost overlay each other. Errors in determining the location of the observed multipath location will change the shape of the ellipse, but have less impact on the search area.

Ellipse Variation as Function of Multipath Delay (Constant Range DME to Aircraft)

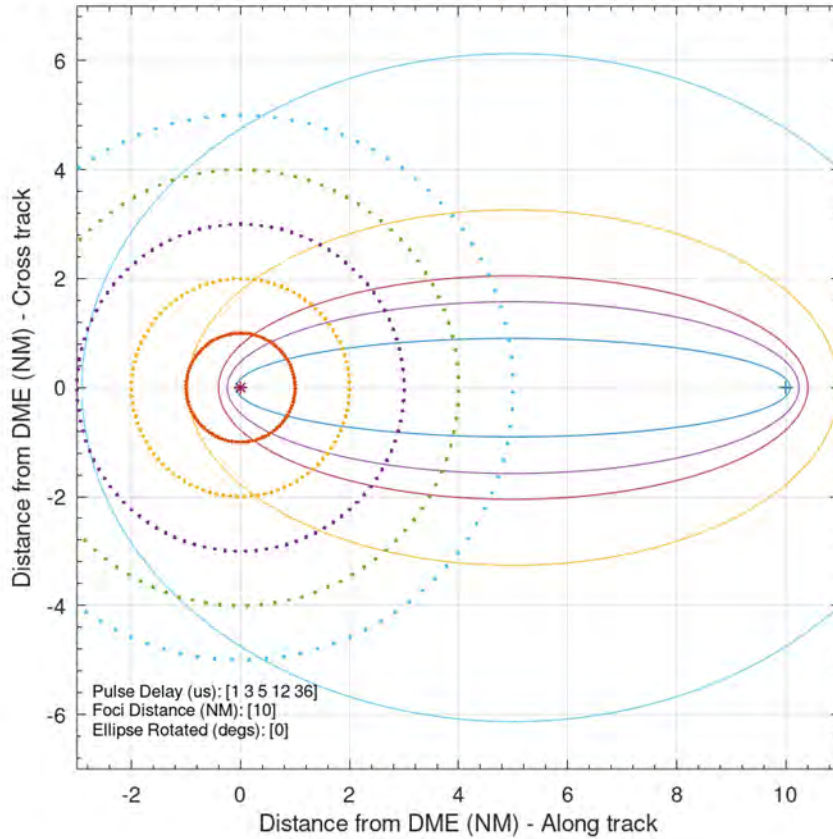


Figure E-9. Ellipse Variation as Function of Transmitter to Multipath is Varied

To provide a sense of the variability, Figure E-10 below shows an ensemble of ellipses drawn for different conditions. It combines the information presented in Figure E-8 and Figure E-9. Each multipath delay in Figure E-8 was varied for the conditions in Figure E-9. The following parameters were varied: the distance between the transmitter and reported multipath location out to 20 nmi, and multipath delays of 1, 2, 5, and 12 μ s. The elevation angle of the ellipse was held constant at zero degrees. There are 4 well defined grouping of plots. Each grouping shows how the ellipse changes as a function of distance between transmitter and reported multipath location for a constant multipath delay. For some groupings, a complete ellipse is observed. This occurs when the distance between the transmitter and the reported multipath location is small. As the distance increases, only the portion of the ellipse nearest the transmitter can be observed. The asterisk is the location of the transmitter. The reported multipath location is on the X-axis to the right. Circular reference lines are shown at distances of 1 and 2 nmi around the transmitter as dotted lines. A 2 nmi area round the site is shown.

Important observations:

1. If the reflecting surface is behind the facility, the distance to the reflector remains constant for a given delay regardless of the distance from the transmitter to the aircraft. The distance is equal to multipath delay in μs divided by two-way propagation delay. Two-way propagation delay is $12.367 \mu\text{s}$ per nmi.
2. As the reflecting surface is rotated from directly behind the transmitter by 90° , the possible location of the reflecting source starts to change as a function of the distance from the transmitter to the aircraft.
3. As the reflecting surface is moved forward of the transmitter toward the reported multipath location, the location becomes very dependent on the distance from the transmitter to the reported multipath location.

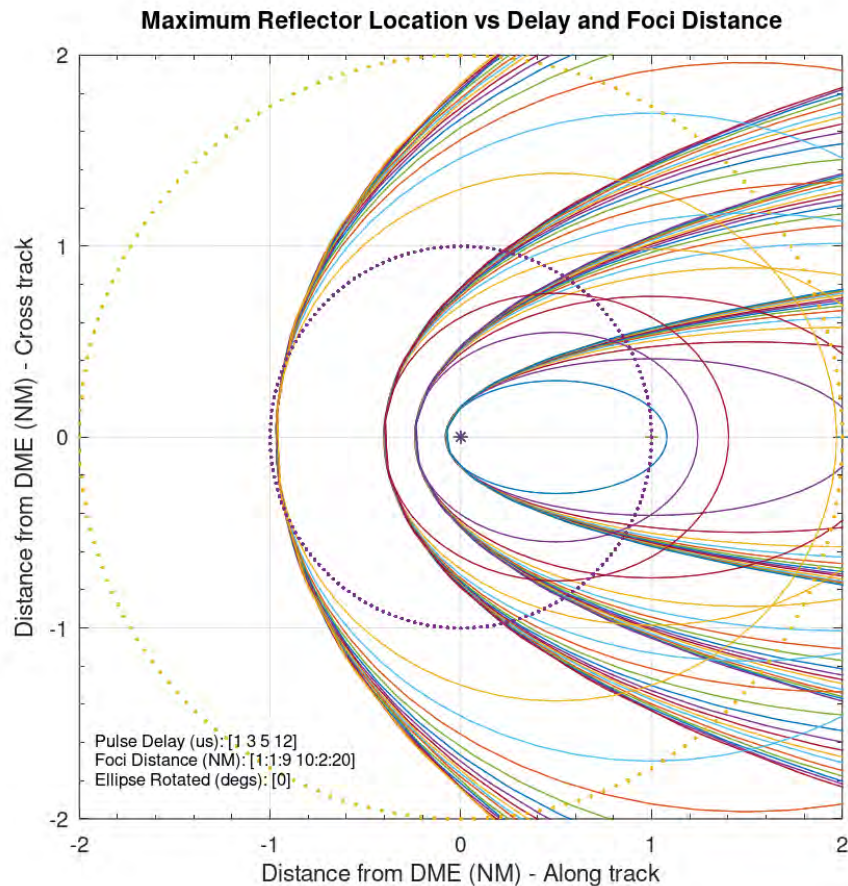


Figure E-10. Ellipse Variation Ensemble

4. Methods to Locate Reflecting Surface

There are two known methods to aid in identifying a multipath reflecting surface:

1. Measured multipath delay; and
2. Scalping.

The measured multipath delay method starts when problems are reported by FI or pilots. Reports will include comments like dropped tracks or DME range errors at some location. Subsequent flights are required to probe the area, measure multipath delay, and record the actual aircraft position of measurement.

The scalloping method starts when FI observes scalloping during an inspection, reports dropped tracks, or DME range errors. The scalloping method has been identified in FAA Order 6820.10, "VOR, VOR/DME, and VORTAC Siting Criteria", and has been used successfully for finding VOR multipath. The same method can be used to identify DME multipath, and the reader is referred to that document instead of restating the method here. This appendix will focus on explaining the measured multipath delay method.

5. Measuring Multipath Delay

The DME system includes a downlink and an uplink channel. The downlink channel starts the ranging process when the DME interrogator (i.e., aircraft) transmits an interrogation pulse-pair to the transponder (ground station). The transponder decodes the interrogation and if valid, transmits a pulse-pair back to the aircraft. Once a valid interrogation is detected by the transponder, it no longer checks for incoming interrogations until it has sent a reply. By design, the blanking is adjustable from 50 to 150 μs . The process is intended to suppress shorter multipath delays described earlier. There is also the ability to increase the receiver dead time to suppress longer delay multipath. The trigger for this function is interrogation amplitude sensitive. The downlink path includes interrogations for all aircraft within the service volume. It is not possible to determine which interrogation was transmitted by a particular aircraft and its position when transmitted. It therefore does not include useful information for locating a reflecting surface.

The uplink channel includes replies to all decoded interrogations plus squitter and ident pulses. Each reply is from the same transmitting location therefore the effects of multipath will be the same for all pulse-pairs. By design, each aircraft interrogation is not periodic and is jittered in time. The interrogator uses this information to determine which reply is in response to the interrogation and determines a DME range. When measuring multipath delay, it is not necessary to know which reply is in response to the interrogation therefore many more pulse-pairs are available for measurement.

To use the ellipse method for locating the reflecting object, the delay of the multipath pulse must be measured. FI does not currently have the ability to record detected video pulses in their aircraft. FI has connected an oscilloscope to an available detected video output from the DME equipment in the aircraft. The technique was reported in Reference BB. The FAA William J. Hughes Technical Center (WJHTC) has also measured multipath while validating the DME math model. Digitized pulses were recorded and processed post flight. The process was reported in Reference V. Both methods used detected video pulses. FI used the detected video output of the FI DME interrogator. The WJHTC used a Rohde & Schwarz EDS-300 DME/Pulse Analyzer. The instrument has a feature called PulseView which allows the capture of digitized video pulses. It is important that DMEs are set to single channel operation and not allowed to operate in scanning mode. This makes sure the detected video being observed is from the desired DME facility.

Before multipath delay can be measured, it must be located. Using the oscilloscope method allows observers on the aircraft to determine the presence of multipath. This may require probing flights in the area of reported problems to determine the area of interest. Once established, the focus can shift to performing the actual measurements. As previously mentioned, the multipath delay will change as a function of the geometry. It is not necessary to perform the delay measurement at the precise location of dropped track or range error. It is more important to have a good measurement of the delay.

When the direct and reflected pulses are heavily overlapping it is very difficult to identify the individual pulses. The user may have to guess at a range of pulse delays. Two ellipses can be drawn, one for the minimum and one for the maximum pulse delay observed. The reflecting source should be somewhere between the two ellipses. An alternate solution is to change the geometry so the delay will change. An orbital flight through the observed multipath point will have the greatest change in geometry over a short distance. The reflecting source may be very directional therefore it is important to investigate over a small area. The desire is to change the pulse delay enough to separate the direct and reflected pulses to be able to measure the pulse delay. The term “measure” has been used in the above discussion. Unless the direct and reflected pulses are clearly separate, the process is really an “estimate” of delay. The full instrumentation package used by the WJHTC allows the capture of large amounts of data, but it does not guarantee the data will be collected in the area of interest. Analysis is completed in post processing. Regardless of capture method used to view the video pulse-pairs, the direct and reflected pulse-pairs must be identified. Since the transponder includes a dead time between transmitted pulse-pairs and it is greater than the pulse-pair spacing, the gaps can be used to identify the direct pulse-pair.

Oscilloscope setup and use is critical. Internal triggering based on the detected video is sufficient. External triggering is not required. Sweep time/span must be set greater than the pulse-pair spacing. It is suggested to use at least 20 μ s for X-channel and 35 μ s for Y-channel. Shorter spans will cause only one pulse of the pair to be displayed with no choice of selecting first or second pulse of the pair. Not all triggers will capture a pulse-pair, but enough sweeps should include pulse-pairs for analysis. Modern digital oscilloscopes allow capturing the waveform and can be very helpful. In areas where multipath is observed, the waveform should be capture for later analysis. Depending on the oscilloscope, many pulse-pairs may be captured. Delay is generally measured at the half-amplitude points. Depending on the waveform, it may be more of a guess.

As mentioned earlier, delay does not have to be measured at the point of dropped track or range error. Try changing the flight profile slightly to determine if other areas show a cleaner multipath signal. Constructing ellipses based on multipath delays measured at several location may aid in identifying smaller areas that are more likely to contain the reflection object. The more accurate the measurement of pulse delay and the associated aircraft position, the better the ellipse will be in identifying the location of the reflecting surface. It is not a precise process. FI has demonstrated that when using the oscilloscope method, the reflecting surface can be located.

6. Ellipse Method

Parameters which define the shape of the ellipse are based on the distance from the transmitter to the aircraft and multipath delay. Orientation of the ellipse is defined by the azimuth from the transmitter to the aircraft. Regardless of the actual implementation, the following steps are required:

1. Determine the distance and azimuth from the transmitter to the aircraft.
2. Compute the values that define the ellipse. Values include semi-major axis, semi-minor axis, eccentricity, and orientation.
3. Compute position values on the ellipse. These are the values which define where a reflector may be located. The values may be defined as latitude and longitude, displacement east and north from the transmitter, or azimuth and distance relative to the transmitter. The choice depends on how the information will be used. If the intent is to automate adding the information to a map, then values in latitude and longitude may be the best choice. If the intent is to manually use the information, azimuth and distance may be the best choice. Google Earth has a tool to measure distance and azimuths. By placing the origin at the transmitter, the cursor can be moved providing the user with azimuth and distance information. Other applications may provide the same features. If manually drawing the information on a paper map, displacements east and north may be more useful.

7. Determining the Ellipse Parameters

This section will define the steps needed to define the ellipse of interest. The intent is not to provide actual software, but to define the process. Simplified equations are provided to demonstrate the process. If used accurately, the simplified equations should be sufficient when defining the ellipse within 5 nmi of the transmitter. Geodetic software is available from many sources that will provide more precise calculations and can be used to automate the process. National Geodetic Survey offers the Geodetic Tool Kit on their web site: <https://www.ngs.noaa.gov/TOOLS/>. Applications like INVERSE and FORWARD can be used to compute the distance and azimuth between points. Applications may be used online or downloaded for use on a local computer.

Step 1 - Compute the Distance between the Transmitter and the Aircraft

$$distance = \sqrt{((lat2 - lat1) * 60)^2 + ((lon2 - lon1) * 60 * \cos(lat1))^2}$$

Where:

- lat1 = latitude of the transmitter in degrees decimal degrees (N is positive)
- lon1 = longitude of the transmitter in degrees decimal degrees (W is negative)
- lat2 = latitude of the aircraft in degrees decimal degrees (N is positive)
- lon2 = longitude of the aircraft in degrees decimal degrees (W is negative)
- distance = distance between transmitter and aircraft in nmi

Step 2 - Compute the Azimuth from the Transmitter to the Aircraft

$$azimuth = \arctan ((lon2 - lon1)/(lat2 - lat1))$$

Where:

- lat1 = latitude of the transmitter in degrees decimal degrees (N is positive)
- lon1 = longitude of the transmitter in degrees decimal degrees (W is negative)
- lat2 = latitude of the aircraft in degrees decimal degrees (N is positive)
- lon2 = longitude of the aircraft in degrees decimal degrees (W is negative)
- Azimuth = azimuth angle from true north to the aircraft (units are either radians or degrees based on algorithm used)

Step 3 - Compute Ellipse Parameters

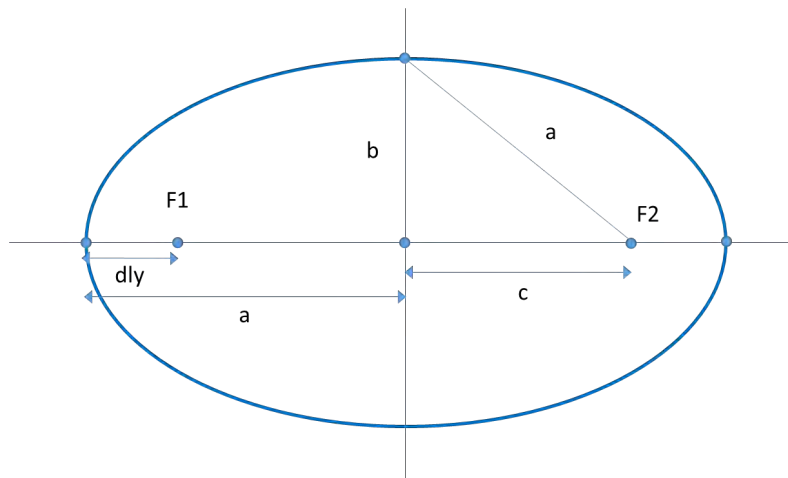


Figure E-11. Ellipse Parameters

$$c = \text{distance from transmitter to aircraft (NM)} / 2$$

$$dly = \text{multipath delay } (\mu\text{s}) / 12.367 (\mu\text{s}/\text{NM})$$

$$a = c + dly$$

$$b = \sqrt{a^2 - c^2}$$

$$ec = c/a = \sqrt{1 - (b^2 / a^2)}$$

Where:

- F1 = focus (transmitting antenna)
- F2 = focus (aircraft)
- c = distance from center of ellipse to focus in nmi
- dly = multipath delay in μs converted to displacement in nmi
- a = semi-major axis in nmi
- b = semi-minor axis in nmi
- ec = eccentricity

Step 4 - Compute Ellipse Using Polar Form

Use of the polar form of an ellipse easily allows conversion to other reference systems. Reference point is one focus of the ellipse. 0° is aligned along the axis through the transmitter and aircraft.

$$r = b^2 / (a - c * \cos(\theta))$$

Where:

a = semi-major axis in nmi

b = semi-minor axis in nmi

c = distance from center of ellipse to focus in nmi

r = distance from focus to point of interest on ellipse for bearing θ in nmi

θ = bearing from focus to point of interest on ellipse (reference is transmitter to aircraft)

Note: θ must be in radians or degrees consistent with trig function

Step 5 - Convert Polar Coordinate of Ellipse in East/North Coordinates

This step will convert the ellipse polar coordinates to east/north coordinates with proper rotation. The previous step computed the ellipse in polar coordinates without rotation.

$$e = r * \sin(\phi - \theta)$$

$$n = r * \cos(\phi - \theta)$$

Where:

r = distance from focus to point of interest on ellipse for bearing θ in nmi
(computed in previous step)

θ = bearing from focus to point of interest on ellipse associated with r (used in previous step)

ϕ = azimuth from transmitter to aircraft computed in step 1

e = displacement of ellipse point from transmitter in easterly direction (nmi)

n = displacement of ellipse point from transmitter in northerly direction (nmi)

Note: θ and ϕ must be in radians or degrees consistent with trig function

Step 6 - Convert East/North Ellipse Coordinate to Geodetic Position

This step will convert ellipse coordinates from east/north to geodetic coordinates. If using software which includes geodetic computes, this step will be replaced by using the appropriate function to move the geodetic position of the transmitter by the range (r), bearing (θ), and azimuth (ϕ) computed in steps 2 and 4.

$$dLat = n/60$$

$$dLon = e / (60 * \cos(Lat1))$$

$$LatE = Lat1 + dLat$$

$$LonE = Lon1 + dLon$$

Where:

- e = displacement of ellipse point from transmitter in easterly direction (nmi)
- n = displacement of ellipse point from transmitter in northerly direction (nmi)
- dLat = displacement of ellipse point from transmitter in northerly direction (degrees)
- dLon = displacement of ellipse point from transmitter in easterly direction (degrees)
- Lat1 = Latitude of the transmitter in degrees
- Lon1 = Longitude of the transmitter in degrees
- LatE = Latitude of the point of interest on the ellipse in degrees
- LonE = Longitude of the point of interest on the ellipse in degrees

8. Summary

Figure E-12 below can be used to help identify the location of a possible reflecting surface without calculating the ellipse. The asterisk represents the transmitter location. Circles are drawn in 1 nmi increments relative to the transmitter. Radial lines are drawn for every 30° of bearing. Each series of lines is drawn for a constant multipath delay. Distance between the transmitter and reported multipath location is varied. Multipath delays of 1, 3, 5, 12, and 36 μs were used. Range values from 1 to 9 nmi in 1 nmi increments, and 10 to 20 in 2 nmi increments are shown. To use the chart, the user would align the zero degree bearing with the azimuth to pulse delay measurement. Distance and relative bearing can be read from the chart. While not precise, it provides an indication of possible locations to search.

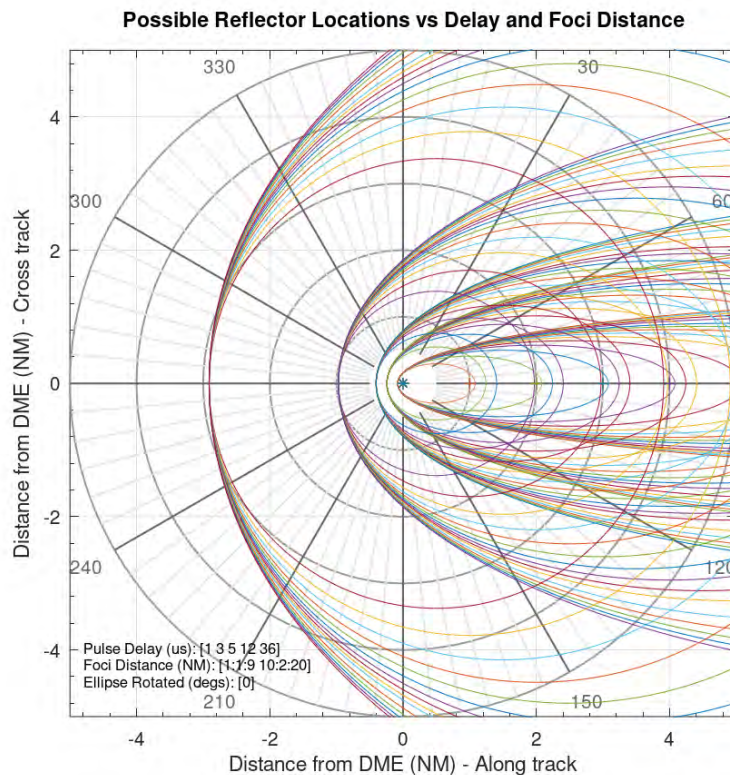


Figure E-12. Locating Possible Reflection Source

9. Use of Fresnel Plots

Searching the internet one can find applications that create an ellipsoid surface showing various Fresnel Zones based on frequency. The surface is output as a Keyhole Markup Language (KML) format file that can be imported into Google Earth. These applications can be used to define the location of possible reflecting surfaces. Fresnel Zones are based on multiples of the half-wavelength of the desired frequency. In order to use this application, a frequency must be calculated whose half-wavelength is equal to the desired multipath delay.

Equation for frequency versus wavelength is:

$$\lambda = v/f$$

Where:

$$\begin{aligned}\lambda &= \text{wavelength (m)} \\ v &= \text{speed of light (} 3 * 10^8 \text{ m/s)} \\ f &= \text{frequency (Hz)}\end{aligned}$$

Equation to convert multipath delay to wavelength is:

$$\lambda (m) = 2 * \text{delay (us)} * \frac{1852 \left(\frac{m}{NM} \right)}{12.367 \left(\frac{us}{NM} \right)}$$

The 2 times multiplier is required to convert the delay from half to full wavelength.

Appendix F. DME Math Modeling

1. Introduction

This appendix describes the results from math modeling studies performed in the development of this document. Math modeling is a tool in the siting engineers' toolbox to assist in making siting decisions. It is not practical to model the entire environment in which the DME facility is installed, therefore it should only be used to assist in the final decision making.

The FAA William J. Hughes Technical Center (WJHTC) has developed a high-fidelity DME computer model that was used in the development of the DME Siting Criteria. The model was validated through flight testing and is summarized in Reference V. The model predicts performance of DME systems in presence of various types of multipath and shadowing. It predicts performance in terms of signal strength, range error, and lock status. The model utilizes user inputs such as geometry of scattering objects, terrain, reflection properties, and flight paths.

The DME Model uses a commercial-off-the-shelf (COTS) software package for electromagnetic field simulation with custom software written to simulate the DME receiver and for Input/Output (I/O).

The ANSYS Electronics Desktop is a COTS product that is used to model the electromagnetic, circuit, and system behavior of electronics systems. The DME Model was developed using High Frequency Structure Simulator (HFSS) and Shooting and Bouncing Rays + diffraction (SBR+), which are included as part of the suite of tools within the ANSYS Electronics Desktop. SBR+ uses an advanced frequency domain physical optics based method and has the following computational capabilities:

1. Coupling between transmitting and receiving antenna pairs;
2. Spatial electric and magnetic field distribution;
3. Incident, scattered, and total fields; and
4. Co-polarization and cross-polarization scattering based on interactions with various objects within a graphic user interface.

SBR+ was used to simulate physical optics reflections of surrounding environments with the capability to enhance them with Physical Theory of Diffraction, Uniform Theory of Diffraction, and creeping waves. The electromagnetic propagation is simulated at multiple discrete frequencies within the bandwidth of the desired DME channel at predetermined observation points. Observation points in the model are points in space at which the performance of the DME is simulated. These points can be along a flight path or evenly distributed on a constant altitude surface.

The results of the incident, scattered, and total electric fields are in the frequency domain and phasor form. A Gaussian filter is applied to the electric fields in order to obtain the characteristic DME pulse shapes. The results are then post-processed by applying an inverse Fourier transform thus converting the frequency domain data to the time domain to

obtain the DME pulses. These pulses are assumed to be the signal incident on the DME receiver and are processed using guidance from the DME Minimum Operational Performance Standards (MOPS). The resulting outputs are: range error, signal strength, lock status, pulse shape analysis, and pulse traces for all observation points.

2. Results and Interpretation

The model offers two basic types of plots to display the results: a 2-dimensional plot, and a 3-dimensional surface heatmap plot. The first plot is used to display the results along a flight path, where distance or radial relative to the DME are on the X-axis, and the performance metric is on the Y-axis. Alternatively, the results can be plotted in a polar coordinate system, particularly when the flightpath is orbital. The heatmap plot is used to display results on a constant-altitude surface which covers a greater area and includes more observation points. The heatmap plots are mostly plotted in a polar coordinate system, where the radial and range defines the physical location of the observation point and the performance metric is quantified using a color spectrum.

A sample model scenario was created to show how the results can be plotted. The scenario consisted of a metallic hangar placed due east at a distance of 3,000 feet from the DME, as illustrated in Figure F-1. The dimensions of the hangar are 300 by 250 feet, the height is 75 feet, and the hangar is rotated 135° as illustrated in the figure.

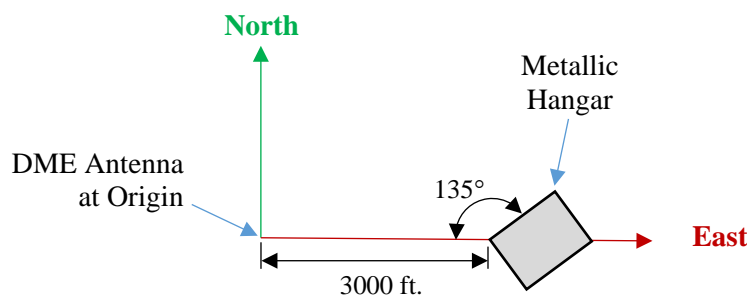
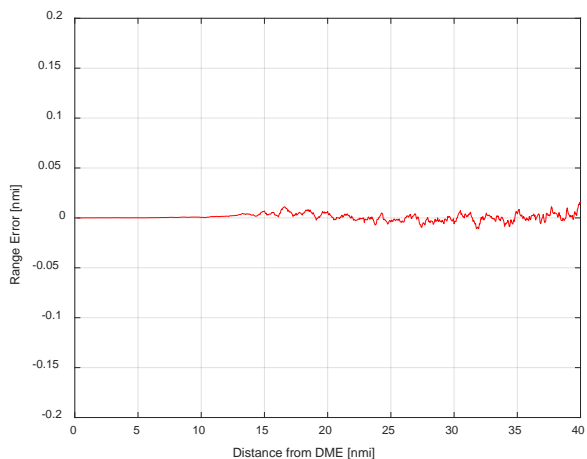
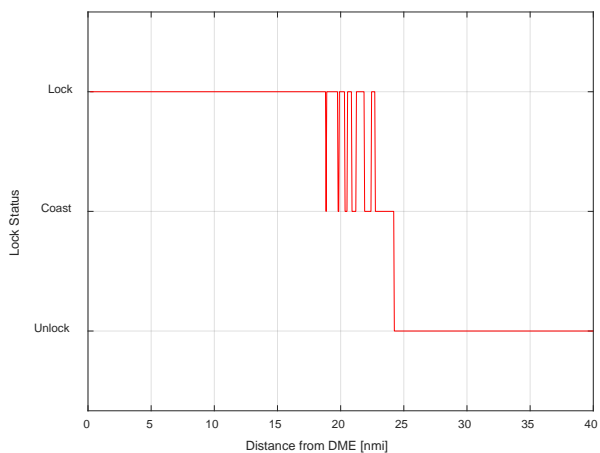


Figure F-1. Sample Model Scenario to Describe Plots

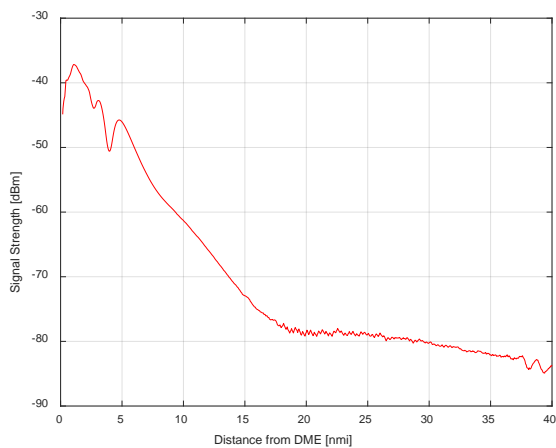
A sample set of results using the 2-dimensional plotting method are given in Figures F-2(a), (b) and (c). These results are of a radial run along azimuth 88° at 1,000 feet Above Ground Level (AGL) of the model scenario described earlier. One benefit of using these types of plots is that they are in a similar format as flight check data. Another benefit is that the number of observation points is small hence a shorter runtime. One drawback of this method is that the effects resulting from the modeled scenario may be slightly offset from the modeled flight path and not captured in the plot. This method works well when studying the impact of structures on DME performance along approaches, arrivals, departures, and airway routes.



(a)



(b)



(c)

Figure F-2. Sample 2-dimensional (a) Range Error, (b) Lock Status Plot, and (c) Signal Strength

A sample set of results using the heatmap plotting method are given in Figures F-3(a), (b), and (c). These results are of the same model scenario described above. Range error and signal strength are plotted using a color-coded scale. In the case of range error, areas of white indicate that the receiver was unable to decode a range value from the received pulse-pairs. The main benefit of utilizing these plots is that it gives a holistic view in terms of extent and magnitude of the impact caused by the scenario being model. A limitation of using this modeling method is the way the lock status is plotted. When an aircraft enters a region where valid DME pulses are no longer decoded, the DME airborne equipment will coast for a certain period of time before losing lock. This is highly dependent on aircraft speed and direction. In the lock status heatmap plot it is not practical to account for possible direction of travel for every observation point; instead only the decode criteria is plotted. If a successful decode was made, it is plotted as a ‘Lock’; otherwise it is plotted as ‘Unlock’. The areas where unlocks occur will end up being smaller than what is plotted. Nonetheless, the plot does indicate areas where coasts and unlocks should be expected.

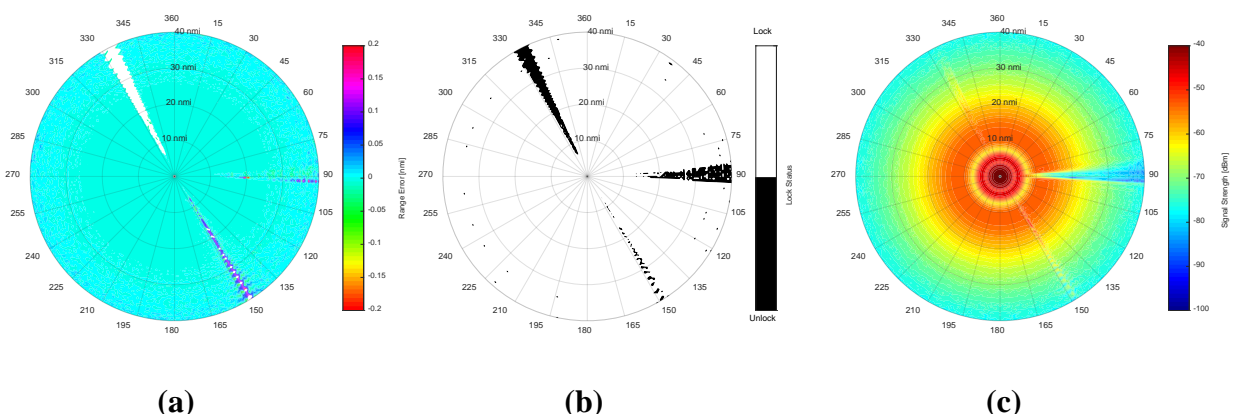


Figure F-3. Sample Heatmap (a) Range Error, (b) Lock Status, and (c) Signal Strength Plot

3. Case Studies

The objects modeled in this appendix were chosen to reflect objects that may be frequently encountered at typical DME sites such as: wind turbines, air traffic control towers (ATCTs), communication towers, solar panel arrays, irrigation systems, and large cylindrical structures. Subsequent sections of this appendix provide analyses for each of these objects. The objects were modeled alone over a flat ground plane, hence only the impact of the object is analyzed. In reality there may be other objects or structures nearby that may exacerbate the effects of the modeled objects. One example is a treeline near the DME that would exacerbate the effects of an ATCT. The treeline reduces the strength of the direct signal causing a larger multipath-to-direct (M/D) ratio bringing the error closer to the DME in the direction of the treeline. The siting engineer must identify such cases where they exist and use engineering judgement and the evaluation tools discussed in Appendix C and E to assess the impact to the DME. Math modeling is also available for such cases.

The modeling and analysis performed in this appendix utilized the heatmap method of modeling and plotting. It is worth noting that only results that showed measurable impact

are included in the analysis, the plots for modeling scenarios that showed no impact were intentionally omitted. The modeling was performed using a transmitter at 1,000W. The antenna used in the modeling was the nominal DME antenna with the main beam of the antenna located at an elevation of 3°, and the base of the DME antenna was placed at a height of 20 feet AGL.

The observation points are defined on a constant-altitude surface at height of 1,000 feet AGL. The altitude was chosen to represent the minimum altitude flight inspection uses during a commissioning flight inspection per USSFIM, 11.4.f.(2)(a). Additionally, the altitude would capture the largest impact caused by the structures.

The increments of the observation points are 1° for azimuth, and 0.4 nmi for range. In some cases, the observation point density was increased to fully capture the effect of the scattering object; the increments are defined in those cases. These observation points are chosen to show extent of the impact that the modeled objects have on a larger portion of the service volume. Due to the large area being simulated, the heatmaps may be subject to under sampling for typical aircraft speeds.

Given these sample spacings, it is possible that there may be small pockets within the service volume where the effect due to signal scattering and/or blockage, which is caused by the objects analyzed below, may be operationally observable, but not expected to be problematic. Operationally observable, but not expected to be problematic as used herein means the interrogator coast period may be exhausted causing the DME flag to be momentarily displayed before DME signal tracking is re-established. It should be realized that this is not a new phenomenon as such pockets likely exist in many service volumes today.

a. Wind Turbines. Wind turbines have become increasingly popular over the past few decades as an alternate energy source. The ideal sites for wind turbines are in flatlands with no other obstructions nearby to impede the wind, similar to the ideal conditions for DME ground stations. Wind turbines are most often located in green sites away from urban areas and airports. The dimensions of these objects vary depending on the model.

The impact of wind turbines on DME performance was assessed by modeling three cases of wind turbines:

1. A single wind turbine;
2. Four wind turbines; and
3. Eight wind turbines.

The distance of the wind turbines relative to the DME were iterated in the model from 1,000 feet to 14,000 feet in increments of 1,000 feet east of the DME. This process was repeated for the aforementioned three cases. Through modeling it was determined that the worst-case configuration of the wind turbine for the heatmap plot was one of the blades being vertical and the wind turbine facing at a heading of 135° true north. The

wind turbines were configured in the worst-case configuration for all of the modeling cases.

In order to assess the impacts of the main wind turbine components, two modeling scenarios were performed; (1) consisting of only the metallic shaft and nacelle, and (2) consisting of only the wind turbine blades. The results showed that the shaft and the nacelle had the largest impact on performance in terms of unlocks and range errors. Whereas the blades had a smaller impact primarily causing range errors.

The wind turbines were located east of the DME and faced heading 135° true north. It was determined through modeling that changing the wind turbines' heading mostly shifted the location where the errors were observed, and had little impact on the magnitude of the errors. The wind turbine model used in the simulations was based on the Vestas V90 wind turbine. Figure F-4 shows the dimensions of the wind turbine model used in the simulations.

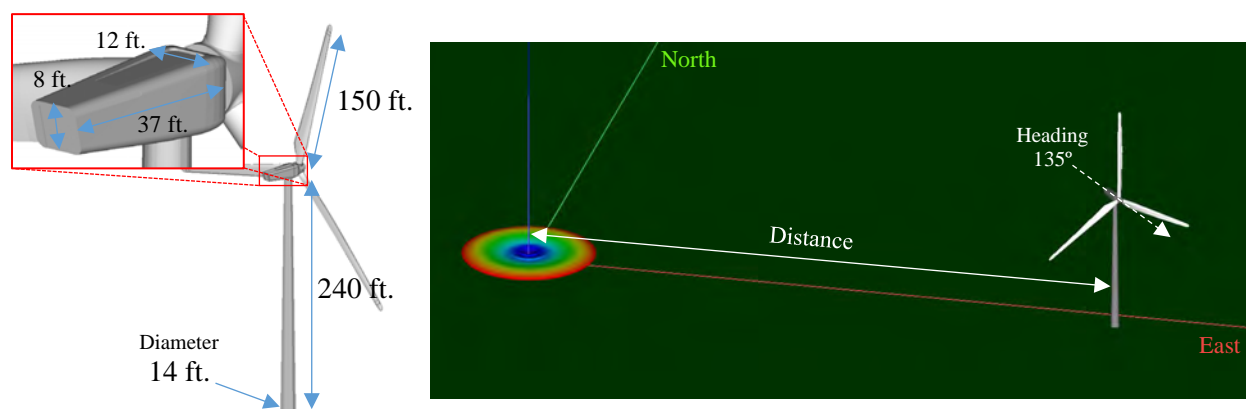


Figure F-4. Wind Turbine (a) Dimensions and (b) Model Set-up

- ii. **Case 1 – A Single Wind Turbine.** Some impact was observed when the wind turbine was located closest to the DME at 1,000 feet away. The impact was primarily loss of lock resulting from shadowing observed behind the wind turbine. There are some areas of range error observed primarily to the north and south of the wind turbine, this range error peaked at around 0.08 nmi and was caused by the blades and the nacelle of the wind turbine. The range error, lock status and signal strength of this scenario for an X-channel transmitter are given in Figures F-5(a), (b), and (c), respectively. The signal strength plot shows that the impact of the single wind turbine is highly localized near the 90° azimuth. The lock status plot shows a likelihood of loss-of-lock to occur particularly if the flight path is radial to the DME near those azimuths. The impact of the single wind turbine was reduced once it was beyond 2,000 feet from the DME. Based on this analysis it is recommended that a single wind turbine located within 2,000 feet of a DME be evaluated for any impact they may have on DME performance.

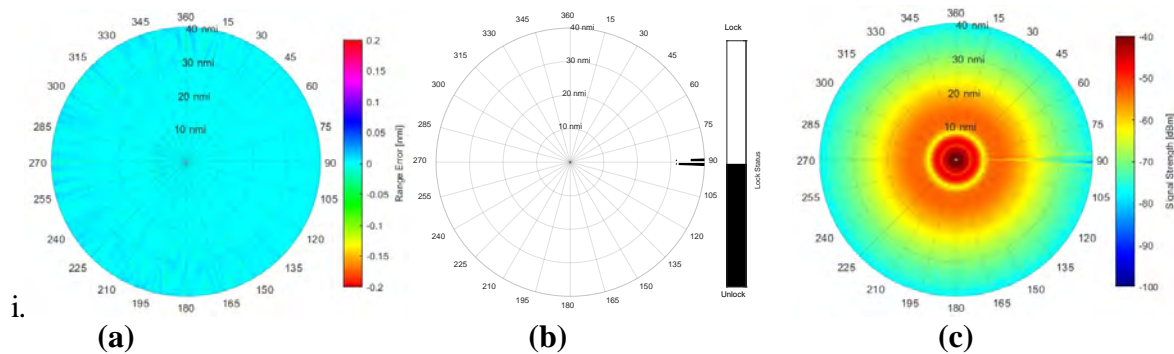


Figure F-5. (a) Range Error, (b) Lock Status and (c) Signal Strength for Case 1 at 1,000 feet

- ii. **Case 2 – Four Wind Turbines.** Some impact was observed when the wind turbines were located closer than 3,000 feet from the DME. The impact was primarily a result of shadowing and was observed behind the wind turbines. The range error, lock status, and signal strength of an X-channel transmitter are given in Figures F-6(a), (b), and (c), respectively. The plots show that the impact of the wind turbines is to the east of the DME, the same direction as the wind turbines. The impact of the four wind turbines reduced once they were beyond 4,000 feet from the DME. Based on this analysis it is recommended that a cluster of four wind turbines separated by 2,000 feet or less, located within 4,000 feet of a DME be evaluated for any impact they may have on DME performance. Beyond 4,000 feet, the wind turbines should also be evaluated if they are below 1.2° subtending angle from the base of the antenna.

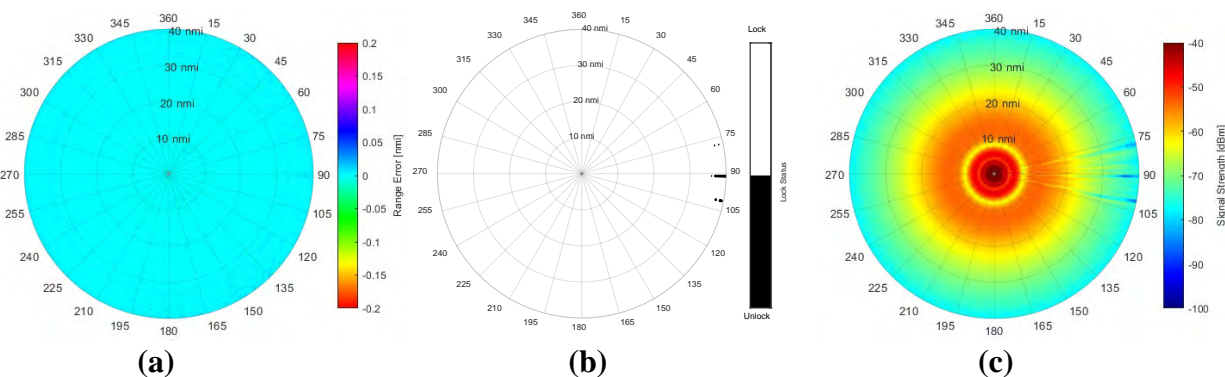


Figure F-6. (a) Range Error, (b) Lock Status, and (c) Signal Strength Results for Case 2 at 3,000 feet

- iii. **Case 3 – Eight Wind Turbines.** A small impact was observed when the wind turbines were located closer than 11,000 feet from the DME. The impact was primarily a result of shadowing and was observed behind the wind turbines. The range error, lock status, and signal strength of an X-channel transmitter are given in Figures F-7(a), (b), and (c), respectively. The plots show that the impact of the

wind turbines is to the east of the DME, the same direction as the wind turbines. The impact of eight wind turbines became negligible once they were past 10,000 feet. Beyond that distance the model showed the impact to be unmeasurable. Based on this analysis it is recommended that a cluster of eight or more wind turbines separated by 2,000 feet or less, be no closer than 10,000 feet from the DME. Beyond 10,000 feet, the wind turbines should also be evaluated if they are below 1° from the base of the antenna.

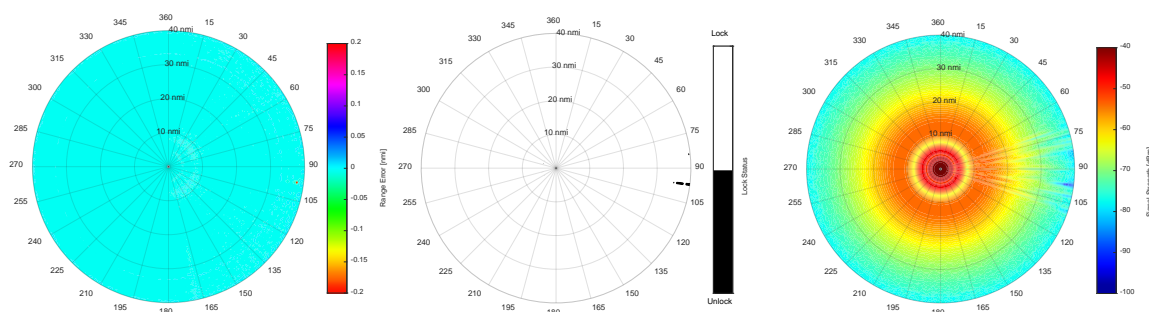


Figure F-7. (a) Range Error, (b) Lock Status, and (c) Signal Strength Results for Case 3 at 5,000 feet

b. Solar Panels. Solar Panels are another renewable energy source that may be encountered at prospective DME sites. In the Northern Hemisphere, the panels are most often configured in an array tilted south by 10-40°. The heights of the panels range from 10-20 feet. Although the panels are optimized to absorb energy in the visible light spectrum, at Radio Frequencies (RF) the panels are reflective due to the many metallic components used to collect and store the energy.

The impact of a solar panel array on DME performance was assessed by modeling a typical solar farm. The solar farm model scenario was created based on measurements gathered from aerial imagery of solar farms in New Jersey. Figure F-8 shows a screen capture of the solar farm used in the model. Two configurations of solar panels were modeled: (1) the complete array was tilted such that the further parts of the array were above the base of the antenna, and (2) the solar array was flat above the ground with no tilt.

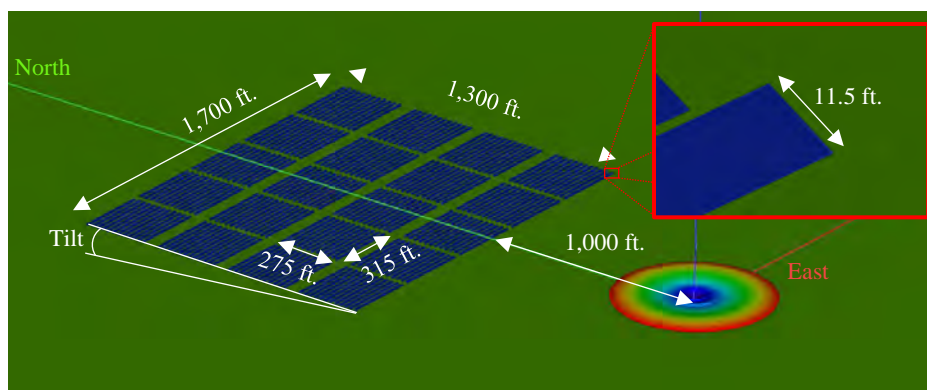


Figure F-8. Solar Panel Array Dimensions

The first solar panel array configuration modeled consisted of a 5° tilt of the array. This brings the northern half of the array above the base of the antenna. The vertical subtending angle measured from the base of the antenna to the highest point of the array equated to 2°. The results of this model scenario are given in Figures F-9(a) through (c). The results show significant performance issues in the direction of the array.

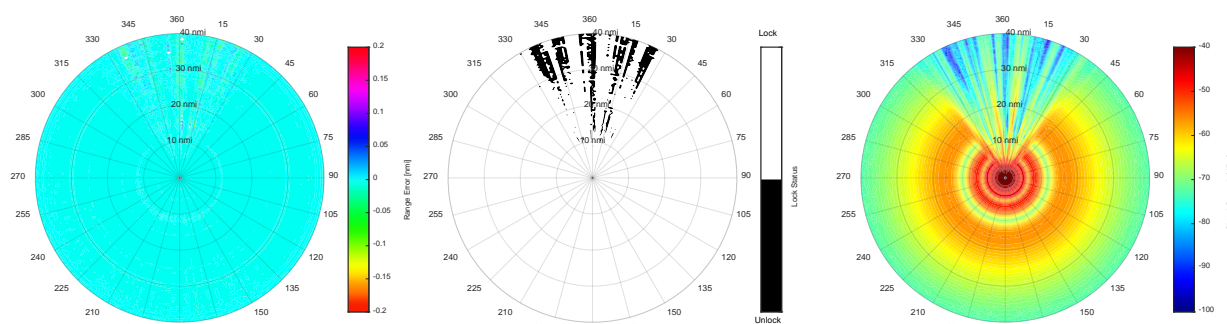


Figure F-9. (a) Range Error, (b) Lock Status, and (c) Signal Strength Results of Solar Array Above Antenna Base

The second solar panel array configuration modeled consisted of a 0° tilt of the array. In this configuration, the array is completely below the base of the antenna. No impact was observed in terms of range error and lock status as a result of this solar farm array. The signal strength plot, shown in Figure F-10, reveals that the solar panel array interrupt the longitudinal reflection that produces a fading null.

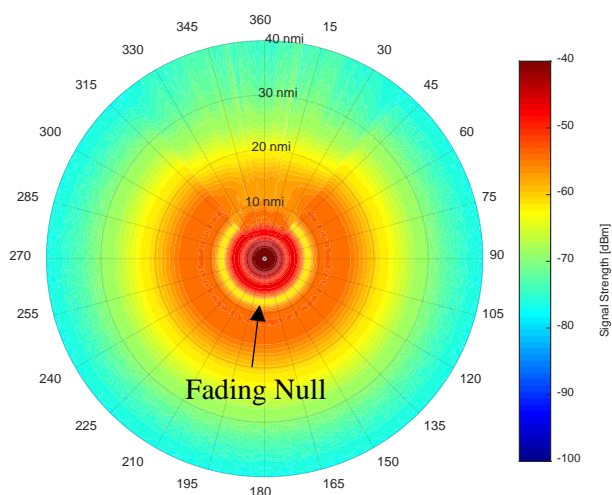


Figure F-10. Solar Panel Array Model Scenario Signal Strength Results at 1,000 feet

An antenna height of 20 feet located in an open area over flat land causes a fading null, which at an altitude of 1,000 feet is observed at around 8 nmi. In the modeled scenario this fading null exists in the azimuth range of 45° clockwise to 315°, which is the same

area that is clear of the solar farm. In the direction of the solar array, the fading null is eliminated by the array's redirection of radiation that would otherwise reflect from the ground to cause the null. However, the signal strength is also decreased in the direction of the array around 20 nmi as a result of the array.

Consider the diagram in Figure F-11, which shows a longitudinal plane of a radial in the direction of the solar panel array. The elevation plane can be divided into three different regions that depend on longitudinal multipath behavior. In Region 1, longitudinal multipath would exist as a result of the radiation leaving the antenna below the elevation angle of ray A. In Region 2, longitudinal multipath would be a result of reflections from the solar array and not the ground. Reflections from the solar panels are dispersed due to the distribution of specular reflection points. In Region 3, longitudinal multipath would again exist as a result of the radiation leaving the antenna above the elevation angle of ray C and reflecting from the ground. Similar behavior is observed when the solar panels are facing a different direction than that depicted in the diagram.

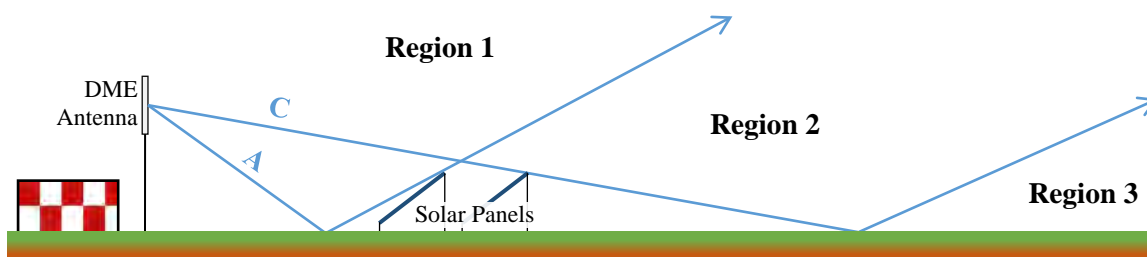


Figure F-11. Longitudinal Multipath of Solar Panel Array

In the model scenario, the null that occurs in the direction clear of the solar panel array and the signal strength decrease that occurs in the direction of the solar panel array are both in Region 2. The reduction of the null is a result of the destructive interference being blocked by the solar panel array, whereas the signal strength decrease is a result of the constructive interference being blocked by the array. Figure F-12 shows the signal strength along radials 15 and 60 where radial 15 is in the direction of the solar panel array, meanwhile radial 60, the baseline, is in the direction with no solar panels. The plot shows that the signal strength along radial 15 is lower than radial 60 between the range of 9 nmi to 30 nmi by an average of 3 db. At the location of the null, 8 nmi, radial 15 shows an increase in signal strength of roughly 10 db. A higher signal strength is also observed along radial 15 at the edge of the service volume.

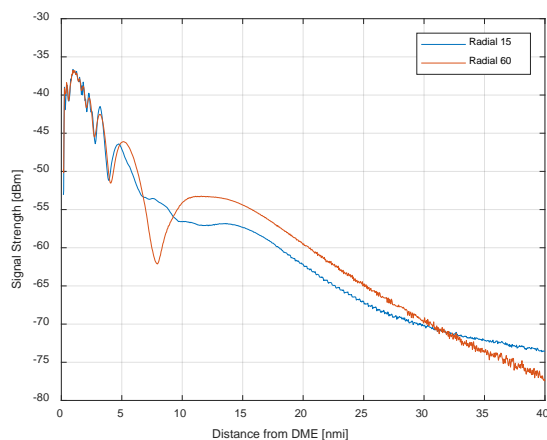


Figure F-12. Signal Strength along Radials 15 and 60 at 1,000 feet

The results of the modeling indicate that the impact of solar panel arrays near DME antennas is overall favorable as long as the height of the DME antenna is above the solar panel array. The resulting siting criteria requirements derived from this analysis is that solar panels can be located anywhere outside of DME antenna near-field boundary as long as all components are below the base of the antenna. Typically, a value of 250 feet should be considered to ensure protection of current and future DME installation. However, this distance may be as short as the 105 feet need to protect to near-field of the dBs 5100A DME antenna, which is the antenna model typically used for new DME installations.

- c. **Center Pivot Irrigation Equipment.** Center pivot irrigation equipment may be found at prospective sites that are located near farmlands. The system typically consists of several segments of pipe joined together by trusses and mounted on wheeled towers that rotate about a fixed center pivot axis. The center pivot and arms are typically 10 to 15 feet in height. A single pipe segment is typically around 180 feet in length. A typical system can consist of a single pipe segment, up to as many as eight segments. Figure F-13 shows the dimensions of the modeled irrigation equipment.

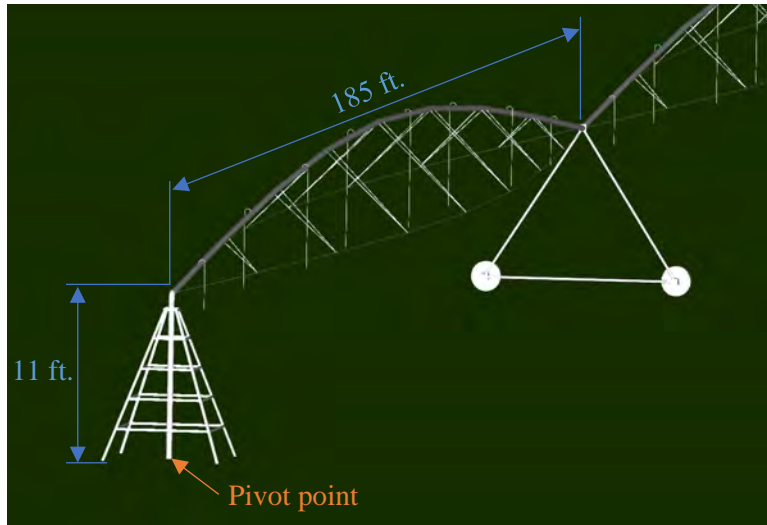


Figure F-13. Irrigation Equipment Dimensions

The impact of irrigation systems on DME performance was assessed by modeling the system in the vicinity of the DME and iterating the position and observing the predicted performance. The first modeling scenario contained a single center pivot irrigation system located directly east of the DME a distance of 1,400 feet. The system was composed of six pipe segments with a total length of 1,085 feet. Figure F-14 shows a screen capture of the modeled scenario. The DME antenna is located at the origin of the coordinate system, indicated by the vertical line, and is hidden in the screen capture. The antenna was placed at 20 feet AGL.

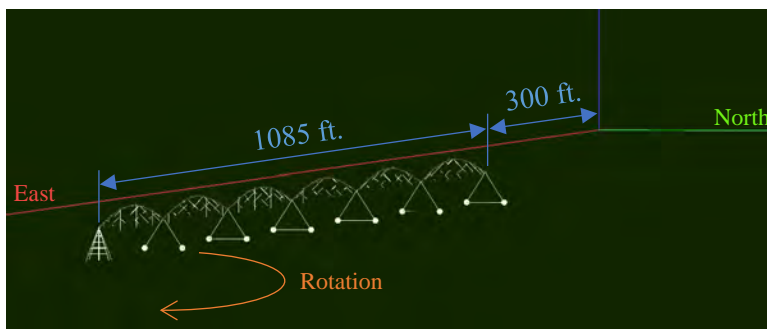


Figure F-14. Screen Capture of Irrigation Equipment in Model

First, the rotation angle of the irrigation system was iterated to determine which general direction showed highest performance impact, i.e., aligned with DME radials, or perpendicular to radials. This modeling showed the highest impact is observed when the rotation angle was such that the irrigation system was perpendicular or close to perpendicular radially to the DME. Second, the distance of the pivot point was iterated along east starting from 300 feet up to 1,500 feet at a 45° angle, the direction that showed the highest impact. The distance iteration is illustrated in Figure F-15.

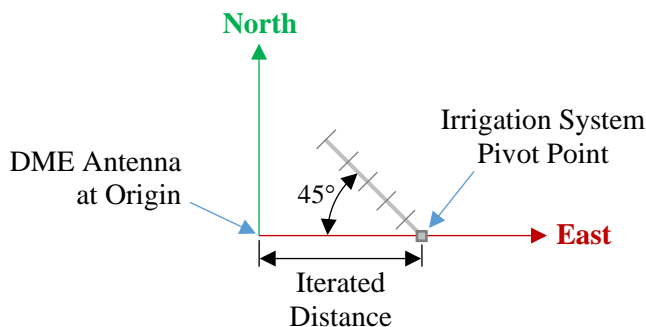


Figure F-15. Illustration of Irrigation System Model Set-up

Figures F-16 (a), (b), and (c) show the range error, lock status, and signal strength results for a 45° orientation of the irrigation system at a distance of 500 feet due east, respectively. At this distance the closest point of the irrigation system is approximately 350 feet from the DME due north east. The results show negligible impact resulting from irrigation equipment. The resulting siting criteria requirements derived from this analysis is that irrigation systems can be located anywhere outside of DME antenna near-field boundary as long as they are completely below the base of the antenna. Typically, a value of 250 feet should be considered to ensure protection of current and future DME installation. However, this distance may be as short as the 105 feet need to protect to near-field of the dBs 5100A DME antenna, which is the antenna model typically used for new DME installations.

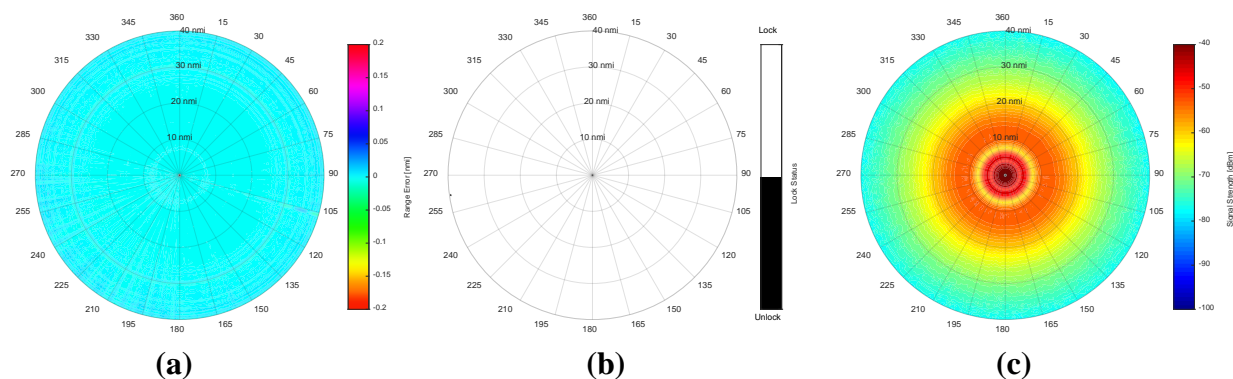


Figure F-16. (a) Range Error, (b) Lock Status, and (c) Signal Strength Results of Irrigation System at 500 feet Distance

- d. Air Traffic Control Towers (ATCTs).** ATCTs pose a unique challenge to siting DME antennas, due to their size and that fact they are present at all major airports and many smaller airports around the United States. The impact of ATCTs is mostly observed along radial paths to or from ATCTs, which can be particularly problematic if the radial intersects an approach procedure.

The impact of ATCTs on DME performance was assessed by modeling the ATCT at various positions and orientations relative to the DME and observing the predicted performance. In reality, there can be many combinations of size, position, and orientation of ATCTs that are unique. The analysis performed here is limited and intended to capture the worst-case scenario of a typical ATCT. The ATCT model used in this analysis was based on the ATCT at the Atlantic City Airport (ACY). This tower design is a standard design found in “FAA Order 6480.7, Airport Traffic Control Tower and Terminal Radar Approach Facility Design Guidelines.” The dimensions and material composition of the ATCT used in the model are given in Figure F-17. The glass portion of the ATCT cab was assumed to be metal as a worst-case scenario.

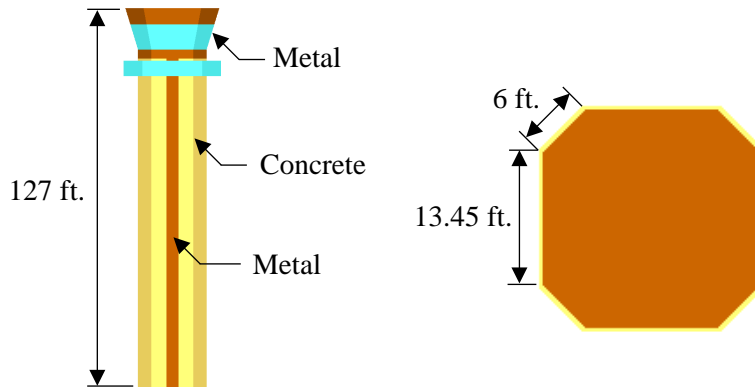


Figure F-17. Dimensions of Model ATCT

The ATCT was placed due east of the DME and the distance was iterated starting at 1,000 feet, as illustrated in Figure F-18. The antenna was placed at a height of 20 feet AGL. After iterating through the distances, the rotation angle of the ATCT was also rotated, as illustrated in Figure F-18.

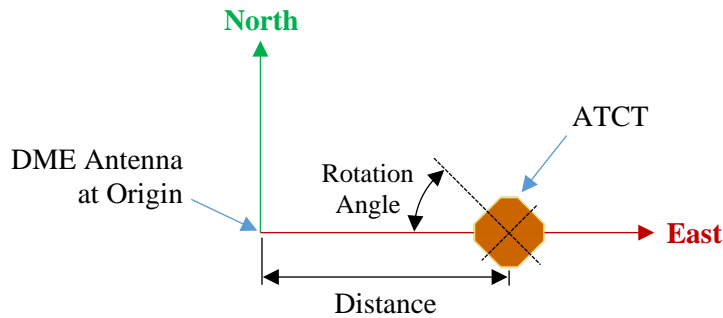


Figure F-18. Illustration of ATCT Model Set-up

At a distance of 1,000 feet and a rotation angle of 0°, the ATCT showed moderate impact on DME performance in terms of range error and loss of lock. Figures F-19(a), (b), and (c) shows the predicted range error, lock status and signal strength results at an

altitude of 1,000 feet above the facility. Some shadowing is observed behind the ATCT around azimuth 90°, which may also lead to unlocks in that area. Moderate range error is observed on the opposite side of the ATCT at azimuth 270°. Some range error is also observed in the north and south which is a result of reflections from the thinner wall.

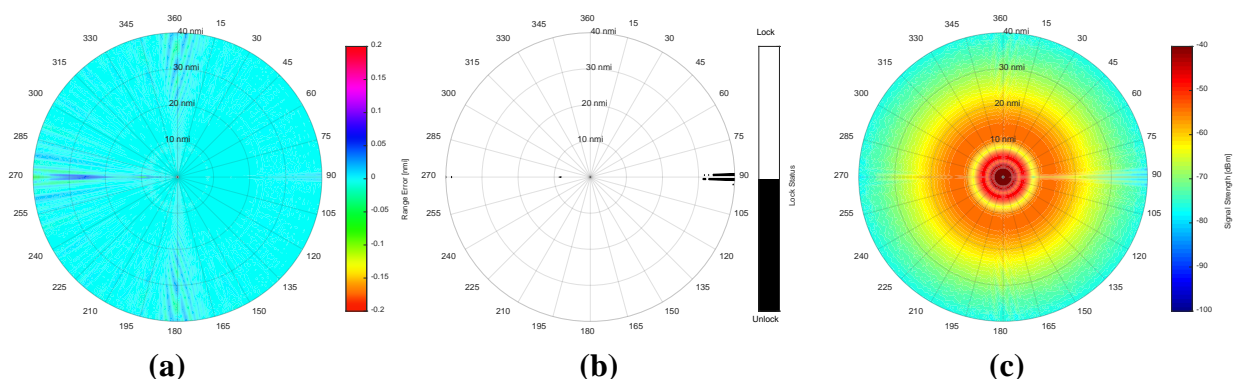


Figure F-19. (a) Range Error, (b) Lock Status, and (c) Signal Strength Results of 1,000 feet Distance

Performance improved as the distance of the ATCT relative to the DME increased until 6,000 feet. At that distance a significant area of unlock was present. At 7,000 feet the impact reduced slightly and past 8,000 feet no further impact was observed. Figure F-20(a) and (b) show the lock status for a distance of 6,000 and 7,000 feet, respectively. In both scenarios the rotation angle of the ATCT was 0°. The pulse-pair waveform showed that the unlocks were caused by time-delay of the first pulse. The scenarios were repeated with Y-channel transmitter, for which the pulse-spacing is 36 μs instead of the 12 μs X-channel pulse-spacing. The results showed no impact for both distances, suggesting that Y-channel transmitters are more immune from multipath resulting from ATCTs.

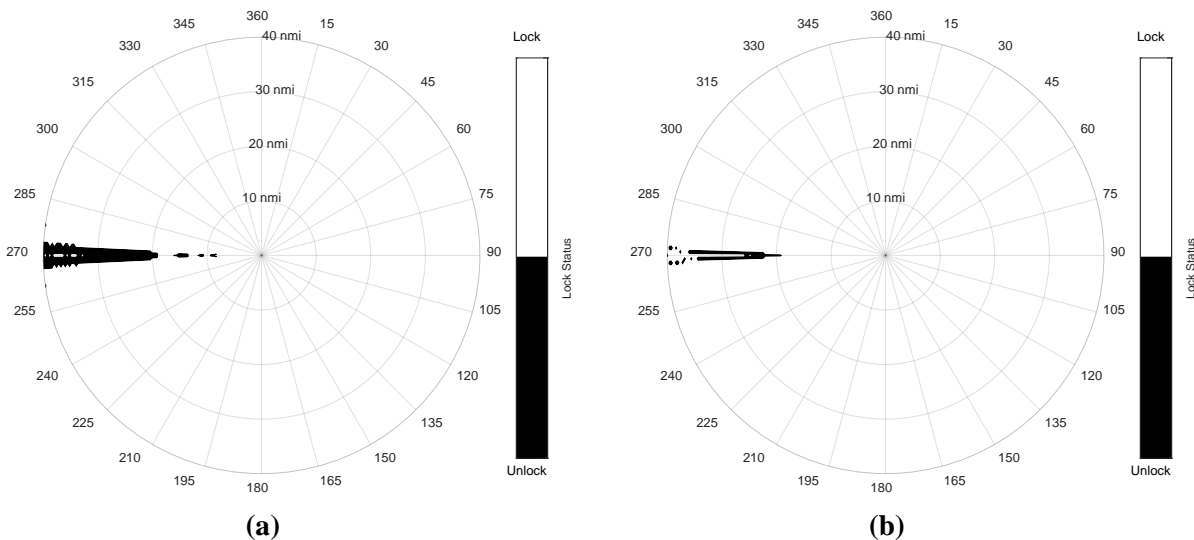


Figure F-20. Lock Status of (a) 6,000 and (b) 7,000 feet ATCT Distance

The ATCT was then rotated by 15° and 30° at 6,000 feet. Figures F-21(a) and (b) show the lock status results for rotation angle 15°, and 30°, respectively, for an X-channel transmitter. Expectedly, the location of the impact shifts as the angle of the ATCT changes. A rotation of 15° shows a narrower impact region compared to the 0° rotation angle, and at 30° the impact is negligible.

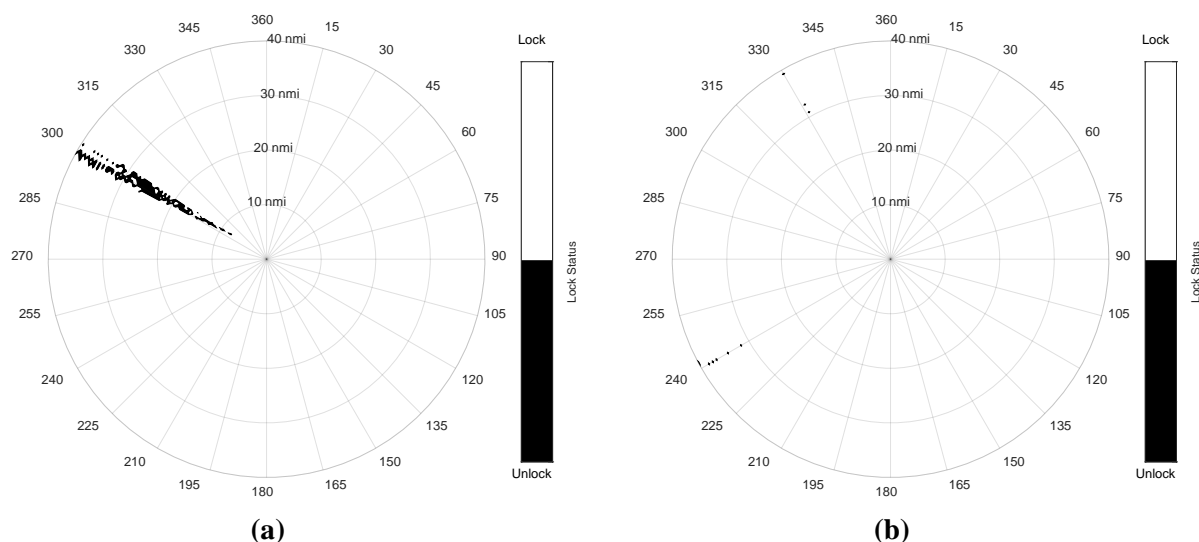


Figure F-21. Lock Status of (a) 15° and (b) 30° at 6,000 feet ATCT Distance

The result of this limited analysis indicates that the severity and location of the impact caused by ATCTs is highly sensitive to reflection geometries. Such geometries that give rise to a multipath delay of 10-15 microseconds cause X-channel DMEs to be more susceptible to unlocks. Due to the narrow shape of ATCTs, errors are observed in a narrow region of the service volume, thus allowing for the DME to be positioned such that errors lie in an unused portion of the service volume. The siting guidance derived from this analysis serves the purpose of protecting the entirety of the service volume.

The siting guidance derived from this analysis are as follows:

1. For X-channel transmitters, ATCTs must be under a 1° elevation angle measured from the base of the DME antenna and farther than 7,000 feet from the DME; and
2. For Y-channel transmitters, ATCTs must be under 2° elevation angle measured from the base of the DME antenna and farther than 4,000 feet from the DME.

In the event that these criteria are not met, the ATCT must be evaluated using the techniques discussed in Appendix C, Appendix E, or math modeling.

- e. **Communication Towers.** Communication towers are likely to be encountered at most prospective DME sites. At airports such towers would support various air-to-ground communication systems. Outside airports, the towers typically support municipal as

well as cellular communication systems. Communication towers are found in many forms and sizes, and it is time-prohibitive to model every model of communication towers. Instead, the modeling analysis focused on the two basic forms that are encountered most often; monopole and lattice towers.

The impact of communication towers on DME performance was assessed by modeling the two basic forms of communication towers mentioned in the previous paragraph. The height of the antennas was chosen to be 190 feet for both structures. This height represents a typical height of communication towers found outside airports. A diagram and dimensions of the towers used in the model are given in Figure F-22. The lateral dimensions of the towers also represent a typical case of communication towers that host cellular antennas.

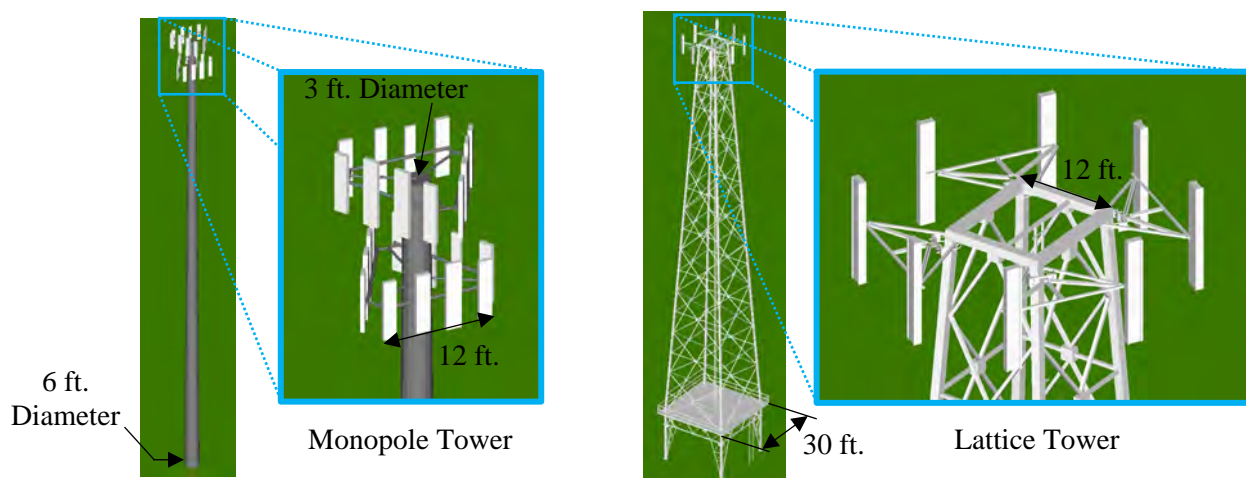


Figure F-22. Diagram of Model Communication Towers

The towers were individually placed due east of the DME and the distance from the DME antenna was iterated starting at 1,000 feet, as illustrated in Figure F-23. The height of the DME antenna was 20 feet AGL. Due to the narrow shape of the towers, their impact may not be fully observed within the previously defined observation point. As such, the observation point increments for this analysis were decreased to 0.5° for azimuth and 0.2 nmi for range.

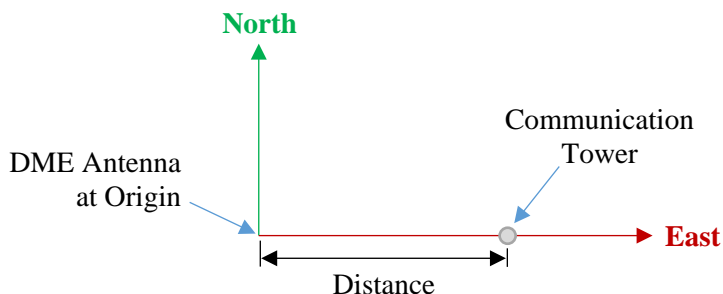


Figure F-23. Illustration of Communication Tower Model Set-up

At a lateral distance of 1,000 feet, modeling shows that the monopole tower will impact DME performance as a result of reflections and shadowing. Figures F-24(a), (b) and (c) show the range error, lock status, and signal strength results for the monopole tower located at 1,000 feet, respectively. The reflections resulting from the tower cause a range error that is observed to the north, west, and south of the DME beyond 30 nmi. This range error amounts up to 0.1 nmi, or 50% of the flight inspection tolerance for range error. The impact of the shadowing is observed behind the tower around azimuth 90°, where a signal strength decrease of 6-10 dBm are predicted in that area. This signal strength decrease produces a small area where continuous loss-of-lock conditions are observed along radial paths around azimuth 90°.

One effect to note on the lock-status plot is the concentric rings of unlocks observed towards the edge of the service volume. These are caused by two main factors; the decreased signal strength at the edge of the service volume combined with the noise in the channel, and the increased observation points. As mentioned earlier in the plot description paragraph, the marked unlock locations may not materialize to actual unlocks due to receiver processing techniques.

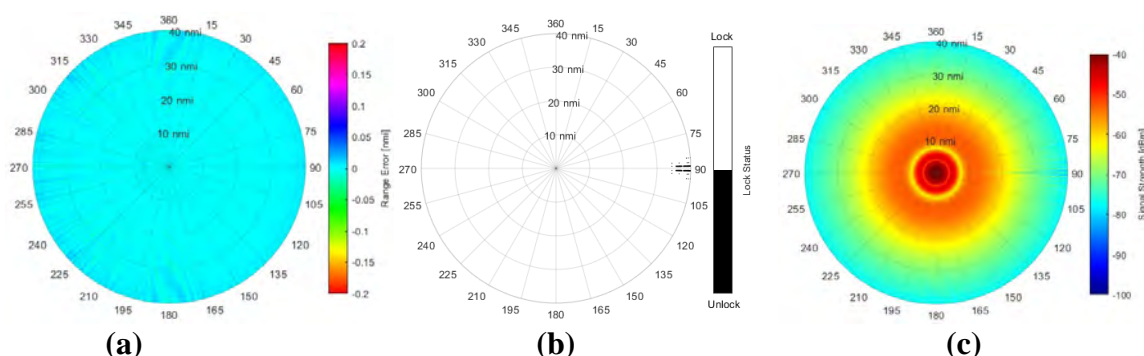


Figure F-24. (a) Range Error, (b) Lock Status, and (c) Signal Strength of Monopole at 1,000 feet

The modeling results for the lattice communication tower showed slightly better performance than the monopole tower with the same vertical dimensions. Figures

F-25(a), (b) and (c) show the range error, lock status, and signal strength results for the lattice tower located at 1,000 feet, respectively.

As in the monopole case, the predominant effect is that of reflection, which causes range errors to the north, west, and south of the DME. Shadowing is also present, although not to the same degree observed in the case of the monopole tower. The beams that make up the lattice structures are of smaller dimensions than the single monopole, thus allowing for more energy to make it past the tower. Shadowing causes discontinuous unlock conditions to the east of the DME, these conditions are unlikely to lead to unlocks.

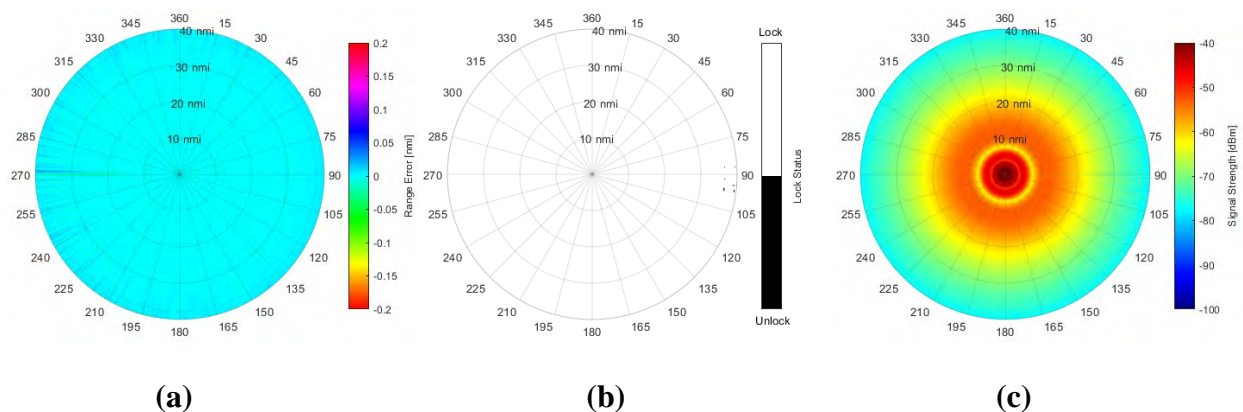


Figure F-25. (a) Range Error, (b) Lock Status, and (c) Signal Strength of Lattice Tower at 1,000 feet

Based on this analysis it is recommended that communication towers be no closer than 4,000 feet from the DME. Beyond 2,000 feet communication towers should be below a 2° subtending angle from the base of the antenna.

- f. **Cylindrical Structures.** Cylindrical structures, such as silos and fuel tanks, pose particular issues to DMEs due to their shapes and the manner in which they reflect radiation. The round shape of a cylinder causes the incident and reflection angle to exhibit a moderate change along the specular reflection points on the cylinder. The net effect of this is that multipath interference is observed throughout a larger portion of the service volume, compared to a structure of a similar size that was not of a cylindrical shape. These types of structures may be encountered at DME sites located at, or outside of, airports.

The impact of cylindrical structures on DME performance was assessed by modeling a cylindrical structure representative of a fuel tank at various distances due east of the DME and observing the predicted impact. The cylindrical structure is composed of metal and has a radius of 80 feet and a height of 60 feet. The dimensions were based on a fuel tank found in a fuel farm in Linden, NJ. The model set-up is illustrated in Figure F-26.

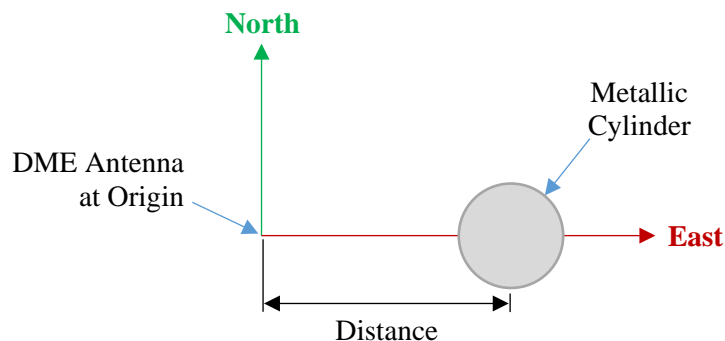


Figure F-26. Illustration of Cylindrical Structure Model Set-up

At distances less than and equal to 2,000 feet, modeling shows that the cylindrical structure will severely impact DME performance of X and Y-channel transmitters, primarily as a result of reflections. Figures F-27(a), (b) and (c) show the range error, lock status, and signal strength results of a Y-channel transmitter for the cylindrical fuel located at 2,000 feet, respectively. The range error plot shows moderate range error in the western portion beyond 25 nmi. The lock status plot shows significant continuous unlocks in the western portion, which will very likely result in unlocks, especially during radial flight paths.

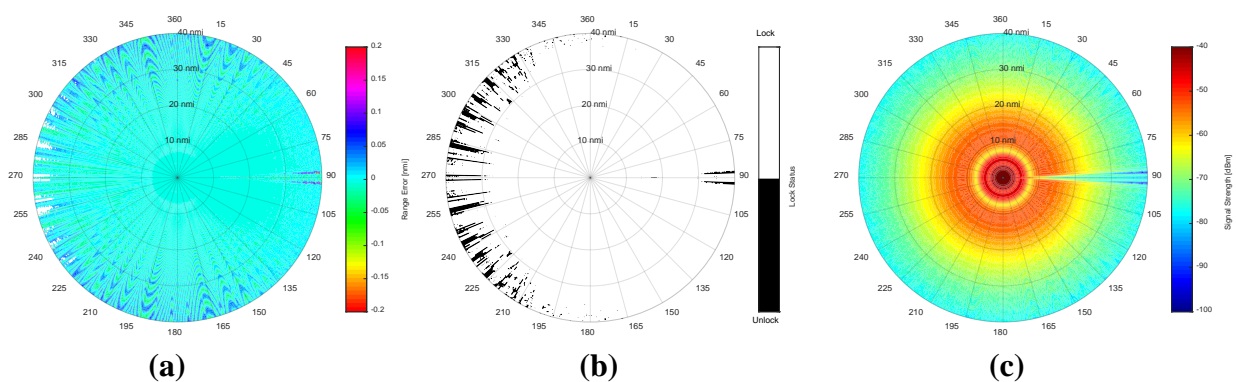


Figure F-27. (a) Range Error, (b) Lock Status, and (c) Signal Strength of Fuel Tank at 2,000 feet

A significant difference between X and Y-channel transmitters was observed when the tank was located at 6,000 feet from the DME. Figures F-28(a) and (b) show the lock status for X and Y-channel transmitters, respectively. At this distance, the path length difference between the direct and tank-reflected signal was similar to the pulse-spacing for X-channel transmitters at locations west of the DME beyond 25 nmi. At these locations the lock status plot for the X-channel showed significant unlocks, whereas no unlocks were observed in the Y-channel lock status plot.

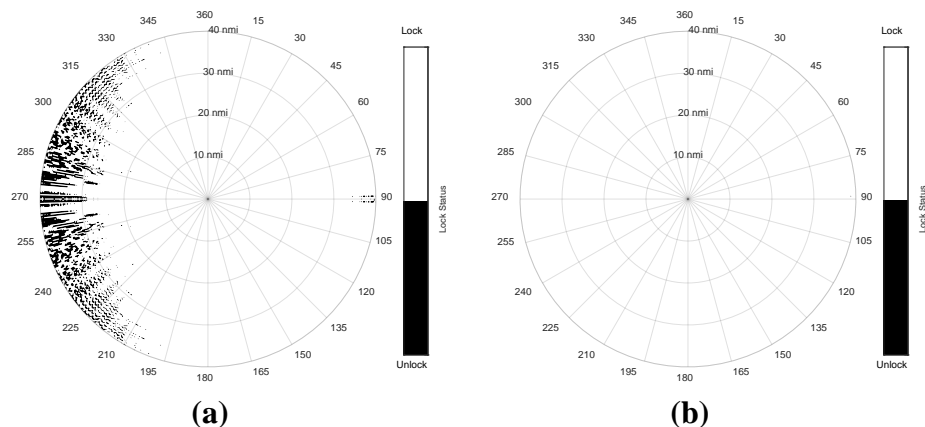


Figure F-28. Lock Status of Fuel Tank at 6,000 feet for (a) X and (b) Y-channel Transmitter

The siting criteria requirements derived from this analysis are as follows:

1. For X-channel transmitters, large cylindrical structures (radius 50-feet or greater) must be under a 0.5° elevation angle measured from the base of the DME antenna and further than 10,000 feet from the DME;
2. For Y-channel transmitters, large cylindrical structures (radius 50-feet or greater) must be under 1° elevation angle measured from the base of the DME antenna and further than 5,000 feet from the DME.

4. Discussion

In this appendix, siting criteria requirements for several types of structures were derived by using the DME math model and analyzing the resulting model data. It is important to note that although the model was extensively validated, the modeling results are only predictions and may be slightly different than reality. Additionally, the coarse grid spacing was used to assess the impact over a large area and small pockets of errors may exist, but are not expected to be operationally significant.